2014

Implementation of Self-Consolidating Concrete for Bridge Applications

Joseph Garet Sweet
West Virginia University

Implementation of Self-Consolidating Concrete for Bridge Applications

Joseph Garet Sweet

Dissertation submitted to
Benjamin M. Statler College of Engineering and Mineral Resources
at West Virginia University

in partial fulfillment of the requirements for the degree of

Doctor of Philosophy in
Civil and Environmental Engineering

Roger H.L. Chen, Ph.D., Chair
Hota V. GangaRao, Ph.D., P.E.
John D. Quaranta, Ph.D.
Felicia F. Peng, Ph.D.
Marvin H. Cheng, Ph.D.

Department of Civil and Environmental Engineering

Morgantown, West Virginia
2014

Keywords: Self-Consolidating Concrete; Caisson Construction; Prestressed Box Girder; Full-Scale Testing

ABSTRACT

Implementation of Self-Consolidating Concrete for Bridge Applications

Joseph Garet Sweet

Self-Consolidating Concrete (SCC) typically refers to a highly-flowable classification of high-performance concrete. Unlike traditional concrete, SCC has the potential ability to flow into and completely fill complex forms under its own weight. A well-designed SCC mix does not need to be vibrated for compaction, unlike a traditional vibrated concrete (TVC) mix. This gives the use of SCC the potential advantages of reduced placement costs and a more worker-friendly construction environment due to the elimination of construction noise and the added ease of placement. The primary objective of this study was to work with contractors, WVDOT officials in order to safely utilize SCC technology on the Stalnaker Run Bridge Replacement, which would be the first WVDOT bridge construction project to utilize SCC. SCC was incorporated for cast-in-place caissons as well as precast/prestressed beam components.

Prior to use of a 4,500 psi mix for the caisson applications, deemed SCC-1, a novel test procedure was developed to assess the uniformity of SCC within a model caisson member. Instead of allowing the entire mock section of SCC to harden prior to dissecting it for core samples, "fresh core" tubes were used to sample the SCC while it was still green. After hardening, the wet cores revealed non-uniformities in the aggregate distribution and hardened properties of the mix as placed within the trial caisson. Despite the non-homogeneity, tests did not indicate a relationship between the absence of aggregates and detrimental effects on the hardened properties of the SCC-1.

SCC-1 was used for the construction of the caissons of Abutment 1, while a traditional caisson mix was used for Abutment 2. Samples taken during casting of the caissons revealed that both caisson mixes exceeded the minimum strength requirement, and specimens of both types exhibited approximately the same modulus of elasticity, around 4,400 ksi. The SCC-1 mix exhibited low Rapid Chloride Permeability and was deemed freeze-thaw durable based on ASTM C 666 testing.

Three precast/prestressed box beams for the Stalnaker Run Bridge were fabricated using a traditional vibrated concrete and two were cast using SCC-2, both of which required a strength of 8,000 psi. Additionally, one extra beam was fabricated and shipped to WVU facilities for testing. All beams were instrumented with a barrage of gages prior to casting. After casting, the SCC-2 mix required 2 nights of steam curing prior to detensioning, while the TVC needed only one. Temperature data collected during curing of the beams indicated maximum temperatures of around 160°F to 170°F, which fall below the PCI-prescribed threshold of 180°F. Specimens collected during construction of the Stalnaker Run Bridge showed some major differences in the hardened behaviors of SCC-2 and TVC. The TVC has a higher modulus of elasticity than the SCC-2 concrete, both at detensioning (19% higher) and at 28 days (21.0% higher). Durability testing of SCC-2 specimens indicate that the SCC-2 concrete from production may not be freeze-thaw durable, and not all specimens exhibited the required durability factor of 80% per project specifications. Results of RCPT testing of both types of concrete

would classify SCC-2 as having predominately "moderate" permeability, while the TVC would be classified as having "high" permeability.

The laboratory beam underwent both destructive and non-destructive testing. The effective prestress in the beam calculated using the observed decompression behavior of the beam (Pe = 707.5 kips or fpe = 159.7 ksi), was within 1.5% of a direct measurement of the residual strain based on strand strain readings, which were taken directly from the strand strain gage readings. The test beam exhibited higher deflection and lower capacity at cracking than the theoretical behavior using PCI design values. Adjustments of the material properties to measured values for SCC-2 gave a good correlation between theoretical and observed load-deflection behaviors. The results of the non-destructive modal analysis did not correlate well with the damage state of the prestressed beam.

Strain data from the Stalnaker Run Bridge data collection station is being collected incrementally. Over a four month period, the magnitudes of measured strain change in the prestressing strand gages ranged from 200 με to 400 με, and 200 με to 500 με for the SCC-2 and TVC beams, respectively. The rate of change in the strain readings for the beams has since decreased drastically.

Acknowledgements

I would like to express my gratitude toward my research advisor, Dr. Roger Chen, for the invaluable guidance and assistance provided throughout my studies. I would also like to thank the members of my research committee, Dr. Hota, Dr. Quaranta, Dr. Peng, and Dr. Cheng, for their insight and guidance in helping to shape this research.

Much of the data collection and experimentation presented herein would not have been possible without the assistance of my colleagues, Kyle Baranowski and T. Alper Yikici. I would also like to recognize the efforts of Dr. Jeong-Hoon Choi, Yun Lin, Binwei Zhang and Susana Rojas in conducting experiments in the laboratory and in the field.

The support from the FHWA and WVDOT was critical to this project, IBRD-0219(293)D. Particularly, I greatly appreciate Mr. Jimmy Wriston and Mr. Mike Mance of WVDOT and Mr. Chien-Tan Chang and Mr. Myint Lwin of FHWA for their valuable technical assistance and guidance in conducting this research. I would also like to thank the Central Supply Company, Euclid Chemical Company, Alcon, BASF Admixtures, and Bilco Construction Company for materials and assistance provided, as well as WVDOH District 8 Engineers Kyle Hall and Steve Schumacher for design and construction details provided through all phases of the research. The assistance of Shelly Foundations, Inc. during the caisson construction and Eastern Vault during fabrication of the prestressed box beams is also appreciated.

Most of all, I would like to thank my family, and my dearest, Renee, for the invaluable patience, understanding and encouragement shown throughout this process.

This document is essentially the same as the final report of the IBRD project submitted to FHWA/WVDOT.

Table of Contents

List of Figures

List of Tables

1 Introduction and Background

1.1 Introduction

Self-Consolidating Concrete (SCC) is a fairly recent technology that has been under development for the past two decades. Compared to traditional vibrated concrete (TVC), SCC is much more fluid, which gives it the ability to flow around rebar and fill formwork without the need for external compaction efforts. The use of SCC is a promising construction alternative, especially when considering situations that arise in many highway bridge applications where tightly-placed reinforcing bars or irregular geometries of structural members would hinder the compaction effort required by traditional concrete mixes. While there have been some applications for this relatively new technology, mostly in the precast building components, at the onset of this research it had not yet been utilized by many state agencies, including the West Virginia Department of Transportation, Division of Highways (WVDOT), for precast bridge girders or cast-in-place applications.

There are many considerations for implementing SCC technology on a wide scale for precast or cast-in-place highway bridge applications. First of all, since the behavior of a particular SCC mix is highly dependent on its ingredients, specifications for mix design with locally available aggregates and admixtures need be developed. Also, there are only a limited number of tests designated for evaluating the performance of a given SCC mix with respect to self-compaction and segregation behaviors, so the performance criteria of acceptable SCC need to be investigated and specified. Certain logistical issues such as formwork design and methods for transporting the SCC to the job site will also have to be addressed before it can be used for cast-in-place applications. In addition, the general curing characteristics and long-term behaviors of the SCC will affect the cracking potential and longevity of the

structure and hence, time-dependent behaviors such as shrinkage, creep and durability need to be studied. Another issue that arises when trying to incorporate SCC into these applications is the lack of familiarity of many people in the concrete industry, including design engineers, ready-mix suppliers, construction workers, and project engineers, with the product since this is such a recent technology. Effective technology transfer or on-site training becomes necessary. Knowledge and experience obtained from this project can benefit not only those who were involved locally but also engineers from the bridge construction industry nationwide.

As part of the Innovative Bridge Research & Deployment (IBRD) program, this research project included laboratory tests using SCC, the development of design, handling, testing, and construction requirements for SCC, and the construction, assessment and monitoring of precast/prestressed and cast-in-place bridge structural members that implement SCC.

1.2 Background

1.2.1 Use of Self-Consolidating Concrete

SCC was first introduced by researchers from the University of Tokyo, Japan in 1989. Since then, Japan has used SCC in bridges, buildings, and tunnels. In addition, a number of SCC bridges have been constructed in Europe in the late 1990's (Ouchi, et al. 2003); in the United States, the application of SCC in highway bridge construction has begun to pick up, and many states have either adopted or are in the process of adopting provisions for its use. In the early 2000's, bridge construction projects using SCC were completed in Kansas, New York, Virginia, and Nebraska (FHWA 2005). An NCHRP Project 18-12, Self-Consolidating Concrete for Precast, Prestressed Concrete Bridge Elements is aimed at increasing the acceptance and use of SCC in highway bridge construction. The U.S. precast concrete industry has applied the technology to architectural concrete since early 2000's. One representative of a

precast supplier estimates that approximately 90% of the precast members produced at their facilities utilize SCC for precast building components (Narchus 2006).

Labor savings are the main advantage of using SCC. When properly designed, it does not require vibration to achieve full compaction and remains stable both during and after placement. In addition to the reduction of labor costs, the use of SCC offers many benefits such as the potential elimination of vibration noise, improved quality and durability, faster construction, and higher strength, resulting in cost savings and less traffic disruption. Properly designed and placed SCC also reduces aggregate segregation, honey combing, and voids in the concrete. Hence, the overall concrete quality improves, as problems associated with vibration are eliminated. It has also been stated that the elimination of vibration improves the concrete's resistance to chloride intrusion and ability to withstand freeze thaw damages (FHWA 2005).

1.2.2 Stalnaker Run Bridge Replacement

This project involves the experimental use of SCC during the Stalnaker Run Bridge replacement (WV State Project S342-219-45.13 00, Federal Project BR-00219(126)E, located on County Route 219/86 in Randolph County, WV), which was scheduled to be replaced during the project. At the time of replacement, the existing bridge had a combination structure that was a simple span concrete deck arch (SCDA) that was at one point widened with a reinforced concrete channel beam on the upstream side, as shown in Figure 1-1. The replacement bridge consists of a single span structure with a concrete deck, prestressed concrete girders, and abutments overlying drilled shaft caissons (see Figure 1-2). The replacement of the bridge included a widening of the structure; the curb-to-curb width increased from 27'-8" for the existing bridge to 33'-0" for its replacement.

Figure 1-1 Old Stalnaker Run Bridge, with temporary bridge in background. View from upstream location.

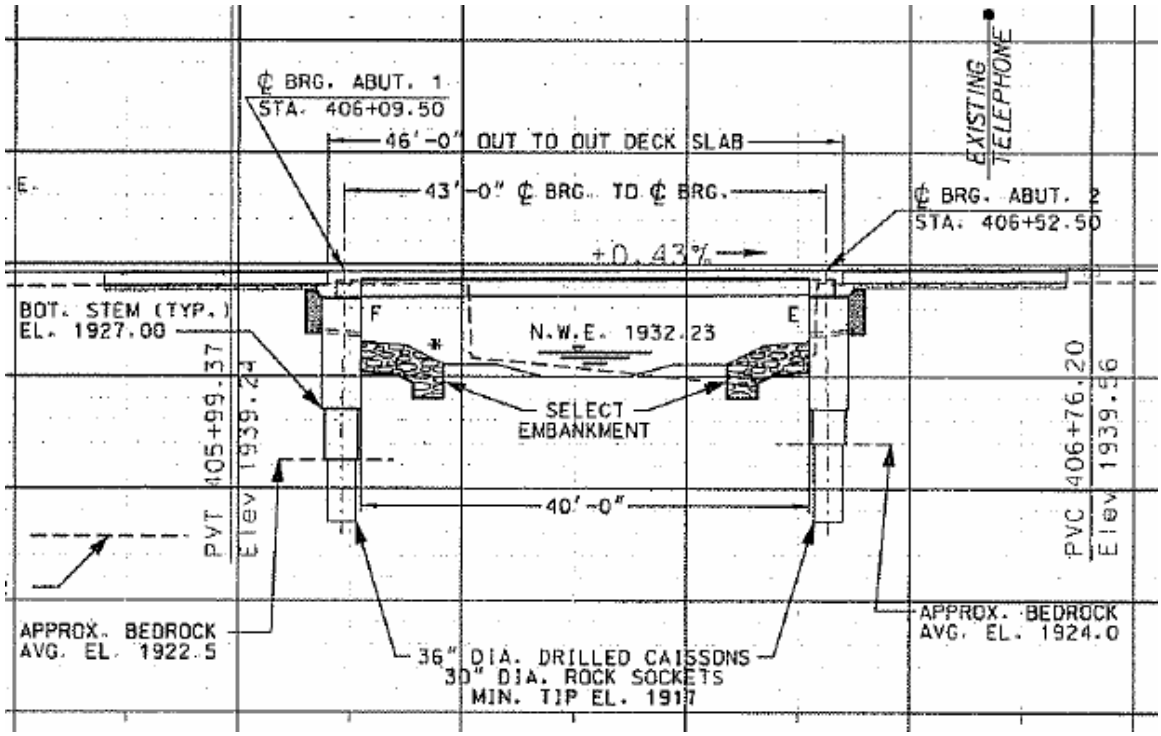

Figure 1-2 Profile of Stalnaker Run Bridge replacement, as indicated in construction plans.

1.3 Research Objectives and Scope

The objectives of this research are to develop the mix design criteria for SCC using local materials widely used in West Virginia, to provide guidelines for transportation of SCC, to specify

construction techniques for cast-in-place SCC applications, to apply SCC technology to components on a highway bridge to be constructed in West Virginia, to monitor the performance of the aforementioned SCC components, and to re-evaluate the applicability of concrete design guidelines for use of SCC.

The scope of this project involved implementing and assessing the efficacy of the use of SCC for the multiple aspects of the Stalnaker Run bridge replacement project. This included use of SCC for the cast-in-place construction of the drilled caissons underlying one of the abutments, as well as two of the five prestressed box girders that were shipped to the construction site. As part of the evaluation process, the other caissons and prestressed box girders for the project were constructed using traditional concrete mixes for the sake of comparison. A trial casting of SCC was performed in the laboratory in preparation for the caisson construction. A third prestressed box beam was also fabricated using SCC and shipped to WVU for testing. Upon completion of the construction, the SCC sections were monitored for a period of over two years.

1.3.1 Pre-Construction

Prior to the bridge construction, guidelines for the use of SCC in the cast-in-place application (caisson construction) and the precast application (precast/prestressed box beams) were established and incorporated into the project provisions. Guidance and assistance were then provided to contractors as they developed SCC mixes to meet the demands of the project. Trial batches were created in WVU laboratories so that fresh and hardened properties of mixes could be ascertained for the purpose of evaluating mixes during the development process.

A cost-effective approach to assessing the suitability of the caisson SCC was devised in which wet conditions anticipated for the field were simulated in the laboratory. A novel method of sampling SCC for assessment of uniformity after placement was developed and employed for this task.

Separate instrumentation plans were devised for the caissons and prestressed beams. Methods were explored for assessment of the uniformity of SCC after placement in the field, including Infrared Thermography and pH investigations for the caissons.

1.3.2 Construction

Each member was instrumented at various locations with sensors which have the ability to detect the temperature, relative humidity and strain levels so these characteristics could be monitored during and after construction. To ensure that the SCC to be used had the same performance characteristics as specified, the fresh properties of SCC were tested on site. As each component was cast, concrete samples were taken to assess shrinkage, strength development, and other material characteristics of the hardened concrete in the laboratory.

1.3.3 Post-Construction

Data collection from the sensors detecting temperature, relative humidity and strain levels began immediately following casting. These measurements were taken periodically to allow for future analysis of the contributions from these factors to the development of material properties as well as to assess the overall behavior and stress development in the structure. A full-scale precast/prestressed box beam that was identical to those used for the bridge was delivered to the WVU Major Units (Structures) Laboratory and tested using non-destructive and destructive methods. Periodic data collection excursions were made to the bridge until a long-term monitoring station was set up on-site, which allowed for continuous data collection and future assessment of performance. Also, based upon the observations during the construction process and the data collected afterward, all specifications developed at the onset of the project were re-evaluated and additions or changes were made accordingly.

1.4 Structure of Document

The body of this document is broken into four major components, with a literature review in Chapter 2 followed by the three chapters detailing the experimentation and data collection pertaining to the use of SCC on the Stalnaker Run Bridge. Efforts relating to the use of SCC for the caissons of the Stalnaker Run Bridge replacement are detailed in Chapter 3, efforts relating to the use of a different SCC mix for the bridge beams are detailed in Chapter 4, and data collected from the completed bridge structure is given in Chapter 5. Chapter 6, includes a discussion on the implementation of SCC in light of the findings of the previous three sections, while Chapter 7 provides a summary of findings from the project.

Chapter 3 discussions include: the creation of project provisions for caisson SCC (deemed SCC-1 in project documents); the SCC-1 and traditional concrete mix designs; the development and execution of a trial caisson casting conducted in the laboratory; and the instrumentation and construction of the caissons in the field using traditional and SCC-1 concrete.

Chapter 4 discussions include: the creation of project provisions for precast/prestressed SCC (deemed SCC-2 in project documents); the SCC-2 and traditional prestressed concrete mix designs; the instrumentation and fabrication of bridge beams using SCC-2 and traditional concrete; and the non-destructive and destructive testing of a full-scale SCC-2 bridge beam in the laboratory.

Chapter 5 gives schematic details of the instrumentation used for long term monitoring of the SCC-1 caissons and the SCC-2 and traditional box beams in the field, as well as some of the strain data and camber measurements collected on site.

Chapter 6 summarizes the findings of the three previous sections, and discusses changes that could be made to future provisions for the implementation of SCC.

Chapter 2

2 Literature Review

To be considered self-consolidating, a mix must have three key characteristics: (1) ability to flow into and completely fill intricate and complex forms under its own weight, (2) ability to pass through and bond to reinforcement material under its own weight, and (3) high resistance to aggregate segregation. These fresh state characteristics of SCC are typically referred to as flowability, passing ability, and segregation resistance, respectively. To make a highly fluid mix that is not prone to segregation, SCC is proportioned differently than traditional concrete and its mix design oftentimes will include different types of admixtures. These variations in proportions and components not only alter the fresh properties, but could ultimately have positive or negative influences on the hardened properties as well. Topics of focus for this literature review include an introduction to SCC, the constituents and mix design of SCC, fresh and hardened properties of SCC and how they are measured, and special topics that are specific to the use of SCC for caisson and precast/prestressed beam construction.

2.1 Behavior of Fresh SCC

In recent years there have been a number of studies aimed at producing standardized testing methods to obtain performance characteristics of SCC. The performance of fresh SCC is most often defined based on assessment of its flowability [or filling ability], passing ability, and segregation resistance.

In 2005, the American Society for Testing and Materials [ASTM] adopted one test for assessing the flowability of SCC: the "Test Method for Slump Flow of Self-Consolidating Concrete," Standard ASTM C 1611 (ASTM Standard C 1610 2006). This technique is conducted in a similar fashion to the

slump test for standard concrete, but instead of measuring the downward displacement, or slump, of a sample after the slump cone is removed, the slump flow of the mix is characterized by measuring the diameter of the sample after cone removal (see Figure 2-1).

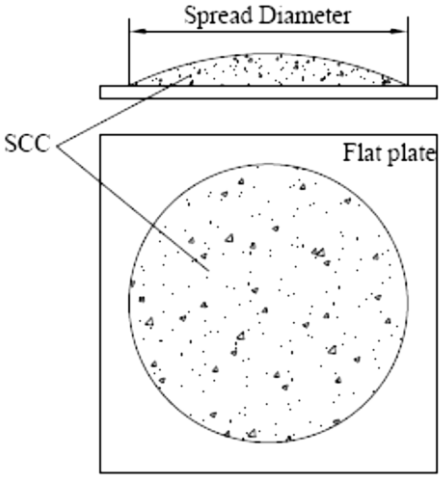

Figure 2-1 Schematic diagram of slump-flow test. (Wang, et al. 2005)

Figure 2-2 Photo of slump-flow (bottom) and J-Ring (top) patties after removal of the Abrams cone.

In addition to the slump flow, the rate at which the mix flows is generally recorded as a T500 (T20) value, or the time that it takes the mix to spread a distance of 500 mm (20 in); another value which is obtained from this setup is the Visual Stability Index, VSI, which is based on observation of the consistency of the mix after spreading. The T500 (T20) gives an indirect representation of the viscosity of the mix, while the VSI gives an indirect representation of the dynamic stability of the mix. This test is relatively quick and simple, and can easily be conducted by project engineers to assess the flowability of an SCC mix as it is delivered for use in the field.

ASTM C 1621 gives guidelines for performing the "Standard Test Method for Passing Ability of Self-Consolidating Concrete by J-Ring," which was released in April of 2006 (ASTM Standard C 1621 2006). This test incorporates a J-Ring (see Figure 2-2) around the base of the slump flow cone; the difference in spread with and without the J-Ring would be indicative of the ability of the SCC mix to flow around reinforcing bars. The J-Ring test would also be efficient for project engineers to conduct as a simple assessment on site.

The slump-flow and j-ring tests mentioned measure primarily the flowability of SCC and the ability of the SCC to flow around rebar (or passing ability), respectively. Two more SCC fresh property tests have been standardized by ASTM for assessment of the static stability of an SCC mix. ASTM C 1610, "Static Segregation of Self-Consolidating Concrete Using Column Technique," and ASTM C 1712, "Rapid Assessment of Static Segregation Resistance of Self-Consolidating Concrete Using Penetration Test" were adopted for this purpose (ASTM Standard C 1610 2006) (ASTM Standard C 1712 2009).

The first segregation test mentioned, ASTM C 1610, is done by first filling a standard-sized segregation column (see Figure 2-3) with fresh SCC, and allowing adequate time (15 ± 1 minute) for any static segregation of the sample to take place. Then, the top portion of the column (1/4 of the

column height) along with all contents is carefully removed and collected such that the weight of aggregates in that portion of the column larger than a #4 sieve can be obtained. Likewise, the same procedure is followed for determining the weight of aggregates contained in the lower one-fourth of the column. The segregation resistance by this method is determined using the relationship:

$$\text{Static Segregation (\%)} = 2 * \frac{[CA_B - CA_T]}{[CA_T + CA_B]} * 100\% \quad (1)$$

where CA_T = Coarse Aggregate Retained from the Top Portion [lb] and CA_B = Coarse Aggregate Retained from the Bottom Portion [lb] of the segregation column. A low percentage would indicate that large aggregates were not settling to the bottom of the column apparatus, while a larger percentage would indicate more segregation. Typical values for an acceptable segregation percent are in the range of zero to 15 percent, though some agencies may apply slightly stricter or looser ranges, and the application is often considered when making this determination. (ACI Committee 237 2007) (BIMB, CEMBUREAU, ERMCO, EFCA and EFNARC 2005)

With the inactive time, the amount of time it takes to sieve the samples, and that for achieving the appropriate moisture state of the aggregates from the static segregation test using the column technique, one can imagine that it would be somewhat impractical to use this method to define site acceptance criteria for SCC, especially when most agencies regulate the time of placement of concrete to within 90 minutes of the time of mixing. Therefore, the penetration test was developed to allow for a more expedited determination of the segregation resistance of SCC that is more practical for field acceptance.

In the penetration test described in ASTM C 1712, the penetration apparatus, shown in Figure 2-4, is placed directly on top of an inverted Abrams cone that is prepared in the same fashion as that for the slump-flow test. After a period of 80 ± 5 s after completion of strike-off, the hollow cylinder is allowed to settle into the surface of the SCC for a period of 30 ± 2 s. The penetration depth, P_d, is

determined using the scale on the penetration apparatus. ASTM C 1712-09 defines the degree of static segregation resistance as follows: an SCC with $P_d \leq 10$ mm is classified as "Resistant," an SCC with 10 mm $\leq$ $P_d \leq 25$ mm is classified as "Moderately Resistant", and an SCC with $P_d \geq 25$ mm is "Not Resistant" to segregation.

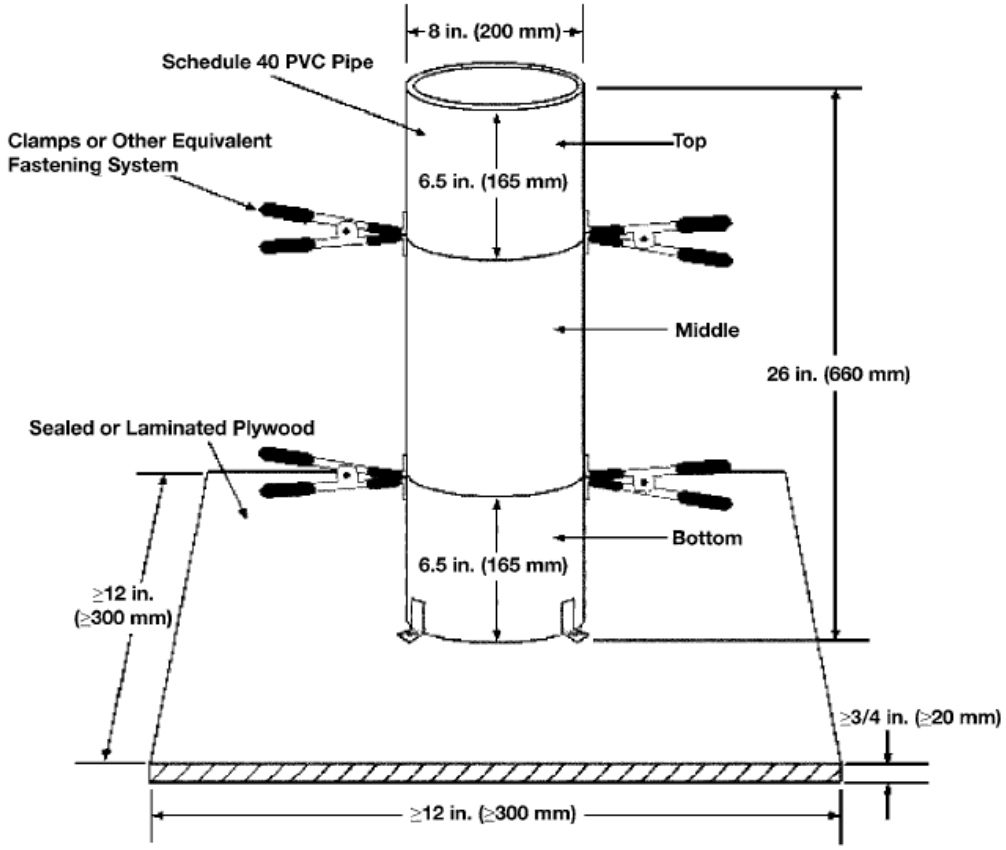

Figure 2-3 Dimensions of Standard Column for Determining Static Segregation of Self-Consolidating Concrete. (ASTM Standard C 1610 2006)

Beyond the ASTM tests, many researchers have used rheological studies to characterize the fresh properties of concrete mixes based on measurements of the yield stress and the plastic viscosity of the concrete sample (Wong, et al. 2000). According to the Bingham model, the yield stress is indicative of a concrete's ability to start flowing, while the viscosity is indicative of the concrete's ability to flow after

stresses exceed the yield stress (Ferraris 1999). Khayat, Assaad, and Daczko have used the rheological properties of SCC to correlate to more common field tests for dynamic stability in order to obtain a greater understanding of the concrete properties that affect self-consolidation (Khayat, Assaad and Daczko 2004). Saak et al. have even proposed methods for using the rheological properties of SCC to control both static and dynamic segregation of the mix (Saak, Jennings and Shah 2001).

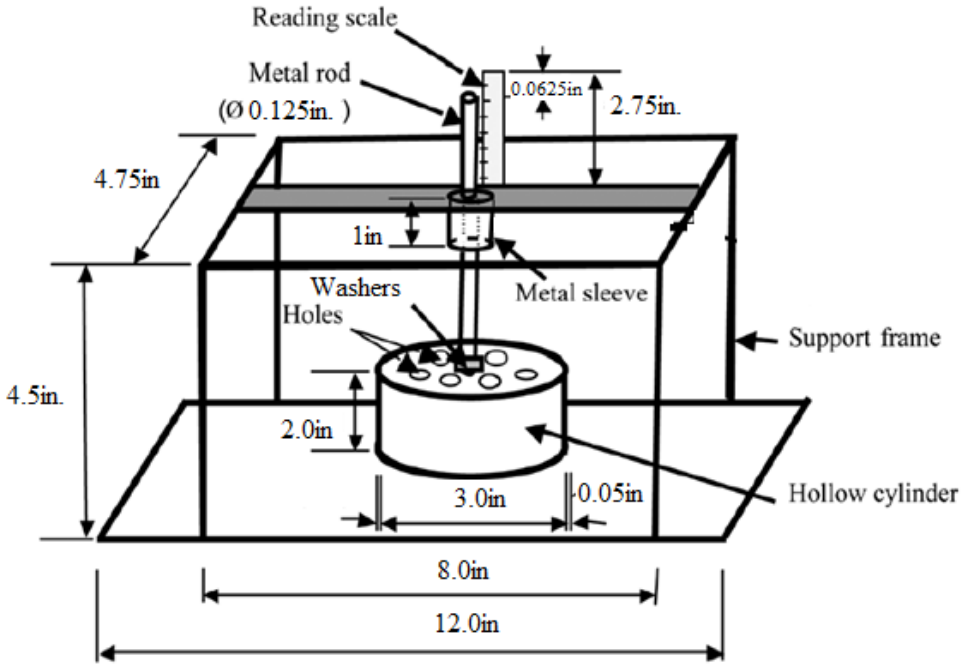

Figure 2-4 Dimensions of the Penetration Apparatus for Rapid Assessment of Static Segregation Resistance. (ASTM Standard C 1712 2009)

2.2 Hardened Properties of SCC

The major differences between SCC and other concrete mix designs are present when the concrete is in its fresh state. Although the magnitude of mechanical properties may differ, SCC will behave in a fashion similar to conventional concrete upon curing; therefore many of the same techniques for assessing standard concrete properties would be suitable for SCC mixes. Techniques for determining the compressive strength of concrete (ASTM C 39), measurement of creep and drying shrinkage over

time (ASTM C 512 and ASTM C 157, respectively), determining permeability (ASTM C 1202), and conducting air void and freeze-thaw analyses (ASTM C 457 and ASTM C 666, respectively) have been well-established and can provide valuable information regarding the short- and long-term performance of concrete. Many of the common tests for hardened properties of concrete can be seen in Table 2-1.

Table 2-1 Common Hardened Property Tests for Concrete

Test	Desired Characteristics	Standard Method(s)
Compression	28-day Compressive Strength	ASTM C 039 AASHTO T22
Modulus of Elasticity	Modulus of Elasticity Poisson's Ratio	ASTM C 496
Split-Tensile Test	Tensile Strength	ASTM C 496
Length Change	Drying Shrinkage	ASTM C 341 AASHTO T160
Air Void Analysis	Air-void Characteristics	ASTM C 457
Chloride Permeability	Resistance to Chloride Penetration	ASTM C 1202 AASHTO T277
Creep	Long-Term Creep (under Compressive Forces)	ASTM C 512 ASTM C 801
Freeze/Thaw Analysis	Durability Characteristics	ASTM C 666 AASHTO T161
Pull-Out Test	Bond with Prestressed Tendons	ASTM C 234 Moustapha Method

In addition to the standardized testing, embedded gages can be used to give time-dependent data relating to the temperature, relative humidity and strain levels of in-situ concrete. Determining relationships between these and other time-dependent characteristics of a concrete mix can help in predicting the short-term and long-term behaviors of reinforced concrete and prestressed concrete members. Of particular importance to this project are the shrinkage and permeability of the caisson SCC, as these could affect the lifespan of the bridge foundation. Likewise, the creep, shrinkage, and modulus of elasticity of the prestressed SCC are directly related to prestress losses, while these (in addition to the permeability characteristics) would also affect the longevity of prestressed box beams.

There have been many studies comparing the mechanical properties of hardened self-consolidating concrete to those of traditional vibrated concrete. In his investigation, Persson concluded that the "creep, shrinkage and elastic modulus of SCC coincided well with the corresponding properties of [traditional vibrated concrete] when the strength was held constant (Persson 2001)."

Numerous others have observed notable differences in the behaviors of SCC and TVC, though. In a compilation of results from over 70 studies, Damone observed that the modulus of elasticity of SCC can be up to 40% lower than TVC for mixes with low compressive strengths, but is generally less than 5% lower at high strengths (Damone 2007). Parra et al. observed SCC moduli of elasticity that were 2% below those of TVC despite the stiffness of the SCC's cement paste being larger; they attributed this to the overall larger quantity of paste in the SCC as compared to the TVC. In this study, the authors also observed splitting tensile strengths that were lower than those of TVC (Parra, Valcuende and Gomez 2011). Due to the potential for large discrepancies in mechanical behavior, the engineering properties of the SCC should be evaluated in a case-by-case basis to ensure satisfactory performance.

2.3 SCC Constituents and Mix Design

SCC is composed of many of the same components that are used to make TVC: large and small aggregates, air, water, cementitious materials, and admixtures. While most of the same constituents are used, the proportioning of the materials needs to be altered so that they exhibit sufficient viscosity to stabilize aggregates and prevent static and dynamic segregation. Obtaining sufficient viscosity in an SCC mix is typically done either by (1) including a low water-to-cementitious material ratio and a high powder content in the mix design, or (2) incorporating an appropriate mixture of high-range water reducing admixture (HRWRA) and viscosity modifying admixture (VMA) into the mix to obtain the desired characteristics. Bonen and Shah categorize these as powder-type SCC and VMA-type SCC,

respectively (Bonen and Shah 2005), while combination-type SCC mixes exhibit elements of both (Shindoh and Matsouka 2003).

Even for a VMA-type SCC, the mix design generally requires a higher content of fine particles than the conventional concrete to increase flowability and to avoid segregation and bleeding. Materials are often used that have a low specific gravity such as: ground granulated blast furnace slag (GGBFS); pozzolans such as fly ash and silica fume; and filler materials. In particular, slag can be added to a mix as a supplementary cementitious material, and silica fume or fly ash can be added as pozzolanic materials. Since supplementary cementitious materials will hydrate on their own in the presence of water, while hydration of pozzolanic materials is a secondary reaction which normally occurs only after the hydration of PC, it has been seen that the use of some types of fly ash, particularly Type F Fly Ash, will lead to a significantly slower rate of SCC strength development when compared to supplementary cementitious materials, such as slag (Slag Cement Association 2002). Therefore, not only should the ultimate desired strength be considered when determining the proportions of powder materials, but also the rate at which that strength needs to be attained.

Altering the types of coarse and fine aggregates used for an SCC mix will have a significant effect on the performance of the SCC in the fresh state as well as when hardened. The geometry of the particles will undoubtedly affect the properties of the fresh mix; in general, rounded aggregates, such as river gravel, would encounter less inter-particle friction than more angular aggregates, such as crushed limestone, so an SCC mix using rounded aggregates should theoretically exhibit better passing ability than a similar mix using aggregates with sharp, jagged surface contours (Kasemsamrarn and Tangtermsirikul 2005).

The size and packing ability of the aggregates will have an effect on the properties of the SCC mix. Using different blends of the same types of aggregate would generally increase the packing ability

of the aggregates, which is beneficial for decreasing HRWRA demand. The flowability, passing ability and segregation resistance of SCC improve with a decrease in the maximum size of coarse aggregate (Koehler and Fowler 2007). Khaleel et al. observed that the compressive and tensile strengths, and stiffness of SCC with a maximum aggregate size of 3/8" was seen to be better than that with 3/4" (Khaleel, Al-Mishhadani and Abdul Razak 2011). However, ACI notes that using fewer large aggregates or a smaller aggregate size can negatively impact the viscoelastic properties of the SCC, so they recommend using the greatest volume and largest coarse aggregate possible while still providing good stability, filling ability, and passing ability of the fresh SCC (ACI Committee 237 2007).

The use of most admixtures, such as air entraining agents and set retarders, for SCC is similar to that of traditional concrete. However, instead of traditional water reducing admixtures, High-Range Water Reducing (HRWR) admixtures are typically used, which allow the cement paste to maintain a higher viscosity than lower-lever water reducers when used to a concentration that the concrete is in a flowable state. Viscosity Modifying Admixtures (VMA) may also be added in the case that more stability is needed in an SCC mix.

The overall texture of a SCC mix will be dramatically altered due to the inclusion of the admixtures. For instance, the addition of large quantities of viscosity modifying admixtures (VMA) to a mix reduces the risk of segregation, but the SCC would then be more likely to exhibit thixotropic effects in which the concrete would show fluid behavior when agitated but would return to a semi-solid state at rest (BIMB, CEMBUREAU, ERMCO, EFCA and EFNARC 2005). This would be beneficial in cases where it is desirable to reduce pressure on the formwork, but the mix would become more susceptible to stoppages or delays between successive lifts during construction.

2.4 SCC for Cast-In-Place Caissons

In the presence of groundwater, the concrete for cast-in-place caissons is oftentimes placed using a tremie pipe that will allow the filling of the wet hole by starting at the bottom. With the orifice of the tremie pipe end remaining below the surface of the concrete and water interface as the pipe is gradually raised (see Figure 2-5) until a point at which all water is removed from the shaft and only clean concrete remains. This process minimizes the mixing of water and concrete during placement and reduces the risk of inclusions in the final structure.

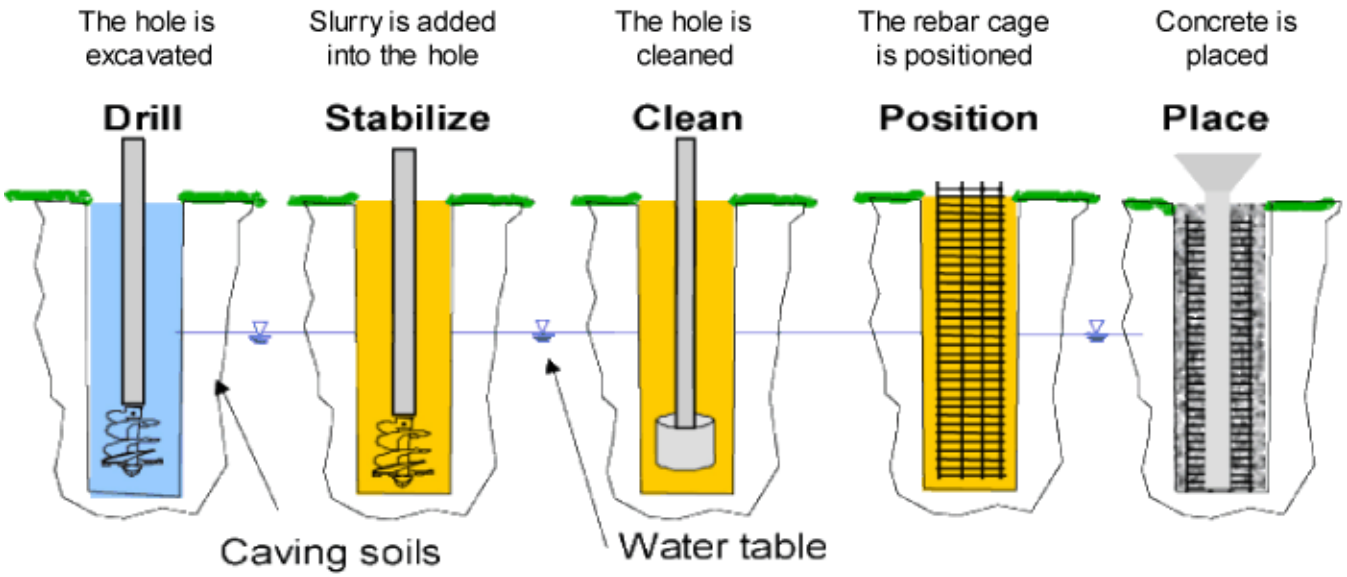

Figure 2-5 Schematic of filling procedure for drilled shaft construction (Florida Department of Transportation n.d.).

In listing some of the more common problems that arise when going through this procedure, Dan Brown lists the following considerations that are often overlooked on the project in the cases of failure:

- "Workability of concrete for the duration of the pour
- Compatibility of congested rebar and concrete
- Control the stability of the hole during excavation and concrete placement, especially with the use of casing
- Drilling fluid which avoids contamination of the bond between the concrete and bearing material or excessive suspended sediment (Brown 2004)."

Of particular importance with regard to using SCC for this type of application are the duration of workability of the concrete and the compatibility of the congested rebar and concrete. Since SCC starts out as a very fluid mixture, the initial workability of the mix should not be an issue; however, if the mix loses workability too rapidly, the concrete in the casing that stabilizes the soil could neck when removing the casing. At a minimum, this situation would make it very difficult to remove the casing. Also, if the aggregate size is too large for the rebar spacing of the rebar cage, the aggregates may have difficulty in passing through the cage; this could lead to large voids around the outside of the cage that could compromise the integrity of the shaft.

2.4.1 Batching and Transportation

For cast-in-place members, considerations need to be made for batching and transportation of SCC that may not be necessary for TVC. For instance, many SCC mixes utilize polycarboxylate HRWRAs that develop workability more slowly than typical HRWRAs. Literature from Grace Admixtures warns that rapid mixing of SCC with this type of admixture can lead to poor reproducibility and induce excess foaming. Instead of a rapidly rotating drum, a normal truck mixer can mix at half speed to induce more of a "folding" motion in the SCC as opposed to a "slapping" motion (Grace Construction Products 2005).

The volume of SCC that one is able to safely transport with a typical truck mixer must also be considered for cast-in-place applications. ACI 237-07 also warns that the fluidity of SCC warrants a limit of transporting no more than 80% of the drum capacity (ACI Committee 237 2007) to prevent spillage.

Transportation time can become an issue with SCC, as well, since the effects of the admixtures are time-dependent. Furthermore, Ghafoori and Diawara warn that extreme temperatures can adversely affect the fresh properties of concrete by accelerating or retarding the rate of hydration and the rate of

moisture loss. In a study simulating various hauling times under extreme temperatures, they noted a loss in slump flow of up to 45% when considering exposure to a 109°F ambient temperature for 80 minutes, as compared to a 70°F ambient condition for the same amount of time. On the other hand, the slump flow when exposed to 31°F ambient temperatures for 80 minutes was 10% higher when compared to the 70°F baseline mix (Ghafoori and Diawara 2010).

2.4.2 Existing Guidelines for SCC in Cast-In-Place Applications

At the time of this study, the WVDOH Standard Specifications for use of traditional concrete in cast-in-place caisson construction included Sections 601 and 625 of the Standard Specifications, and Materials Procedure MP711.03.23. Section 601 prescribes mix proportion, batching and delivery, site acceptance, and placement requirements for traditional cast-in-place concrete. Section 625 gives guidelines that are specific to the construction of drilled caisson foundations. Section 601 refers to Section 703 for specification of chemical admixtures to be used in concrete, which is significant because the existing Section 703 does not address the use of VMAs that are oftentimes used in SCC. Materials Procedure MP711.03.23 provides guidelines for mix qualification of concrete.

The general procedure followed by the contractor for a caisson concrete used in a WVDOT project would be to: (1) develop a mix that satisfies the material requirements of Section 601 [and 703], as well as the strength requirements of 601 or more stringent project requirements, (2) test the mix in accordance with MP711.03.23 and submit results to the Department for approval, and (3) use for construction of the caissons in accordance with Sections 601 and 625. Section 601 requires that Step 2 is conducted by a Division approved laboratory (West Virginia Department of Transportation 2000).

Beyond what was prescribed for use of traditional caisson concrete, some agencies did include provisions for cast-in-place SCC at the time of this project. Utah (UDOT) (Utah Department of Transportation 2008), Illinois (IDOT) (Illinois Department of Transportation 2007), and Rhode Island

(RIDOT) (Rhode Island Department of Transportation 2006) had some sort of provisions for cast-in-place SCC, while New Jersey (NJDOT) (NJDOT 2007) had specifications expressly for the use of SCC for drilled shaft applications. Moreover, Hodgson et al. had recently conducted research that had concluded with the successful implementation of SCC for a drilled shaft application in South Carolina (Hodgson, et al. 2005).

All state regulations listed included some sort of material requirements for cast-in-place SCC. For instance, UDOT dictated a maximum pozzolan content (<30%), maximum nominal aggregate size, which varies by application, a particular aggregate gradation for SCC, and a maximum *w/cm*, which also varies by application. IDOT regulated coarse aggregate types, and the maximum ratio of fine aggregates to total aggregates, *FA/TA*, to below 50%.

Not surprisingly, states generally required a trial batch to demonstrate adequate performance of an SCC mix design as part of the pre-qualification process. Timing of the trial batch varied from 21 days prior to use (IDOT) to 60 days prior to use (NJDOT). Fresh properties requirements typically included measurement of air content, slump-flow, T_{50} time, J-Ring value, VSI, and sometimes included L-box, Segregation Column, and pumpability. NJDOT had an additional requirement that the fresh properties are measured with time to ensure adequate workability of caisson SCC for at least 2½ hours after batching. In all cases, the trial batch was required to meet compressive strength requirements, and NJDOT also requires performance of Hardened VSI assessment.

Acceptance criteria of SCC delivered to the job site generally required similar tests from state-to-state, but at different frequencies. For instance, IDOT required slump-flow, VSI, and J-Ring or L-Box to be performed on the first two trucks and every 50 yd^3 thereafter; hardened VSI was required for first truck of SCC and every 300 yd^3 thereafter. NJDOT required measurement of slump-flow, VSI, air

content and compressive strength at a rate of 3 times per Lot, with hardened VSI performed at least once per day.

2.5 SCC for Precast/Prestressed Box Beams

2.5.1 Considerations for SCC in Precast/Prestressed Applications

Since it is most cost effective to remove precast/prestressed beams from the casting beds as quickly as possible, the time at which concrete reaches the minimum strength requirement for detensioning is critical for beam manufacturers. Without careful mix design, the nature of SCC mixes could take longer than necessary to develop the desired strength, though. NCHRP Report 628 indicated that an increase in binder content of SCC, while leading to a higher 56-day compressive strength, could lower the 18-hour modulus of elasticity and the 7-day flexural strength. This report also observed that highly-fluid SCC (defined as having a 28 to 30 inch spread) has been seen to develop lower compressive strengths at 18 hours of steam curing and lower 18-hour modulus of elasticity than similar concrete having a low slump-flow and a lower dosage of HRWRA (Khayat and Mitchell 2009).

Aside from obtaining the adequate strength to release prestressing forces, concrete properties will affect the beam strength and deflection characteristics. The initial camber and short-term losses of prestress forces in a prestressed beam are heavily dependent upon the elastic properties of the concrete [particularly the initial modulus of elasticity] at the time of prestress release. Likewise, the creep, shrinkage and the eventual stiffness of the concrete will affect the long-term camber, deflections and loss of prestress forces after transfer (Precast/Prestressed Concrete Institute 1999) (Precast/Prestressed Concrete Institute 2003).

PCI Interim Guidelines warn that although modulus of elasticity values of traditional concrete and SCC are sometimes similar, for some SCC mixes the modulus of elasticity may be only 80 percent

of that for normal high-performance concrete. Furthermore, they also note that (1) the creep potential of SCC is higher than that of conventional concrete made with the same raw materials and the same 28-day strength, and (2) shrinkage potential increases as the paste content of a mix increases, so shrinkage strains could be higher for many SCC mixes (Precast/Prestressed Concrete Institute 2003). The respective creep and drying shrinkage of SCC mixes observed in NCHRP Report 628, which investigated the use of SCC specifically for precast/prestressed purposes, were 10% to 20% higher and 5% to 30% higher when compared to high-performance concrete (HPC) mixes made with similar water-to-cementitious material ratios. Drying shrinkage strains observed in the NCHRP project ranged from 500 to 1000 με after 300 days (Khayat and Mitchell 2009).

Also of importance when utilizing SCC for precast/prestressed applications is the bond that develops between the SCC and the prestressing strands. If this bond is not sufficient, the beam could experience reduced stiffness and the lower capacity due to longer bond development lengths in the member. In the studies investigated by Damone, there was not a significant difference in the concrete-strand bond when considering SCC in comparison to TVC (Damone 2007). These sentiments were echoed by Staton et al., who saw transfer lengths in concrete cast with SCC that were statistically equal to those when cast with a high-strength concrete mix. The researchers did, however, observe a slight reduction in the transfer lengths for SCC mixes that utilized VMA (Staton, et al. 2009).

2.5.2 Analysis of Prestressed Beam Behavior

Common analysis methods for predicting the load and deflection behavior of prestressed concrete beams in flexure are detailed in the design guidelines of the American Concrete Institute (ACI) as well as those of the Precast/Prestressed Concrete Institute (PCI). Another traditional analysis method for predicting the load-deflection behavior behavior of PC beams is a moment-curvature analysis, as outlined originally by Burns (Burns 1964).

Traditional analyses of prestressed members involve some basic assumptions with regard to the beam behavior. The first is that concrete strains vary linearly over the depth of the section when under loading, as depicted in Figure 2-7(a). Also, it is assumed that a perfect bond exists between the concrete and the prestressing strands, as well as between the concrete and any non-prestressed reinforcement in the section. Due to the initial elongation of the pre-tensioned strands, the strands and the concrete would have initial deformations as illustrated schematically in Figure 2-6(a) and (b), whereas any non-prestressed reinforcement is assumed to have a deformation equivalent to that derived for the concrete at the same depth.

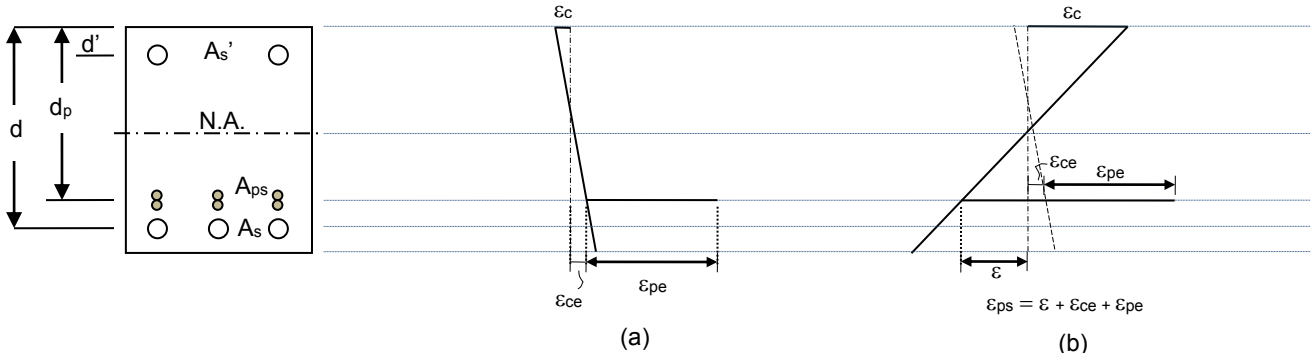

Figure 2-6 Sectional response of a rectangular prestressed beam section (a) under self-weight, and (b) under external loading. [Adapted from (Burns 1964)].

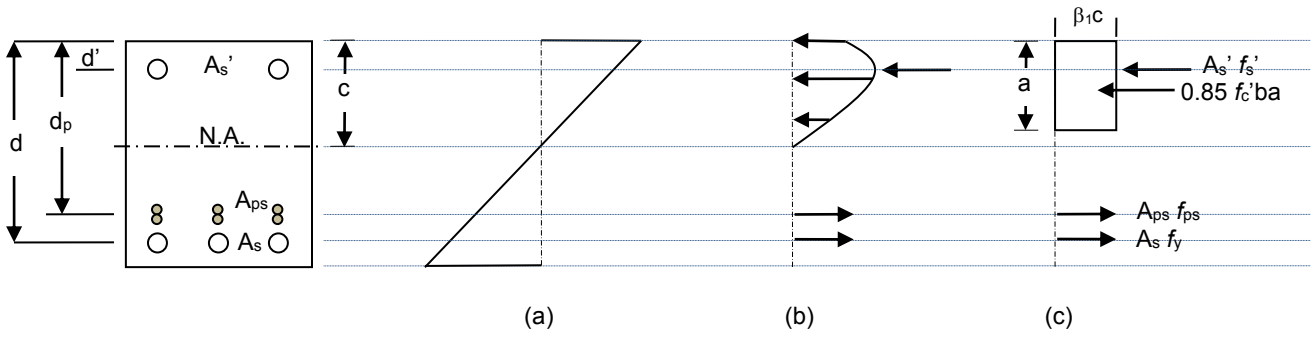

Figure 2-7 Flexural resistance of rectangular prestressed beam section at ultimate stage: (a) strain profile, (b) theoretical stress distribution, and (c) simplified stress distribution using rectangular stress block.

Due to the philosophical and procedural similarities of the ACI and PCI methods of analysis, these will be discussed concurrently in the next sub-section; a brief introduction to the moment-curvature analysis technique will follow. A depiction of the section geometry and member strains of a beam section when subjected to various loads in schematically shown in Figure 2-6.

2.5.2.1 ACI and PCI Equations for Analysis

Both the ACI and PCI methods base the calculation of the nominal flexural resistance of a PC beam on Whitney's simplification of the compressive component into an equivalent rectangular block, which is shown in Figure 2-7(c).

PCI gives the following design equations for strength at cracking and at the ultimate stage (Precast/Prestressed Concrete Institute 1999):

Cracking Moment: $$M_{cr} = (f'_r * S_2) + P_e * \left(r^2/c_2 + e\right) \quad (2)$$

Nominal Moment: $$M_n = A_p * f_{ps} * \left(d_p - a/2\right) \quad (3)$$

From basic structural analysis, the theoretical deflection at "x" due to a point load, P, acting at a point of distance "a" along a simply-supported beam along a span, L, is given by the relationship:

Deflection at x: $$\Delta = \frac{P\,a\,(L-x)}{6\,E\,I\,L}\,(x^2 + a^2 - 2Lx) \quad (4)$$

To determine the maximum deflection at cracking, Δ_g, we can use loading values for P_L based on M_{cr} and the gross section moment of inertia, I_g. To find the mid-span deflection of the beam at the ultimate stage, we can assume a bi-linear deflection behavior per PCI:

Deflection at Failure: $$\Delta_{TOT} = \Delta_{cr} + \Delta_g \quad (5)$$

The contribution of the deflection that occurs beyond Δ_g must consider the cracked moment of inertia for the section. PCI gives this relationship for the cracked section when using the bi-linear deflection analysis:

$$I_{cr} = n \cdot \rho_p \cdot \left(1 - 1.6\sqrt{n \cdot \rho_p}\right) \cdot b \cdot {d_p}^3 \quad (6)$$

2.5.2.2 Moment-Curvature Analysis

A moment-curvature analysis, as outlined by Burns, is typically more precise than the ACI or PCI calculations since it takes into account the non-linear stress-strain relationship of the concrete, whereas PCI calculations use a constant value for concrete stiffness. The primary objective of this type of analysis is to create the moment-curvature relationship for the beam cross-section. Using the established sectional response, a more precise load-deflection relationship for the member can be created using the following relationship between deflection, Δ, and curvature, φ:

$$\Delta_{AB} = \int_A^B x\varphi \, dx \quad (7)$$

The moment-curvature method considers that the initial strain of the tendons is greater than that of the surrounding concrete, due to the pretensioning of the strands. However, strain compatibility is maintained beyond the initial state, with subsequent changes in the strand strains and the surrounding concrete strains being equal. For all calculations, it is assumed that the strain variation along the depth of the cross section is linear.

The moment-curvature analysis of a prestressed beam prior to cracking is performed by first prescribing a loading that would result in a nominal stress or strain state at a particular location in the section (e.g. the loading that would result in zero strain in the concrete at the locations of the strands). Then, the forces in the prestressing strands are adjusted to account for the change in loading. Next, the stresses resulting from the prestressing effect and loading are calculated using the adjusted prestressing forces. Finally, the section stresses are converted to resulting strains based on the non-linear stress-strain behaviors of the concrete and steel. The relationship between strain and curvature is illustrated in Figure 2-6. The analysis remains valid for the prescribed state so long as none of the resulting concrete

stresses exceed the modulus of rupture for the concrete, as this would require the cracked section analysis that will follow (Burns 1964).

The cracked section analysis is an iterative process that requires balancing the internal compressive and tensile forces, as shown in Figure 2-7(b), when assuming a maximum compressive strain of concrete. The following process is used for establishing the moment-curvature relationship of the section for loads that exceed cracking:

1. Prescribe the concrete strain of the top fiber.
2. Assume a depth to the neutral axis, *c*.
3. Compute internal forces based on strain compatibility and the measured or assumed stress-strain relationships of the concrete and prestressing strands.
4. Check to see if the internal compressive force from concrete, C, equals the sum of the tensile forces from all strands, T, based on the assumed value of *c*.
5. If C ≠ T, revise assumption of *c* and return to Step 3.
6. Once equilibrium is satisfied, use the final value of *c* to find the curvature, φ, and the corresponding moment.

2.5.2.3 Decompression Loading

The loading at which the concrete stress in the bottom fibers of the beam (σ_2) go from a state of compression to a state of tension is the so-called decompression loading. This loading is valuable to the analysis of the beam because it can be used to approximate the effective prestressing force in the strands, P_e, using the relationship:

$$\sigma_2 = \frac{P_e}{A_c}\left(1 + \frac{e * c_2}{r^2}\right) + \frac{(M_0 + M_D + M_L)}{S_2} = 0 \quad \textbf{(8)}$$

where e, c_2, r, A_c and S_2 are section properties, and M_O, M_D and M_L are indicative of the non-factored load state of the beam.

2.5.2.4 Camber of Precast/Prestressed Beam

Brewe and Myers outlined methodology for determining the initial and long-term cambers of prestressed SCC girders (Brewe and Myers 2010). In this model, the initial beam camber can be derived from the camber due to prestressing, Δ_{ps}, and the deflection due to dead load, Δ_d. For the long-term camber, adjustments are made to the short term to account for the loss of prestress, Δ_{loss}, and the camber due to creep, Δ_{cr}.

The initial camber is calculated using the modulus of elasticity of the concrete at the time of release, and the transformed section properties at the time of release, whereas the long-term adjustments are calculated using the long-term modulus of elasticity of concrete and long-term section properties.

The upward camber from prestressing forces can be calculated as:

$$\Delta_{ps} = \frac{A_{ps} f_{pt} e L^2}{8 E_{ci} I_{tr}} \quad \textbf{(9)}$$

where f_{pt} is the stress in the prestressing strands immediately after transfer, and I_{tr} is the transformed-section moment of inertia of the beam upon release. The other component of the initial camber is the downward deflection from dead load, which is calculated as:

$$\Delta_{di} = \frac{5 M_d L^2}{48 E_{ci} I_{tr}} \quad \textbf{(10)}$$

where M_d is the moment due to self-weight.

Adjustments for the long-term camber occur from the prestress losses, which are calculated using the relationship:

$$\Delta_{loss} = \frac{A_{ps} \Delta f_{pLT} e L^2}{8 E_c I_t} \quad \textbf{(11)}$$

where Δf_{pLT} represents the long-term prestress losses, and I_t is the transformed-section moment of inertia based on long-term behavior.

The final component of the long-term camber is the upward camber resulting from the creep of concrete. This can be taken as the creep coefficient of the concrete times the initial camber of the beam, or:

$$\Delta_{cr} = (\Delta_{ps} - \Delta_d)\psi_b \quad \textbf{(12)}$$

where ψ_b is the creep coefficient of the concrete at the appropriate age, and Δ_d is the dead-load contribution calculated using the long-term values E_c and I_t.

2.5.3 Guidelines for SCC in Precast/Prestressed Applications

The existing WVDOH Standard Specifications at the time of this study included Section 603, which prescribes most facets of mix design, placement and fabrication of prestressed/precast concrete members using traditional vibrated concrete. Similar to the cast-in-place concrete specifications, the material requirements in Section 603 refer to Section 703 for specification of chemical admixtures to be used in concrete, which is significant because the existing Section 703 does not address the use of VMAs that are oftentimes used in SCC. Unlike the specifications for cast-in-place concrete, though, Section 603 does not directly reference Materials Procedure MP711.03.23 for mix qualification of prestressed concrete, and essentially defers to ACI 318 procedures for mix design and testing.

The general procedure followed by the contractor for gaining approval of a prestressed concrete mix to be used in a WVDOT project would be to: (1) develop a mix in accordance with ACI 318 that satisfies the material requirements of Section 603 [and 703], as well as the strength requirements given in the project documents, (2) report strength achieved from a newly-tested batch, or from historical data, to the Department for approval, and (3) use for fabrication of the prestressed beams in accordance with Section 603 (West Virginia Department of Transportation 2000). Section 603 specifies that either an independent laboratory or PCI certified plant personnel should execute Steps 1 and 2 of this process.

As was the case with SCC for caisson concrete, at the onset of this study some agencies included provisions for use of SCC for precast and/or prestressed concrete applications. New Jersey Department of Transportation (NJDOT 2007) had specifications for use of precast SCC, Florida Department of Transportation (FDOT 2005) had specifications in place for precast/prestressed SCC, PCI had interim guidelines for the use of SCC (Precast/Prestressed Concrete Institute 2003), and foreign guidelines existed in Europe (BIMB, CEMBUREAU, ERMCO, EFCA and EFNARC 2005). Furthermore, a research study in North Carolina had outlined Special Provisions used for prestressed SCC projects in Maine, North Carolina and Virginia (Zia, Nunez and Mata 2005).

Since it applied to numerous applications, PCI Interim Guidelines gave a thorough description of many of the factors of importance when utilizing an SCC mix for precast/non-prestressed, precast/prestressed, or architectural applications (Precast/Prestressed Concrete Institute 2003). These Guidelines included considerations for mix design, fresh properties, testing, and quality control of SCC for these applications. However, since these were meant to act as a guideline instead of hard-line specifications, much was left up to the user's discretion in terms of specifics for SCC mix design, required fresh properties, and mix qualification. The document does include a number of design guidelines that give the reader a good understanding of how certain fresh properties could affect the placement of SCC [e.g. an SCC with a spread in the range of 22" to 26" would likely be good for applications with "low" or "medium" element shape intricacy, but problems could arise with high element shape intricacy]. Guidelines were also given for the required air content of SCC in relationship to maximum aggregate size and severity of freeze-thaw exposure.

Similar to the PCI Interim Guidelines, the European Guidelines for SCC provided a good basis for assessing the important factors for use of SCC, however they did not provide many definitive paradigms for its utilization. The European Guidelines provided recommendations for mix design and

desirable workability characteristics, as well as explanations of the types of tests that can be used for assessment. They also recommended conducting trial castings prior to any use of SCC in the field.

New Jersey DOT specifications required the use of a Type F or a combination of Type F and VMA when using SCC for precast applications, but the only other mix design requirement specific to SCC was that the FA/TA was to be below 0.5, by mass. The specifications did require a mix qualification to be done, with results submitted at least 45 days prior to use; for this qualification batch, the air content of the SCC was to be within the top half of the allowable range, as was the slump-flow (26 in. to 28 in.). The acceptable slump flow range during production when using prestressed SCC was specified as 24 in. to 28 in. The NJDOT specifications also required hardened VSI testing to be done during the qualification, as well as at least once per day during production.

FDOT specifications require a laboratory trial batch, followed by a field demonstration of the use of SCC prior to submittal for use on precast/prestressed projects. Material requirements detailed include a maximum FA/TA of 0.5, with a VMA required if FA/TA is less than 0.45, and a 20% increase in the permissible amount of cement content over that for traditional concrete. Fresh properties include a maximum target spread of 25 in., a maximum passing ability (J-Ring Value) of 2.0 in., and a static segregation of less than 15%. The mock up, or field demonstration, is to include the production and placement of at least 9.0 yd^3 of SCC, along with determination of the workable period as well as later assessment of the aggregate distribution within the mockup products. Some vibration of SCC is permitted under FDOT specifications if delays occur or if it is determined that minimal vibration leads to better consolidation.

Special Provisions that have been used by Maine, North Carolina and Virginia for precast/prestressed SCC, as described by Zia et al (Zia, Nunez and Mata 2005), are highlighted in Table 2-2 Test Requirements detailed in Special Provisions for use of prestressed SCC. [Zia et. al, 2005] and

Table 2-3. As can be seen, Virginia generally has the most stringent requirements, with a slightly lower allowable spread, inclusion of required permeability tests, and the most prescriptive placement requirements. Since North Carolina and Virginia may not have as heavy of exposure to freeze-thaw cycles as does Maine, the only appearance of freeze-thaw test requirements was in the Maine Special Provisions. It is also noteworthy that Virginia did not allow any vibration whatsoever under their Special Provisions, while the Maine and North Carolina allowed exceptions to be made under the discretion of the Engineer.

Table 2-2 Test Requirements detailed in Special Provisions for use of prestressed SCC. [Zia et. al, 2005]

States	Maine	North Carolina	Virginia
Test Requirements			
Slump Flow Test	24 to 32 in.	24 to 30 in.	23 to 28 in.
Visual Stability Index (VSI)	1 as Max.	Report	Unspecified
J-Ring Test Value	Not Required	< 0.5 in.	< 0.5 in.
L-Box Test (H2/H1)	Not Required	0.8 to 1.0	Not Required
Shrinkage Test	Not Required	Max. 0.04% at 28 days	Max. 0.04% at 28 days
Permeability Test	Not Required	Not Required	Max. 1500 coulombs at 28 days
Freeze-thaw Test	Max. 3% mass loss or 20% change in E (dynamic)	Not Required	Not Required
Hardened Air Void Analysis	Required	Not Required	Not Required

Table 2-3 Placement Requirements detailed in Special Provisions for use of prestressed SCC. [Zia et. al, 2005]

States	Maine	North Carolina	Virginia
Placement Requirements			
Location of Placement	Unspecified	Unspecified	Placed from one side to other or pumped from bottom upward
Placement between lifts	Unspecified	Unspecified	Concrete not allowed to lose flow and unable to combine with next lift
Vibration	External vibrator allowed with delay in lifts and loss of slump	Not allowed without Engineer's permission	Not permitted
Finish	Unspecified	Unspecified	Smooth finish without holes larger than 3/8"

Chapter 3

3 Cast-In-Place Caissons

The caissons for the Stalnaker Run Bridge were designed to consist of a 1.1-m (3.5 ft) diameter, 1.8-m (6 ft) deep drilled shaft overlying an integral 0.9-m (3ft) diameter, 3.7-m (12 ft) deep rock socket, as shown in Figure 3-1. The breastwall of each abutment is supported by three caissons, as shown in Figure 3-2. The reinforcing cage for the caissons was comprised of 20 No. 11 longitudinal reinforcing bars that were confined using No. 4 hoops with outer radii of 76 cm (2.5 ft) and at a typical spacing of 15 cm (6 in.). In the original design, the longitudinal reinforcing bars were evenly spaced, leaving approximately 4.5 cm (1.8 in.) clear spacing between bars, but then, in order to satisfy AASHTO design guidelines for rebar spacing, was re-designed to include 2-bar bundles, increasing the clear spacing to approximately 9 cm (3.5 in.), as shown in Figure 3-1.

As mentioned previously, it was decided to use SCC for the caissons underlying one of the two abutments (Abutment 1), while using a traditional concrete mix for those of the other (Abutment 2). Figure 3-2 depicts the plan view of the bridge abutments, and also indicates which three caissons were constructed using SCC. Due to the proximity to the stream, and based on the water tables indicated on boring logs provided with the construction plans, it was assumed that the drilled holes for the caissons would fill with water at a rate sufficient to warrant casting in "wet hole" conditions, as defined by Section 625 of the WVDOT Standard Specifications (West Virginia Department of Transportation 2000), and consequently that construction of all caissons would utilize tremie placement techniques.

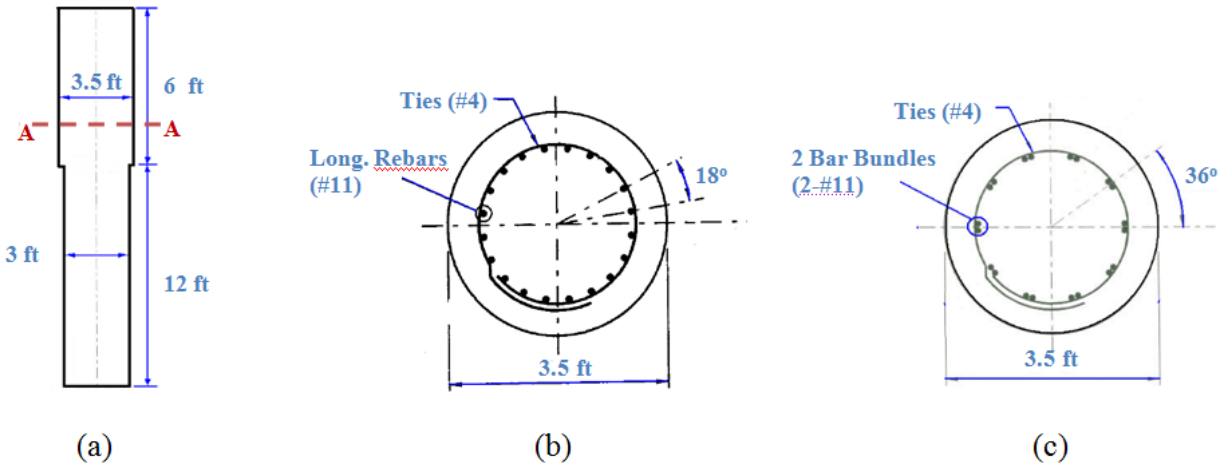

Figure 3-1 Schematic of caissons, elevation view. (b) Original and (c) Revised longitudinal reinforcement configurations, Section A-A.

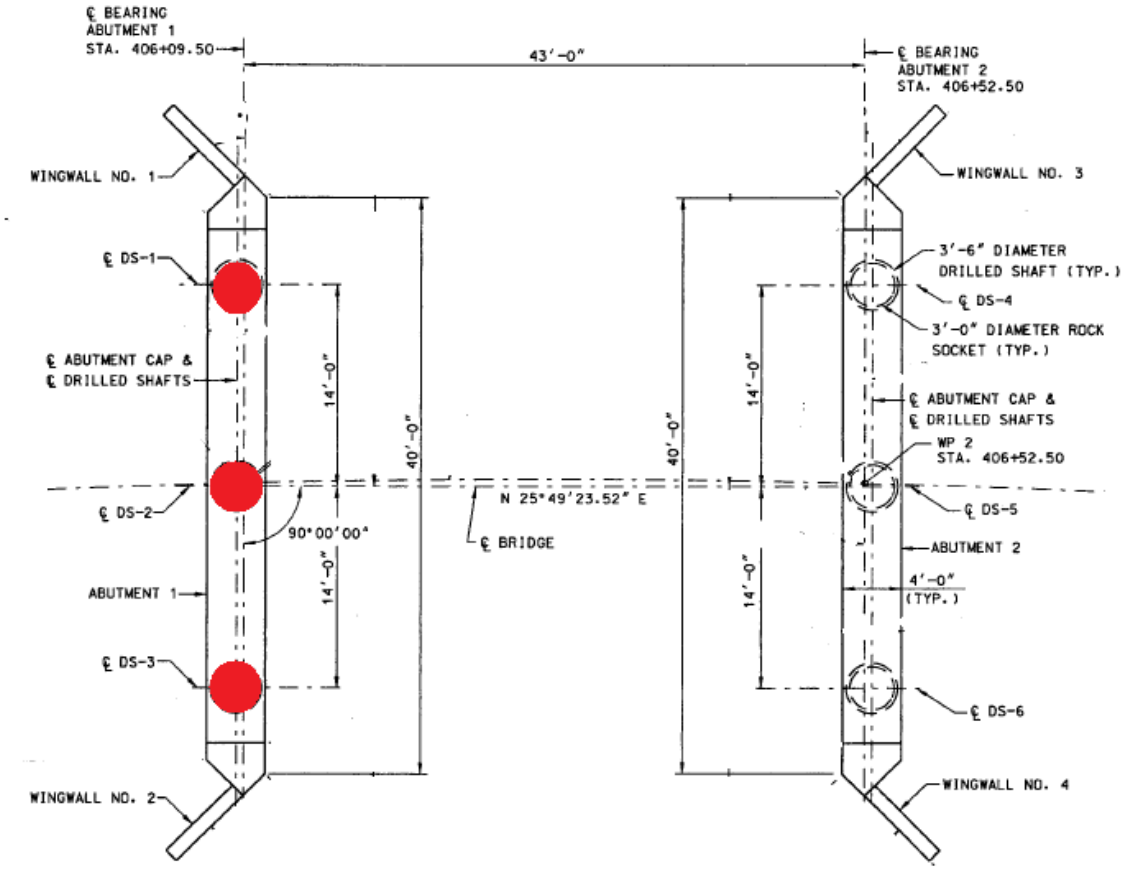

Figure 3-2 Plan view of Stalnaker Run replacement abutments, from construction plans. Shaded areas indicate caissons constructed using SCC.

3.1 Research Approach for Cast-In-Place Caisson SCC

To implement SCC for the cast-in-place caissons of the Stalnaker Run Bridge Replacement, the researchers' experiences with SCC along with the pertinent information presented in Chapter 2 was used to devise a research plan. Special Provisions were necessary to communicate the material, testing and performance requirements of the caisson SCC to the contractors and WVDOT officials. Researchers did provide assistance in development and testing of the caisson SCC, but the contractor was ultimately responsible for submission of the mix design and testing information to WVDOT for final mix design approval prior to use on the bridge.

A test apparatus for conducting a casting of a mock-up caisson section was developed for this process. Initially, the trial caisson casting was devised with the intention of assuring that SCC created by the project Special Provisions would perform satisfactorily in this simulated environment and give the option to modify the provisions should it not. However, due to delays in obtaining a suitable SCC mix from the supplier, combined with a tight construction timeline, this test was conducted at a point after finalization of the Special Provisions. Ultimately, while the trial caisson did not provide an opportunity to modify the Special Provisions, it did give researchers and Engineers an opportunity to assess the hardened properties and filling ability of the caisson SCC and make any necessary changes prior to construction.

Just prior to caisson casting, the rebar cages of the caissons were mounted with temperature sensors and strain gages for data collection efforts, as were ducts for non-destructive testing. Additionally, at the time of caisson construction, samples were collected for later assessment of the hardened properties of the caisson SCC, as well as those of the traditional caisson concrete. The hardened property testing was done to ensure that concrete of adequate quality was used for construction, while the non-destructive testing was done to verify uniformity of the concrete as placed.

3.2 Special Provisions for C-I-P SCC (SCC-1)

It was necessary to write Special Provisions that could be inserted into the project documents in order to communicate the requirements for caisson SCC to contractors, field engineers and Division personnel. These included adaptations to current WVDOT construction practices [particularly WVDOT Standard Specifications Sections 601, 625, and 703; and WVDOT Materials Procedure MP 711.03.23], as well as prescription of new testing to be done in order to ensure satisfactory behavior of the caisson SCC, particularly in the fresh state; these appeared in the project documents in the form of Special Provisions as well as addendums to the General Notes for the project. Efforts were made to write these in such a manner that would promote equal opportunity for all potential concrete suppliers to bid on this project.

For the sake of clarity, the SCC mix design for the caisson portion of the Stalnaker Run Project was deemed SCC-1 in the project documents, while the SCC mix design for the beams was deemed SCC-2. These designations will be conformed to within this chapter as well as throughout the report in its entirety.

The project provisions for SCC-1 were devised based on the researchers' previous laboratory experiences with SCC, other researcher relating to SCC drilled shafts, and recent guidelines for cast-in-place SCC. The main points of the project requirements for SCC-1 will be discussed in this section; guidelines for Class SCC-2 concrete will discussed in Section 4.2. The provisions, as submitted to WVDOT as recommendations for inclusion of SCC as a material for the Stalnaker Run Bridge caisson applications, can be seen in Appendix A.2.

3.2.1 Mix Design Requirements

Any differences in mix components and quantities that result from the use of SCC had to be outlined in the Special Provisions. Since viscosity modifying admixtures (VMAs) are not typically used

for traditional concrete, but were not addressed in the WVDOT Standard Specifications, it was noted in the Special Provisions that use of a VMA for the SCC was permissible so long as appropriate documentation was submitted to the Division; these requirements were written into the addendum for Section 707 of the Standard Specifications.

A summary of material information and mix proportion information for SCC-1 is shown in Table 3-1 and Table 3-2. The maximum size of coarse aggregate was limited to ¾ in., with #67 gradation being permissible provided all aggregate pass the ¾" sieve. Blending of aggregate gradations to increase stability of the mix was permitted to help increase the stability of the SCC mix; although it was required that the aggregate blend contained one gradation that had a maximum aggregate size of ¾ in. Although not depicted on either of these tables, the maximum permissible ratio of fine aggregate to total aggregate, *FA/TA*, for SCC-1 was 0.5. The amount of water was also limited to 4.75 gallons per 94-lb bag of cement, which correlates to a maximum *w/cm*=0.42. The amount of cementitious materials for SCC-1 was to be between 610 lb and 750 lb per cubic yard of concrete.

Table 3-1 Mix requirements for Class SCC-1 concrete used for the Stalnaker Run Bridge Project.

Class of Concrete	Design 28 Day Compressive Strength [psi]	Target Cement Factor [bags / c.y.] *	Maximum Water Content [gal/bag cement] **	Standard Size(s) of Coarse Aggregate*** [Number]	Entrained Air [%]
SCC-1	4500	6.5≤C.F.≤8	4 ¾	67****, 7, 78, 8, 9	**6**

*An equal volume of pozzolanic additive may be substituted for Portland cement up to the maximum amount in In **addition to the material and proportioning requirements shown in these tables, the SCC-1 was to have a target spread of 21 in., and a J-ring value below 1.5 in. in the fresh state, as well as the project-mandated 4,500 psi 28-day compressive strength.**

.

** When using pozzolanic additives, volumes of these materials shall be considered as cement for purposes of establishing maximum water content.

***For SCC-1, blending up to two coarse aggregate types is permitted, but the aggregate blend must contain (at least) one aggregate type that has a maximum aggregate size of ¾ inches.

****Coarse aggregate gradation using #67 aggregates is allowed only if it is graded such that 100% of all aggregates pass through a sieve with ¾-inch nominal opening size. Such a gradation of #67 aggregate will be considered in this provision to have a maximum aggregate size of ¾ inches.

In addition to the material and proportioning requirements shown in these tables, the SCC-1 was to have a target spread of 21 in., and a J-ring value below 1.5 in. in the fresh state, as well as the project-mandated 4,500 psi 28-day compressive strength.

Table 3-2 Upper limits on supplementary cementitious material quantities for Class SCC-1 concrete.

MATERIAL	QUANTITY
Fly Ash	1 Bag (15%)
Ground Granulated Furnace Slag	3 Bags (45%)
Microsilica	1/2 Bag (8%)

3.2.2 Pre-qualification of Mix Design

Like a typical cast-in-place concrete for any WVDOT Division of Highways project, the SCC-1 was subject to approval by the Division prior to use in the field. The testing and submission requirements for trial batches necessary for approval of a mix design are detailed in MP 711.03.23. However, these requirements were refined in light of the different test methods and fresh behaviors of SCC.

The overall process included the creation and testing of two batches of SCC-1. As is typical practice under the MP 711.03.23, each batch was required to meet more stringent fresh property tolerances during the qualification than would be mandated for field acceptance; these included a slump-flow [ASTM C1611] in the upper half of field tolerances [Field: 21 in. ± 2 in., Qualification: 21 in. to 23 in.] and an acceptable air content within a 1% range [6% ± 0.5%]. Other fresh property requirements included a Visual Stability Index (VSI) [ASTM C1611], below 1.0, a T_{50} [ASTM C1611] between 2 sec. and 7 sec., a J-Ring value [ASTM C1621] below 1.0 in., and a static segregation [ASTM C1610] below 12%.

The initial measurement of the fresh SCC-1 properties was to be done at a pre-established time that would correlate to the anticipated time of travel for delivery to the job site. Not only were the fresh properties to be measured at this initial time, but a tentative workable period was to be established for the mix by measuring these properties every 30 minutes afterward until the measured spread fell below 12 in. The workable period would be the time period from the anticipated delivery until the interpolated time at which the spread or j-ring value was tested to be outside of the range of the field acceptance limits [19 in. and 1.5 in., respectively].

Table 3-3 Site acceptance criteria for SCC-1 used for Stalnaker Run Bridge.

Spread ASTM C1611	J-Ring Value ASTM C 1621	V.S.I. ASTM C1611	T_{50} ASTM C1611	Air ASTM C231
53±5 cm (21±2in)	**≤3.8 cm (≤1.5 in)**	**≤1.5**	**2sec≤ T_{50} ≤7sec**	**6%±1.5%**

For each batch, it was also required to perform hardened compressive strength testing on cylinders cast from the SCC-1 at the time of initial testing. Seven specimens were cast from each batch to be tested in compression at the following times: one cylinder at age 24 hours ± 4 hours (the exact age to the nearest hour at time of test shall be noted on the report); one cylinder at age 3 days; one cylinder at age 7 days; one cylinder at age 14 days; and three cylinders at age 28 days. Since no previous data had been collected pertaining to production of SCC-1, the production batch was required to exceed the project specified 28-day compressive strength (4,500 psi) by 1,300 psi; if the 5,800 psi 28-day strength requirement was not met, a re-design of the mix was necessary. For Class SCC-1 Concrete, three additional cylinders were also to be cast for later assessment of the hardened Visual Stability Index. No rodding or vibration was to be done to any of the SCC-1 specimens cast for hardened property assessment.

3.2.3 Acceptance and Placement

The acceptance criteria for SCC-1 delivered for use in the Stalnaker Run Bridge is summarized in Table 3-3. Since it was anticipated that only about one truckload of concrete would be used for each caisson to be constructed, the Special Provisions prescribed fresh property testing of each truckload of SCC-1 upon delivery to the job site.

In addition to the fresh property requirements, three (3) specimens were to be cast from each batch to verify that the 4,500 psi compressive strength requirement is met, and two were to be cast for hardened VSI determination. Again, these were to be cast in a single lift without rodding or tamping.

For the most part, the construction techniques when using the SCC-1 were to be very similar to those for the traditional caisson mix. The biggest difference was that the requirement to vibrate the top portion of the caisson was removed in the case of the SCC-1 construction. Although the use of a tremie pipe during construction was anticipated due to "wet-hole" conditions, this method was specified for the SCC-1 caissons to eliminate any uncertainty about acceptable drop height of the SCC mix. Test holes were originally specified in the provisions to ensure proper construction of the caissons with SCC, however these were later struck in lieu of a smaller laboratory trial, which will be discussed in detail in Section 3.4.

3.3 Caisson Concrete Mix Designs

Due to the location of the bridge, there were only two ready-mix concrete producers that could feasibly supply the concrete for the bridge project: Central Supply and JF Allen/Alcon. At the onset of the project, WVU Researchers worked with both companies and their respective admixture suppliers to develop SCC mix designs that would be suitable for this project. However, once the contracting company for the construction, BILCO Construction Company, had determined that Central would be supplying the concrete for the caissons, efforts were then shifted to finalize their SCC mix design and

perform further testing on the mix. These efforts included: (1) initial development based primarily on strength and spread requirements, (2) refinement in the laboratory and more intensive testing of the fresh and hardened properties, and (3) creation of a full-scale trial batch at the ready-mix plant for final assessment of mixing procedures, admixture quantities, and pumpability of the SCC mix. Based on the findings from this mix development process, a final SCC mix design was determined and tests were conducted in the laboratories of the admixture supplier, and ultimately approved by WVDOT for use on the bridge project. Only results from the final mix design will be discussed in this section.

The mix proportions for the final, approved SCC mix included 750 lb/yd^3 of total cementitious materials, a 15% by weight replacement of cement with Class F Fly Ash, a water-to-cementitious materials ratio (*w/cm*) of 0.38, and a fine aggregate to total aggregate ratio of 0.50. This mix design incorporated a high-range, water reducing (HRWR) admixture, a viscosity modifying admixture (VMA) and an air-entraining agent (AEA). The final, WVDOT-approved 1-yd^3 SCC-1 mix design used for the Stalnaker Run Project can be seen in Table 3-4.

Table 3-4 1-yd^3 theoretical mix designs approved for Stalnaker Run Bridge caisson construction.

Component	Traditional Caisson Mix	SCC-1 Caisson Mix
Type I Cement [a]	564 (334)	638 (378)
Class F Fly Ash [a]	70 (42)	112 (66)
Water [a]	250 (148)	285 (169)
Coarse Aggregate [a]	1743 (1034)	1400 (830)
Fine Aggregate [a]	1220 (723)	1388 (823)
w/cm	0.394	0.381
AEA[b]	2.0 (130.4)	0.35 (22.8)
Type A(D) WRA [b]	6.0 (391.2)	--
Type F HRWRA [b]	--	4.5 (293)
Type S VMA[b]	--	0.75 (49)
Type D Retarder [b]	--	5.0 (326)

[a] lb/yd^3 (kg/m^3)
[b] oz/100 lb cementitious materials (mL/100kg)

A WVDOT "Class B Modified" mix design was used for the traditional caissons. This traditional caisson concrete had the same strength requirements as the SCC, and was designed to have a 7½" (190.5 mm) slump and a target of 7% entrained air. As shown in Table 3-4, this particular mix incorporated 634 lb/yd^3 (376 kg/m^3) of total cementitious materials, an 11% by weight replacement of cement with Class F Fly Ash, a *w/cm* of 0.39, and a fine aggregate to total aggregate ratio of 0.41. This mix incorporated an ASTM C494 Type A and D water reducing admixture (WRA) and an air-entraining agent.

3.4 Laboratory Trial Caisson

To ensure adequate filling of the caissons on site, it was decided to first conduct a trial casting in the laboratory of a member with cross-sectional dimensions similar to those of the actual construction, and in a manner that would most closely simulate the actual field conditions. Site conditions for this particular construction indicated that the field caissons would be cast in the presence of groundwater, so pumping or tremie placement would be necessary by WVDOT standard construction practices (West Virginia Department of Transportation 2000). The desired characteristics of the test apparatus were as follows: (1) same cross-section as the bridge caissons, (2) water-tight, and able to sustain pressures from casting SCC, (3) accessible for concrete sampling at various locations, and (4) reusable and inexpensive.

3.4.1 Trial Caisson Test Concept

Using the original cross section dimensions for the drilled shafts, with a 3.5-ft (1.07 m) diameter, it was determined that a member height of approximately 5 ft (1.52 m) would be sufficient to assess the stability of the SCC. In order to avoid expensive or labor-intensive dissection of a large mass of hardened concrete, it was decided to remove the SCC from the form while still in the fresh state, which would also allow the setup to be reusable. For concrete removal, the outer walls were made to allow

them to open after placement of concrete such that the formwork and the rebar cage could be salvaged prior to the concrete setting.

Sampling would be done prior to opening the formwork walls using an experimental technique, referred to in this report as "fresh coring." To collect the fresh core samples, plastic drain tubes would be inserted into the fresh SCC down from the top of the concrete until they reached the base of the form. The locations of these cores were selected to get representations of the concrete both inside and outside of the rebar cage.

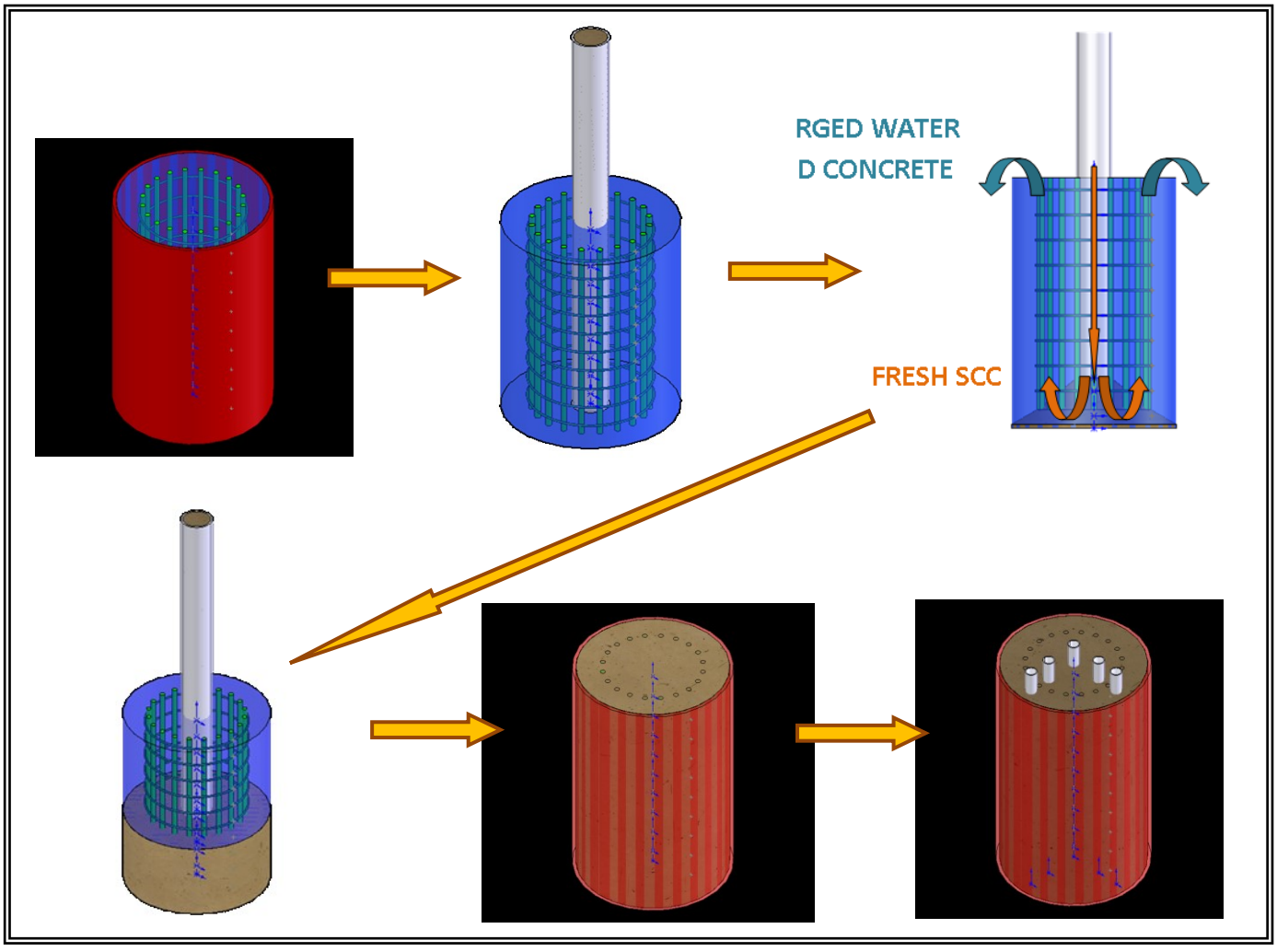

Figure 3-3 Schematic filling procedure for trial caisson testing.

The methodology for this testing is illustrated in Figure 3-3. The steps for filling and sample collection for this test are as follows:

1. The formwork is made to be water-tight, and the rebar cage then lowered into position.
2. The entire apparatus is filled with water.
3. The plugged hose orifice is lowered to the bottom of the apparatus.
4. While leaving the hose orifice near the base, SCC will be fed through the pump to gradually purge water from the apparatus.
5. When all of the water has been purged, additional SCC is added to the point where only non-diluted concrete remains.
6. The pump hose is removed, and any excess SCC is removed from the top of the form using a screed.
7. Fresh cores tubes are inserted at the desired locations by applying slight twisting motion while maintaining a downward pressure.
8. Tops of core tubes are secured while formwork walls are opened.
9. Excess SCC is removed from around the fresh cores, which are then individually collected and capped.
10. The formwork and rebar cage are cleaned for reuse.

Fresh property tests were done prior to filling the formwork, and specimens were collected for testing hardened properties both before and after pumping.

3.4.2 Preliminary Tests

Before casting of the trial caisson, there were two critical elements of the experiment that warranted further investigation. First, it was decided to see the extent to which concrete could be compromised if excessive mixing of concrete and groundwater were to occur. Second, since an experimental process was to be used to sample the SCC in the test caisson while in the fresh state, the feasibility of inserting fresh core tubes into concrete, and the appropriate timing for doing so, were explored.

3.4.2.1 Effects of Mixing with Groundwater

A simple experiment was devised to explore the possible detrimental effects of concrete mixing with ground water, albeit an extreme case. To illustrate this, the 8-bag SCC mix was first created in the laboratory. This was then placed directly into two water-filled 6”x12” cylinder molds until the water was completely replaced with concrete. After curing, the compressive strengths were then compared to cylinders that were cast in the traditional fashion. An image of the cylinder before and after filling, and of the specimen after demolding can be seen in Figure 3-4. Placement of the SCC was done from a height just above the water line as to reduce effects of drop height. Also, the cylinders were overfilled with concrete such that sufficient volume was present upon eventual loss of bleed water; excess concrete was removed using a strike-off bar as part of the finishing process.

Figure 3-4 SCC specimen cast into water-filled cylinder mold.

It can be seen from the specimen shown in Figure 3-4 that this type of casting can have significant aesthetic effects on concrete. Not only were large bleed channels visible in the specimen, but the surface texture is much sandier than a typical specimen, with much of the cementitious materials near these bleed channels being transported away.

The compressive testing of these cylinders was done to quantify the extent to which this affected the hardened properties of the concrete. Both cylinders that were cast into water-filled molds only resisted 16,000 lbs of compressive force when tested at 28 days in accordance with ASTM C39. This would correspond to an f_c' of 566 psi; in contrast, the average 28-day compressive strength obtained when casting compressive cylinders of the same batch of concrete under normal conditions was 5,650 psi. Therefore, it can be seen that in extreme cases of concrete mixing with water, it is feasible that the concrete only obtains a fraction of the strength that it would if under dry conditions.

3.4.2.2 Tube Insertion into SCC for Fresh Coring

To explore the feasibility of the fresh coring procedure at different times, a small batch of SCC-1 was first created in the laboratory. Three 6"x12" cylinders were filled within the first 15 minutes after batching. Then, at three different times [½ hr, 1½ hrs, and 2½ hrs], a length of the 4-inch diameter fresh coring tubes was inserted into a cylinder using a slight twisting motion.

It was seen that tube insertion was feasible at all three times. In all three cases, the depth of concrete inside of the tube was slightly lower than that outside of the tube. This difference was measured to range between $^3/_8$ in. and ½ in., with no correlation between difference and time of insertion.

To further evaluate whether segregation was forced within the specimens, they were allowed to cure for a number of weeks prior to saw cutting to expose the internal aggregate distribution of each. Figure 3-5 shows an image of the aggregate distribution of the saw-cut specimen for which the tube was inserted after 1½ hours. As with all cores, this specimen exhibited a reasonably uniform aggregate distribution with large aggregates on top of the specimen. At all times, there was only a minor disturbance of the aggregates near the boundary of the tube, with a slight reorientation of these boundary aggregates. Upon evaluation of all cores, it was determined that the fresh tube insertion would be a

viable method for sampling of the trial caisson SCC, and for this particular SCC mixture the timing of insertion [within reason] would not have a significant effect on the cores collected.

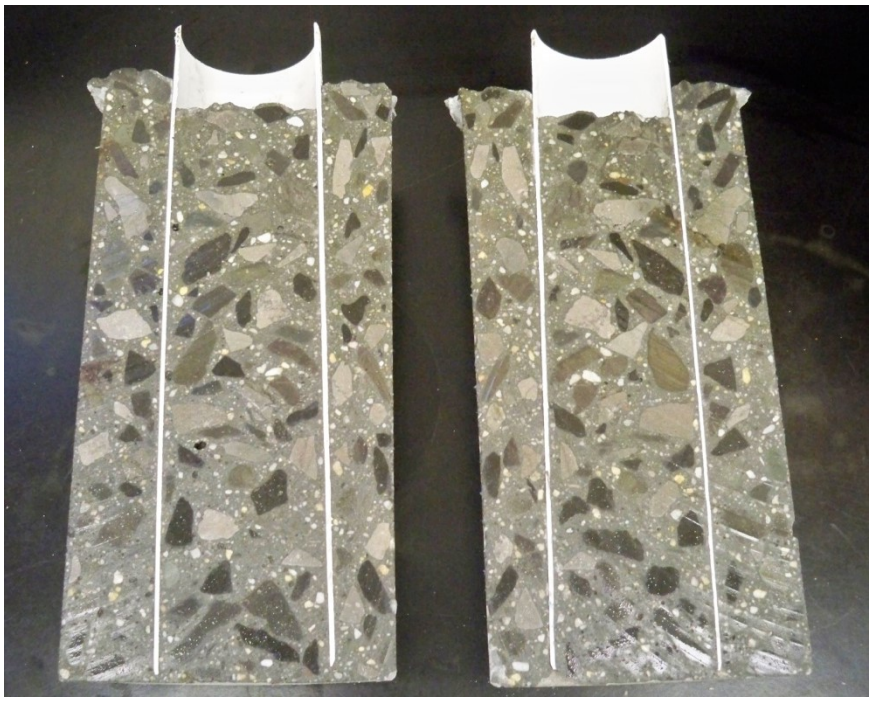

Figure 3-5 Aggregate distribution in 6"x12" cylinder after "fresh core" tube (4”dia.) insertion into 1.5-hour-old SCC.

3.4.3 Apparatus

In order to achieve an inexpensive, yet reusable setup, the 5-foot outer walls of the formwork were constructed out of plastic corrugated culvert pipe. A wooden base was custom made to fit snugly into the bottom of the formwork. A retaining pool was used to collect purged water and purged concrete during casting. A picture of the apparatus in its entirety can be seen in Figure 3-6.

Figure 3-6 Picture of laboratory trial caisson formwork and setup.

(a) **(b)** **(c)**

Figure 3-7 Test caisson apparatus components. (a) Schematic, top view. (b) Hinged rear seam. (c) Front seam with handles, L-brackets bolted together.

To allow the formwork to open, a hinge effect was created on one side by creating a release on the one side of the apparatus by cutting a seam down the height of the pipe, and notching the corrugations on the opposite side of the pipe using a "V" pattern, to allow it to swing open as desired. L-brackets were attached along the length of both sides of the seam, allowing the seam to be clamped or

bolted shut. The modifications to the culvert pipe that allowed for a hinge action are illustrated in Figure 3-7. To seal the apparatus and make it water-tight, a combination of weather sealing strips, silicone caulk, and an asphalt-based roof cement was used around the front seam and the base.

A section of reinforcing cage was fabricated such that the passing ability of the SCC could be assessed. Although the two-bar bundled configuration with the larger spacing (3.5 in.) was to be used on all cages for the actual bridge construction, it was decided to use the single rebar configuration with the smaller spacing (1.8 in.) for the laboratory trial caisson. This was thought to provide a more conservative experiment to account for variability of construction on site, and to possibly illustrate the advantage of SCC in its ability to flow through a more congested space. The size of rebar, and the size and spacing of the hoops remained consistent with the field caisson design. All steel rebar in the cage was coated with a two-part epoxy, which is not specified in the actual bridge design, but included for the trial caisson to prevent rusting of the rebar so it would be reusable. The fully-assembled rebar cage can be seen in Figure 3-8.

The final major element of the apparatus design was the method of sampling the SCC following placement into the formwork. To collect "fresh core" samples, 4-inch (100 mm) diameter SDR35 drain pipes were used to contain the samples. These had slightly sharpened edges on the lower surface to minimize displacement of aggregates during insertion. The tubes were outfitted with appropriate-sized caps to seal the fresh core specimens upon completion of sampling.

3.4.4 Test Conditions / SCC Properties

Upon delivery, the fresh properties of the trial caisson SCC were measured prior to pumping; the concrete exhibited a 19.75-inch spread, a fresh air content of 3.5%, and a unit weight of 146.4 lb/yd^3. The segregation resistance via the column segregation test was measured to be 0.1%. The ambient conditions at the time of delivery included temperatures in the mid-sixties (^{o}F) with light showers upon

delivery, and increased temperatures to 75°F with mostly cloudy skies by the end of casting. Pumping operations began at around 11:00 am on July 19, 2009, and it took approximately 10-15 minutes to completely fill the formwork. Fresh property testing of the SCC after pumping was foregone due to increasing concrete temperatures.

Test specimens were cast using SCC sampled both before and after pumping. The specimens created using non-pumped SCC included 4"x8" cylinders for compressive strength testing, 6"x12" cylinders for both splitting tensile strength and modulus of elasticity testing, and 3"x3"x11" prisms for length change monitoring. Specimens cast using pumped SCC included only 4"x8" prisms for compressive strength determination. The results of the hardened property testing for compressive strength, splitting tensile strength, and modulus of elasticity of the non-pumped and pumped caisson specimens can be seen in Table 3-5. Similarly, the trends for the length change of the non-pumped SCC prisms can be seen in Figure 3-9.

A noticeably lower strength was observed from concrete taken after pumping; it is uncertain as to whether the pumping process induced extra air, since this was not tested post-pumping, but that might help explain the significant difference in observed compressive strengths. Although these were tested 10 days later than project-mandated 28 day testing [this delay was due to the construction of the actual SCC-1 caissons], the 38-day strength exceeded the required field compressive strength for the project, 4500 psi, as well as the required compressive strength requirement for mix qualification, 5800 psi; it is expected that 28-day results would yield results at or near the mix qualification requirement of 5800 psi. The total shrinkage strains measured from the shrinkage prisms was 890με at 280 days, and a later measurement at about 2 ½ years yielded 924με.

Figure 3-8 Assembled rebar cage prior to trial caisson testing.

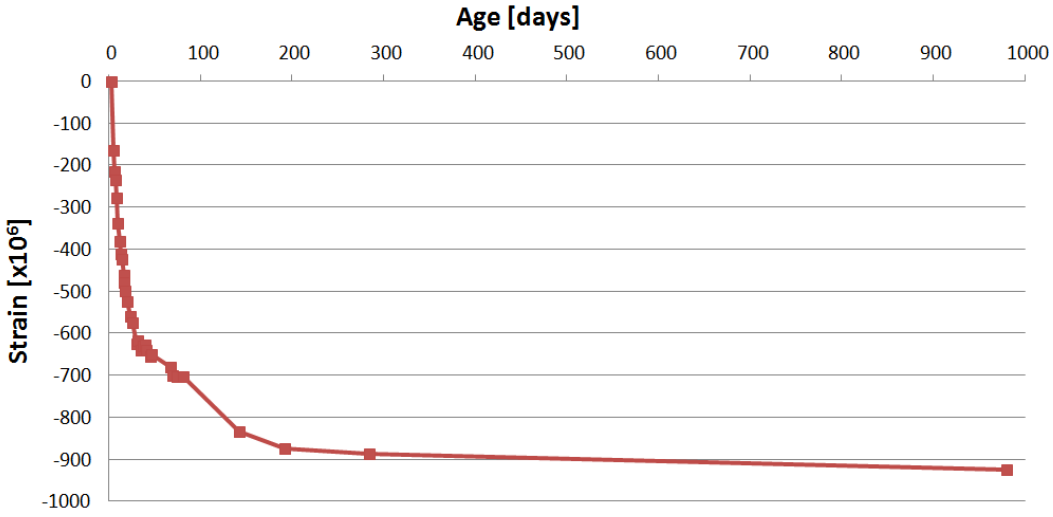

Figure 3-9 Shrinkage data from non-pumped SCC-1 concrete sampled upon delivery to trial caisson experiment.

Table 3-5 Hardened properties of trial caisson SCC specimens.

Age [days]	Compressive Strength 4"x8" cylinders [psi]		Splitting Tensile Strength 6"x12" cylinders [psi]	Modulus of Elasticity 6"x12" cylinders [psi]
	Non-Pumped	Pumped	Non-Pumped	Non-Pumped
7	5,930	4,480	470	4.46×10^6
16	7,020			
38	8,450	6,390	520	4.76×10^6

3.4.5 Fresh Coring

To collect samples, "fresh cores" were taken from the caisson while it was still in the fresh state. To do this, 4-inch (100 mm) diameter plastic drain pipes were inserted into the fresh SCC down from the top of the concrete until they reached the base of the form. The locations of these cores were selected to get representations of the concrete both inside and outside of the rebar cage. As could be seen in Figure 3-3, the desired locations for fresh cores included one core in the center of the rebar cage, two cores located just on the inside of the cage, and two cores equidistant from the outside of the cage and the inside of the formwork walls.

Some movement of the rebar cage occurred during casting, though, so the locations of the cores were also shifted from those depicted schematically in Figure 3-3 to those shown in Figure 3-10. The desired number of representative cores were still taken from locations at the center of the cage, just inside and just outside of the cage, although the locations were shifted accordingly.

After all five tubes were inserted and the concrete was approaching initial set, the formwork walls were opened so that all concrete could be removed. For the fresh cores, a collector plate was first slid underneath of the tube so that it could be lifted in its entirety without losing any concrete, and then the caps were placed on both ends of the tubes so that the sample could be easily removed and stored.

By the time the initial testing was performed and concrete placement began, a couple of hours had passed since the truck had left the plant and the concrete temperature had already begun to rise; the concrete had already begun to stiffen by the time the formwork was ready to be removed. While the two

outer cores were removed rather easily upon opening of the formwork walls, the other three required significantly more effort to remove. A pneumatic chisel was used to chip away the hardening concrete from the three inside tubes, which resulted in some cracking of these specimens.

Figure 3-10 Locations of trial caisson fresh core tubes, as placed.

The plastic tubing was cut from the hardened concrete cores after approximately one month. Initial inspection of the cores was done to visually map the locations at which cracking had occurred. The locations of cracks that were observed at this time can be seen in Figure 3-11. In this figure, the top portion of each core represents the portion of the 6-foot tall core tube that was not filled with concrete. No cracking occurred on the two outer specimens, Core #4 and Core #5, which were easily removed from the caisson formwork without use of the pneumatic hammer, so the cracking in the three inner cores was likely due to the retrieval process.

3.4.6 Allocation of Cores for Testing

Next, it was desirable to assess the uniformity of the concrete from casting using the cores. This would involve using a wet saw to cut the cores into smaller specimens for specified testing. From each core, this included four 4-inch (10 cm) tall specimens for hardened visual stability assessment, three 6-inch (15cm) tall specimens for compressive testing, and two 2-inch (5 cm) tall specimens for Rapid Chloride Permeability Testing (RCPT). Since some cracking had occurred during removal of the inner cores and center core, fragmenting each of these in a different way, it was not possible to select the exact same depths for each core from which to cut the specimens. The approximate locations from which each of the specimens was removed can be seen in Figure 3-11. The numbers to the right of each are the distances from the base of the test caisson to the approximate center of the respective specimen.

3.4.7 Hardened VSI - Aggregate Distribution within Trial Caisson

Hardened specimens were collected for the purpose of assessing the uniformity of the concrete after placement into the formwork. For the Hardened VSI analysis, the 4 inch by 4 inch (10 cm by 10 cm) cylinders from the locations shown were first saw-cut longitudinally, and then further surface preparations was done so that petrographic analysis of the aggregates and air voids could be done at each location. The preparation and procedures for the aggregate distribution analysis will be discussed in this section, while the air void distribution will be discussed in the next section.

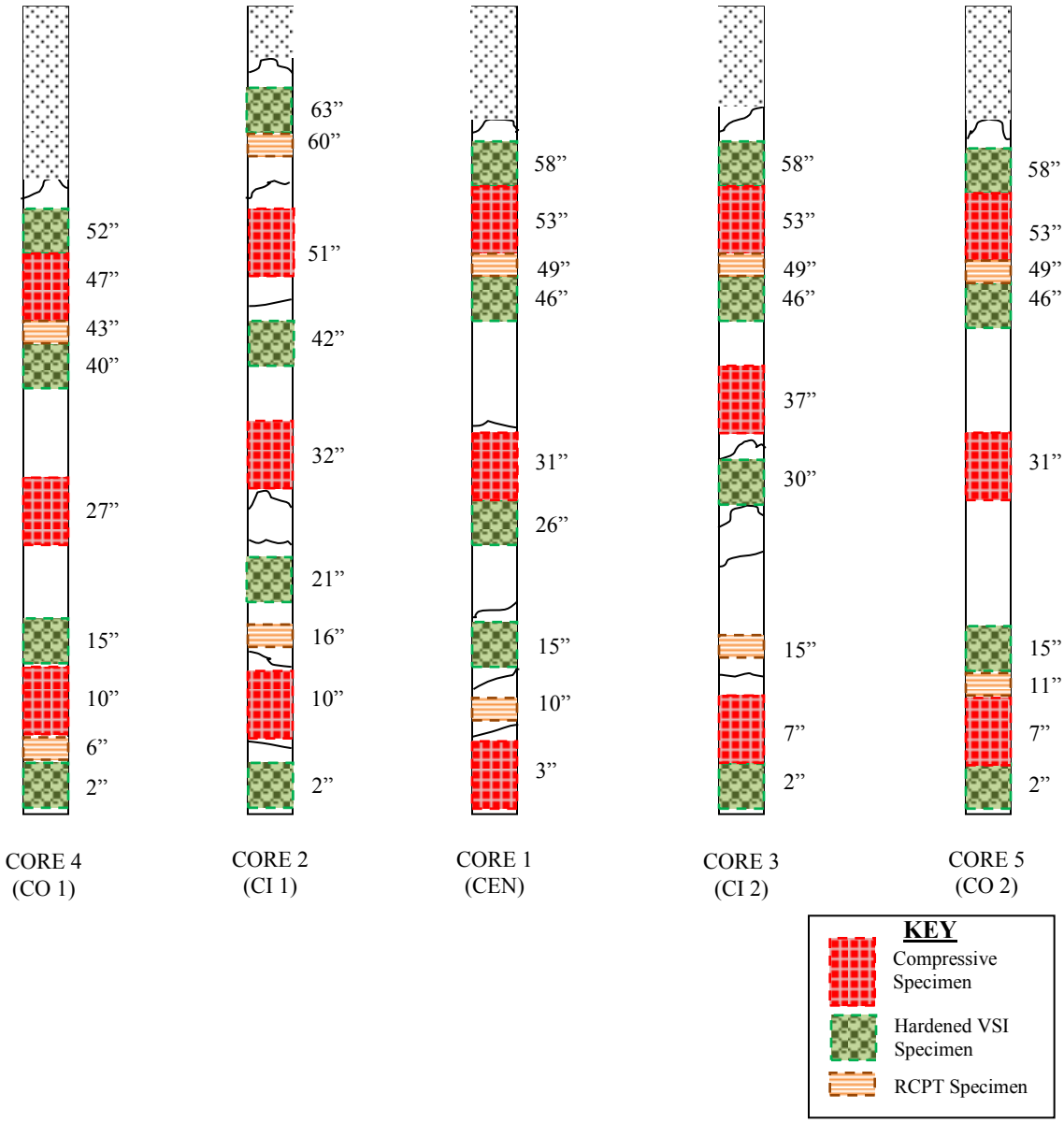

Figure 3-11 Locations of specimen removal from Trial Caisson cores. Numbers indicate approximate height to center of specimen.

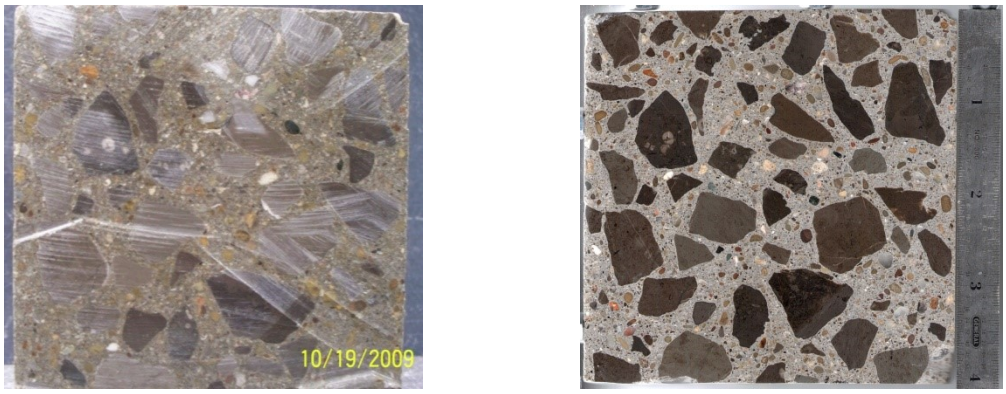

(a) (b)

Figure 3-12 Images of Hardened VSI Specimen CEN-1. (a) Before polishing, dampened surface; (b) After polishing, dry surface.

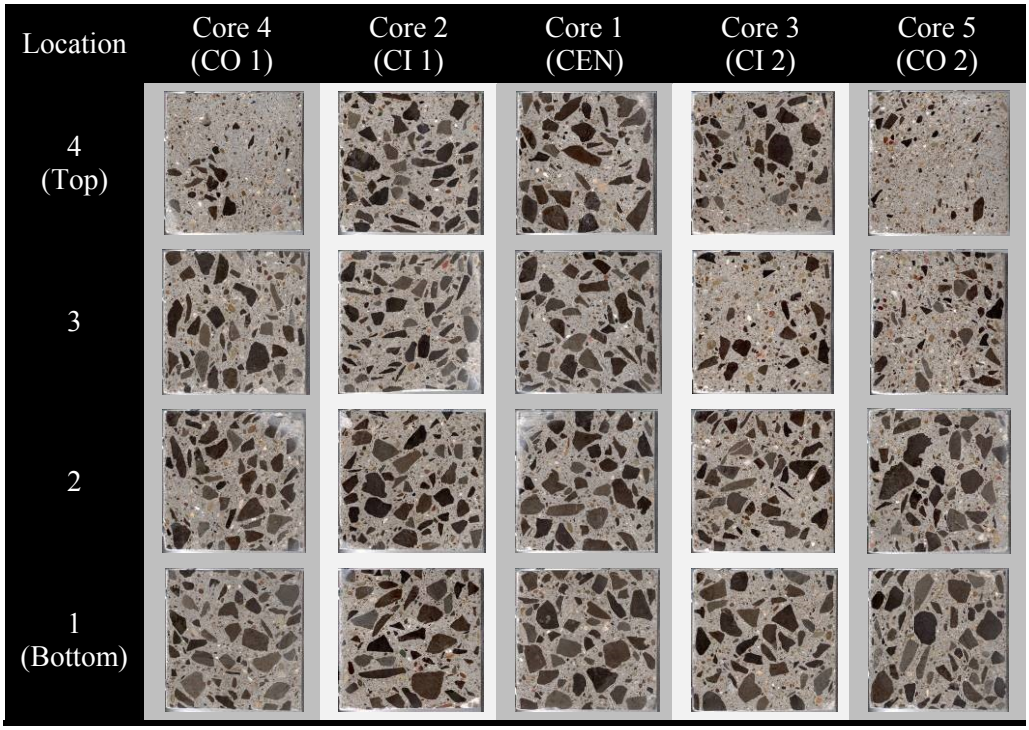

Figure 3-13 Hardened VSI specimens after polishing.

For easier distinction between aggregates and paste, the specimens needed to be prepared prior to analysis. Many researchers have used polishing as a means of preparation for this type of analysis (Yurtdas, et al. 2011) (Sutter 2007) (Jakobsen, et al. 2006). Preparation of the Hardened VSI specimens of this study included surface preparation for each specimen, followed by digitizing of the surface.

After the specimens were cut longitudinally, any large ridges were removed using a cup grinding wheel. Next, they were polished using a handheld, right-angle wet-polisher; the polishing pads used for polishing, in sequence, had grits of 50, 100, 200, 400, 800 and 1500. This produced a glossy surface in which it is easy to distinguish between paste and aggregates. At this point, the surface of each was scanned to create a high-resolution digital image of the plane. A comparison of these surfaces before and after polishing can be seen in Figure 3-12. Figure 3-13 shows all hardened VSI specimens collected after the polishing procedure had been administered.

It can easily be seen from Figure 3-13 that in some locations a distinct difference in the amount of large aggregates present in the samples existed, particularly along the depths of Cores 3, 4 and 5. Therefore, further analysis was conducted to quantify the amount of large aggregate present at within each sample.

For the sake of consistency, as the specimens may vary slightly in size, the area of consideration was reduced slightly for the analysis. Due to the nature of the original coring process, it is expected that some aggregates near the edge of the specimen that would have otherwise been on the boundary were either removed or reoriented as the tube was inserted into the fresh concrete. As a result, the width of the area of interest was therefore reduced from the entire concrete plane, approximately 4 in. (10 cm), to 3.5 in. (8.9 cm) for this investigation. Similarly, the height of the area of interest was reduced from approximately 4 in. (10 cm) to 3.9 in (9.9 cm) to account for any imperfections that may have occurred along the edge during saw cutting or polishing procedures.

A program called JMicroVision was used to aid the processing of the digital images to conduct aggregate counts. With this program, the user can define a scale, define boundaries, and separate objects based on color properties and size using manually defined thresholds. To determine the amount of large aggregates present within the sample, the edges of aggregates with a linear dimension greater than 4 mm

were defined using this program. Figure 3-14 shows the boundaries of large aggregates, as defined when using this program, in the area of interest as described above.

From these images, the percentage of the area of interest that is composed of large aggregates was determined for each of the cores. Comparisons of the total percentage of large aggregates at the four locations of each respective core are shown in Table 3-6. As one might already expect based on Figure 3-13, Table 3-6 also depicts a large variation in the aggregate distributions of both outer cores, particularly the top specimens, and to a lesser extent in the top of Core 3.

3.4.8 Hardened VSI - Air Void Distribution within Trial Caisson

After determination of the aggregate quantities of the 20 Hardened VSI core specimens, sections from the same cores were then prepared for air void analysis. To develop a visible contrast between the air voids, the polished surface was dyed with black ink, and then after the dye was completely dry a white Barium Sulfate powder was used to fill all voids. To ensure voids were filled completely, the powder was tamped into the surface using a rubber stopper, which forced it into all contours of the specimen; all excess powder was subsequently wiped from the specimen, leaving only blackened paste and aggregate fractions, with white powder-filled voids.

The specimen surfaces were then digitized at a high-resolution (3,200 dpi) into an 8-bit TIF file using an office scanner. Figure 3-15 shows the digital image of Specimen CEN-1 after surface preparation. A magnifying glass was used to check the quality of the digital image in comparison to the specimen, as well as to ensure that all voids were in fact from air voids within the paste and not such things as voids within porous aggregates or cracks; appropriate alteration (typically blackening) of the digital image was done upon identification of such anomalies within the digital image.

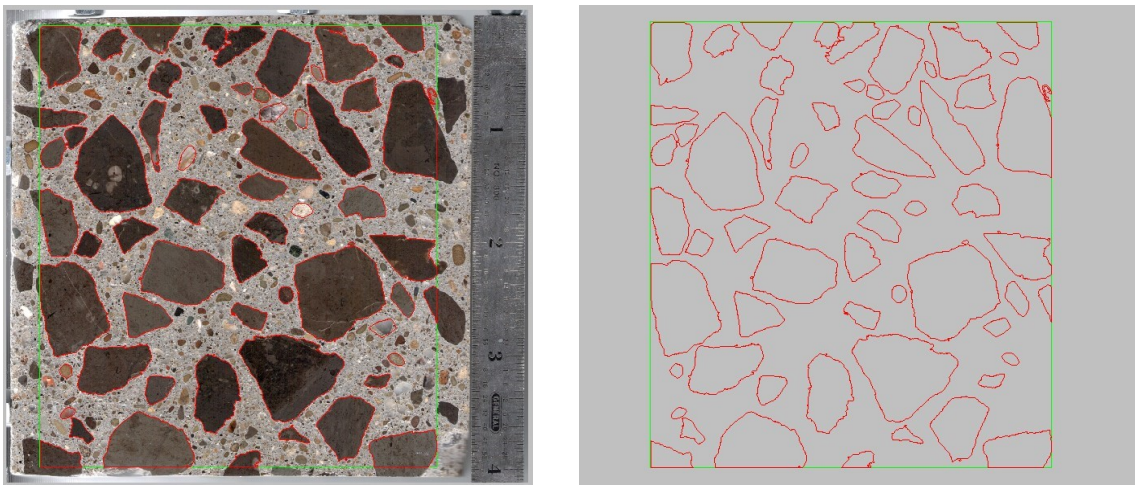

(a) (b)

Figure 3-14 Boundaries of large aggregates in Hardened VSI Specimen CEN-1. (a) Specimen with large aggregates outlined; (b) Aggregate outlines only.

Table 3-6 Aggregate distribution of trial caisson cores.

Location		Height @ Center of Specimen, in. (cm)	Tot. # C.A.	Tot. Area C.A. in^2 (mm^2)	% Area C.A. (% Total)
Core 1 (CEN)	4 (top)	58 (147)	67	5.42 (3501)	39.93%
	3	46 (117)	61	5.02 (3245)	36.80%
	2	26 (66)	65	5.70 (3675)	41.28%
	1 (bottom)	15 (38)	69	6.57 (4241)	48.12%
Core 2 (CI1)	4 (top)	63 (160)	77	5.26 (3397)	38.30%
	3	42 (107)	93	4.82 (3111)	35.30%
	2	21 (53)	86	5.27 (3398)	38.55%
	1 (bottom)	2 (5)	73	5.87 (3785)	42.86%
Core 3 (CI2)	4 (top)	58 (147)	71	3.68 (2374)	26.92%
	3	46 (117)	78	3.04 (1963)	22.22%
	2	30 (76)	82	4.88 (3146)	35.58%
	1 (bottom)	2 (5)	63	5.46 (3520)	39.71%
Core 4 (CO1)	4 (top)	52 (132)	40	1.34 (867)	9.79%
	3	40 (102)	84	5.12 (3306)	37.48%
	2	15 (38)	67	5.47 (3532)	40.04%
	1 (bottom)	2 (5)	75	5.60 (3612)	40.95%
Core 5 (CO2)	4 (top)	58 (147)	65	1.32 (854)	9.69%
	3	46 (117)	114	3.40 (2193)	24.83%
	2	15 (38)	75	5.68 (3665)	41.44%
	1 (bottom)	2 (5)	73	6.08 (3922)	44.49%

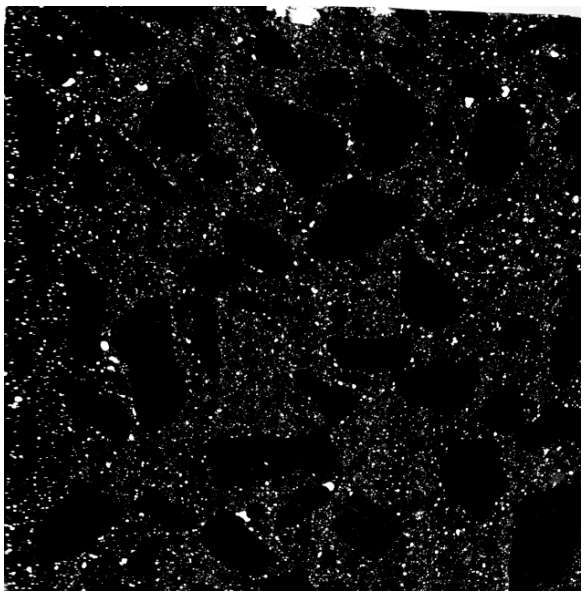

Figure 3-15 Scanned Image of Hardened VSI Specimen CEN-4 after preparation for air void analysis.

The analysis used a shareware program, Bubblecounter, to assess the air void structure of each specimen. The results will be discussed in Section 3.4.11.

3.4.9 RCPT Specimens

At approximately 6 months after casting of the trial caisson, the selected Rapid Chloride Permeability Test (RCPT) specimens were tested in accordance with ASTM C1202 to determine the extent to which non-uniformity of constituents within the member could potentially affect the durability of the concrete at different locations. This test subjects 2"x4" disc specimens to a 60V electric charge to measure the electric transport properties of the concrete, which is often taken as an indirect assessment of the permeability of the concrete. Details of the procedures and apparatus used for this testing can be found in APPENDIX B.1. Results of the RCPT testing by location within the test caisson are shown in Table 3-7.

Table 3-7 Results of Rapid Chloride Penetration Testing on Samples from Trial Caisson Cores.

	Height @ Center of Specimen [in. (cm)]	Initial Current [mA]	Total Charge Passed [Coulombs]	Penetration Depth [cm]	Non-Steady-State Chloride Migration Coefficient [$\times 10^{-12}$ m^2/s]
CORE 1 TOP	49 (124)	113	**3322**	2.02	20.42
CORE 1 BOTTOM	10 (25)	116	**3045**	1.36	13.57
CORE 2 TOP	60 (152)	90	**2415**	1.29	12.67
CORE 2 BOTTOM	16 (41)	71	**1822**	1.27	12.39
CORE 3 TOP	49 (124)	136	**4046**	1.61	16.39
CORE 3 BOTTOM	15 (38)	106	**2762**	1.31	13.04
CORE 4 TOP	43 (109)	114	**3035**	1.75	17.60
CORE 4 BOTTOM	6 (15)	77	**1849**	1.29	12.66
CORE 5 TOP	49 (124)	100	**2813**	1.20	11.81
CORE 5 BOTTOM	11 (28)	92	**2621**	1.22	12.01

The initial current, total charge passed, penetration depth, and calculated non-steady-state chloride migration coefficient for the specimens taken at the bottoms of the cores were often lower than those from the tops of the same cores. In some cases there is a very large discrepancy between values when the top specimen displays higher values than the bottom. These large discrepancies indicate not only that a non-uniform distribution of materials existed within the concrete of the trial caisson, as shown in the previous sections, but that this non-uniform distribution could potentially lead to durability issues. Despite these differences, most specimens would be considered to exhibit Moderate Chloride Ion Penetrability by ASTM C1202, having between 2000 and 4000 Coulombs pass during the test, with only two specimen (Core 2 and Core 4 Bottom) exhibiting a Low Chloride Ion Penetrability, and one specimen (Core 3 Top) exhibiting a High Chloride Ion Penetrability.

3.4.10 Compressive Core Specimens

The compressive core specimens were first prepared by reducing their dimensions to approximately 2.7" x 5.45" using a concrete core drill and a concrete chop saw. These were then subjected to two different rounds of testing. First, non-destructive pulse velocity testing (ASTM C597-

09) was conducted to assess the uniformity and relative quality of the concrete at the different locations. Next, the cores were capped using a mortar capping process and tested destructively per ASTM C69 to determine the compressive strength. All compressive core specimens were exposed to ambient laboratory conditions for a period of several months prior to testing, and maintained an air dried condition throughout testing.

3.4.10.1 Ultrasonic Testing of Compressive Cores

The ultrasonic pulse velocities of the compressive cores were determined in accordance with ASTM C597-09, and in particular using the procedures detailed in APPENDIX B.3. The weight and outer dimensions of each specimen were determined for use in the dynamic modulus calculations.

A breakdown of the pulse velocities for each of the cores can be seen in Table 3-8 Ultrasonic pulse velocity results for core specimens.. Also in this table, the percent difference of pulse velocities are shown when compared to: (1) the second compressive specimen from each core, and (2) the average pulse velocity from all 15 compressive specimens. It can be seen that for the Center Core and Inner Core 2, all pulse velocities measured were reasonably close to the second specimen in their respective cores. Furthermore, all specimens in these two cores were within 2.25% of the mean pulse velocity. However, more substantial differences are seen for specimens CI1 C1, CO1 C1, and throughout the length of Outer Core 2. The results of CI1 C1 are unusually low due to the presence of a void within the specimen, since the signal received was not only delayed in arriving, but much weaker upon arrival than in other specimens.

To compare the elastic behavior of the concrete at different locations, the densities were calculated for each specimen using measured weights and average top and bottom diameters, and the Poisson's Ratio was assumed to be constant for all specimens. In Table 3-8, the dynamic modulus of each core when considering the density is compared to the average dynamic modulus for all specimens

when calculated in the same manner. It can be seen from this data that, disregarding the results from core CI1 C1, that the dynamic modulus was as much as 117% of the average, and as low as 88% of the average for the group of specimens.

3.4.10.2 Destructive Testing of Compressive Cores

After completion of the ultrasonic pulse velocity testing, the specimens were prepared for destructive testing via mortar capping to create the smooth, parallel surfaces specified for testing under ASTM C39. Figure 3-16 shows the compressive core specimens during the mortar capping process.

Table 3-8 Ultrasonic pulse velocity results for core specimens.

Specimen		Length [mm]	Travel Time [us]	Pulse Velocity [m/s]	% Diff – MEAN	E / E_{MEAN}
Center Core	CEN C3 (top)	138.53	30.60	**4526.55**	1.70%	1.0508
	CEN C2	138.65	30.87	**4491.50**	0.91%	1.0343
	CEN C1 (bot)	139.83	30.72	**4551.18**	2.25%	1.0385
Inner Core 1	CI1 C3 (top)	140.24	31.77	**4414.23**	-0.82%	0.9833
	CI1 C2	138.06	31.19	**4426.42**	-0.55%	0.9819
	CI1 C1 (bot)	139.48	35.41	**3938.86**	-11.50%	0.7952
Inner Core 2	CI2 C3 (top)	138.81	31.56	**4398.60**	-1.18%	0.9638
	CI2 C2	137.87	31.64	**4357.08**	-2.11%	0.9512
	CI2 C1 (bot)	138.53	31.30	**4426.19**	-0.56%	0.9950
Outer Core 1	CO1 C3 (top)	137.17	31.04	**4418.58**	-0.73%	0.9434
	CO1 C2	138.79	30.87	**4496.03**	1.01%	1.0338
	CO1 C1 (bot)	136.77	28.74	**4758.23**	6.91%	1.1693
Outer Core 2	CO2 C3 (top)	137.20	31.85	**4307.54**	-3.22%	0.8815
	CO2 C2	138.27	30.35	**4555.77**	2.36%	1.0441
	CO2 C1 (bot)	137.29	29.23	**4696.72**	5.52%	1.1338
MEAN VALUE		*138.36*	*31.14*	***4450.90***		

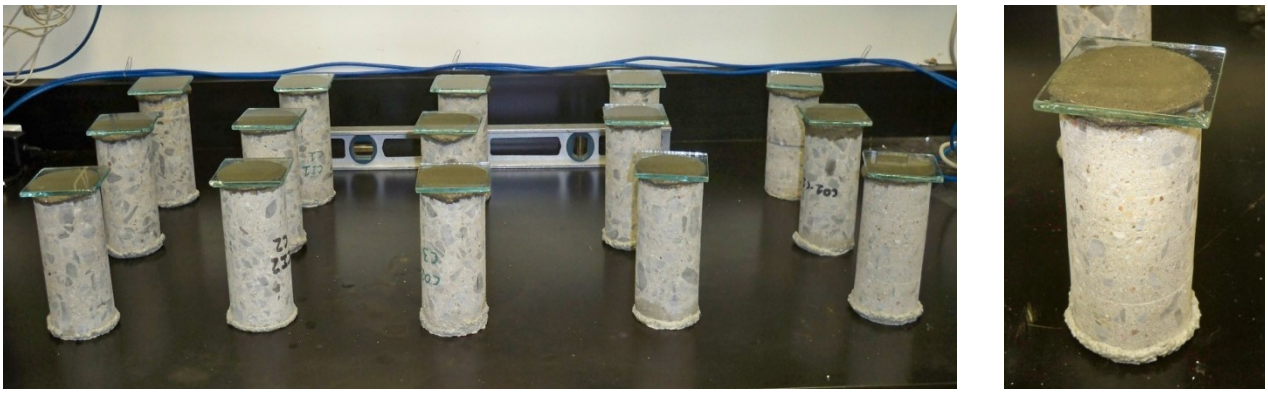

Figure 3-16 Trial caisson compressive cores during mortar capping.

After mortar capping, the core specimens were tested in accordance with ASTM C39 to determine the compressive strength of each. They were each loaded until failure at a rate of approximately 35 psi/s. The results from the compressive tests are summarized in Table 3-9.

It can be seen by comparing Table 3-9 to Table 3-6 that there is not a direct correlation between the aggregate content of the cores and the compressive strength, as determined from a limited sample size in accordance with ASTM C39. For the most part, the pulse velocity results given in Table 3-8 have a better correlation to the aggregate content, with an increase in aggregate content having a corresponding increase in pulse velocity.

3.4.11 Discussion of Results from Trial Caisson

Results from the hardened VSI testing indicated a non-uniformity of aggregates in three of the five cores. The aggregate content of each sample is shown in relationship to the height of the specimen in Figure 3-17. The largest discrepancies were seen in the cores taken from outside of the rebar cage, Cores 4 and 5, indicating that some blockage likely occurred.

The hardened VSI testing also revealed a general increase in the air content of the samples with an increase in distance from the base, as shown in Figure 3-18. This trend would indicate either an

overall migration of air from the bottom of the trial caisson to the top, or a non-uniformity of the concrete as it came off the truck.

Table 3-9 Results from compression testing of trial caisson cores.

Specimen		Area [in^2]	Ultimate Load [lbs]	Failure Type	Compressive Strength [psi]	$f_c' / (f_c')_{MEAN}$
Center Core	CEN C3 (top)	5.688	36,300	2	6,382	0.937
	CEN C2	5.691	35,700	2	6,273	0.921
	CEN C1 (bot)	5.690	38,700	3	6,802	0.999
Inner Core 1	CI1 C3 (top)	5.689	39,400	3	6,926	1.017
	CI1 C2	5.693	42,500	4	7,466	1.096
	CI1 C1 (bot)	5.692	41,800	3	7,343	1.078
Inner Core 2	CI2 C3 (top)	5.686	38,500	2	6,771	0.994
	CI2 C2	5.685	38,700	4	6,808	1.000
	CI2 C1 (bot)	5.687	39,700	4	6,981	1.025
Outer Core 1	CO1 C3 (top)	5.671	34,700	3	6,118	0.898
	CO1 C2	5.677	29,400	3	5,179	0.760
	CO1 C1 (bot)	5.596	33,800	3	6,040	0.887
Outer Core 2	CO2 C3 (top)	5.679	46,800	2	8,240	1.210
	CO2 C2	5.690	43,600	3	7,663	1.125
	CO2 C1 (bot)	5.688	40,700	3	7,155	1.051
MEAN VALUE					*6,810*	

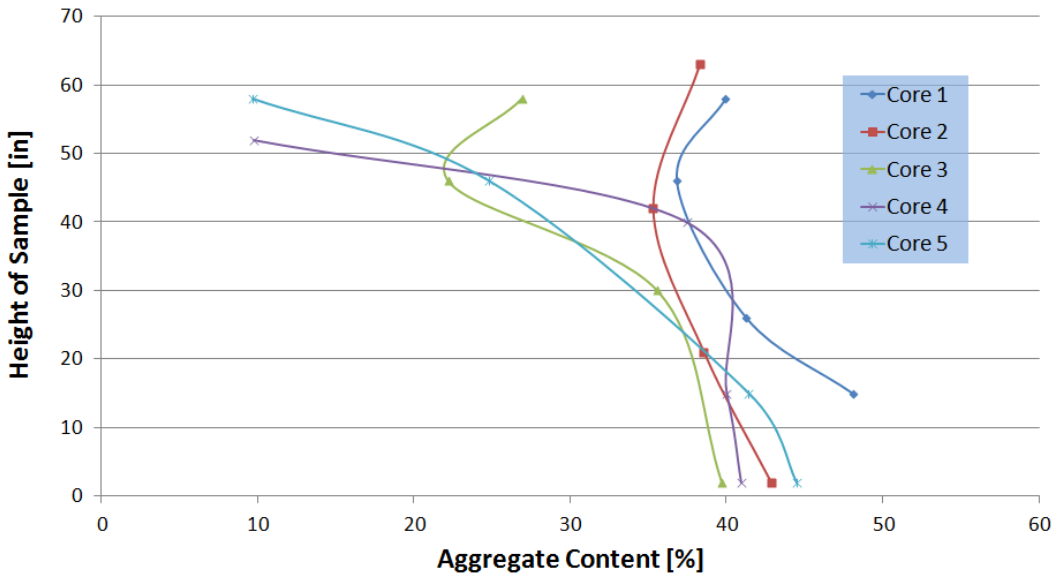

Figure 3-17 Aggregate distribution of trial caisson from hardened VSI samples.

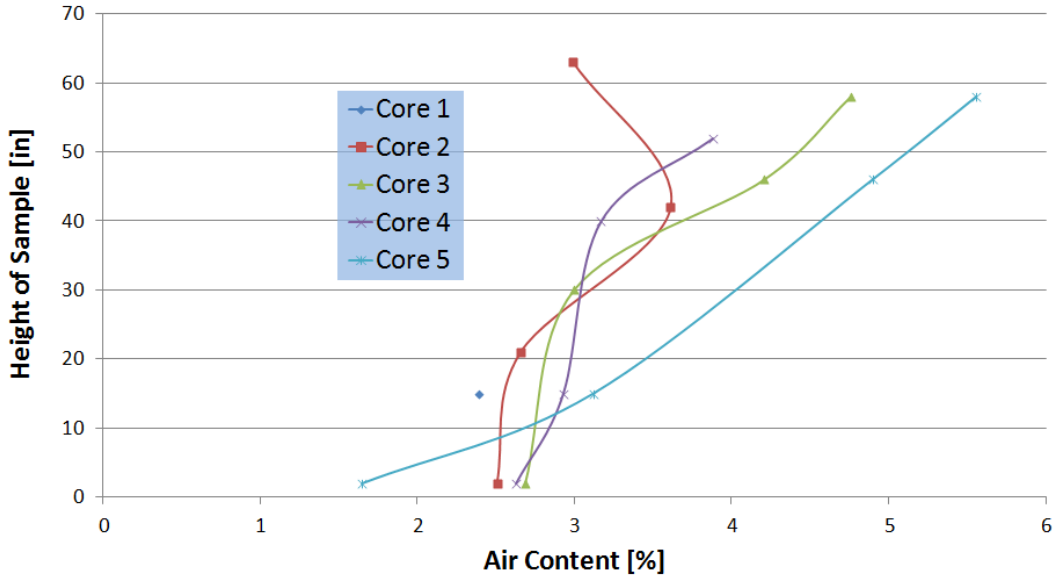

Figure 3-18 Air distribution of trial caisson from hardened VSI samples.

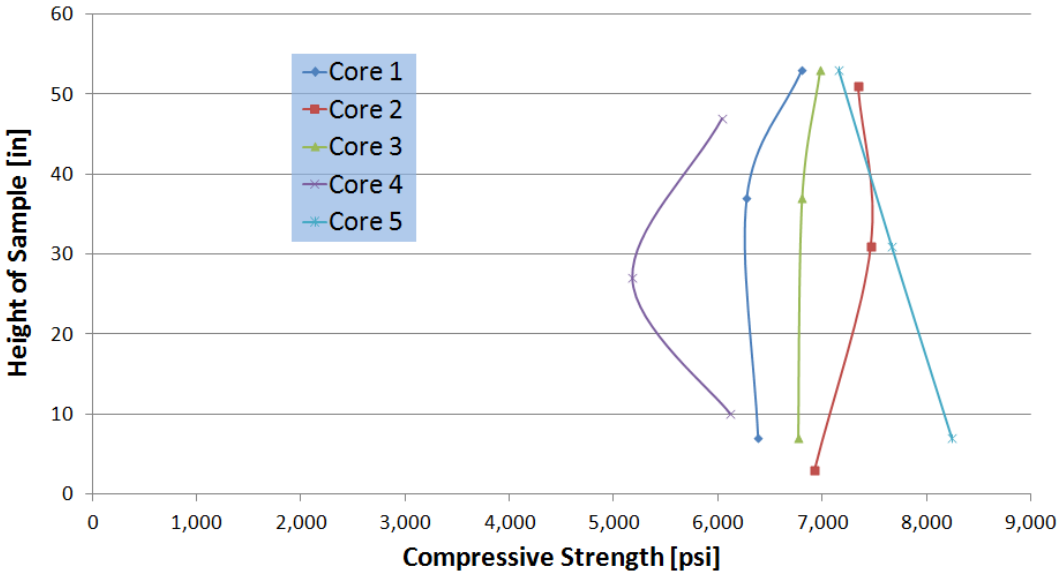

Figure 3-19 Compressive strengths at different locations within trial caisson, from compressive core specimens.

Since these non-uniformities were observed among the core specimens, it is of interest to determine exactly how they could potentially affect the material properties and durability of the caisson structure. Figure 3-19, Figure 3-20 and Figure 3-21 show the respective pulse velocities, compressive strengths and chloride permeability results when plotted versus location within each core.

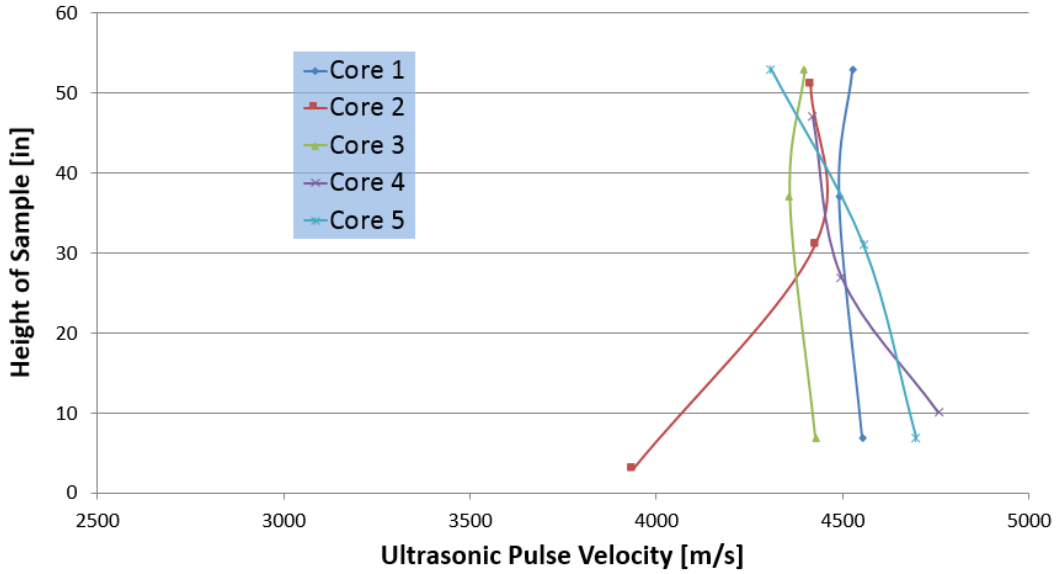

Figure 3-20 Ultrasonic pulse velocities at different locations within trial caisson, from compressive core specimens.

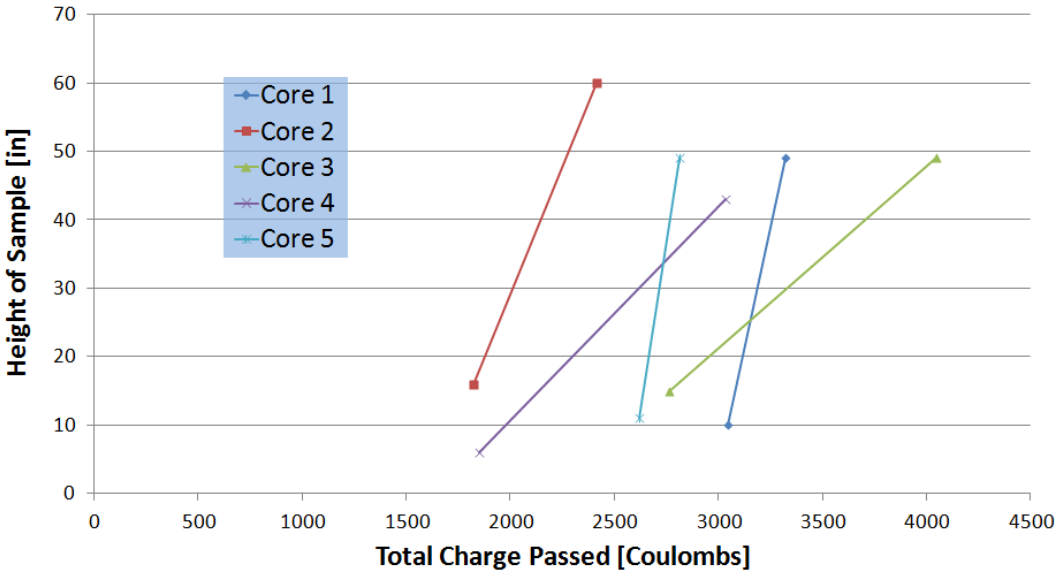

Figure 3-21 Chloride penetrability at different locations within trial caisson, from RCPT specimens.

One might expect to see a correlation between the compressive strength and the aggregate distribution, but this was not observed in this case. For the most part, compressive strength was fairly consistent along the length of any given core. The magnitude of the strength did not necessarily

correlate to aggregate content, with Core 1 [Center] and Core 4 [Cage Outer 1] exhibiting the lowest strengths, while Core 2 [Cage Inner 1] and Core 5 [Cage Outer 2] exhibited the highest strengths. Typically the compressive strength of concrete decreases with an increase in air content (Neville 2004), but this trend was not clearly represented in the data, either. Although there is a size effect from using smaller specimens, no single specimen exhibited a compressive strength lower than the project-specified 4,500 psi requirement.

Pulse velocities in most compressive cores ranged from 4,300 m/s to 4,760 m/s. This range of values seems reasonable based on the results of Lin et al.; tests of numerous concrete mixes of varying aggregate content and *w/c* gave Lin et al ultrasonic pulse velocities of 28-day specimens ranging from around 4,100 m/s to around 4,650 m/s (Lin, et al. 2007). The 3,940 m/s ultrasonic pulse velocity obtained from the bottom sample of Inner Core 1 appears to be an outlier; although one might infer that a large crack or void was present that might have affected the transmission of the ultrasonic pulse, this was not reflected in the results of the destructive compressive testing of this specimen.

Most of the RCPT results from the trial caisson core specimens indicate moderate permeability, and results from the tops of the cores typically showed an increased permeability, showing a direct relationship to the air content and an inverse relationship to the amount of aggregates present at those locations. The preliminary air-void spacing factor seen in the samples were typically between 0.25 to 0.35 mm, which is higher than that recommended for good freeze-thaw durability, 0.2 mm (ACI Committee E-701 2003).

It is of note that the overall air content for this batch was lower than that required for field production, though, and an increase in total air should reduce the spacing factor, assuming that this would correlate to a larger quantity of small air voids being created. Lomboy and Wang observed a distinct correlation between the spacing factor and the content of air voids smaller than 300 microns, but

saw no such correlation between porosity and chloride permeability (Lomboy and Wang 2009). Based on this, the higher air content that would be expected in the field could improve the freeze-thaw characteristics of the mix, but would not necessarily be a detriment to the permeability of the concrete.

In general, the nature of the testing did not allow for a strong statistical assessment of the concrete properties at any given location, since there was only one specimen per location. However, under this worst-case scenario, which includes a rebar spacing of only about ½ of what would occur in the field, and using these results as indications of the range of properties that could occur within the caissons, it was not seen that even large variations in the materials would be detrimental to the hardened properties of the SCC-1 concrete.

3.5 Stalnaker Run Caisson Construction

Casting of the caissons for the Stalnaker Run Bridge replacement began on July 17, 2009, using the approved SCC-1 mix design given in Table 3-4 to cast the caissons for Abutment 1 of the bridge. The following week, on July 23, 2009, the caissons for Abutment 2 of the bridge were cast using a traditional caisson concrete, a high-slump Class B Modified mix. The instrumentation, construction details, data collection and results from these castings will be discussed throughout this section.

3.5.1 Instrumentation and Monitoring Plan

A number of different tests were conducted in attempt of evaluating the SCC-1 and traditional caissons of the Stalnaker Run Bridge. Much of the information was collected either at the time of casting or shortly thereafter, however the monitoring plan also provided the means to monitor the strain of the SCC-1 caisson at a limited number of locations after the construction is completed. The discussion of the caisson instrumentation and monitoring plan found in this section is broken down into

three portions: pre-construction instrumentation, data collection and sampling during construction, and post-construction monitoring.

3.5.1.1 Pre-construction Instrumentation of Caissons

The rebar cages were instrumented prior to placement into the wet holes to allow for data collection at a later date. The types of gages placed prior to casting included concrete embedment strain gages [Vishay EGP-5-350, see Figure 3-22] to measure strains in concrete, foil strain gages [Omega KFG-5-350-C1-11L3M3R, see Figure 3-23] to measure strains on the longitudinal rebars, analog temperature sensors [Analog Devices TMP36GT9Z, see Figure 3-24], and data-logging temperature/humidity hygrochrons [Embedded Data System DS1923-#F5 iButton, see Figure 3-25].

All gages used for instrumentation of the caissons were protected from mechanical and water damage prior to casting, with the exception of the embedment strain gages, which were already designed to be durable under these conditions. The foil strain gages were sealed and protected from water damage using the MB-AE 10 system from Vishay. The analog temperature sensors were protected using a combination of shrink tubing and a latex polymer sealer. Each iButton hygrochron was encased in a hard plastic enclosure and sealed using a latex polymer sealer; one side of the enclosure was comprised of a layer of Gore-Tex® fabric to permit passage of water vapor such that relative humidity could be monitored.

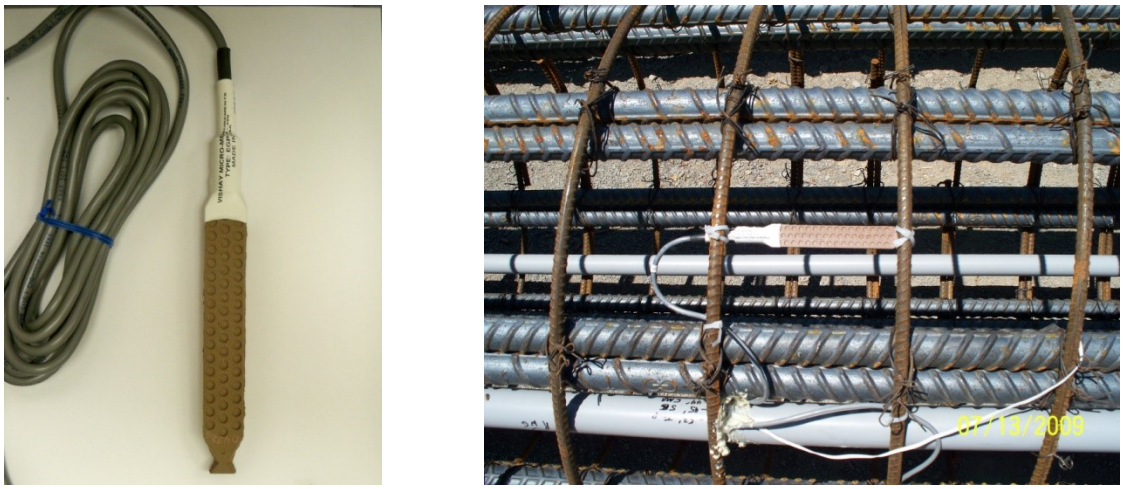

Figure 3-22 Concrete embedment strain gage, before and after affixing to caisson rebar cage.

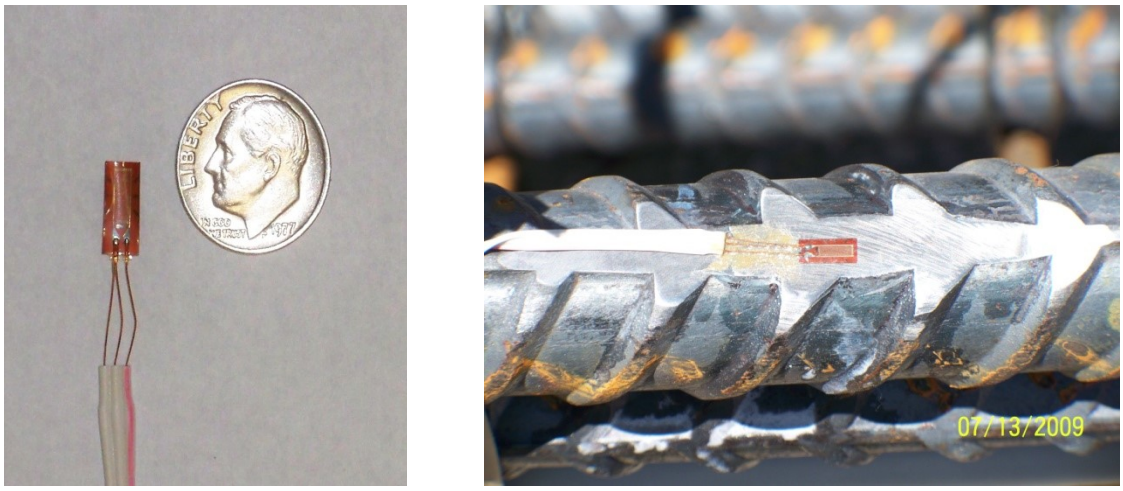

Figure 3-23 Foil strain gage, before and after mounting on steel rebar (before protection).

Figure 3-24 Analog temperature sensor, before and after attaching wire and protection.

Figure 3-25 Thermal logging hygrochrons, before and after protecting and mounting on steel cage.

For both sets of three caissons (those for Abutment 1 and those for Abutment 2), the upstream caisson was designated as "heavily-instrumented," while the center and the downstream caissons were "moderately-instrumented," meaning that more gages were placed in upstream caissons. The locations of the gages for the heavily monitored caissons are displayed in Figure 3-26 and Figure 3-27. It can be seen from these figures that each of the heavily-instrumented caissons contained four (4) concrete embedment strain gages, two (2) steel strain gages, three (3) analog temperature sensors, and three (3) data logging hygrochrons. The instrumentation for the moderately-reinforced caissons was similar, but each contained only one (1) embedment strain gage, one (1) steel strain gage, and three (3) analog temperature sensors, with no hygrochrons used for these caissons. The embedment and steel strain gages for the moderately instrumented caissons were both at the top location shown in Figure 3-26, while the analog temperature sensors were in the same locations as those depicted in this figure.

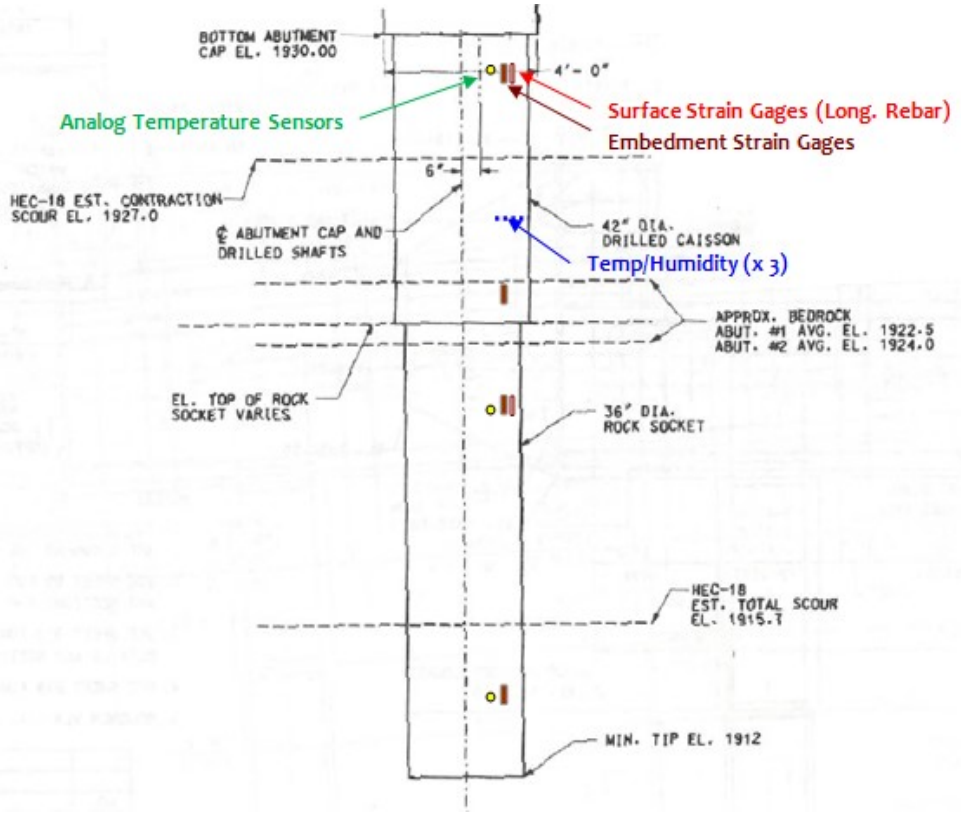

Figure 3-26 Gage locations for heavily-instrumented caissons. Elevation view.

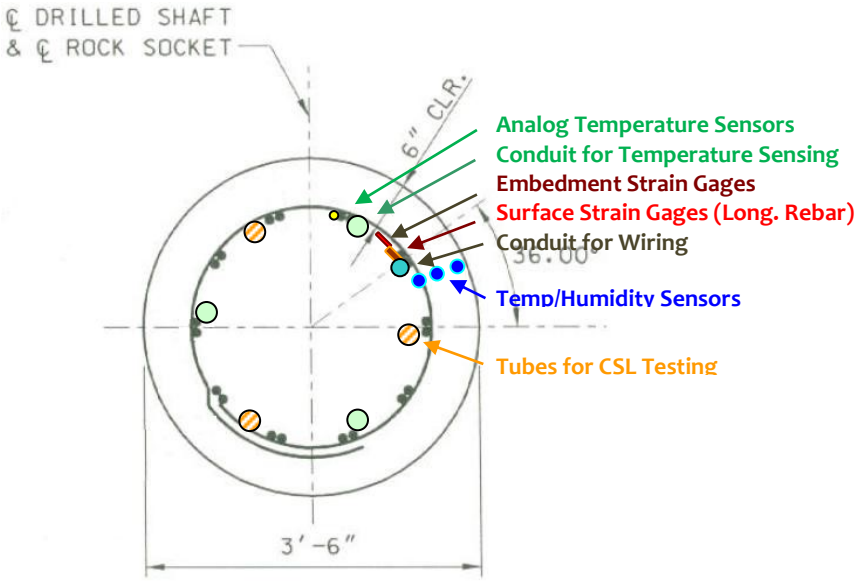

Figure 3-27 Gage locations for heavily-instrumented caissons. Plan view.

The wires for all caisson gages were protected by running them up the inside of the cages through PVC conduit. In order to prevent short circuiting of the gages due to water penetration, all

openings in the conduit were sealed prior to cage placement using expanding foam. The wiring conduit and instrumentation, as affixed the rebar cage, can be seen in Figure 3-28.

Figure 3-28 Rebar cage after installation of all gages.

3.5.1.2 Data Collection and Sampling during Caisson Construction

Upon delivery of the SCC-1 to the job site, the fresh property tests were conducted as prescribed in the project Special Provisions. The class B Modified concrete would be tested per standard procedures.

In addition to the tests required in the project documents for on-site quality control, samples were collected upon delivery of concrete to the job site so that assessment of the hardened behaviors. Specimens collected included 4”x8” cylinders for compressive strength determination and RCPT assessment, 6”x12” cylinders for splitting tensile strength and modulus of elasticity determination, 3”x3”x11” prisms for shrinkage measurement, and 3”x4”x16” prisms for freeze-thaw testing.

During the actual casting of the caissons, small samples of fresh concrete, purged groundwater, and purged concrete were collected and tested for the purpose of a pH investigation that will be discussed briefly in Section 3.5.3.

3.5.1.3 Post-Construction Monitoring of Caissons

Infrared thermal integrity testing was to take place in the hardening caissons in attempts of detecting any construction flaws. Access along the depth of the caissons would be provided by conduit placed within the cage prior to construction, as was shown in Figure 3-27.

After completion of the caisson construction, the lead wires from the caisson gages were to remain intact such that subsequent readings could be taken. Strain and temperature readings would be taken throughout the first 48 hours after casting of each set of caissons. Eventually these lead wires would be extended to long-term monitoring stations for continuous monitoring, which will be described in Section 4.

3.5.2 Casting of Caissons

The SCC mix developed in this project was ultimately used to construct the three caissons for Abutment 1 of the bridge replacement project on July 16, 2009. The caissons for the other abutment were cast using a high-slump WVDOT "B Modified" mix design on July 23, 2009. The mix designs for each type of concrete are the same as those given in Section 3.3.

On each respective day of casting, the water-filled holes were checked for debris using an underwater camera. Once acceptability of the holes was verified, the rebar cages were lowered into their respective holes for that day's casting (see Figure 3-29).

Figure 3-29 Placement of rebar cage for use in Stalnaker Run caisson, Abutment 2.

The fresh properties measured for all concrete as delivered by each truck to the site can be seen in Table 3-10. The majority of the high-range water reducing (HRWR) admixture that was added to the SCC-1 was done on site after transport, while the chemical admixtures for the B Modified concrete were all added at the plant prior to transport. All fresh property testing of the SCC-1 mixes was done after pumping, while testing of the B Modified batches was done prior to pumping. Specimens for hardened property assessment of these mixes will be discussed in more detail in Section 3.5.6. It was noted that the field SCC-1 specimens for hardened testing initially remained unprotected from the environment for a period of about 3.5 hours after casting; these specimens likely achieved a higher initial temperature than the B Modified specimens, which could have altered the structure of hydration products, and thereby affected the hardened properties (Neville 2004).

Both types of concrete were placed into "wet hole" conditions using a tremie pipe, which was fed using a pump system. No slurry was used for concrete placement, but a removable steel casing was

used for the drilled shaft portion of the construction. Both sets of caissons were cast successfully, and they eventually became integral parts of their respective bridge abutments.

Table 3-10 Fresh properties of Stalnaker Run caisson concrete.

Fresh Property	SCC-1					B Modified		
	Truck 1	Truck 2	Truck 3	Truck 4		Truck 1	Truck 2	Truck 3
Spread, in (cm)	19.5 (49.5)	19 (48.3)	--	--		--	--	--
Slump, in (cm)	--	--	--	--		7.0 (17.8)	7.25 (18.4)	7.75 (19.7)
T_{50}, seconds	2.2	4.55	--	--		--	--	--
J-Ring Value, in (cm)	1.25 (3.2)	0 (0)	--	--		--	--	--
Static Segregation, %	--	0%	--	--		--	--	--
Air Content, %	6.8	7	5.5	6.5		4.8	7.2	6.5
Unit Weight, lb/ft^3 (kg/m^3) ASTM C136	141.0 (2259)	140.9 (2257)	143.9 (2305)	--		145.6 (2332)	140.8 (2255)	142.2 (2278)
Concrete Temp., ^{o}F (^{o}C)	86 (30)	85.5 (29.7)	79 (26.1)	85 (29.4)		79 (30)	76 (29.7)	78 (26.1)

The caisson casting on the SCC side did experience more delays during construction than the casting on the B Modified side. These delays were mainly because of the (1) difficulties the concrete producer had in meeting the requirements for air content after adding the high-range water reducing (HRWR) admixture on site, (2) the extra testing that was required for site acceptance since this type of concrete was new to most of the parties involved, and (3) the concrete trucks were more limited in the amount of SCC that they could carry due to its extra fluidity in comparison with the traditional mix. As a result, it took approximately five hours on the first day of casting to place all three caissons using SCC, as opposed to about three hours on the second day of casting for the three using the traditional mix.

These delays could be minimized, if not eliminated completely or reversed, with increased familiarity with SCC by the producers and the testers in the field, most apparently in the time it takes to set up and conduct the acceptance testing done by field technicians. A simple procedural adjustment could have also helped eliminate the problematic high air content that delayed acceptance of the trucks;

Hodgson et al recommend avoiding field adjustment of chemical admixtures, as this was observed in their study to result in excessive air entrapment when addition of HRWR is accompanied by rapid mixing in the field (Hodgson, et al. 2005).

3.5.3 pH Investigation

The purpose of the pH investigation was to explore whether differences in pH can be seen in mortars of different water-to-cementitious material ratios (w/cm), and understand how the pH measurements will change with the degree of hydration of cement in a mix. Initial laboratory pH tests on fresh mortar were done to see the effects of a potential introduction of supplementary water into concrete during casting of caissons when in the presence of ground water. The initial laboratory experiments will first be discussed, followed by the data collection from the Stalnaker Run Bridge construction.

3.5.3.1 pH Investigation of Laboratory Mortars

The mortar mixes for the initial investigation included the same materials that would eventually be used by Central Supply for the SCC used for construction of the drilled shafts. The mortar mixes included no admixtures, but the proportions of the sand, cement and fly ash remained consistent with the initial SCC-1 mix designs. Two different water-to-cementitious materials ratios were used, 0.4 and 0.5. The mix quantities used for each mix can be seen in Table 3-11. Each batch created approximately 2.5L of concrete.

Table 3-11 Mix quantities of mortars for preliminary pH investigation.

	Sand [g]	Type I Cement [g]	Fly Ash [g]	Water* [g]
w/cm = 0.4	**2139**	**1005**	**176**	**491**
w/cm = 0.5	**2139**	**1005**	**176**	**606**

*Oven-dried sand (0% free moisture) was used to create the mortars, so an additional amount of water was included in the mix to account for the absorption of the sand, 0.81%.

After mixing, each batch was split into three samples for measurement. A pH and temperature meter, an Extech PH220 Palm pH, was used to take measurements of the temperature and pH for each mix until significant stiffening of the mortar occurred, at least one hour after mixing. Plots including both the temperature and pH for the 0.4 and 0.5 water-to-cementitious ratio mortar mixes can be seen in Figure 3-30 and Figure 3-31, respectively. It should be noted that a small amount of bleed water was seen in the 0.4 w/cm mortar after about 30 minutes, and a significant amount was seen after the same time for the 0.5 w/cm mix.

A comparison of the pH measurements versus time can be seen in Figure 3-32. It can be seen from this figure that the mortar mix with the higher water-to-cementitious ratio exhibits a slightly lower pH in the fresh state. Overall, the pH readings of both mixes tend to increase with time, presumably due to increased hydration of the cement particles. At the time of significant stiffening of the mortars, it appears that the 0.4 w/cm mix exhibited a pH that was approximately 0.1 lower than the 0.5 w/cm mix.

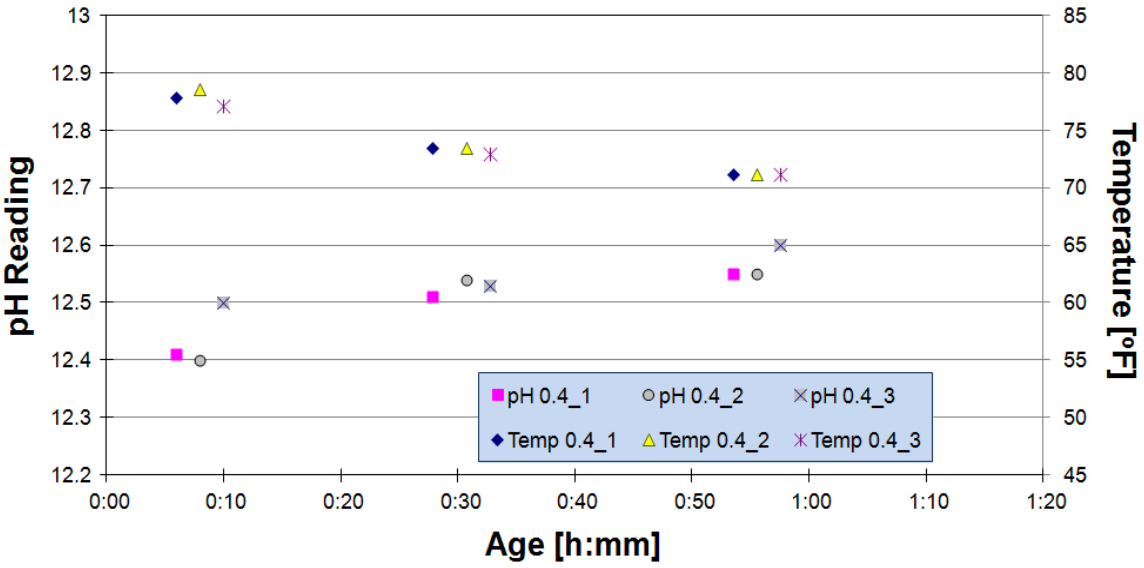

Figure 3-30 Temperature and pH measurements at different times for mortar mix with w/cm=0.4.

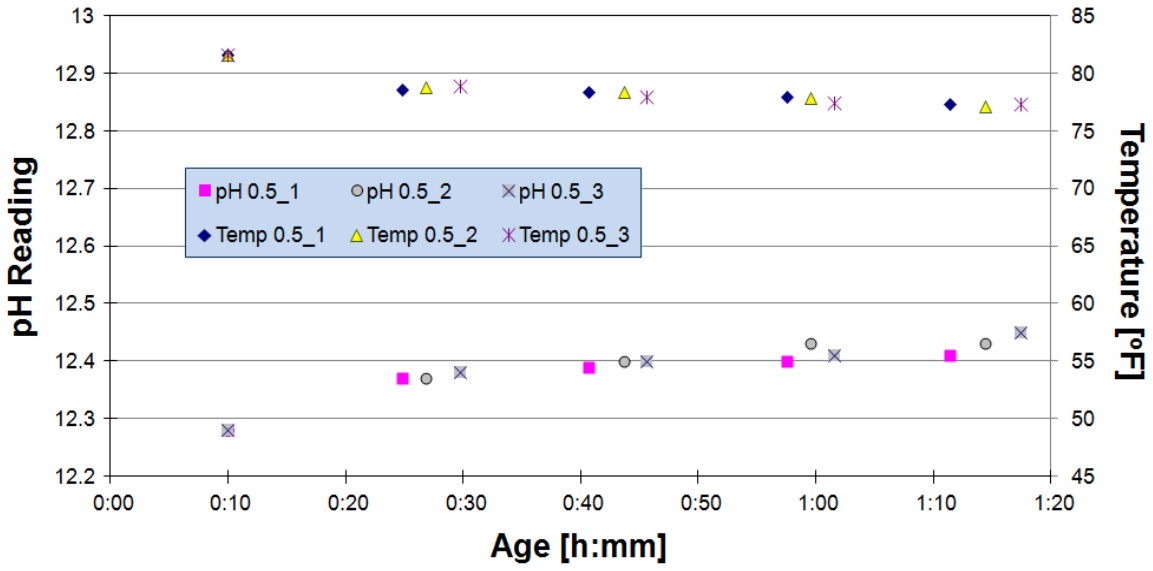

Figure 3-31 Temperature and pH measurements at different times for mortar mix with w/cm=0.5.

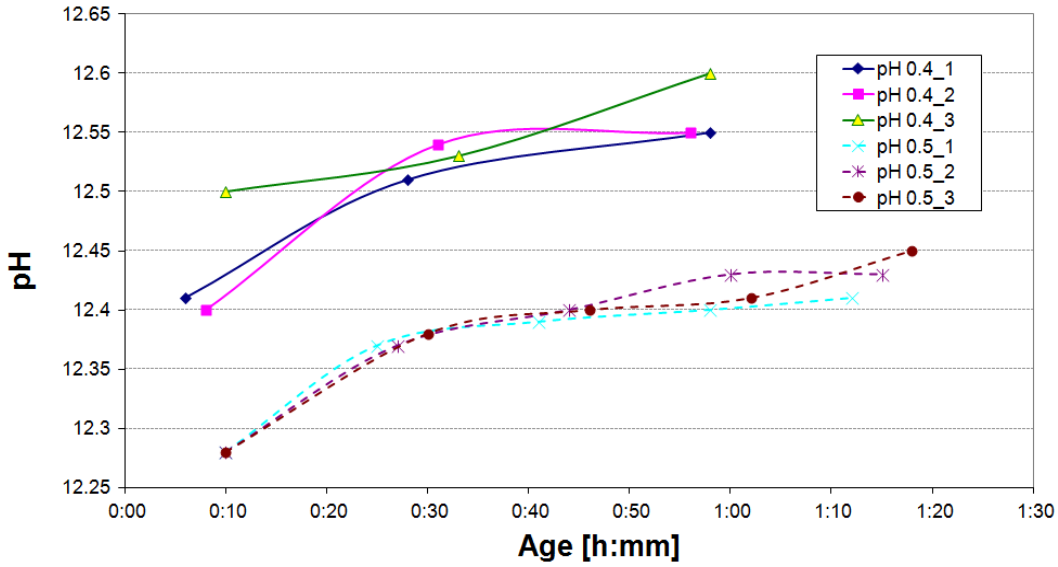

Figure 3-32 Comparison of pH measurements versus time for mortar mixes with w/cm of 0.4 and 0.5.

3.5.3.2 Field pH Measurements

During casting of the SCC-1 caissons for Abutment 1, samples of the purged water were collected during filling of each caisson as an indication of the amount of mixing occurring between the concrete and the groundwater present. The sampling was done using a glass container attached to line.

During collection, the container was lowered to the level at which water was being purged from the caisson to collect a sample and then retrieved; meanwhile a worker measured the depth of the water/concrete interface. A similar process was done to collect purged groundwater for the B Modified caissons of Abutment 2, although the tops of the caissons were more accessible to workers due to a cofferdam structure around the construction, allowing for more direct access to the tops of the caissons, so the glass sample containers did not have to be lowered using a line. The measured pH of the purged ground water taken at various depths for all six caissons can be seen in Figure 3-33.

At the end of filling of the B Modified caissons, the top surfaces of the caissons were easily accessible such that the purged concrete could be directly sampled upon completion of filling. Therefore, it was possible to observe the pH of the purged B Modified concrete, which is also represented in Figure 3-33. Furthermore, the pH of a sample of B Modified concrete taken upon delivery can be seen in comparison with the purged concrete from each batch in Figure 3-34.

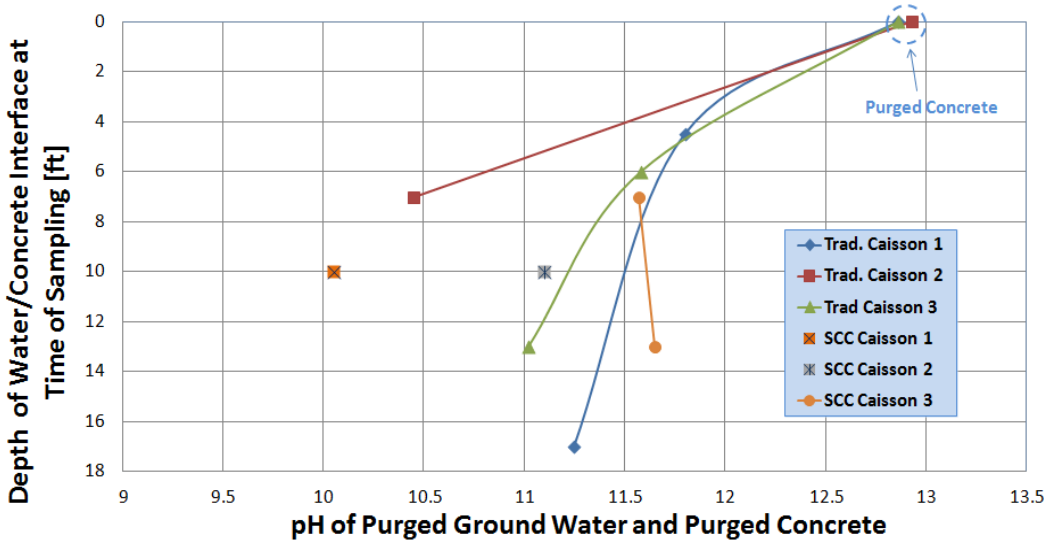

Figure 3-33 pH of purged groundwater (or purged concrete) vs. depth of pour for all Stalnaker Run caissons.

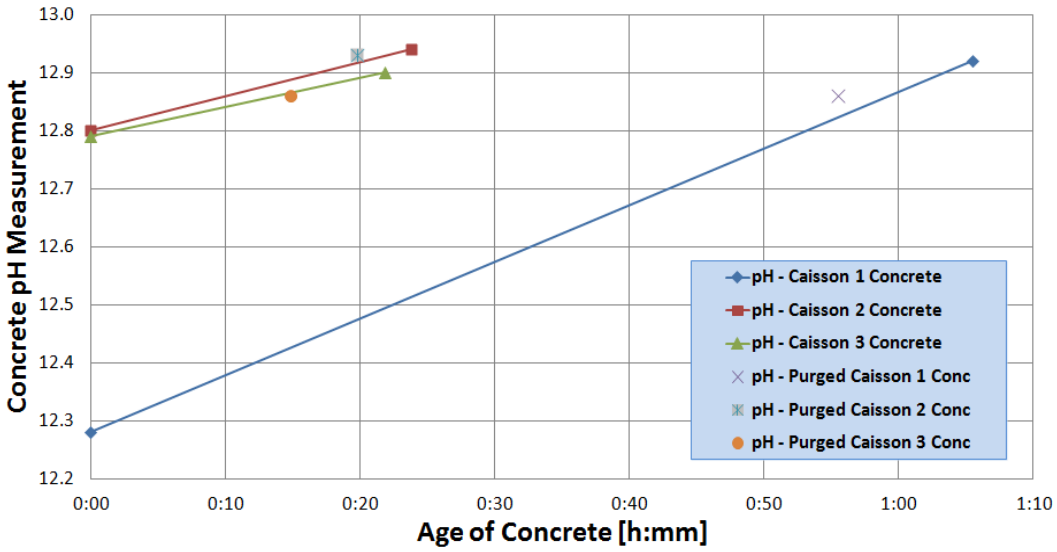

Figure 3-34 pH of concrete samples from casting of B Modified caissons.

Figure 3-34 indicates that the pH of the purged B Modified concrete was very close to that of the same concrete sampled from the truck and tested at approximately the same time after delivery. The overall magnitude of the field pH measurements of the B Modified concrete are larger than those of the laboratory mortars since (1) the mortars are based on the SCC-1 mix design, which has a higher percentage of Fly Ash, and (2) the laboratory mortars did not contain any admixtures, which could further alter the pH of the pore water. Since the purged concrete from all three B Modified caissons had a pH that was within 0.05 of the concrete that was not exposed to the groundwater, it is believed that any caisson concrete that was tainted with the groundwater was successfully purged during the casting process.

3.5.4 Inspection of Caissons after Casting

Two methods of inspection were done for both sets of caissons after casting. As was prescribed in the construction documents for the caissons, the Contractor arranged for cross-hole sonic logging (CSL) testing, a form of ultrasonic testing, after full curing. Additionally, Researchers conducted thermal probe testing on the hardening caisson concrete within the first 48 hours after casting. Infrared

thermal integrity testing has been reported by Mullins as a promising technique for detection of drilled shaft defects, since it has the ability to detect anomalies beyond radius of the rebar cage, as opposed to the ultrasonic techniques used for CSL testing that is limited to anomaly detection within the rebar cage. Therefore, a similar thermal integrity testing was incorporated into the quality assurance regimen for both types of caissons.

Both types of non-destructive techniques utilized embedded tubes to allow exploration of the entire depth of the caisson. The CSL testing used 2½" steel tubes, while the thermal probe testing utilized 1½" PVC conduit tubes for exploration of the shafts; the tubes were placed around the perimeter of the cage in an alternating configuration approximately 60° apart. The schematic locations of the tubes with respect to the rebar cage can be seen in Figure 3-35.

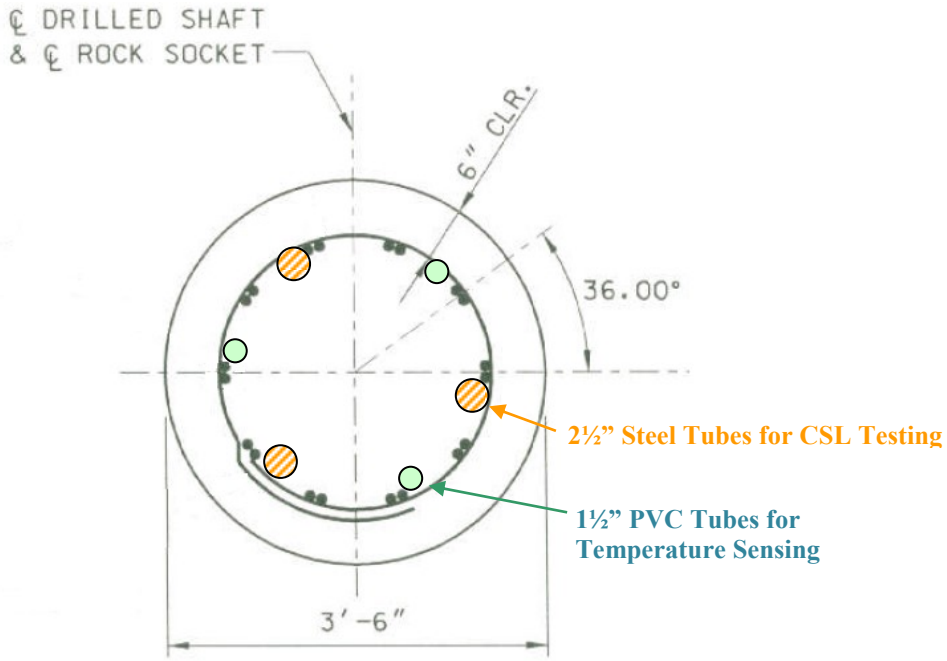

Figure 3-35 Locations of tubes for CSL and Infrared Thermal Integrity Testing of caissons.

3.5.4.1 Infrared Thermal Integrity Testing

To explore the temperature profile along the depth of each caisson at the locations indicated in Figure 3-35, a probe was used to take instantaneous temperature measurements, and a rotary

measurement device was used to measure the depth of the probe during testing. The probe consisted of three Infrared Thermocouples [Exergen Micro IRt/c] encased in ¾" diameter PVC tube, oriented such that they would measure outward at 120° from each other. A picture of the probe can be seen in Figure 3-36.

Figure 3-36 Probe for Infrared Thermal Integrity Testing.

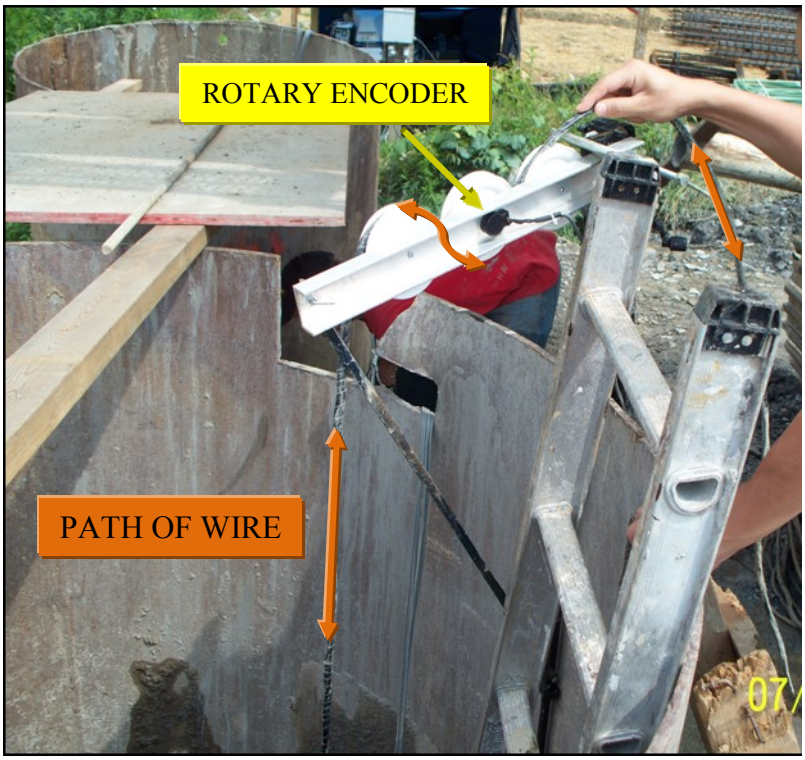

Figure 3-37 Depth tracking system for Infrared Thermal Integrity Testing.

Additionally, a digital rotary encoder, integral with a pulley system, was used to track the depth of the probe during the exploration, shown in Figure 3-37. As the wire was fed through the three-pulley system to allow the probe to descend/ascend down/up the conduit pipe, the calibrated rotary encoder was

used to track the travel of the probe, which corresponds to the depth of the probe at any given time. The instruNet Model 100 data acquisition system with instruNetWorld software was used to collect temperature and depth data during the testing. A sample of the processed data from one pass down the temperature sensing tube can be seen in Figure 3-38.

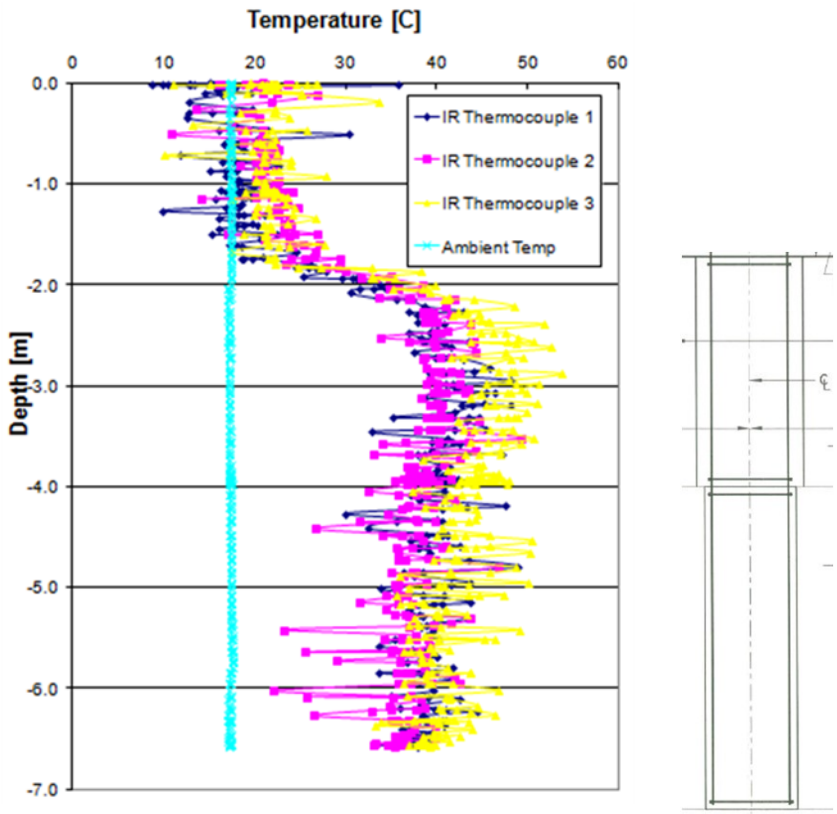

Figure 3-38 Infrared Thermal Integrity Testing results from B Modified Caisson #2; Tube #2 @ 20 hrs after casting.

A distinct rise in the temperature was observed using the infrared thermometers. However, there is a considerable amount of scatter in the readings, so much so that it would be difficult to pinpoint any particular defects in the caisson based on this data. While it is believed that there is still merit in this technique as a non-destructive evaluator of caisson integrity, it is apparent that modifications to the equipment and/or techniques used in the field for this investigation are necessary for obtaining truly meaningful results.

3.5.4.2 Cross-hole Sonic Logging of Caissons

After at least five days of curing, an outside contractor tested all caissons for both abutments with cross-hole sonic logging (CSL) using three tubes per caisson. Figure 3-39(a) shows a typical log of the CSL testing of an SCC caisson and Figure 3-39(b) shows a typical log of the CSL testing of a Class B Modified caisson. It was reported by the testing agency that no defects or anomalies were detected within the testing limits for any of the six caissons. All six were deemed to be in "Good" condition using Olson Instruments' CSL Condition Rating Criteria, meaning that no signal distortion or decreases in signal velocity greater than 10% were observed in the logs.

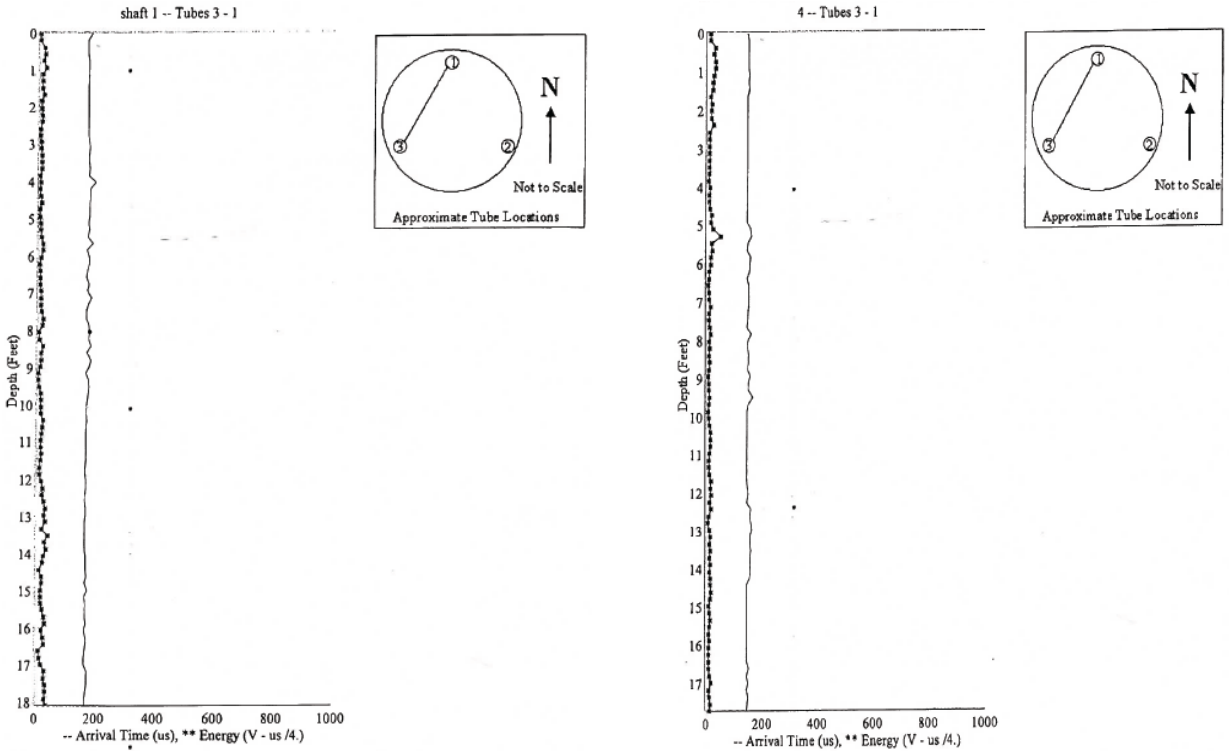

(a) **(b)**

Figure 3-39 Typical CSL results for (a) SCC-1 and (b) B Modified caissons.

3.5.5 Initial Field Data

As was mentioned at the beginning of Section 3.5, both thermal data and strain data were collected for the first 48 hours after casting both sets of caissons. This will be presented in the next two subsections.

3.5.5.1 Thermal Data

The temperature data collected from the thermal loggers of the heavily-instrumented SCC-1 and B Modified caissons is shown respectively in Figure 3-40 and Figure 3-41. When comparing the SCC-1 sensors located approximately 2", 4" and 6" from the outside of the caisson, respectively, a noticeable temperature gradient can be seen, even within that small distance. Furthermore, it is apparent when comparing these two figures that the traditional B Modified mix design has a higher peak temperature than the SCC-1. When comparing the temperatures from the 4" sensor, the peak B Modified reading is approximately 12^{o}F higher than the SCC-1 reading; communication with the innermost temperature logger, #42, was lost, but one would expect to see a similar discrepancy between the temperature profiles had that data been recovered.

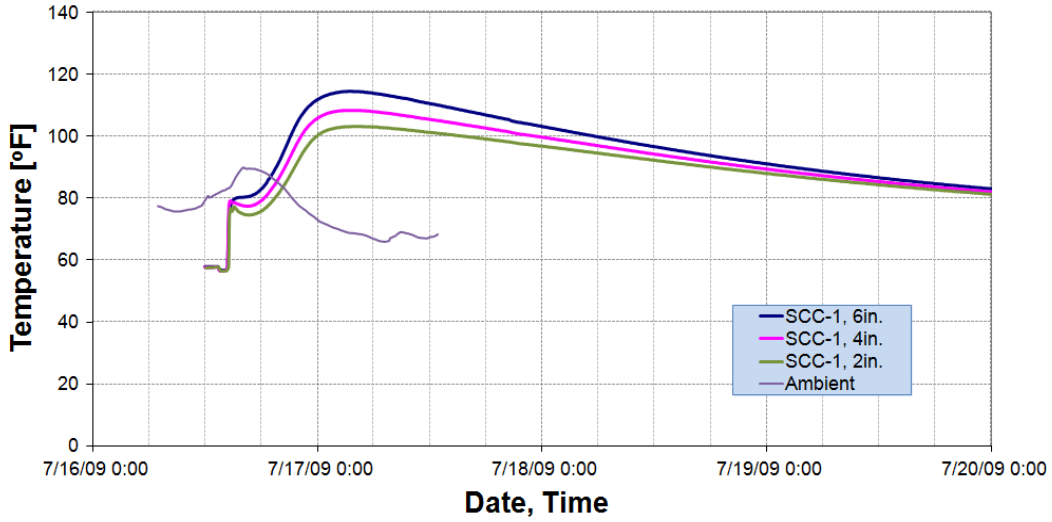

Figure 3-40 Temperature from Thermal Loggers, SCC-1 Heavily-Instrumented Caisson.

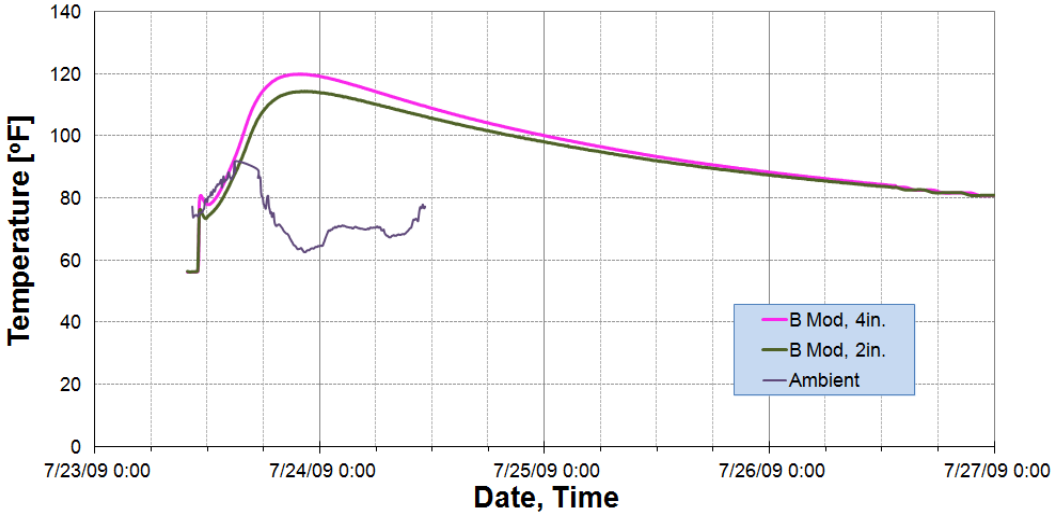

Figure 3-41 Temperature from Thermal Loggers, B Modified Heavily-Instrumented Caisson.

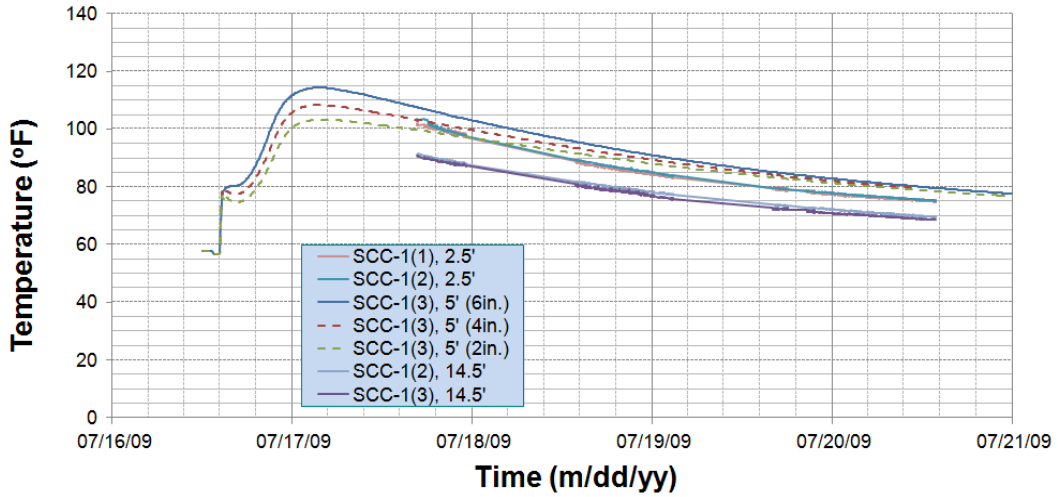

Figure 3-42 Comparison of all thermal data for SCC-1 caissons, Stalnaker Run Bridge.

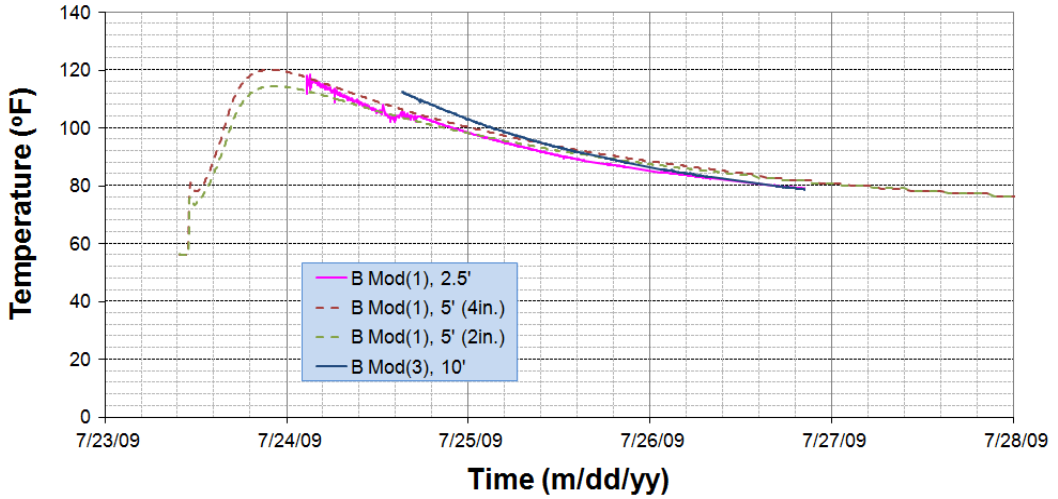

Figure 3-43 Comparison of all thermal data for B Modified caissons, Stalnaker Run Bridge.

The temperature data collected from the analog temperature sensors provided reliable data in only 6 of the 18 cases for the sensors used on the bridge, with others losing connectivity or shorting out. The analog data is presented in comparison with the thermal loggers for the SCC-1 and B Modified caissons in Figure 3-42 and Figure 3-43, respectively. It can be seen from the data presented in Figure 3-42 that the maximum temperature differential observed along the depth of the SCC-1 caissons was the

approximately 17°F difference seen between sensors in Caisson 3. Not enough useable temperature data was collected from the analog thermal sensors in the B Modified caissons to make a similar observation.

While the analog temperature sensors may be a useful, inexpensive means for conducting this type of investigation in the future, more measures are necessary with this technology to assure the longevity and protection of these sensors prior to doing so, especially in wet environments.

3.5.5.2 Strain Data

The strain data collected show limited information from the first three days after placement of each type of concrete. In the case of the SCC-1 caissons, inclement weather conditions contributed to multiple system shutdowns, as well as significant losses of data, so data collected was somewhat sporadic, as shown in Figure 3-44. The gages for the SCC-1 caissons were also re-zeroed approximately 10 hours after the end of construction, right around the time when the concrete temperature was peaking. The more complete history of the B Modified caissons is shown in Figure 3-45; data collection for these began immediately with no unexpected losses or power outages occurring at the onset.

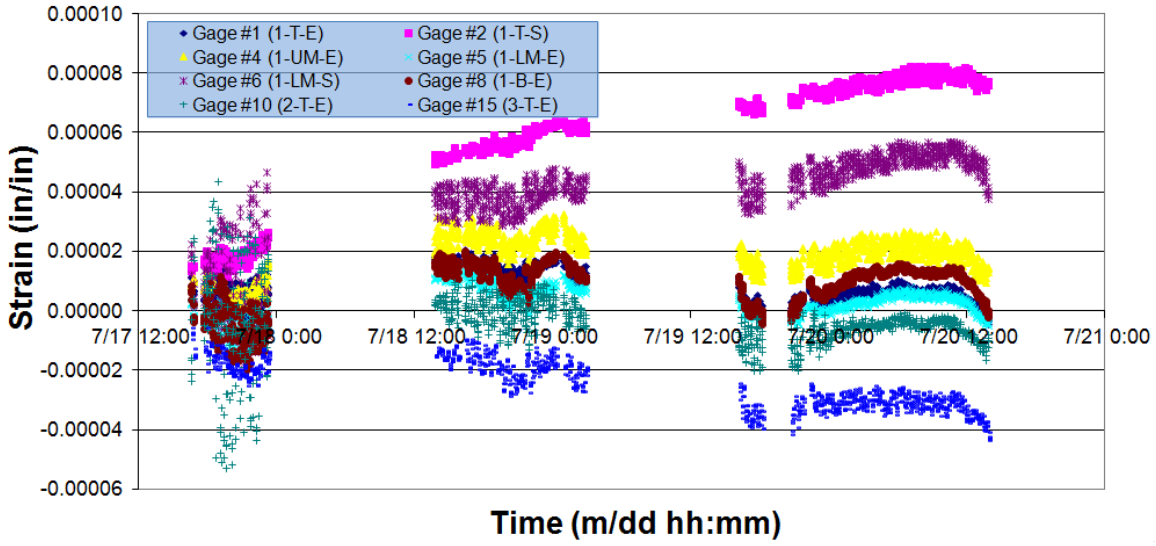

Figure 3-44 Strain data collected from SCC-1 Caissons.

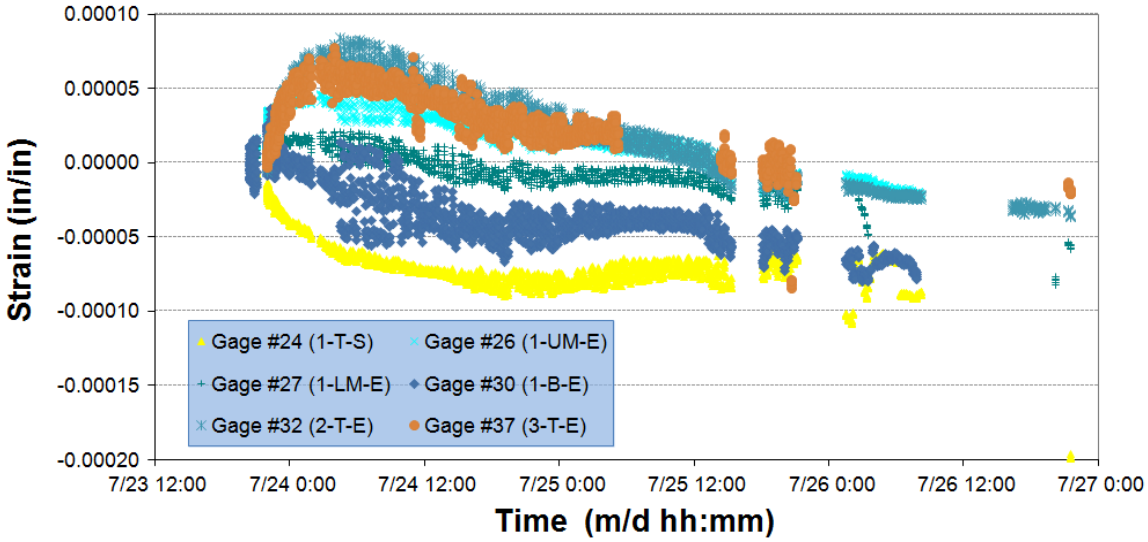

Figure 3-45 Strain data collected from B Modified Caissons.

Since these members were not exposed to any external forces, the internal strains experienced came as a result of thermal effects and concrete shrinkage. In the SCC-1 caissons, the readings ranged from -40 to 80 με after three days, while in the B Modified caissons these ranged from -90 to 90 με after three days.

3.5.6 Hardened Properties of Caisson Concrete

Compressive strength (ASTM C39) development curves for the final approved SCC mix, the trial caisson SCC, and both types of concrete for the bridge caisson castings are shown in Figure 3-46. Similarly, split tensile strengths (ASTM C496), modulus of elasticity values (ASTM C469), rapid chloride permeability test (RCPT) results (ASTM C1202, see also APPENDIX B.1), and freeze-thaw durability characteristics (ASTM C666; see also APPENDIX B.2) for these concrete batches are summarized in Table 3-12. In addition, the total shrinkage (ASTM C157) development trends of the trial caisson and the field batches can be seen in Figure 3-47. Each value shown in Figure 3-46, Table

3-12 and Figure 3-47 represents a mean value obtained from at least three different specimens, with the exception of the freeze-thaw results, which is derived from only two specimens.

It can be seen from Figure 3-46 that all mixes, including all B Modified caisson batches, exceed the required design 28-day compressive strength of 4,500 psi (31 MPa). It is also evident from comparing the 1-day compressive results of SCC Truck 2 to those of the final project mix that the early temperature exposure did have an effect on the development of the hardened properties of the field specimens.

From this small sample size, more truck-to-truck variability was seen among the compressive strengths of SCC than those of the traditional caisson concrete; the range of 28-day strengths for the two SCC batches appears to be almost twice as much as that for the three traditional batches. Truck 1 of the traditional mix exhibited the highest Modulus of Elasticity (Table 3-12), but there was not a significant difference in the average measured modulus of any of the other specimen groups taken from the field.

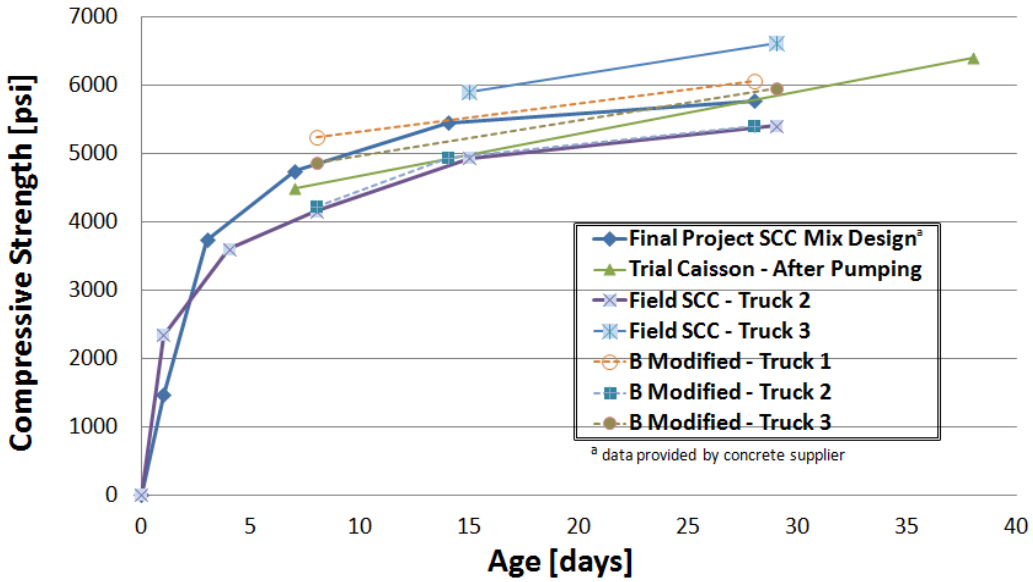

Figure 3-46 Compressive strength development curves for caisson concrete.

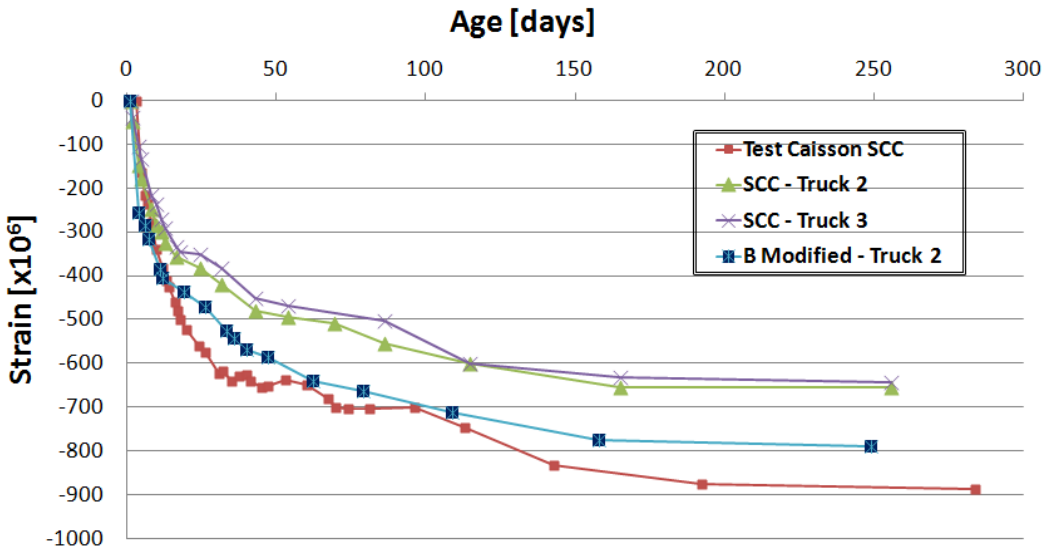

Figure 3-47 Total shrinkage trends for caisson concrete.

Table 3-12 Hardened properties of caisson concrete.

Hardened Property	Lab SCC	Field SCC	B Modified		
	Trial Caisson	Truck 2	Truck 1	Truck 2	Truck 3
Modulus of Elasticity, ksi (GPa)	4,760 (32.8) @ 38 days	4,400 (30.4) @ 29 days	4,910 (33.8) @ 28 days	4,420 (30.5) @ 28 days	4,370 (30.2) @ 28 days
Split Tensile Strength, psi (MPa)	517 (3.57) @ 38 days	432 (2.98) @ 29 days	566 (3.90) @ 28 days	494 (3.40) @ 28 days	597 (4.12) @ 28 days
RCPT- Total Charge Passed (coulombs)	1439 @ 140 days	1906 @ 112 days			
Freeze-Thaw Durability Factor			96.7% / 98% 300 cycles @ 15 mo.		

The measured splitting tensile strengths of the field SCC were lower than the traditional mix. The SCC for the trial caisson exhibited a substantially larger splitting tensile strength than the Truck 2 SCC mix, thought, so one could conclude that the elevated initial temperature of the field SCC specimens had an adverse effect on the splitting tensile strength of the mature concrete. The RCPT results for both field SCC batches tested would classify as low permeability concrete per ASTM C1202, and the Durability Factors obtained from freeze-thaw testing would indicate that the SCC-1 is freeze-thaw durable.

The shrinkage data in Figure 3-47 also shows that the field SCC exhibits a lower total shrinkage than the other three mixes, and that the two field SCC mixes exhibited similar shrinkage strains. One would expect the SCC, with the higher cement content, to undergo more shrinkage than the B Modified concrete (Heirman, et al. 2008), as was the case with the trial caisson mix. It is apparent from this, along with the comparison of the field SCC to the trial caisson SCC of the same mix design, that the initial environmental exposure had a significant influence on the overall shrinkage results of the SCC field specimens.

3.5.7 Durability Characteristics of Caisson Concrete

The durability characteristics assessed for the caisson concrete included testing of the freeze-thaw durability and the rapid chloride permeability testing. These will be discussed individually in this section.

3.5.7.1 Freeze-Thaw Durability of Caisson Concrete

Two 3”x4”x16” prisms were cast during the caisson construction using SCC-1 for the purpose of freeze-thaw testing in accordance with ASTM C666. These specimens were water cured until the start of testing, which commenced approximately 15 months after caisson construction. Testing followed Procedure A of ASTM C666 (samples remained surrounded by water throughout freezing and thawing), and each specimen was placed in its own container such that it could be surrounded by the desired amount of water.

The test setup and procedures described in Appendix B.2 were followed for the testing. Periodic testing was done of the SCC-1 specimens, starting after 30 cycles, and every 30 cycles thereafter until 300 cycles was reached.

The changes in the relative dynamic moduli calculated using the fundamental transverse frequencies for the two SCC-1 specimens can be seen in Figure 3-48, and those calculated using the fundamental longitudinal frequencies can be seen in Figure 3-49. Very similar trends were seen when calculating this value using the different frequencies for this calculation, as can be seen when comparing these two figures.

Both sets of data would indicate that the SCC-1 used in the construction was sufficiently freeze-thaw durable. The average durability factor, DF, calculated using the transverse frequencies was 96.7% after 300 cycles, and an average DF of 98% was calculated using the longitudinal frequencies after 300 cycles.

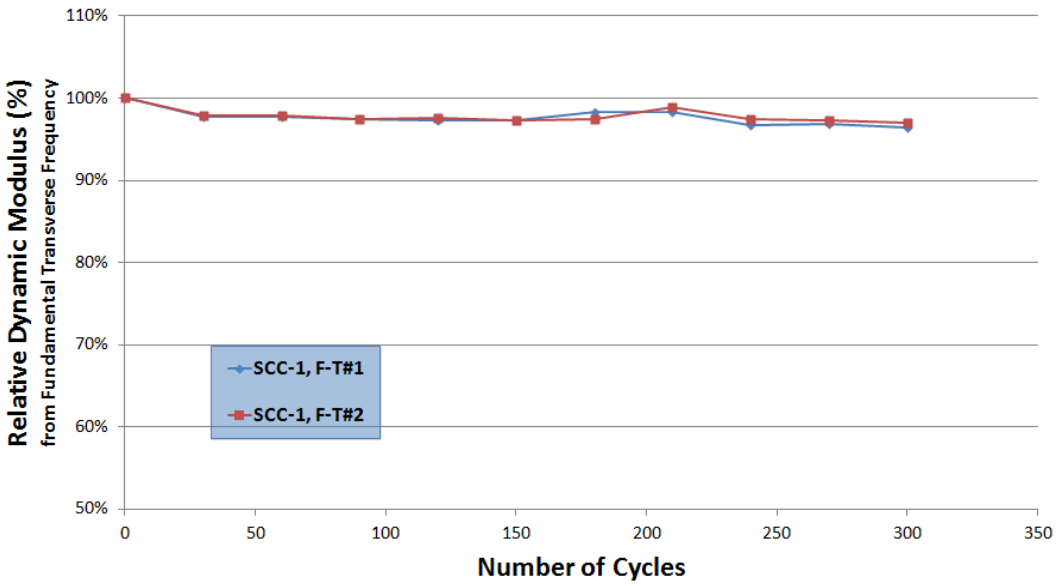

Figure 3-48 Relative dynamic moduli of SCC-1 caisson specimens based on fundamental transverse frequency measurements.

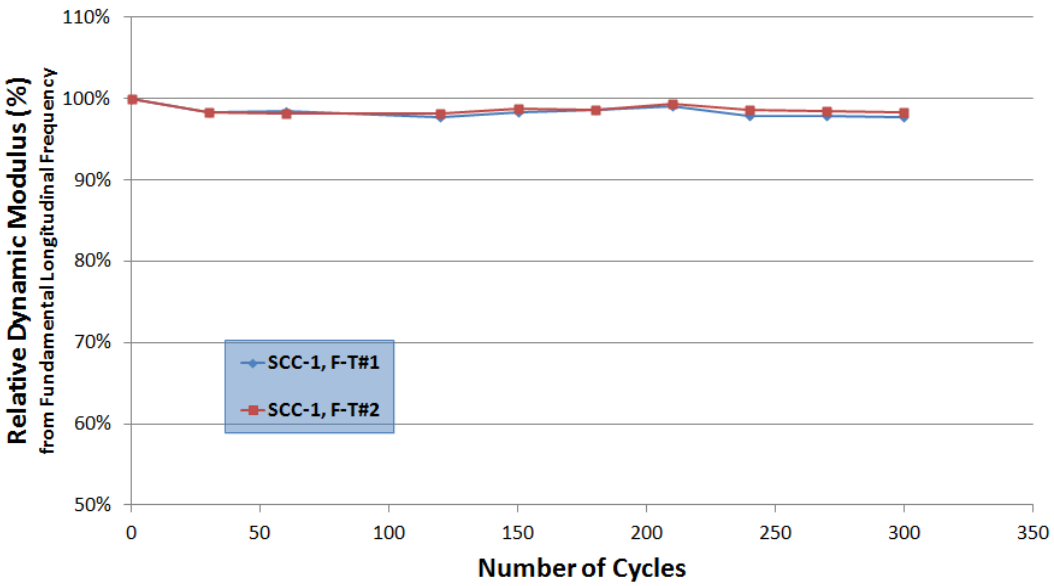

Figure 3-49 Relative dynamic moduli of SCC-1 caisson specimens based on fundamental longitudinal frequency measurements.

3.5.7.2 Rapid Chloride Permeability of Caisson Concrete

The procedures described in Appendix B.1 were used to test the rapid chloride permeability of specimens collected from the field during caisson construction. Specimens cast using both types of concrete specimens were tested. SCC-1 specimens were tested at approximately 45 days after casting. No B Modified specimens were cast during the construction for the purpose of RCPT testing, so specimens from a batch with the same mix design that was delivered at a later date were used as a basis of comparison. The results from the RCPT testing of the SCC-1 field specimens and the B Modified mix can be seen in Table 3-13.

Two of the three SCC-1 samples would be rated as "low" permeability by ASTM C1202, with the other being "moderate" permeability. The B Modified specimens exhibited slightly higher permeability than the field SCC-1 specimens, with all three being classified as "moderate" permeability under the same criteria.

Table 3-13 Results of Rapid Chloride Penetration Testing on caisson concrete samples.

	Age at Time of Testing [days]	Initial Current [mA]	Total Charge Passed [Coulombs]	Penetration Depth [cm]
SCC-1 (1)	111	65	1822	0.716
SCC-1 (2)	112	84	2283	0.973
SCC-1 (3)	113	60	1612	0.648
B Modified (1)	215	87	2294	1.367
B Modified (2)	313	79	2541	1.511
B Modified (3)	315	98	3335	1.392

3.6 Summary of Findings from Caisson Portion of Study

An SCC-1 mix design was developed for use in casting the laboratory trial caisson, as well as for the three SCC caissons for the Stalnaker Run Bridge. The fresh properties for the mix, as provided by the concrete and admixture suppliers, included a 23-inch (584mm) spread, a j-ring value of 0, and an air content of 5.5%. It is noted that although blending of more than one type of aggregate was permitted by the project specifications, this mix design utilized only #67 aggregates for the sake of simplicity and ease of production, but including an aggregate blend could help densify this mix, in turn reducing the amount of cementitious materials necessary and improving performance (Nanthagopalan and Santhanam 2009).

3.6.1 Trial Caisson Results

Prior to using SCC-1 concrete for the caissons of the Stalnaker Run Bridge, a trial caisson apparatus was devised such that the wet hole conditions of the field application could be reasonably simulated in the laboratory using a novel approach. One of the key features to the trial caisson experiment was the development of a novel "fresh core" sampling method, in which concrete specimens are removed from concrete-filled formwork while still in the fresh state, allowing the trial caisson testing apparatus to be reusable and relatively inexpensive. The fresh coring technique is possible in this

particular SCC mix design because of its suitable mix proportion quantities and favorable consistency; testing would need to be conducted to determine whether the technique would be feasible for TVC or even SCC mixes with higher packing densities, though.

Investigation into the uniformity of the SCC after placement into the trial caisson formwork revealed disparities between aggregate contents at different locations, particularly for the samples taken from outside of the rebar cage, indicating that blocking of aggregates likely occurred during placement. The percentage of coarse aggregates, by cross-sectional area, typically ranged from 35% to 45%; the uppermost specimens from the cores taken from outside the cage had less than 10% coarse aggregate.

Accompanying the differences in aggregate content were variations in hardened properties by location, particularly chloride permeability and compressive strength. Most of the RCPT specimens from the trial caisson would exhibit Moderate Chloride Ion Penetrability per ASTM C1202, with two cores exhibiting Low Penetrability and one exhibiting High Penetrability. Compressive strengths ranging from 5,180 psi to 8,240 psi, with no discernable tie between the compressive strength and aggregate content at any particular location. The Ultrasonic Pulse Velocity test results ranged from a low of 3,940 m/s to a high of 4,760 m/s. For the most part, results did exhibit an increase in pulse velocity with an increased aggregate content. Aside from the pulse velocity results, however, observed differences in hardened properties do not necessarily correlate to the aforementioned aggregate content, so the aggregate blocking would not necessarily be detrimental to the in-situ performance of the concrete. The amount of blocking that occurred during the trial caisson experiment was also compounded by the fact that the spacing of longitudinal rebars in the cage for the experiment was only about one-half of what would be used in the field.

3.6.2 Field Implementation of Caisson Concrete

SCC-1 was used for the three caissons cast beneath Abutment 1 of the Stalnaker Run Bridge, while a WVDOH Class B Modified concrete mixture was used for the three caissons for Abutment 2 one week later; both involved casting into wet-hole conditions using a tremie pipe with a pump truck. The casting of the SCC-1 caissons consisted of four deliveries of concrete occurring over a period of about five hours, whereas the casting of the B Modified caissons only took three truckloads and was finished in approximately three hours. Lack of experience of those conduction and overseeing the acceptance testing of SCC-1 and those making on-site adjustments to the admixture content, combined with the concrete supplier's self-imposed limitation on the volume of SCC that their trucks could carry, led to these delays. However, it is believed that delays such as these could be overcome with increased familiarity with the product, testing procedures, and delivery methods.

Various methods were utilized in attempt of assessing the uniformity of concrete after placement. Based on preliminary laboratory investigations, it is noted that the pH of the pore water of concrete can help determine the extent to which the concrete mixed with groundwater during placement. Although on-site data collection was insufficient to draw solid conclusions in this regard, it is believed that this technique warrants further investigation. Field data collected during Infrared Thermal Integrity Testing exhibited too much scatter to provide any evidence of voids in the member, but slight adjustments to the equipment and procedures are believed to be sufficient to provide meaningful results in this regard. Third-party Crosshole Sonic Logging testing did not reveal any abnormalities within the concrete caissons of either bridge abutment.

3.6.3 Hardened Properties of Caisson Concrete

Both SCC-1 and the Class B Modified mixture had 28-day design strengths of 4,500 psi. Cylinders taken from the field indicate that the compressive strengths of both types of concrete delivered

surpass this project requirement by at least 500 psi. Modulus of elasticity testing revealed no discernable difference in the stiffness of the two types of concrete, although splitting tensile strength tests indicate that SCC-1 had a lower tensile strength than the B Modified mixes. Rapid Chloride Permeability Testing of two of three SCC-1 specimens indicated a "low" permeability, with the third being classified as "moderate" permeability; RCPT testing of concrete with the same mix design as the B Modified concrete used for caisson construction would be classified as "moderate" permeability. Freeze-thaw durability of SCC-1 specimens indicated good freeze-thaw durability, with Durability Factors of 97% to 98%.

4 Precast/Prestressed Box Beams

The superstructure for the Stalnaker Run Bridge was comprised of five prestressed box beams supporting an integral deck. The beams had identical specifications for geometry, reinforcement layout, prestressing forces, and concrete strength requirements. Beam outer dimensions were 48 in. wide by 17 in. tall, as shown in Figure 4-1(a), which shows the outer dimensions and strand pattern as indicated by the fabricator's shop drawings. It can be seen that each beam had a total of twenty-nine (29) ½-diameter, low-relaxation seven-wire strands, which were located in three rows; each strand had an initial tension of 3,200 psi, with some being debonded for 6, 8 or 10 feet. A chamfered 38 in. wide by 6 in. tall void is present in the center of the cross section, and along the length of most of the beam, as shown in Figure 4-1(b) and (c); the absence of this void creates an approximately 10 in. long diaphragm in the center of the beam, as well as 45 in. long solid end sections. The concrete to be used for fabrication of the beams was to have a compressive strength of 6,000 psi at the time of detensioning, as well as a 28-day compressive strength of 8,000 psi.

It was decided to use SCC to fabricate two of the bridge beams, while the other three would be fabricated using a traditional prestressed concrete mix design. The two SCC beams were to be placed adjacent to each other on one side of the bridge, while the traditional concrete beams would be placed on the opposite side of the bridge as well as in the center, as shown in Figure 4-2. Additionally, a third SCC beam would be manufactured and shipped to WVU facilities for testing.

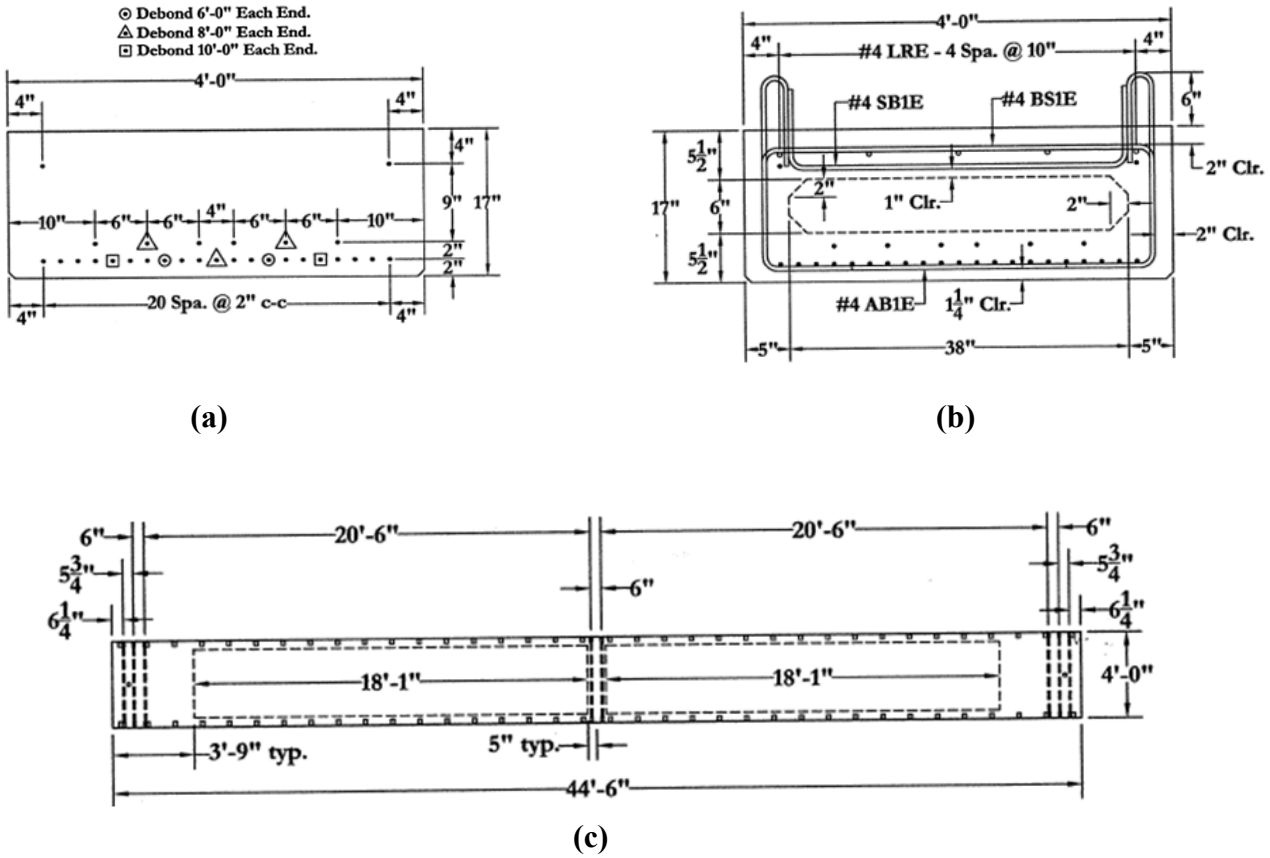

Figure 4-1 Prestressed box beam details, as provided by fabricator: (a) Cross-section detailing strand pattern; (b) cross-section detailing void dimensions; and (c) plan view of beam design.

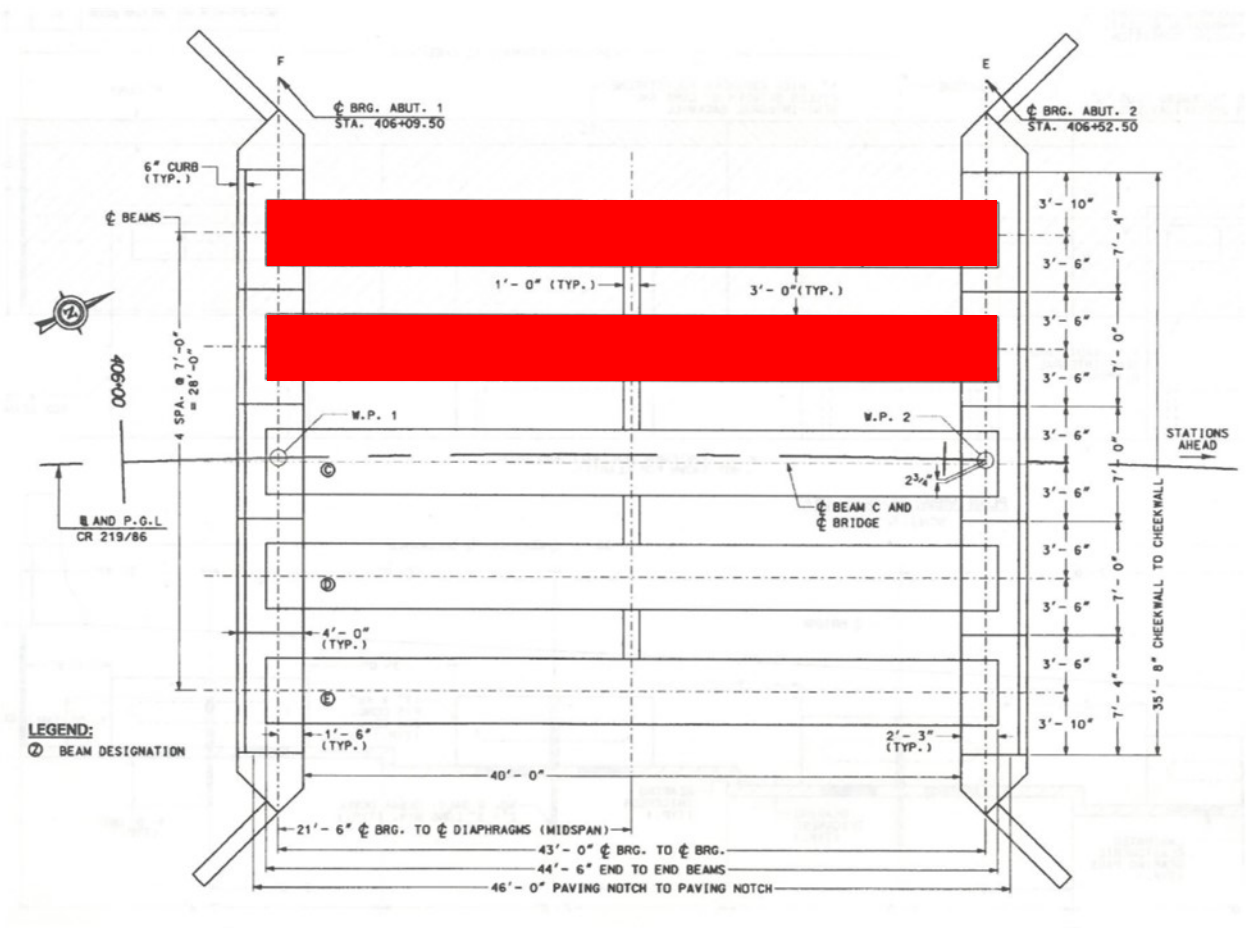

Figure 4-2 Plan view of Stalnaker Run Replacement Bridge, from project plans. Shaded areas indicate prestressed box beams fabricated using SCC.

4.1 Research Approach for Precast/Prestressed SCC

As was the case for implementing SCC for the cast-in-place caissons of the Stalnaker Run Bridge Replacement that were discussed in Chapter 3, the researchers' experiences with SCC along with the pertinent information presented in Chapter 2 was used to devise a research plan for implementing SCC for the precast/prestressed box beams. Special Provisions were developed to communicate the material, testing and performance requirements of the precast/prestressed SCC to the contractors and WVDOT officials. Researchers provided some assistance in development and testing of the

precast/prestressed SCC, but again the contractor was ultimately responsible for submission of the mix design and testing information to WVDOT for final mix design approval prior to use on the bridge.

With the caisson portion of this study, a trial caisson section was devised to ensure adequate performance of the caisson SCC. Instead of a mock section for the precast/prestressed beam SCC, a full-scale bridge beam was cast in order to assess the performance of the SCC beams. This was cast at the same time as the SCC box beams that were to be used on the Stalnaker Run Bridge. All beams, including the TVC beams for the Stalnaker Run Bridge, were instrumented with temperature, humidity and strain sensors at a time when the reinforcement for the prestressed beams was being secured in the casting bed prior to casting.

Temperature and strain measurements were recorded throughout the casting and detensioning processes. Maximum temperatures were compared to the maximum allowable temperatures prescribed by PCI. Strain profiles and camber at detensioning were compared to theoretical values to assess the validity of existing design guidelines when dealing with SCC. Test specimens were taken during casting to evaluate and compare the hardened properties of the TVC and the SCC, particularly the compressive and tensile strengths, stiffness, shrinkage and permeability characteristics of the mixes.

The laboratory beam was subjected to a barrage of testing, including destructive load testing and non-destructive modal analysis. The destructive testing was done in stages, with an increasing amount of load applied and released such that each subsequent loading would increase the damage state of the beam. The modal analysis was done in between destructive tests in order to determine the extent to which the mode shapes of vibration are indicative of the damage state of the beam. Strain, load and deflection data were collected throughout the destructive loading of the beams such that the observed behavior could be compared to the theoretical behavior of the beam; this included a comparison of observed load-deflection behavior to the theoretical behavior when (1) the parameters used for the

theoretical calculations include the original design characteristics of the beam, and (2) the parameters were refined based upon the measured material properties and observed characteristics of the beam.

4.2 Special Provisions for Precast/Prestressed SCC (SCC-2)

It was necessary to write guidelines that could be inserted into the project documents in order to communicate the requirements of SCC for precast/prestressed beam fabrication to contractors, inspectors and Division personnel. These included adaptations to current WVDOT construction practices, as well as prescription of new testing to be done in order to ensure satisfactory behavior of the beam SCC; these appeared in the project documents in the form of Special Provisions as well as addendums to the General Notes for the project. Efforts were made to present these in such a manner that would promote equal opportunity for all potential fabricators to bid on this project.

For the sake of clarity, the SCC mix design for the caisson portion of the Stalnaker Run Project was deemed SCC-1 in the project documents, while the SCC mix design for the beams was deemed SCC-2. These designations will be conformed to within this chapter as well as throughout the report in its entirety.

The project provisions for SCC-2 were devised based on the researchers' previous laboratory experiences with SCC as well as recent guidelines for the use of SCC for precast/prestressed applications. The main points of these will be discussed in this section; guidelines for Class SCC-1 concrete were discussed in Section 3.2. The provisions, as submitted to WVDOT as recommendations for inclusion of SCC as a material for the Stalnaker Run Bridge precast/prestressed applications, can be seen in APPENDIX A.3.

The general procedure followed by the contractor for gaining approval of a prestressed concrete mix to be used in a WVDOT project, as outlined in Chapter 2, are to (1) develop a mix design based on project requirements and Section 603 of the Standard Specifications, (2) perform necessary testing of the

mix and submit results to gain Department approval for use, and (3) fabricate beams in accordance with Section 603 of the Standard Specifications (West Virginia Department of Transportation 2000). Section 603 specifies that either an independent laboratory or PCI certified plant personnel should execute Steps 1 and 2 of this process.

This general procedure was maintained in the Special Provisions, but with supplemental clauses that are specific to the use of SCC. However, in light of the inherent differences between hardened properties of SCC and TVC, and to ensure better quality control for the first use of SCC on a WVDOT project, the mix qualification process was expanded to include a modified version of MP711.03.23 such that more testing would be done for the SCC than typically required of other prestressed concrete mixes.

4.2.1 Material Requirements

Any differences in mix components and quantities that result from the use of SCC-2 had to be outlined in the Special Provisions. Since viscosity modifying admixtures (VMAs) are not typically used for traditional concrete, but were not addressed in the WVDOT Standard Specifications, it was noted in the Special Provisions that use of a VMA for the SCC-2 was permissible so long as appropriate documentation was submitted to the Division; these requirements were written into the addendum to Section 707 of the Standard Specifications.

Table 4-1 Mix requirements for Class SCC-2 concrete used for the Stalnaker Run Bridge Project.

Class of Concrete	Compressive Strength @ Release [psi]	Design 28 Day Compressive Strength [psi]	Maximum Water Content [gal/bag cement] *	Entrained Air **[%]**
SCC-2	6000	8000	4 ¾	**5**

***An equal volume of pozzolanic additive may be substituted for Portland cement up to the maximum amount in Table 4-2 Upper limits on supplementary cementitious material quantities for Class SCC-2 concrete.. When using pozzolanic additives, volumes of these materials shall be considered as cement for purposes of establishing maximum water content.**

A summary of material information and mix proportion information for SCC-1 is shown in Table 4-1 and Table 4-2. The maximum size of coarse aggregate was limited to ¾ in., with #67 gradation being permissible provided all aggregate pass the ¾" sieve. Blending of aggregate gradations to increase stability of the mix was permitted to help increase the stability of the SCC mix, although it was required that the aggregate blend contained one gradation having a maximum aggregate size of ¾ in. Although not shown on either of these tables, the maximum permissible ratio of fine aggregate to total aggregate, FA/TA, for SCC-1 was 0.5. The amount of water was also limited to 4.75 gallons per 94-lb bag of cement, which correlates to a maximum w/cm=0.42. Unlike for SCC-1, there were no limits on the maximum or minimum amounts of cementitious materials permitted in SCC-2, as it was determined that economy and performance would dictate the amount used for production.

Table 4-2 Upper limits on supplementary cementitious material quantities for Class SCC-2 concrete.

MATERIAL	QUANTITY
Fly Ash	1 Bag (15%)
Ground Granulated Furnace Slag	2 Bags (30%)
Microsilica	1/2 Bag (8%)

In addition to the material and proportioning requirements shown in these tables, the SCC-2 was to have a producer-defined target spread that was limited to a maximum of 25 in. and a J-ring value below 1.5 in. in the fresh state, as well as the project-mandated compressive strengths at the time of release of prestressing forces and at 28 days.

4.2.2 Pre-qualification of Mix Design

Prior to use during fabrication of the box beams, the SCC-2 was subject to approval by the Division. Although Section 603 of the Standard Specifications does not stipulate the use of MP 711.03.23 for mix approval of prestressed concrete, and simply refers to ACI 318 for guidance, the

Special Provisions used these procedures for the basis of acceptance of the SCC-2. The MP711.03.23 requirements were further refined in light of the different test methods and fresh behaviors of SCC.

The overall process included the creation and testing of two batches of SCC-2. As is typical practice under the MP 711.03.23, each batch was required to meet more stringent fresh property tolerances during the qualification than would be mandated for acceptance during production; these included a slump-flow [ASTM C1611] in the upper half of field tolerances [Production: Target Spread ± 2 in., Qualification: Target Spread to Target Spread plus 1 in.] and an acceptable air content within a 1% range [5.0% ± 0.5%]. Other fresh property requirements included a Visual Stability Index (VSI) [ASTM C1611], below 1.0, a T_{50} [ASTM C1611] between 2 sec. and 7 sec., a J-Ring value [ASTM C1621] below 1.0 in., and a static segregation [ASTM C1610] below 12%.

Similar to the qualification of Class SCC-1 concrete, the "workable period" was also to be determined for Class SCC-2 concrete. This included measurement of the fresh properties at an initial time, as well as every 30 minutes afterward until the measured spread fell below 15 in. The workable period would be the time period from the anticipated delivery until the interpolated time at which the spread or j-ring value was tested to be outside of the range of the field acceptance limits [2 in. below Target Spread, and 1.5 in., respectively].

For each batch, it was also required to perform hardened property testing on specimens cast from the SCC-2 at the time of initial testing. Due to the increased complexity in behavior of the prestressed concrete box beams, more hardened testing was required for SCC-2 than was required for the caisson concrete. Prescribed hardened property testing included: compressive strength; modulus of elasticity; creep, shrinkage; rapid chloride permeability; freeze-thaw durability; and bond strength.

Cylinders were to be cast from each batch and tested in compression and modulus of elasticity at the following times: one cylinder at age 24 hours; one cylinder at age 3 days; one cylinder at age 7 days;

one cylinder at age 14 days; and three cylinders at age 28 days. Three additional cylinders were also to be cast for later assessment of the hardened Visual Stability Index. The prescribed number, size, and testing schedule for the creep, shrinkage, freeze-thaw, and rapid chloride permeability tests are shown in Table 4-3. All specimens using Class SCC-2 concrete for purpose of testing compressive strength, creep, shrinkage, modulus of elasticity, freeze thaw resistance, rapid chloride permeability, hardened visual stability index (VSI) and bond with prestressing steel tendons were to be cast in a single layer with no rodding or vibration.

Table 4-3 Details of durability testing for SCC-2 mix qualification.

TEST	*TESTING STANDARD*	*# OF SPECIMENS*	*SPECIMEN SIZE*	*LOAD MAGNITUDE*	*AGE AT INITIATION OF LOADING*
Creep	***ASTM C 512***	***6***	***6" (152 mm) x 12" (305 mm) cylinders***	***40% of Compressive Strength***	***2 days***
Drying Shrinkage	***ASTM C 490***	***3***	***3" x 3" x 11"***	***Air Exposure***	***7 days***
Rapid Chloride Permeability	***AASHTO T277***	***3***	***4" (102mm) x 2" (51 mm) cylinders***	***60 ± 0.1 V***	***90 days***
Freeze-Thaw	***AASHTO T161***	***6***	***3" x 4" x 16"***	***(freeze-thaw cycles)***	***14 days***

Additional hardened property testing to be done included assessment of the bond between SCC-2 and prestressing strands. This was to be done using a simple pull-out test procedure based on the Moustafa Method (Logan 1997). Bond testing was required for both SCC-2 concrete and the traditional prestressed concrete mix for the sake of comparison.

4.2.3 Acceptance and Fabrication

The acceptance criteria for SCC-2 for use in the fabrication of the Stalnaker Run Bridge prestressed box beams is summarized in Table 4-4. The Special Provisions prescribed fresh property testing for each batch of SCC-2 produced, or at least once per 10 yd^3.

In addition to the fresh property requirements, three (3) specimens were to be cast during casting of each beam to verify that the 8,000 psi compressive strength requirement is met, and two were to be cast for hardened VSI determination. Again, these were to be cast in a single lift without rodding or tamping.

Table 4-4 Acceptance criteria for SCC-2 used for fabrication of prestressed box beams.

Spread ASTM C1611	*J-Ring Value ASTM C 1621*	*V.S.I. ASTM C1611*	*T50 ASTM C1611*	*Air ASTM C231*
Target ±5 cm (Target ±2in)	***≤3.8 cm (≤1.5 in)***	***≤1.0***	***2sec≤ T50 ≤7sec***	***5% ±1.0%***

The batching and placement operations when using Class SCC-2 concrete were to be planned to ensure that casting of the prestressed box beams is completed during the pre-established workable period of the concrete, such that no vibration of the concrete is necessary at any point during construction. Batching, transportation and delivery of the Class SCC-2 was to be planned by the Beam manufacturer such that there is a continuous feed of SCC into the formwork, and therefore, no delay between subsequent layers.

4.3 Mix Development

The contractor for the Stalnaker Run Bridge replacement project, BILCO Construction, subcontracted the fabrication work for the prestressed box beams of the bridge to Eastern Vault/American Block Company. Eastern Vault is a precast company in Princeton, WV that specializes in precast burial vaults, masonry blocks, and precast/prestressed box beams. Their facilities for beam fabrication included three casting beds, each greater than 150 ft in length; a 1.3 yd^3 central pan mixer is used for batching, and distributed to the casting beds one batch at a time in individual hoppers, via forklift. Mix development for the SCC-2 concrete was done by Eastern Vault with the assistance of their admixture supplier, BASF Construction Chemicals.

The first attempt at mix qualification was done in June of 2009, and was witnessed by WVDOT officials and WVU researchers. Since the RCPT results of the batches tested in June 2009 did not satisfy the project requirements, Eastern Vault petitioned WVDOT to allow them to alter the mix design to include silica fume. Due to impending construction deadlines, WVDOT made an allowance for use of a new mix for beam production on an "at risk" basis, provided that: (1) some early age information for the new mix design was provided to WVDOT prior to fabrication of the beams using SCC, and (2) all testing required for qualification is completed and submitted to the WVDOT. The testing conducted for the mix qualification process will not be discussed in detail in this document.

The mix components for the two prestressed concrete mixes used for production can be seen in Table 4-5. As can be seen in this table, both mixes had similar contents of total cementitious materials and similar *w/cm*, but the SCC-2 mix had a higher FA/TA ratio, employed a partial replacement of cement with silica fume, and used a different admixture combination.

Table 4-5 1-yd^3 Theoretical mix designs used for prestressed box beam fabrication.

Component	TVC PC Beam Mix[a]	SCC-2 PC Beam Mix[a]
Type III Cement[b]	785 (466)	734 (435)
Silica Fume[b]	--	58 (34)
Water[b]	279 (165)	289 (171)
Coarse Aggregate[b,c]	1808 (1073)	1443 (856)
Fine Aggregate[b,c]	985 (594)	1431 (778)
w/cm	*0.353*	*0.365*
AEA[d]	38 (315)	65 (534)
WRA 1[d]	85 (704)	--
HRWRA 2[d]	--	115 (954)
VMA[d]	--	15 (123)
Set Retarder[d]	12 (99)	16 (131)

[a] information courtesy of Eastern Vault/BASF
[b] lb/yd^3 (kg/m^3)
[c] aggregate weight in SSD condition
[d] fl.oz./yd^3 (mL/m^3)

4.4 Beam Fabrication

Fabrication of the prestressed box beams started in the middle of September 2009, approximately two months after the in-situ construction of the SCC drilled shafts, which took place in the middle of July of the same year. The three traditional prestressed box beams were cast on the 16th of September, almost one week prior to the SCC-2 box beams on the 21st. A pan mixer with a 1.3 yd^3 maximum capacity was used for fabrication, so this was the typical batch size used for the casting. Researchers instrumented the casting beds prior to fabrication and collected samples of both types of concrete during casting for later testing and comparison of hardened properties.

In total, 22 batches of SCC-2 were mixed for casting the three beams; five batches that were tested did not satisfy the fresh concrete requirements and were discarded. Table 4-6 shows results of the in-situ fresh property testing of the SCC-2 concrete, which was required to be performed at a frequency of once per beam.

The traditional box beams were constructed in multiple phases: the lower reinforcement was placed, then the lower portion of concrete was cast and vibrated, followed by the placement of the voids and the top of rebar, and finally the top portion of the concrete was placed and vibrated. Fabrication of the three traditional beams took almost one complete working day; casting began around 9am and finished after 4pm, with a half-hour lunch break following completion of the first beam. Figure 4-3 shows the casting process for the traditional beams, with the bottom portion of the concrete placed and vibrated prior to assembly of the void and top reinforcement.

The casting procedure for the SCC-2 beams was simpler than that of the traditional beams; all reinforcement and voids for the SCC-2 beams were first secured and then all concrete was placed at once without vibration. Casting of the three SCC-2 beams took about half the time of the traditional

casting, and was done in an afternoon. Placement of the concrete began at around 1 pm and ended around 4 pm. Figure 4-4 shows the fully-assembled rebar cage and void during SCC-2 beam casting.

Table 4-6 Fresh properties of SCC-2 batches measured during production of PC beams.

Test Time	Beam #	Slump Flow *(23±2in)* [in]	J-Ring Value *(<1.5in)* [in]	50 cm Flow Duration *(2-7 sec)* [sec]	VSI *(<1)*	Air Content *(4 to 6)* [%]	Concrete Temp. [°F]	Ambient Temp. [°F]	Batch Used in Beams?
13:30	1	20.5	0.5	-	0	5.6	76	64	No
13:45	1	22 ¼	0.25	2.65	0	7	76	64	No
14:00	1	22	0	(1) 2.12 (2) 1.85	0	6.8	83.2	64.5	No
14:35	1	23 7/8	1 1/8	2.00	0	5.4	83.9	65	Yes
15:15	2	21 ¼	0	(1) 2.35 (2) 2.68	0	5.5	83.9	65	Yes
16:25	3	20 ½	-	2.93	0	5.5	83.9	65	No
16:45	3	19 ½	-	1.78	0	5.5	83.9	65	No
17:10	3	21	0.25	2.5-2.22	0	5.5	83	65	Yes

The ambient conditions near the casting bed were recorded using a digital hygrochron. The temperature and humidity data collected can be seen in Figure 4-5; in this figure, the shaded regions represent the approximate periods during which the two sets of beams were fabricated. The values in this plot are not indicative of the accelerated steam curing conditions to which the beams were exposed, though, as the ambient hygrochron was not exposed to the elevated temperatures.

Release of prestressing forces was conducted after sufficient concrete strength had been achieved. After steam curing throughout the first night, the traditional concrete reached sufficient strength for removing formwork and release of prestressing force on September 17th. The SCC-2 concrete needed two nights of steam curing, and reached sufficient strength for formwork removal and prestress release on the 23rd. Steam curing operations were halted at least two hours prior to cutting in both cases. To allow for removal of the steel sidewalls of the form beds, all instrumentation wires were

temporarily disconnected. After removal of the sidewalls, all gages were then reconnected and data acquisition operations resumed prior to cutting of the strands. The strands were cut using an oxy-acetylene torch in a symmetric sequence, as specified by PCI.

Figure 4-3 Picture of concrete, void and upper rebar placement during traditional beam casting.

Figure 4-4 Pre-assembled formwork during placement of concrete in single lift for SCC-2 beams.

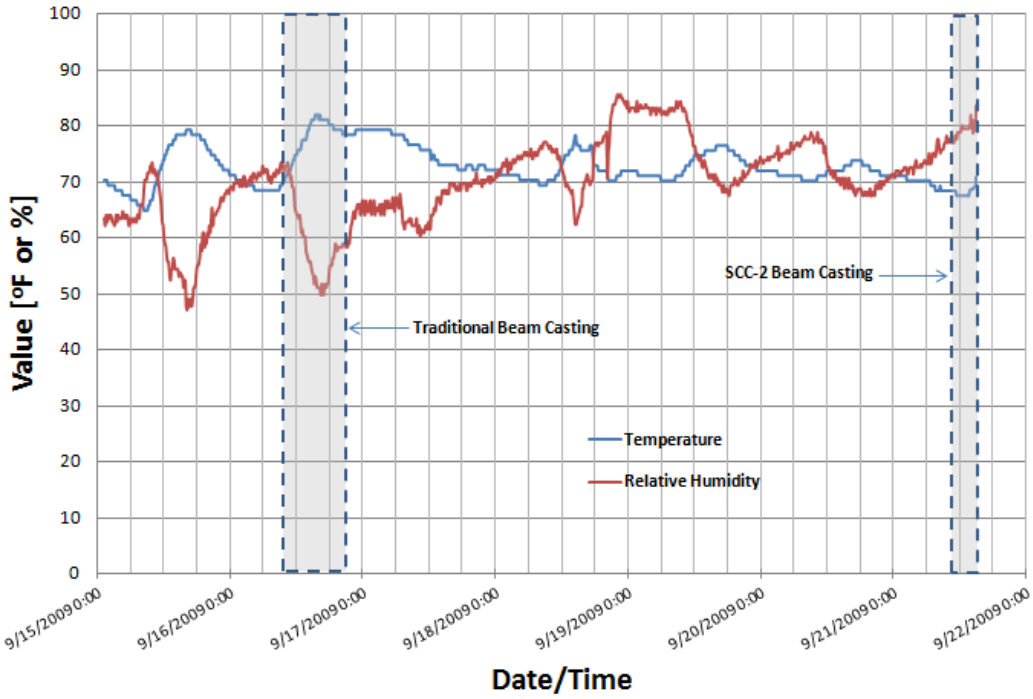

Figure 4-5 Ambient conditions near casting beds during fabrication of prestressed box beams.

Pre-installed strain gages and temperature sensors for all traditional and SCC-2 beams were monitored throughout their respective casting, curing, and detensioning. Concrete samples of both types were also collected for hardened property testing, including: compressive and splitting tensile strengths, modulus of elasticity, shrinkage, creep, rapid chloride permeability, and freeze-thaw durability. Also, some initial measurements of strand slip-in and bond development length would be taken. These will all be discussed in the subsequent sections.

4.4.1 Beam Temperatures during Fabrication

Prior to the casting of all traditional and SCC box beams, numerous temperature gages were secured into the formwork. These included both analog and data-logging temperature sensors. Each of the five beams that were to be placed on the bridge was instrumented with one logging temperature sensor, and one analog temperature sensor. The SCC-2 beam that was to be tested at WVU was

instrumented with a total of seven analog temperature sensors [Analog Devices TMP36GT9Z, as were shown in Figure 3-24], and one data logging temperature/humidity hygrochron [Embedded Data System DS1923-#F5 iButton, as were shown in Figure 3-25]. The locations of all sensors are detailed in Figure 4-6. The numbering system used for the temperature sensors can be seen in Table 4-7.

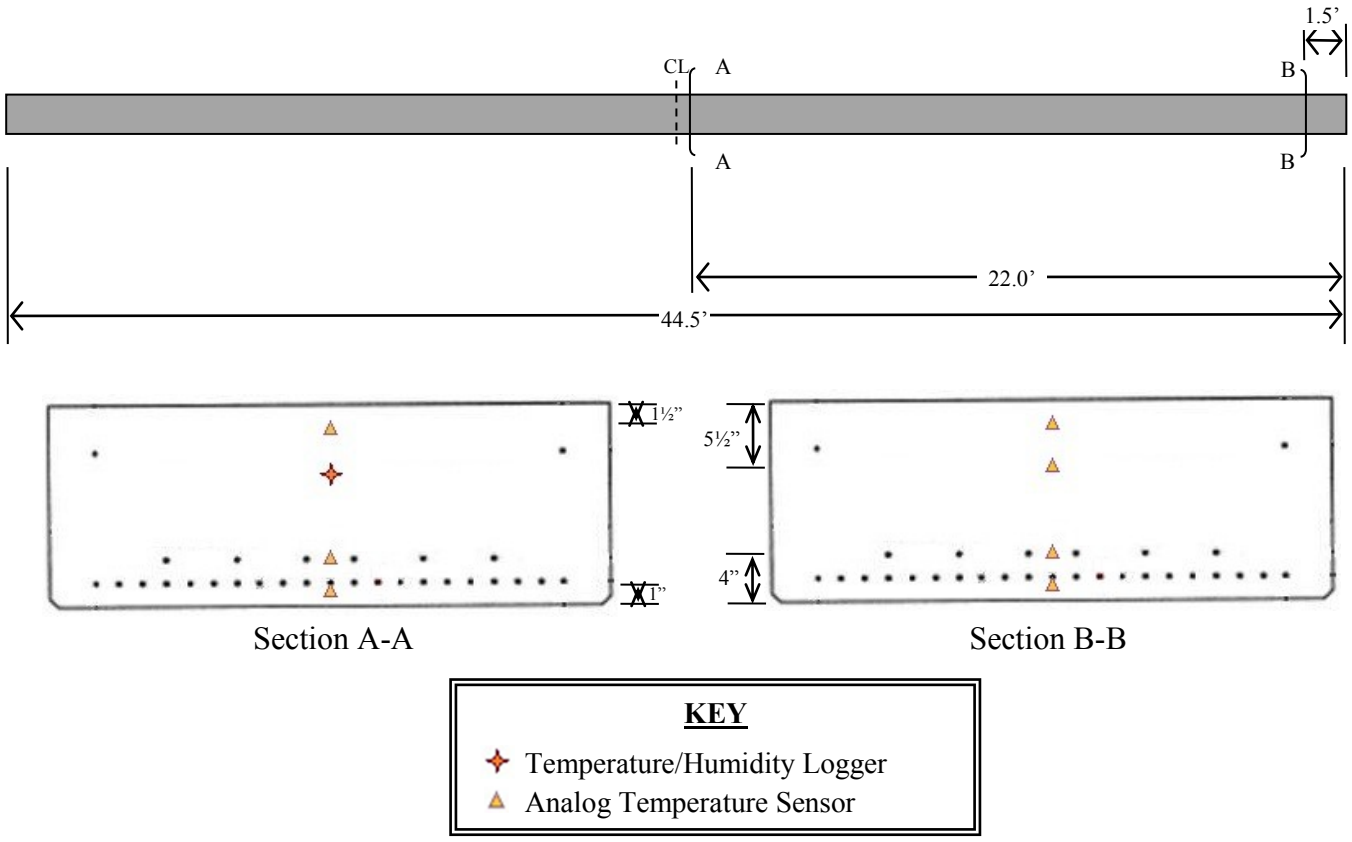

Figure 4-6 Locations of temperature sensors (where applicable), as placed during instrumentation of prestressed box beams.

Temperature readings were taken at various locations during construction and throughout curing of the SCC-2 and the traditional box beams. I-buttons that were used in each beam required no external data acquisition equipment, so data was continuously sampled at a pre-designated rate once these were initiated. Provided the I-buttons remain protected and communication could be maintained, data can be collected from the I-buttons at any time. For both sets of beams, the I-buttons were activated prior to casting, and data was collected after detensioning. Data from the I-buttons collected prior to beam

fabrication through the first five days afterward can be seen in Figure 4-7 and Figure 4-8 for the traditional and SCC-2 beams, respectively. It can be seen from these figures that some data sets are incomplete; communication with the I-button for Traditional Beam 3 was lost during beam fabrication, so no data could be collected, while data was collected only one time from SCC Beam 1 prior to losing communication with the sensor in that beam.

Table 4-7 Temperature sensor designations for prestressed beam instrumentation.

Section Designation	Gage Type & Location	Traditional Beam 1	Traditional Beam 2	Traditional Beam 3	SCC-2 Lab Beam	SCC-2 Beam 2	SCC-2 Beam 3
Section A-A	Analog, Top				SCC24		
	Hygrochron	Trad21	Trad20	Trad19[a]	SCC21[a]	SCC20	SCC19
	Analog, Mid	Trad24[b]	Trad23[b]	Trad22[b]	SCC25	SCC23	SCC22
	Analog, Bot				SCC26		
Section B-B	Analog, Top				SCC27		
	Analog, TopMid				SCC28		
	Analog, Mid				SCC29		
	Analog, Bot				SCC30		

[a] Communication with sensor lost during fabrication or curing.
[b] Lapse in temperature data due to data acquisition shut down.

Unlike the stand-alone I-buttons, the analog temperature sensors were dependent upon an external voltage supply and a data acquisition system to obtain readings. A complete set of data was recorded for the SCC-2 beams, from casting through detensioning. For the traditional beams, however, there was an unexpected system shutdown during the evening, so no data was collected for a period of about 15 hours until the system was restarted the next morning. The data collected from the analog sensors for the SCC box beams can be seen in Figure 4-9. In Figure 4-9, the readings from gages in the same location within the beams, Gages 22, 23, and 25, which are at the bottom of the 20 foot sections, are highlighted to allow for a more direct comparison of temperature trends within the different beams.

None of the observed temperatures exceeded the PCI maximum temperature of 180^0F (80^0C) (Precast/Prestressed Concrete Institute 1999). Based on the I-button data shown in Figure 4-7 and

Figure 4-8, it appears that the SCC-2 beams reached slightly higher temperatures than the traditional beams; however, based on the trends seen in the temperature data, with higher temperatures in beams cast later in the day, it is possible that Traditional Beam 3 achieved a higher peak temperature than the other two traditional beams and would have been closer to the maximum observed for the SCC beams. The measured internal temperatures for the beams at the times of detensioning were in the ranges of 130-150^{0}F for the traditional beams, and 110-120^{0}F for the SCC-2 beams.

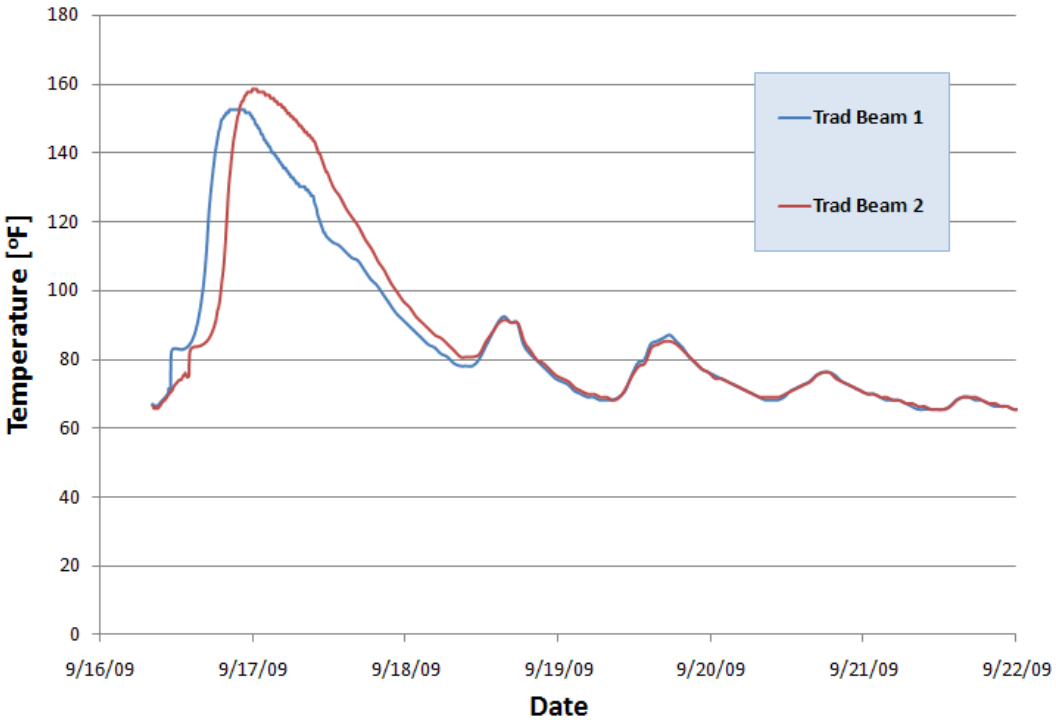

Figure 4-7 I-Button temperature data from traditional box beams during fabrication.

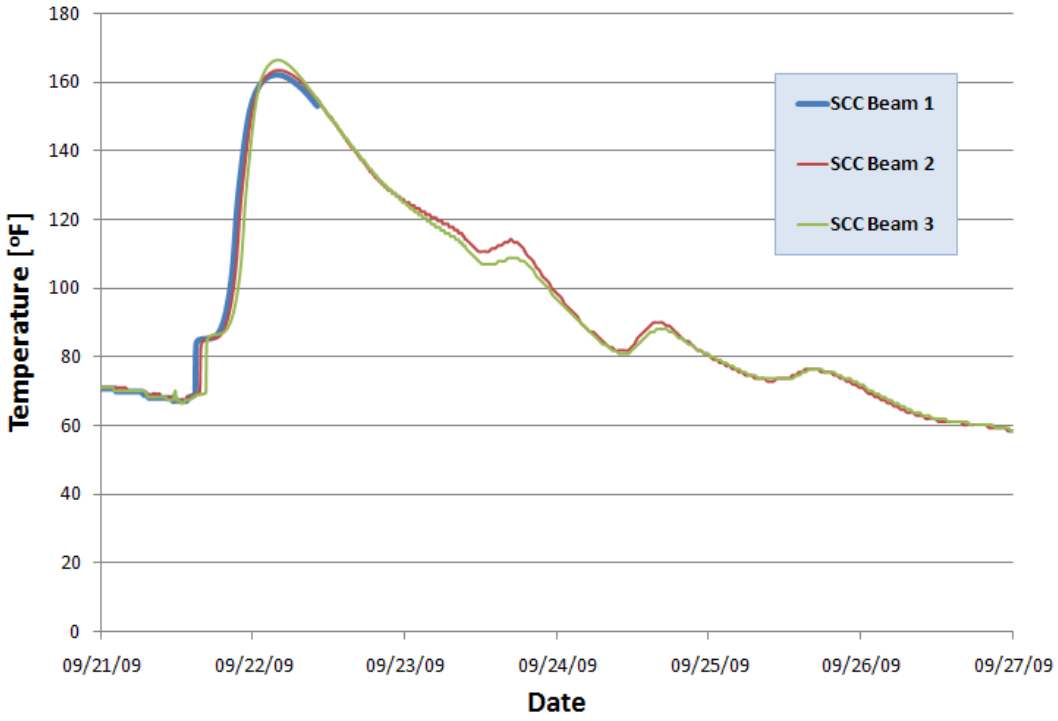

Figure 4-8 I-Button temperature data from SCC-2 box beams during fabrication.

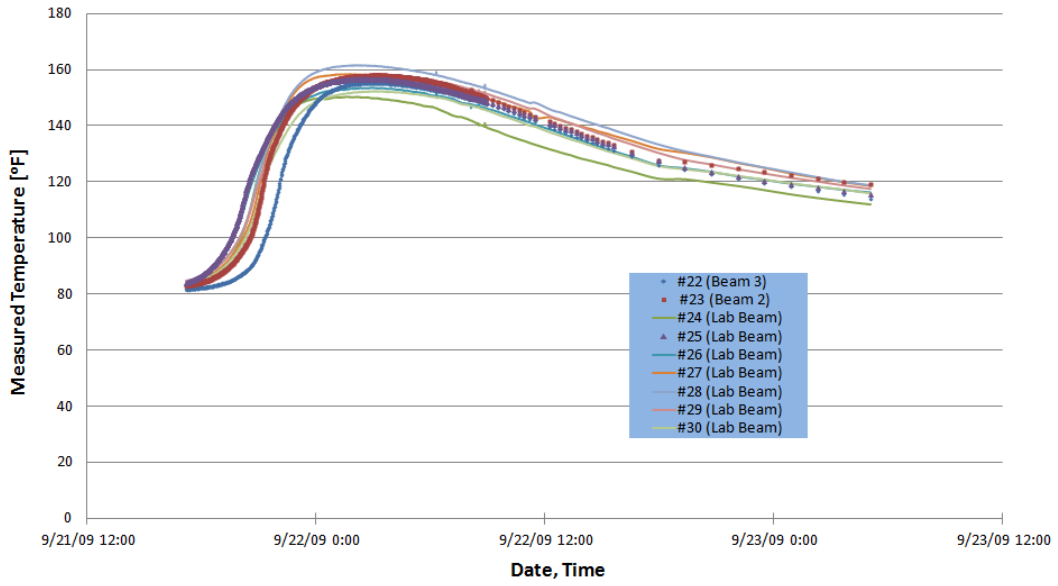

Figure 4-9 Analog temperature data from SCC-2 box beams during fabrication.

4.4.2 Strain Measurements from Fabrication

In addition to temperature instrumentation, all traditional and SCC box beams were equipped with numerous strain gages secured into the formwork prior to fabrication. These included surface-mounted strain gages located on the prestressing strands to directly measure the steel strain and embedded concrete strain gages to measure concrete strain at various places. Each of the five beams that were to be placed on the bridge was instrumented with a total of two steel strand strain gages and four embedment concrete strain gages. The SCC-2 beam that was to be tested at WVU was instrumented with a total of six embedded concrete strain gages [Vishay EGP-5-350, as were shown in Figure 3-22] and five steel strand strain gages [Omega KFG-2N-120-C1-11L3M3R, see Figure 4-10]. The locations of all sensors are detailed in Figure 4-11, while the numbering used for the strain gages for all beams can be seen in Table 4-8.

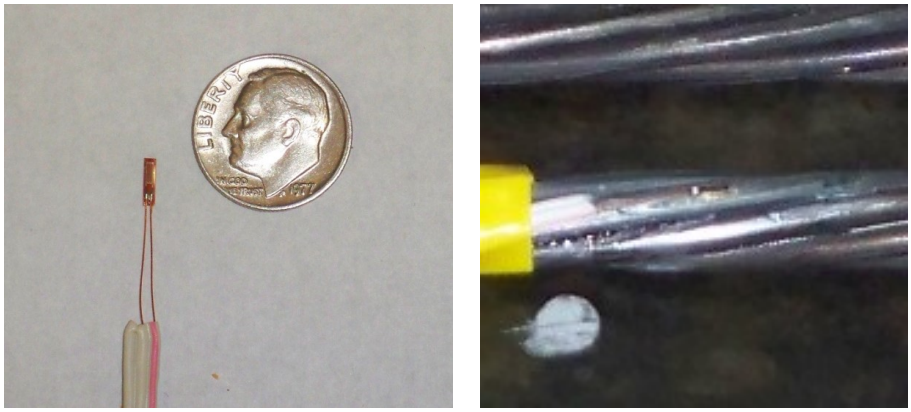

Figure 4-10 Foil strand strain gage, before and after mounting on prestressing strand.

The strand strain gages used were prewired strain gages with steel temperature compensation. All strand strain gages for the SCC and TVC beams were affixed to the prestressing strands using Micro-measurements M-Bond AE-10 adhesive system before tensioning.

The strain readings taken during tensioning of the strands for the SCC-2 beams can be seen in Figure 4-12. These readings would correlate to stresses ranging from 188 ksi to 198 ksi using the stress-strain relationship for ½-inch Grade270 seven-wire strands established by Devalapara and Tadros (Devalapura and Tadros 1992). This compares reasonably well to the initial design stress for the strands, 202.5 ksi, especially when considering that Devalapara's relationship is formulated from the lower bound curve of strand data.

Table 4-8 Strain gage designations for prestressed beam instrumentation.

Section Designation	Gage Type & Location	Traditional Beam 1	Traditional Beam 2	Traditional Beam 3	SCC-2 Lab Beam	SCC-2 Beam 2	SCC-2 Beam 3
Section A-A	Strand	Trad5, Trad6	Trad3, Trad4	Trad1, Trad2	SCC5, SCC6	SCC3, SCC4	SCC1, SCC2
	Embedment, Lower	Trad16, Trad17	Trad11, Trad12	Trad7, Trad8	SCC16, SCC17	SCC11, SCC12	SCC7, SCC8
	Embedment, Upper	Trad18	Trad13	Trad9	SCC18	SCC13	SCC9
Section B-B	Strand				SCC36		
Section C-C	Strand				SCC35		
	Embedment, Lower				SCC31		
	Embedment, Upper				SCC32		
Section D-D	Strand				SCC34		
Section E-E	Embedment, Lower				SCC33		
	Embedment, Upper	Trad15	Trad14	Trad10	SCC15	SCC10	SCC14

The strain changes experienced at several locations during detensioning of the traditional and SCC-2 PC beams can be seen in Figure 4-13 and Figure 4-14. In all cases, a gradual change can be seen over the five to six minute period during which the 29 prestressing strands were cut, with the resulting strain change depending on the location of the gage.

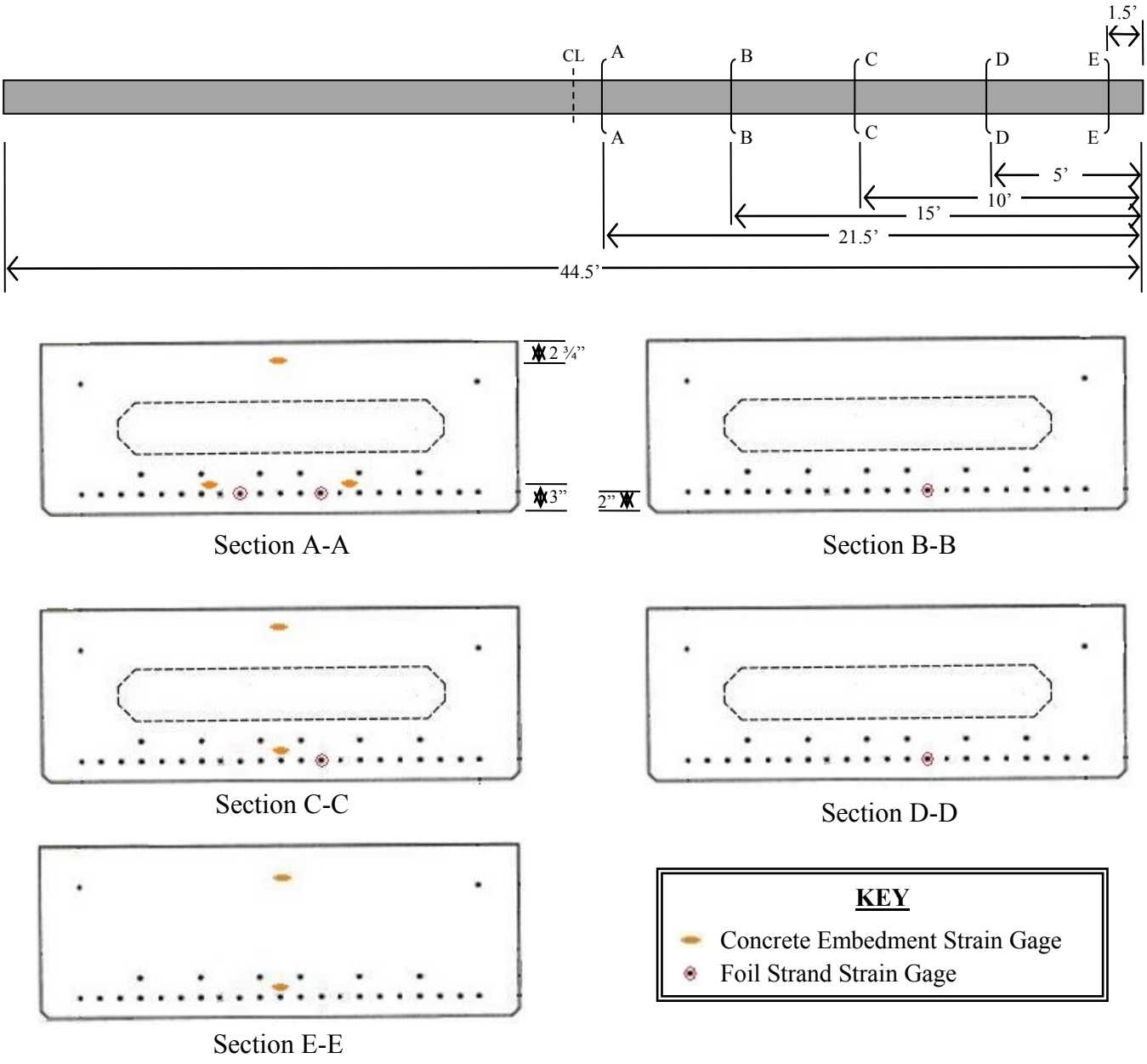

Figure 4-11 Locations of strain gages (where applicable), as placed during instrumentation of prestressed box beams.

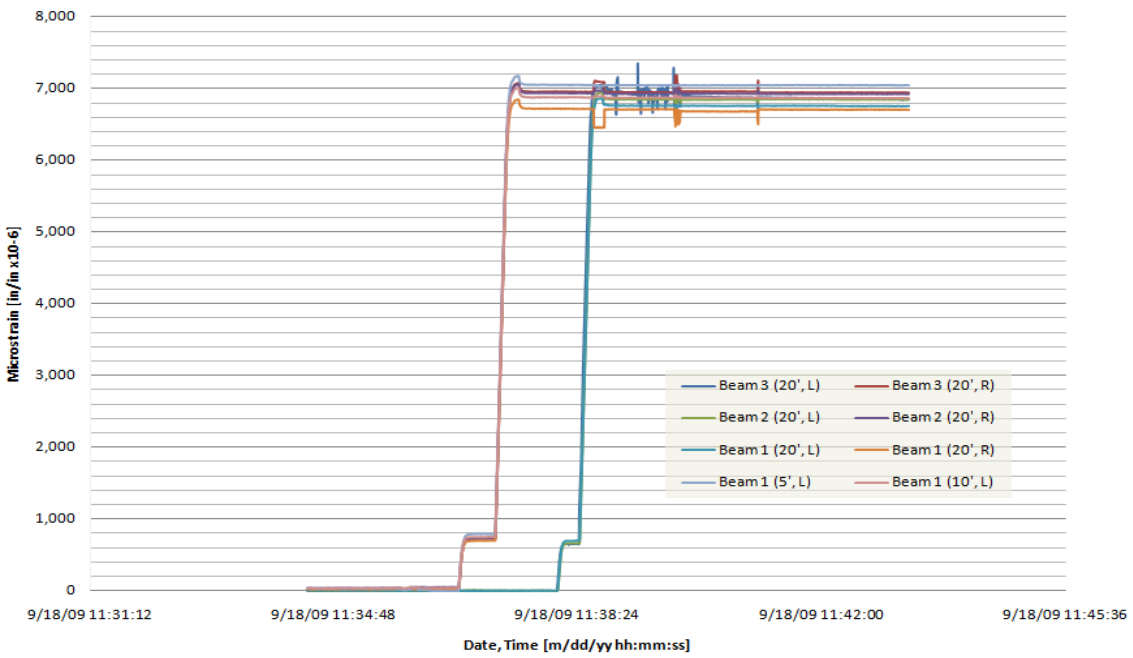

Figure 4-12 Prestressing strand strains as recorded during tensioning, SCC-2 box beams.

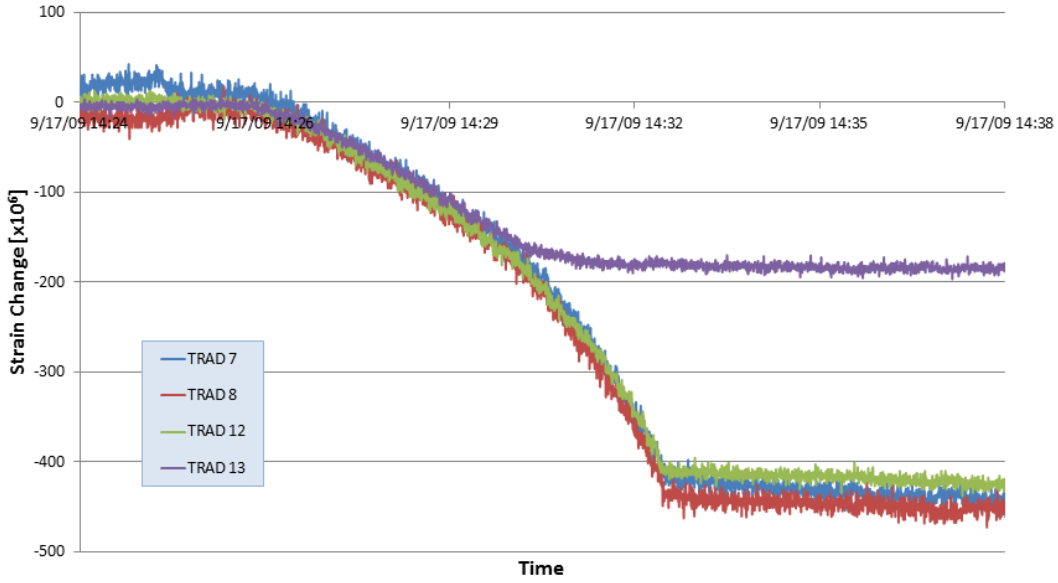

Figure 4-13 Strain readings [με] of select concrete embedment gages during detensioning of traditional PC beams.

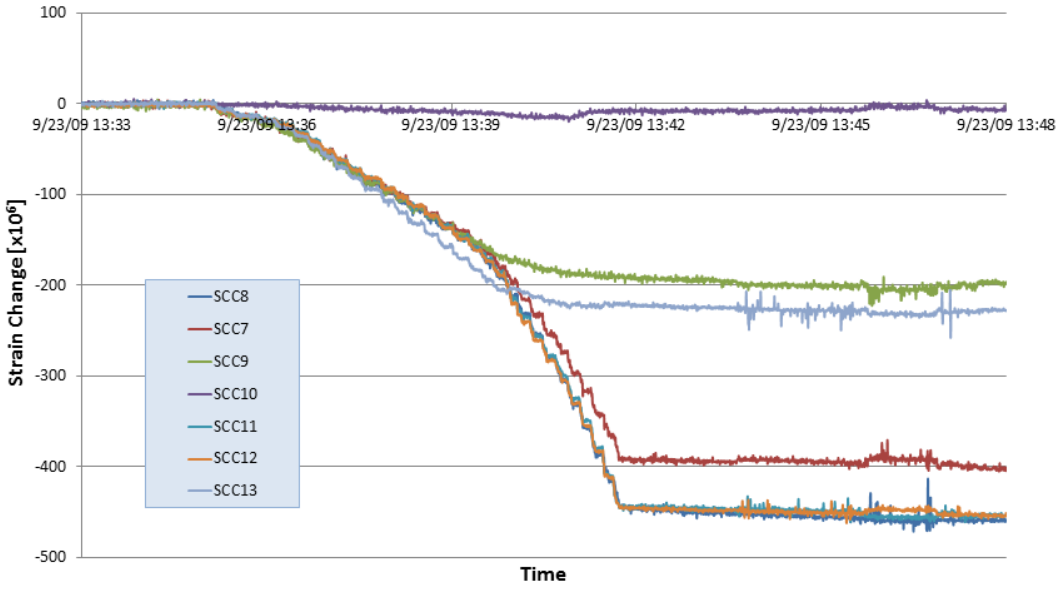

Figure 4-14 Strain readings [με] of select concrete embedment gages during detensioning of SCC-2 PC beams.

In addition to the concrete strain gages, the strand strain gages monitored the strain changes in strands during the detensioning process, as shown in Figure 4-15 and Figure 4-16 for midspan tendons during the detensioning of the TVC and SCC-2 beams, respectively. It can be seen by comparing the two figures that the strand strain gages for the TVC beams experienced a wider range of readings during detensioning, as compared to the output from the SCC-2 beams. The strain gages from each pair strand gages on two of the three TVC beams, i.e. Gages #3 and #4 from TVC Beam 2 and Gages #5 and #6 from TVC Beam 1, were very close to one another [Gage #1 from TVC Beam 3 was non-responsive]. This could indicate that there was more batch-to-batch variation in the mechanical properties of the traditional concrete than there was in the properties of the SCC that was used for beam fabrication.

A summary of the strain changes of all gages during detensioning can be seen in Table 4-9, with negative changes indicating a shortening of the beam at that location. On average, the strand strain gages and embedment gages near the bottom of the SCC-2 beams indicated a slightly larger contraction during detensioning than did those of the traditional beams. The slightly smaller elastic strain changes experienced within the traditional beams during detensioning are reflected to a degree in the average

initial cambers measured by the fabricators, shown in Table 4-10. As a whole, though, there was not a substantial difference between the initial cambers of the two types of beams.

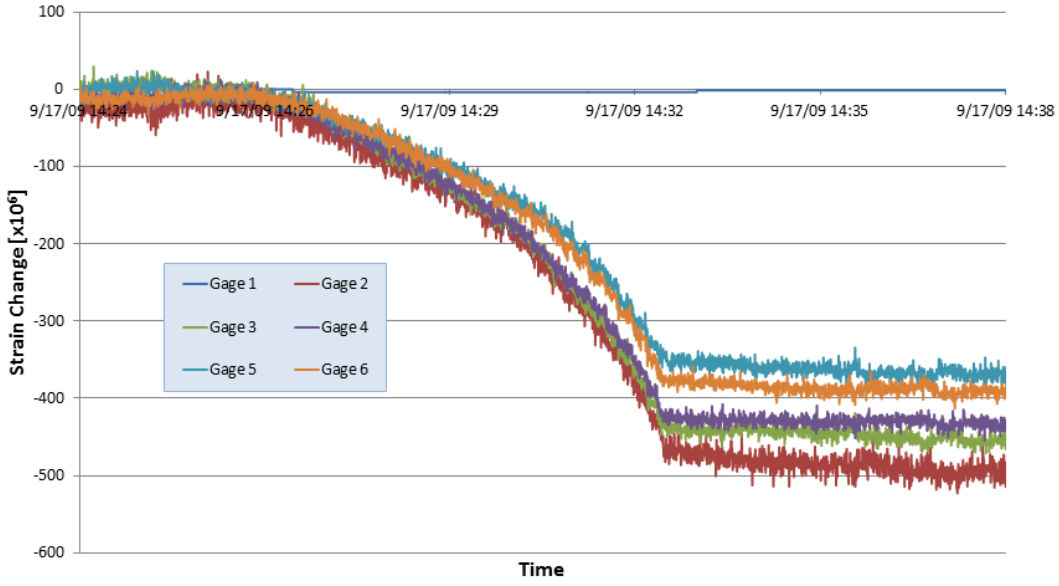

Figure 4-15 Strain readings [με] of midspan strand strain gages during detensioning of Traditional PC beams.

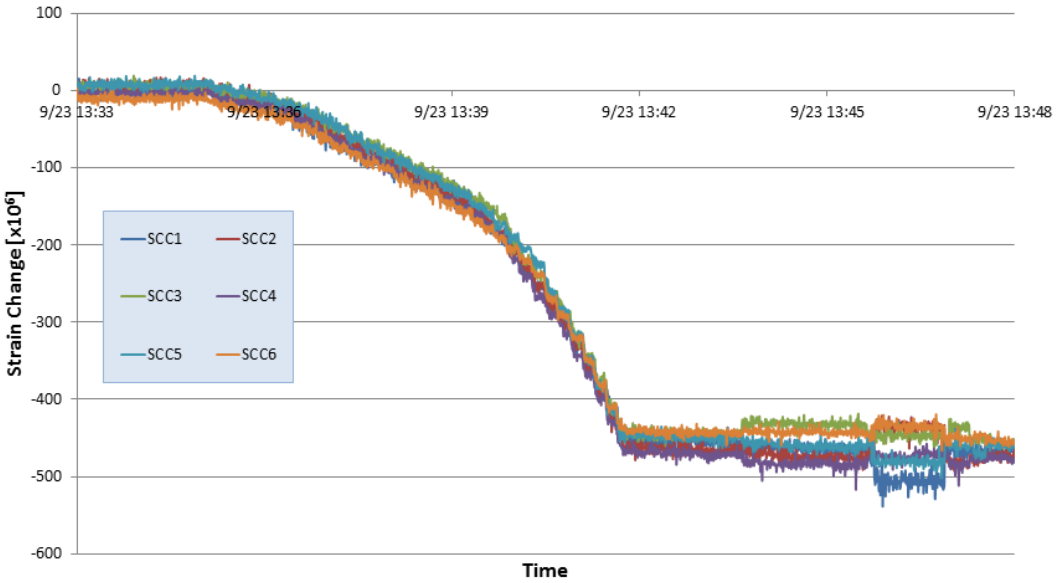

Figure 4-16 Strain readings [με] of midspan strand strain gages during detensioning of SCC-2 PC beams.

Table 4-9 Observed strain changes during detensioning of prestressed beams, in microstrain.

Section Designation	Gage Type & Location	Traditional Beam 1	Traditional Beam 2	Traditional Beam 3	SCC-2 Lab Beam	SCC-2 Beam 2	SCC-2 Beam 3
Section A-A (21.5 feet from end)	Strand[a]	#5 (-352) #6 (-378)	#3 (-446) #4 (-431)	#1 (XX) #2 (-409)	#5 (-445) #6 (-442)	#3 (-458) #4 (-469)	#1 (-465) #2 (-479)
	Embedment, Lower[b]	#16 (-357) #17 (-382)	#11 (-395) #12 (-408)	#7 (-421) #8 (-421)	#16 (-366) #17 (-307)	#11 (-445) #12 (-443)	#7 (-389) #8 (-445)
	Embedment, Upper[c]	#18 (-175)	#13 (-177)	#9 (-188)	#18 (-236)	#13 (-223)	#9 (-192)
Section B-B (15 feet)	Strand[a]				#36 (XX)		
Section C-C (10 feet)	Strand[a]				#35 (-513)		
	Embedment, Lower[b]				#31 (-384)		
	Embedment, Upper[c]				#32 (-137)		
Section D-D (5 feet)	Strand[a]				#34 (-407)		
Section E-E (1.5 feet)	Embedment, Lower[b]				#33 (-377)		
	Embedment, Upper[c]	#15 (-17)	#14 (-18)	#10 (-24)	#15 (-27)	#14 (XX)	#10 (-11)

Also shown in Table 4-10 are the moduli of elasticity results from 6”x12” cylinders made from concrete sampled before delivery to each respective beam, steam cured along with the beam, and tested at the precast facilities in accordance with ASTM C469 on the day of detensioning. There is a moderate correlation between the magnitudes of the cambers presented in Table 4-10 and the measured stiffness of the concrete used for each beams, particularly with the stiffest traditional concrete yielding the lowest camber.

Table 4-10 Initial cambers of prestressed box beams, as measured by fabricators.

	Traditional Beam 1	Traditional Beam 2	Traditional Beam 3	SCC-2 Lab Beam	SCC-2 Beam 2	SCC-2 Beam 3
Measured Initial Camber	7/8”	1-1/8”	1-1/8”	1-1/8”	1-1/4”	1-1/4”
Concrete Modulus of Elasticity, psi (from 6”x12”)	5.79 x10^6	5.25 x10^6	5.76 x10^6	4.45 x10^6	4.58 x10^6	5.07 x10^6

4.4.3 Hardened Properties of Beam Concrete

Numerous specimens were collected during fabrication of the TVC box beams and the SCC-2 box beams. These included: 6”x12” cylinders for measurement of creep, modulus of elasticity, compressive strength and splitting tensile strength; 4”x8” cylinders for measurement of compressive strength and rapid chloride permeability testing; 3”x3”x3” prisms for length change measurement; and 3”x4”x16” prisms for freeze-thaw durability testing. The batches that were selected to make the test specimens for each beam were the same ones whose fresh properties were tested and accepted for use in the beam casting, totaling one batch per beam.

The test specimens were initially cured under the same conditions as the beams; all specimens were placed on the casting bed next to the beams and steam cured with the beams until the concrete had gained enough strength and the strands were cut. After transport to WVU facilities, the specimens were stored in a high-humidity curing room at a relatively constant temperature until they were recalled for their respective testing.

The mechanical testing for compressive strength, tensile strength, and modulus of elasticity was performed at the precast plant on the first day of testing (the day strands were cut), and the other tests were performed at the West Virginia University Concrete Laboratory. Results of the compressive, splitting tensile, and modulus of elasticity tests at the time of detensioning and at 28 days are shown in Table 4-11 and Table 4-12, respectively.

Although the moduli of elasticity of the box beam SCC specimens were lower than those of the traditional box beam concrete with similar compressive strengths, in all cases the observed modulus exceeded the ACI approximation based on the compressive strength of the cylinders. Additionally, a disparity can be seen between the compressive strengths obtained from the 6”x12” cylinders, which had previously been loaded for modulus testing, and the 4”x8” cylinders that were not previously loaded;

this was fairly consistent between mature SCC and traditional specimens, but a significant effect was not seen for the traditional concrete cylinders at the time of detensioning.

Table 4-11 Hardened properties of prestressed box beam concrete at time of detensioning (1 or 2 days).

	E (6"x12") [psi]	E (ACI, calculated) $=57{,}000\,[f_c'(6"x12")]^{0.5}$ [psi]	f_{ci}' (6"x12") [psi]	f_{ci}' (4"x8") [psi]	f_{ST}' (6"x12") [psi]
Trad. Beam 1	5.79 x10^6	4.78 x10^6	7,038	7,202	578
Trad. Beam 2	5.25 x10^6	4.28 x10^6	5,647	5,677	394
Trad. Beam 3	5.76 x10^6	4.42 x10^6	6,013	6,088	451
Trad. AVG	**5.60 x10^6**	**4.49 x10^6**	**6,233**	**6,322**	**474**
SCC-2 Beam 1	4.45 x10^6	4.38 x10^6	5,895	6,366	492
SCC-2 Beam 2	4.58 x10^6	4.18 x10^6	5,376	6,167	573
SCC-2 Beam 3	5.07 x10^6	4.42 x10^6	6,019	6,380	514
SCC-2 AVG	**4.70 x10^6**	**4.33 x10^6**	**5,763**	**6,304**	**526**

Table 4-12 Hardened properties of prestressed box beam concrete at 28 days after casting.

	E_c (6"x12") [psi]	E_c (ACI, calculated) $=57{,}000\,[f_c'(6"x12")]^{0.5}$ [psi]	f_c' (6"x12") [psi]	f_c' (4"x8") [psi]	f_{ST}' (6"x12") [psi]
Trad. Beam 1	6.81 x10^6	4.82 x10^6	7,144	9,828	511
Trad. Beam 2	6.02 x10^6	5.19 x10^6	8,306	7,878	514
Trad. Beam 3	5.78 x10^6	4.88 x10^6	7,315	8,343	550
Trad. AVG	**6.20 x10^6**	**4.96 x10^6**	**7,589**	**8,683**	**525**
SCC-2 Beam 1	4.93 x10^6	4.89 x10^6	7,369	8,316	585
SCC-2 Beam 2	4.96 x10^6	4.77 x10^6	7,021	8,396	520
SCC-2 Beam 3	5.50 x10^6	4.97 x10^6	7,628	9,032	628
SCC-2 AVG	**5.12 x10^6**	**4.88 x10^6**	**7,339**	**8,581**	**578**

4.4.4 Durability Characteristics of Beam Concrete

Certain properties of the SCC and TVC concrete used for casting were measured to explore any potential durability issues that the prestressed beams may exhibit. The durability tests conducted include freeze-thaw testing and rapid chloride permeability testing.

4.4.4.1 Freeze-thaw Testing of Beam Concrete

Three 3”x4”x16” prisms and three 3”x3”x11.25” prisms were cast during beam fabrication using SCC-2 for the purpose of freeze-thaw testing in accordance with ASTM C666. Likewise, two 3”x4”x16” and two 3”x3”x11.25” prisms were cast using the traditional concrete. Although all ten specimens underwent freeze-thaw testing, the smaller specimens will be referred to as “Shrinkage” specimens in this summary since the smaller prisms were outfitted with gage studs for the purpose of precisely monitoring length change during testing; the larger specimens will be referred to as “Freeze-Thaw” specimens.

After the initial steam curing, all prisms were demolded and soaked in water until the start of testing. The freeze-thaw testing for the SCC-2 specimens commenced approximately 7 months after beam fabrication, while the Traditional beam concrete underwent testing separately, starting at about 12 months after beam fabrication. Testing followed Procedure A of ASTM C666 (samples remained surrounded by water throughout freezing and thawing), and followed the general procedures outlined in APPENDIX B.2.

Periodic testing was done of the SCC-2 specimens, starting after 5 cycles and every 30 cycles thereafter, until 300 cycles was reached. The Traditional specimens were tested starting after 30 cycles, and every 30 cycles thereafter until 300 cycles was reached.

The changes in the relative dynamic moduli calculated using the fundamental transverse frequencies for the six SCC-2 specimens and four Traditional beam specimens can be seen in Figure 4-17 and Figure 4-18, respectively. Similar trends were seen when calculating this value using the fundamental longitudinal frequencies for this calculation, which are shown in Figure 4-19 for both types of specimens, although it appears as if the transverse method was more sensitive to the minor damage that occurred and showed a more reasonable pattern of degradation of the SCC-2 specimens. In these

figures, and throughout this section, the specimen designation "s#_" refers to 3"x3"x11" specimens that are instrumented with gage studs for length measurement, and the designation "f-t#_" will refer to the larger 3"x4"x16" freeze-thaw specimens.

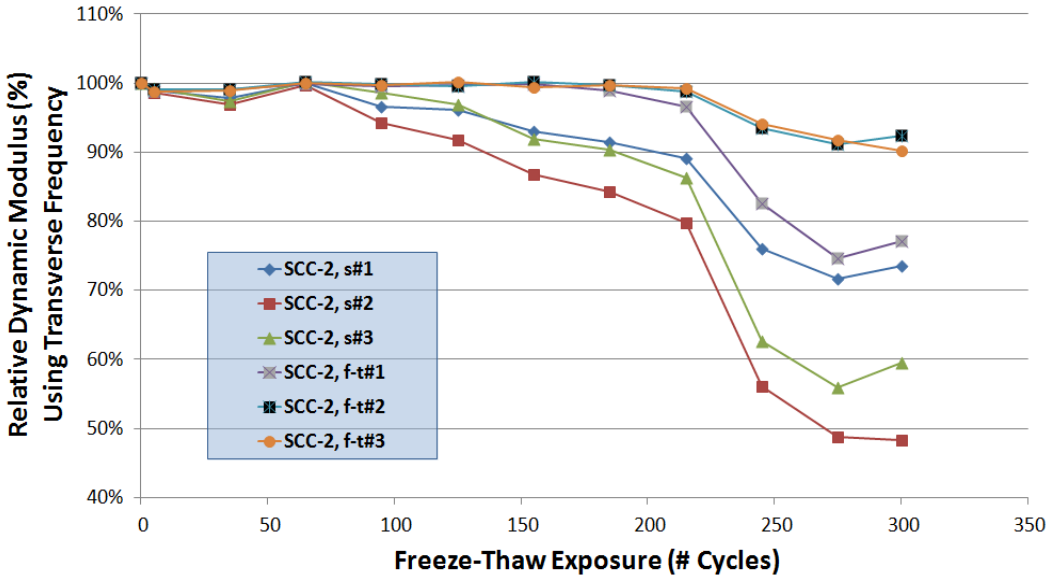

Figure 4-17 Relative dynamic moduli of SCC-2 beam specimens based on fundamental transverse frequency measurements.

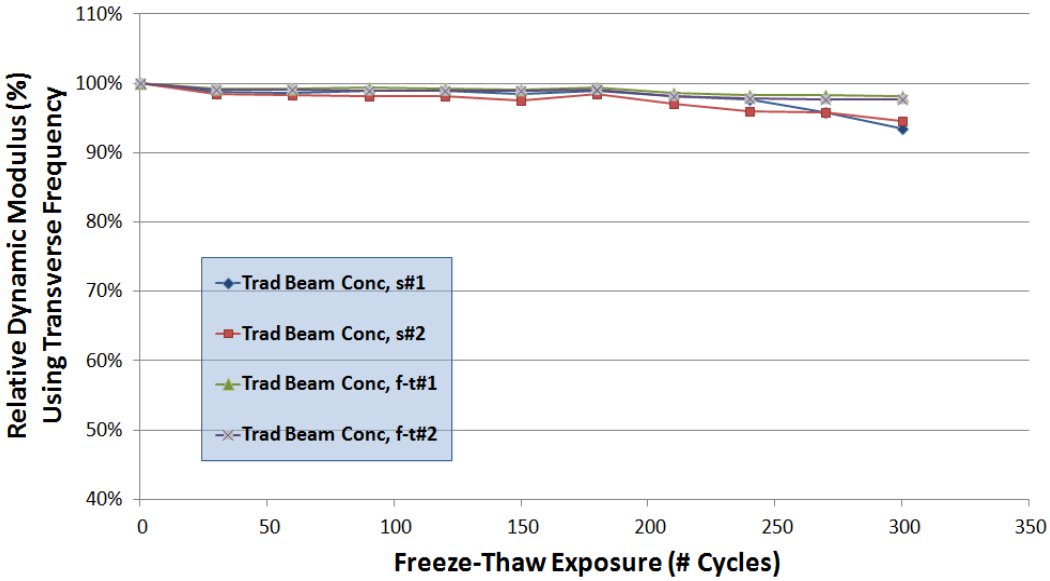

Figure 4-18 Relative dynamic moduli of traditional beam concrete specimens based on fundamental transverse frequency measurements.

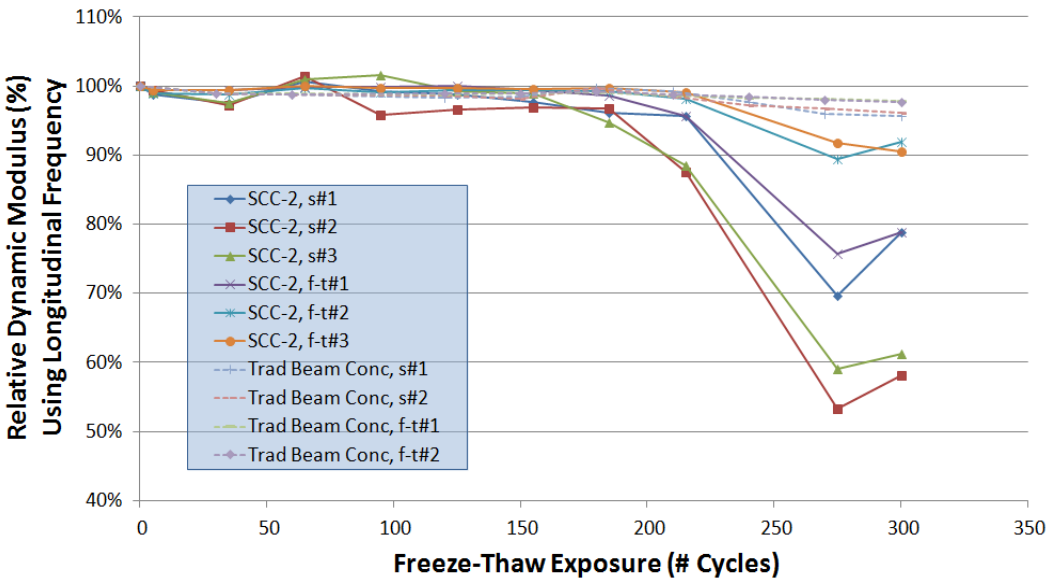

Figure 4-19 Relative dynamic moduli of SCC-2 and traditional beam concrete specimens based on fundamental longitudinal frequency measurements.

Results for the three SCC-2 Shrinkage specimens and the Traditional concrete are shown in Figure 4-20. Based on these results and according to ASTM C666, SCC-2 Specimens s#2 and S#3 could have been removed from testing after 245 cycles based on their length change exceeding 0.1%, while SCC-2 Specimen s#1 did not reach this level until the end of the 300 cycles. None of the measured elongations of the traditional beam concrete specimens exceeded 0.1% at any point during testing.

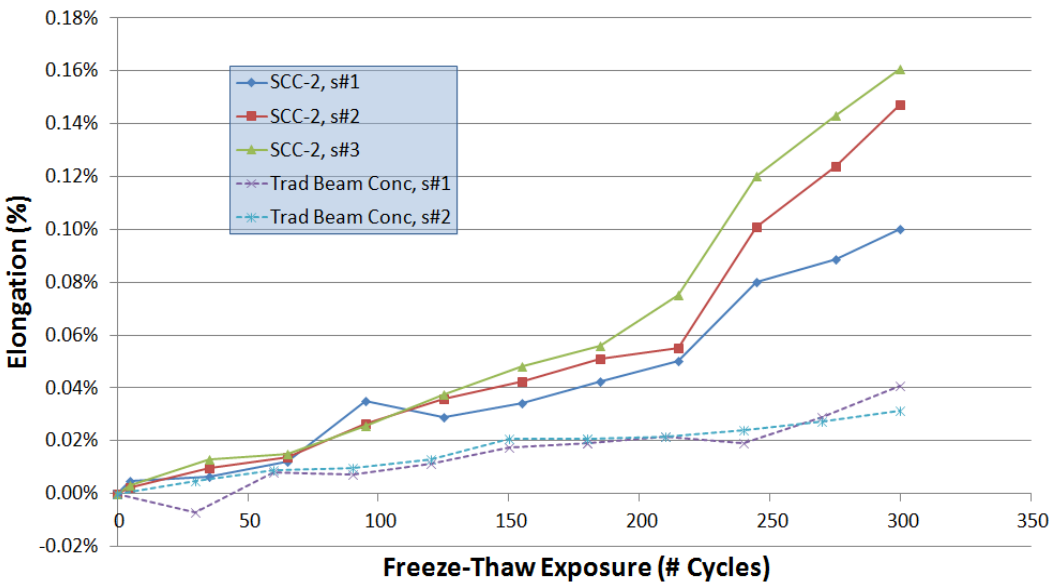

Figure 4-20 Elongation of 3"x3"x11" beam concrete prisms during freeze-thaw testing.

It is apparent from Figure 4-17 through Figure 4-20 that the traditional beam concrete used for the prestressed beams would be considered freeze-thaw durable, while the SCC-2 concrete would not. It is noted that the SCC-2 specimens tested at WVU did perform better than those tested by an outside agency for the SCC-2 mix qualification, although much of this disparity could be explained when considering that the WVU tests were initiated when the specimens had matured more than 7 months, as opposed to the 14 days of maturity gained by the specimens for mix qualification.

4.4.4.2 Rapid Chloride Permeability Testing of Beam Concrete

RCPT testing was conducted for each type of beam concrete in accordance with ASTM C1202 using 2 inch (50 mm) thick by 4 inch (100 mm) diameter disc cut from the 4 x 8 inch (100 x 200 mm) cylinders. The specimens were prepared and tested according to the procedure shown in APPENDIX A.1. The total charge passed through the specimen for SCC-2 and traditional beam concrete specimens can be seen in Table 4-13 and Table 4-14, respectively. These results are from tests conducted at approximately two, four, and five months after casting.

The SCC-2 exhibits lower chloride permeability when compared to the traditional concrete. All SCC-2 specimens except one would be classified as "moderate" permeability under the ASTM C1202 definition, while many of the traditional beam concrete specimens would be classified as "high" permeability.

Table 4-13 Rapid Chloride Permeability Testing results from SCC-2 beam concrete specimens.

Specimen	Age [days]	Adjusted Charge Passed [Coulombs]	Permeability Class	AVG
SCC-2 Beam 1(1)	65	4067	High	3808
SCC-2 Beam 1(2)	66	3529	Moderate	
SCC-2 Beam 1(3)	69	3829	Moderate	
SCC-2 Beam 1(1)	126	2515	Moderate	2541
SCC-2 Beam 1(2)	136	2573	Moderate	
SCC-2 Beam 1(3)	135	2535	Moderate	
SCC-2 Beam 2(1)	127	2905	Moderate	2769
SCC-2 Beam 2(2)	134	2602	Moderate	
SCC-2 Beam 2(3)	133	2801	Moderate	
SCC-2 Beam 3(1)	124	3831	Moderate	-

Table 4-14 Rapid Chloride Permeability Testing results from traditional beam concrete specimens.

Specimen	Age [days]	Adjusted Charge Passed [Coulombs]	Permeability Class	AVG
TRAD Beam 1(1)	62	5705	High	6150
TRAD Beam 1(2)	63	6595	High	
TRAD Beam 1(1)	126	2576	Moderate	2255
TRAD Beam 1(2)	148	1934	Low	
TRAD Beam 2(1)	128	4488	High	4496
TRAD Beam 2(2)	147	4503	High	
TRAD Beam 3(1)	127	4143	High	-

4.4.5 Shrinkage and Creep of Beam Concrete

Shrinkage of concrete and creep of loaded concrete members are known to contribute to the loss of prestress forces of prestressed concrete beams after fabrication. It was therefore desirable to explore

these characteristics of both types of beam concrete in order to understand how using SCC would ultimately affect the fundamental behaviors of the prestressed beams.

4.4.5.1 Shrinkage of Beam Concrete

To assess the shrinkage characteristics of the concrete after removal from the formwork, three 3”x3”x11” prismatic samples were taken from the WVU Test Beam (Beam 1) SCC, and three were taken from Traditional Beam 2. All specimens were steam cured before demolding, and initial measurements were taken at 27 hours after casting. The shrinkage prisms were kept in a climate controlled environment with a temperature of 24±1°C and relative humidity of 28±12%, and readings were taken periodically using a comparator gage corresponding to ASTM C157 specifications.

The average shrinkage strains obtained from the 3”x3”x11” prisms of each type of concrete are shown in Figure 4-21. The shrinkage strains shown in this plot encompass all chemical and drying shrinkage that occurs in the specimen after the initial reading was taken. Each point shown in this figure represents the average shrinkage of three specimens of the particular concrete type.

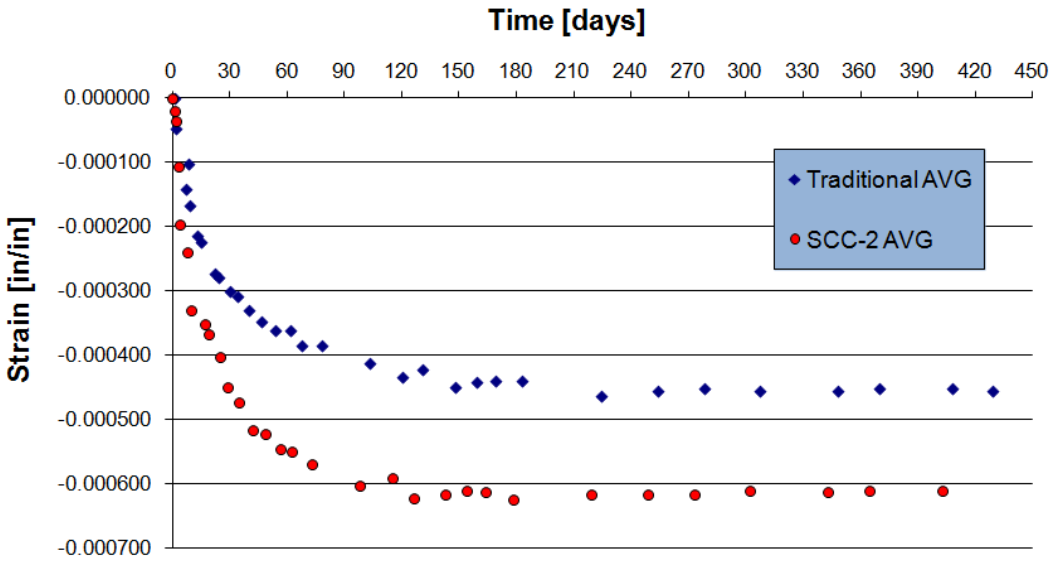

Figure 4-21 Measured total shrinkage of SCC and Traditional Beam Concrete.

The SCC-2 exhibited more shrinkage strain than the traditional beam concrete, with an average measured strain of 609με for the SCC-2 prisms as compared to an average measured strain of 455με for the traditional prisms after more than a full year of air exposure.

4.4.5.2 Creep of Beam Concrete

The general procedures for creep testing of the beam concrete are outlined in APPENDIX B.4. SCC-2 specimens for this testing were steam cured with the accompanying girders for approximately 2 days, while the traditional beam concrete specimens were steam cured with their girders for only the first night after casting.

The three traditional beam concrete creep specimens were loaded 4 days after casting, while the three SCC-2 creep specimens were loaded 3 days after casting; both types were loaded to a stress (f_{cci}) of 2,193 psi using a manual hydraulic jack. The creep coefficients for the SCC-2 and traditional prestressed concrete specimens can be seen in Figure 4-22.

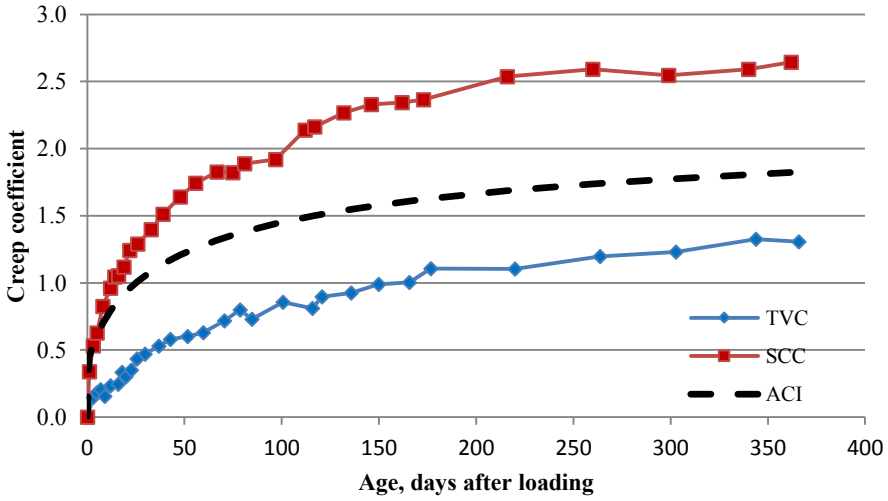

Figure 4-22 Creep strain from traditional and SCC-2 concrete specimens.

Thus, the creep coefficient of the SCC is about 2.27 at 173 days, calculated using the measured creep strain 1,096 με (at 173 days) and the initial elastic strain of 483 με. The maximum measured

creep coefficient of the SCC is about 2.58 at 362 days, based on a 2,193 psi compressive loading applied on the 3rd day after casting. In contrast, the TVC creep coefficients were approximately 1.11 and 1.31 at the same time after exposure to the same load magnitude.

The specific creep is sometimes used to correlate the creep behaviors of concrete that are tested at different stress levels. For the SCC-2 specimens, the observed specific creep was 0.50 με/psi at 173 days, and 0.57 με/psi at 362 days.

4.5 Laboratory Beam

In June 2010, the third full-scale SCC-2 prestressed box beam was delivered to the WVU Major Units (Structures) Laboratory. The beam was placed beneath the load frame onto roller bearings that would give the beam a clear span of 43 feet, which is the same span as the bridge beams' designed center-of-bearing span length. Figure 4-23 shows the beam resting on its roller supports and positioned under the loading frame that is ultimately used for static load testing. Prior to testing of the beam, baseline strain readings were taken using the previously-embedded strain gages, and additional instrumentation mounted to the beam included: 6 concrete strain gages installed on the top and bottom surfaces of the beam; 3 clip gages; 5 LVDTs and 2 load cells.

Figure 4-23 Full-scale box beam in WVU laboratories after placement on roller supports.

Two types of testing were performed on the laboratory beam: one being non-destructive and the other being destructive. The non-destructive testing uses an instrumented sledgehammer and accelerometers to evaluate the vibration characteristics of the beam; this was done multiple times to see the effects resulting from various levels of damage. The destructive testing involves the static loading and unloading of the beam near mid-span to incrementally increasing loads, meanwhile observing changes in the beam's deflection using external LVDTs, and internal strains using the various gages that were placed prior to fabrication.

In general, the testing scheme consisted of progressively increasing static loading with intermittent dynamic characterization. The magnitude of the statically-applied load incrementally increases until failure. Additionally, crack investigations were done to determine the loading at which the bottom of the beam undergoes decompression and to take crack measurements. The general testing scheme for the beam can be seen in Figure 4-24.

Each of the peaks in Figure 4-24 represents a separate 4-point static loading, with a subsequent release of the static loading. The values marked in this figure indicate the load, in kips, per actuator, as is the typical designation that will be used throughout this report; more about the static loading test

configuration will be discussed in Section 4.5.1. After release of the initial static load, a smaller load of approximately 13 kips per actuator was often applied to compare the behavior of the beam at various states of damage; these are marked as the smaller peaks immediately following the larger peaks. The points at which the non-destructive vibration testing was done are also marked in this figure. The results of the dynamic beam tests will be discussed in Section 4.5.2.

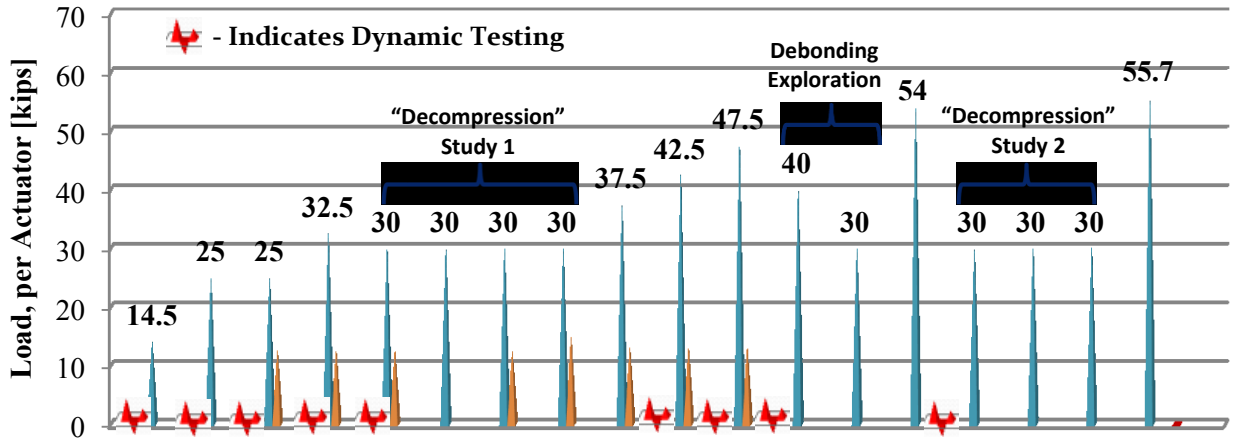

Figure 4-24 Testing scheme for prestressed SCC-2 laboratory beam.

4.5.1 Static Loading of Beam

The static loading configuration consisted of roller supports with a span of 43 feet, which corresponds to the distance between centers of bearing for the Stalnaker Run Bridge beams, with two symmetric strip loads applied to create a 5-foot constant moment zone, as shown in Figure 4-25.

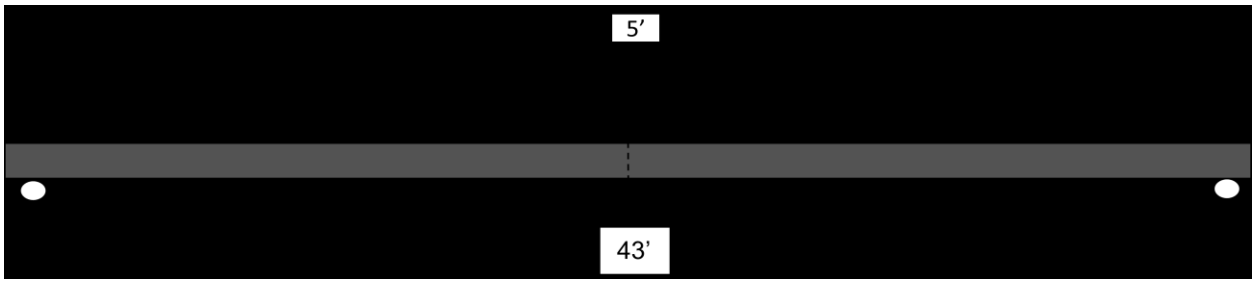

Figure 4-25 Schematic test setup for 4-point bending of prestressed SCC-2 laboratory beam.

A steel spreader beam apparatus was fabricated to create the 5-foot constant moment zone in the center of the beam during destructive tests, as shown in Figure 4-26. During testing, two actuators were used to apply (equal) loading to a spreader beam, which was then distributed as two strip loads across the width of the prestressed beam via cross beams. The jacking force was applied using either a hand pump or an electric pump. To ensure equal pressure application by the actuators during application of jacking forces, both hydraulic lines coming from the pump were teed off so they could connect to both jacks and provide identical inlet pressures. The applied jacking forces were measured using load cells placed beneath each jack.

Figure 4-26 Spreader beam apparatus used for static testing of laboratory beam.

4.5.1.1 Data Collection

Throughout this static testing procedure, and for each load application indicated in Figure 4-24, measurements were taken from load cells as well as the pre-installed strain gages. The strain data taken from the constant-moment zone strain gages during loading of the beam to 14.5 kips, and the subsequent unloading, can be seen in Figure 4-27. For this particular test, loading was applied starting at approximately 1½ minutes after initiation of data acquisition, and that target load was achieved at around 7½ minutes; loading was released at 10¼ minutes. An increase in strain is indicative of an elongation, while a decrease in strain indicates a shortening at that location; in Figure 4-27, the strand strain gages, lower embedment gages, and lower concrete surface gages give positive strain readings, while the upper embedment gage and upper concrete surface gages are negative.

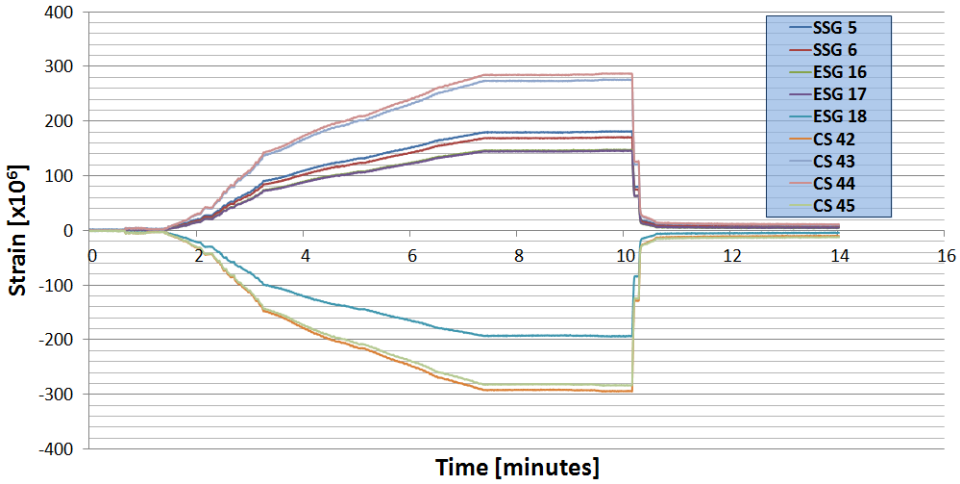

Figure 4-27 Strain data recorded with mid-span gages; 14.5-kip loading of laboratory beam.

At a minimum, deflection measurements were recorded using two LVDTs on opposite edges of the beam's mid-span, although other locations were monitored for most load cases. Initially, deflections were monitored on the non-instrumented half of the beam as well as the end containing the gages, and

good agreement was seen between readings taken at the same distance from opposite supports of the beam, as shown in Figure 4-28.

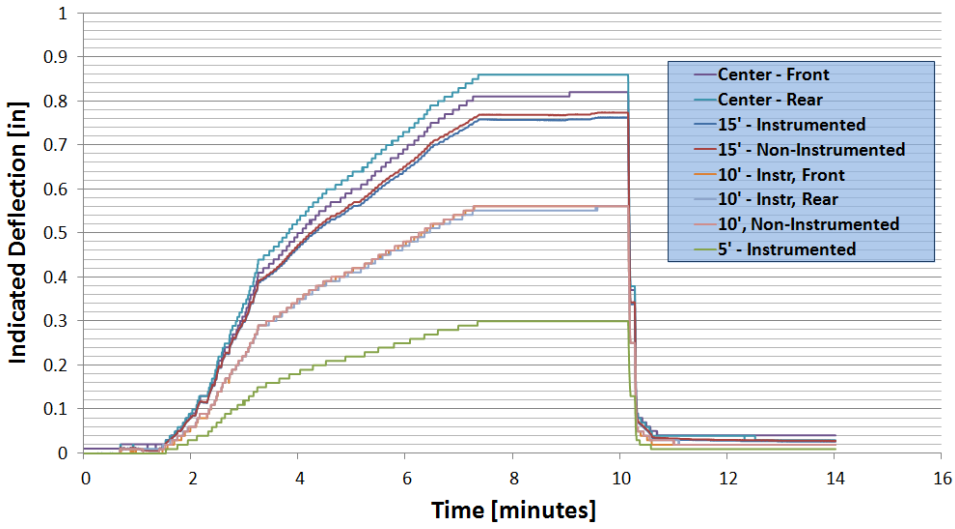

Figure 4-28 Deflection data recorded at various locations during 14.5-kip loading of laboratory beam.

In addition to the load, strain and deflection data that was collected each time the beam was loaded, intermittent data collection was done. This included the collection of beam camber data in between load cycles, which entailed measuring the distance from a taunt string line stretched along the underside of the beam the beam's bottom surface at pre-defined locations. Also, decompression and debonding studies were done after cracking had occurred in the beam at the times depicted in Figure 4-24; these will be discussed in more detail in the following sections.

4.5.1.1.1 Decompression Study 1 – Clip Gage

Initial investigations into the decompression loading included attaching a clip gage to the bottom of the beam which bridged a known crack, as shown in Figure 4-29. The floating core of the LVDT for the clip gage was held in position via a threaded rod that was affixed to an L-bracket on the opposite side of the crack. The hardware was mounted to the bottom surface of the beam such that only 1 inch

remained between the inside faces of the LVDT mounting block and the L-bracket; this yielded a more distinct transition on the curves produced from this testing than earlier attempts that included larger spans between hardware.

Figure 4-29 Clip gage used for decompression investigation.

To determine the load at which decompression at the bottom fibers of the beam occurred, the readings of this clip gage were monitored during 30-kip loadings of the beam. A typical result from this type of gage is shown in Figure 4-30. In this figure, the results from the clip gage (or "Crack LVDT – Center") are compared with the readings from a concrete surface gage located on the bottom of the beam, CS 43. This particular concrete surface gage was located adjacent to the crack, so its readings indicated a gradual elongation to the point of decompression, at which point the crack served as a stress release that reduced the rate of strain in regards to the increase in loading. Similarly, the readings of the clip gage increased slowly to a point at which the crack opened, at which time the rate of change increased significantly. For this study, the decompression loading was defined as the point at which the two slopes intersect. A value of 18.3 kips was determined to be a representative decompression load from the data collected throughout four trials, one of which is illustrated in Figure 4-30.

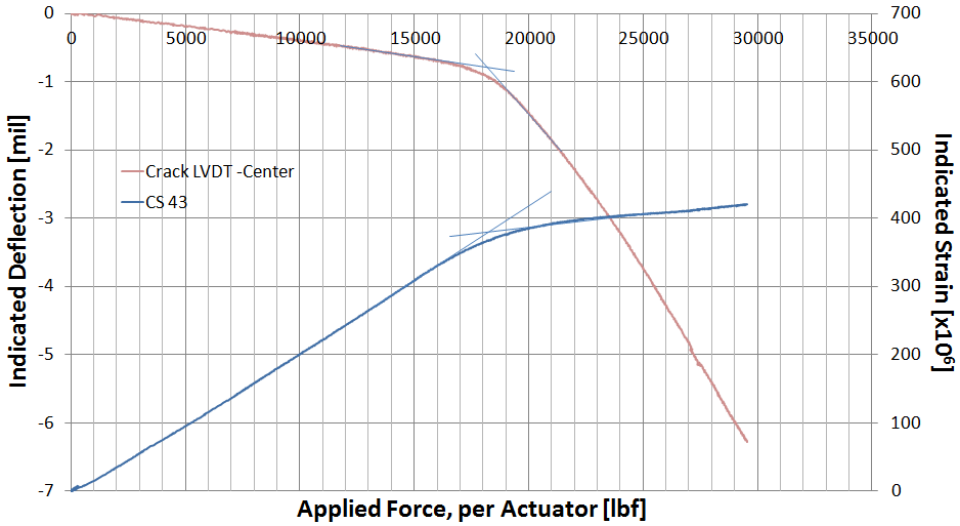

Figure 4-30 Typical result from decompression investigation of cracked prestressed beam.

4.5.1.1.2 Debonding Study

As an initial exploration into whether debonding of the prestressing strands had occurred after the beam experienced large loads, the crack profiles for seven cracks located within the constant-moment zone of the beam were observed after the 47.5 kip load case was completed. The crack widths at up to five (5) different depths for each crack were measured when the beam was subjected to loadings, P_L, of 20 kips, 30 kips, 35 kips, and 40 kips per actuator. Prior to application of loading, each crack was marked with reference marks oriented parallel to the longitudinal axis of the beam, and at 1 in., 3 in., 5 in., 7 in., and 9 in. up from the bottom of the beam.

To collect crack width data, loading was first applied to the smallest target load, 20 kips, and held while crack width measurements were taken at each location; the 1" measurements were not taken for Cracks #2 and #3 since the clip gage hardware was mounted in the vicinity, so there was not enough clearance to use the scope for observation. The loading was then increased to each subsequent load and held while necessary measurements were taken. To assess crack widths, a USB digital scope [IHARA Model UM-02] was used for crack observation, with a corresponding image capture and analysis

program, UM-CAM, was used for linear measurement of the crack width. This digital scope has the capability of achieving around 80x magnification with the low-magnification setting [based on a 22" display screen], and 320x magnification with the high-magnification setting; the high magnification setting was used for this application, which allowed for a precision of measurement of approximately 0.01 mm. The progressive crack growth at one particular location can be seen in Figure 4-31.

The crack profiles for the seven cracks at the four desired loads are given in Figure 4-32. For a perfect bond between concrete and the prestressing strands, one would expect that the crack profiles would increase linearly along the depth, or even be smaller at the locations of highest restraint [in this case, the heaviest reinforcement would be at 2" to 4" from the bottom edge]. It can be seen from this figure that most of the cracks observed had an essentially linear profile; Cracks #4 and #7 were even slightly smaller at the depth of the prestressing strands, demonstrating a good bond. Crack #1, however, had approximately the same width at 3" from the bottom as it did at 1", possibly indicating some debonding at that location; this possible stress release also coincides with a slightly larger overall crack width at this location. The bond between SCC-2 and the prestressing strands will be discussed in more detail in a later section.

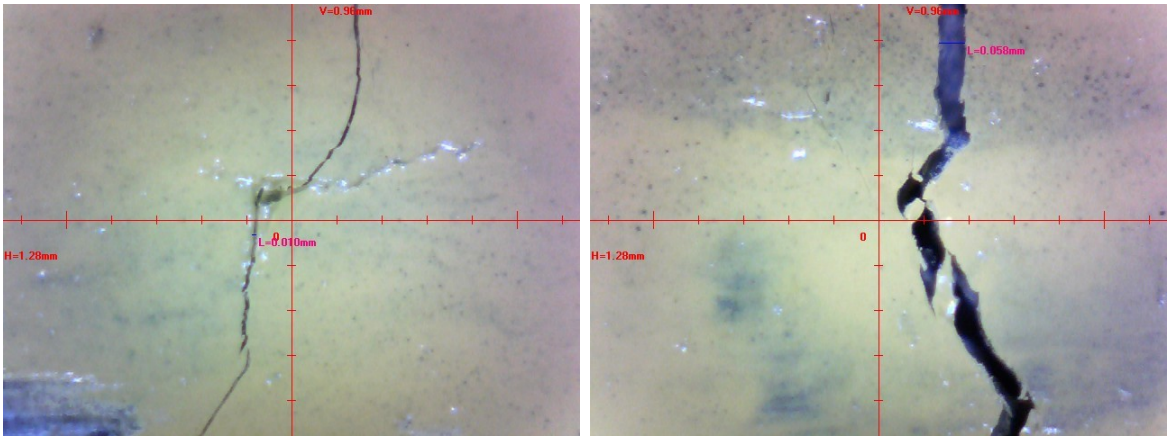

(a) **(b)**

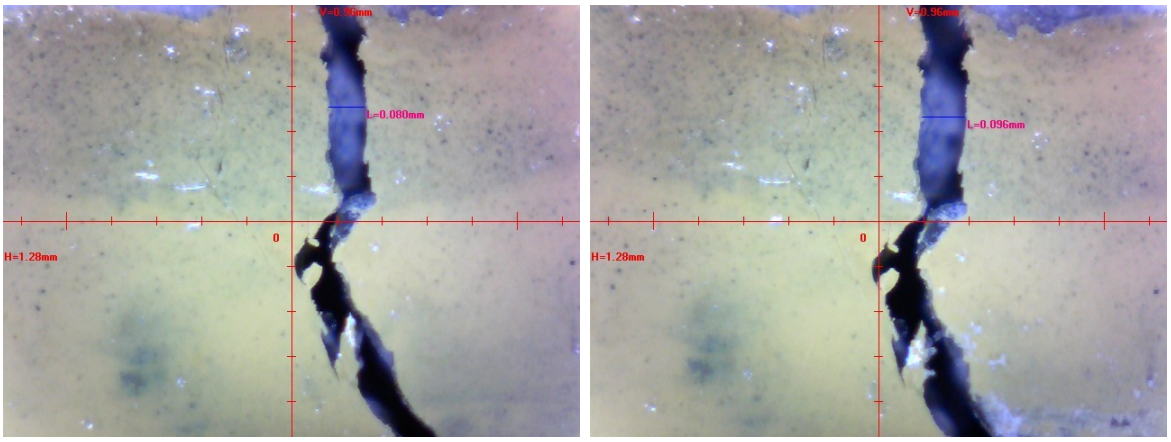

(c) **(d)**

Figure 4-31 Width of Crack 2 @ 3in. from bottom of beam. Loading of (a) 20k, (b) 30k, (c) 35k, and (d) 40k.

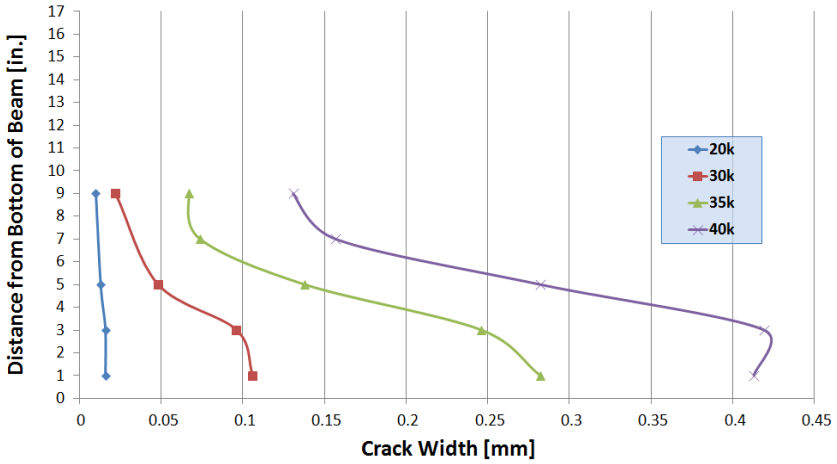
Distance from Bottom of Beam [in.]
Crack Width [mm]
20k
30k
35k
40k

(a)

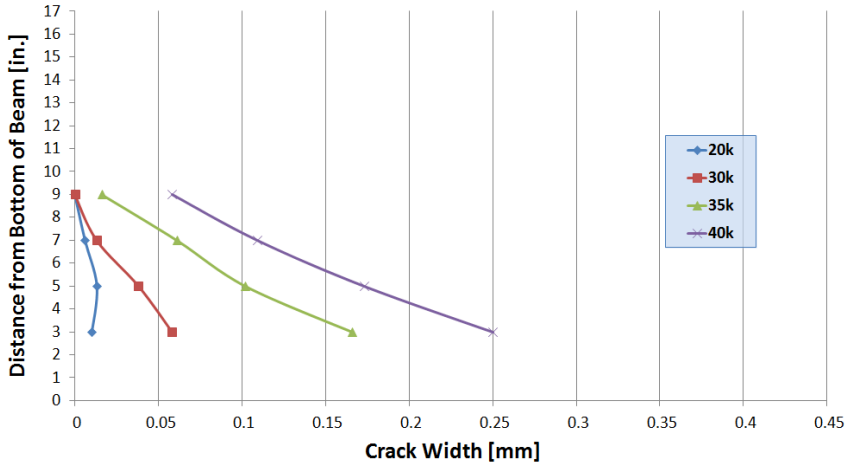
Distance from Bottom of Beam [in.]
Crack Width [mm]
20k
30k
35k
40k

(b)

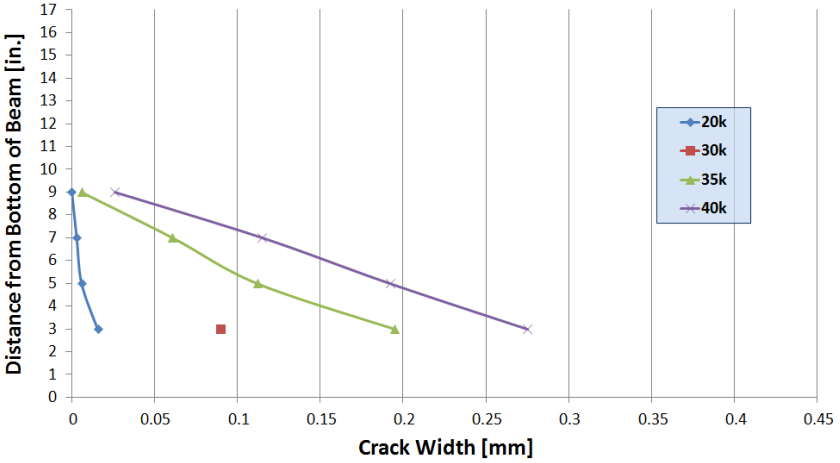
Distance from Bottom of Beam [in.]
Crack Width [mm]
20k
30k
35k
40k

(c)

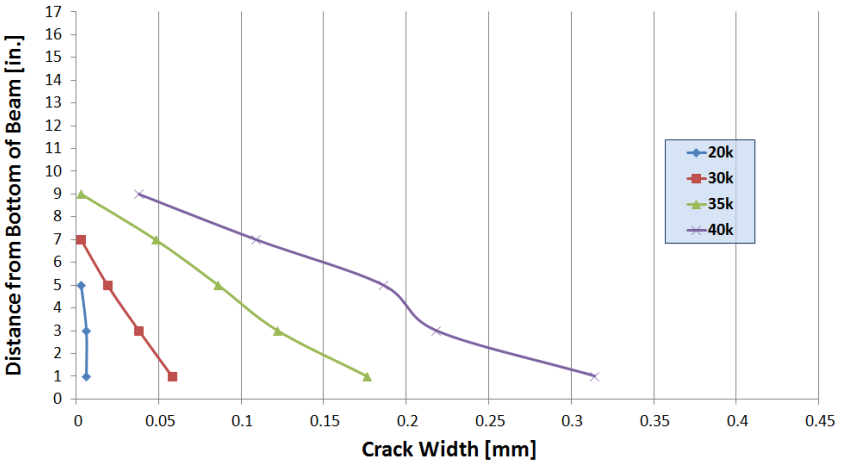
Distance from Bottom of Beam [in.]
Crack Width [mm]
20k
30k
35k
40k

(d)

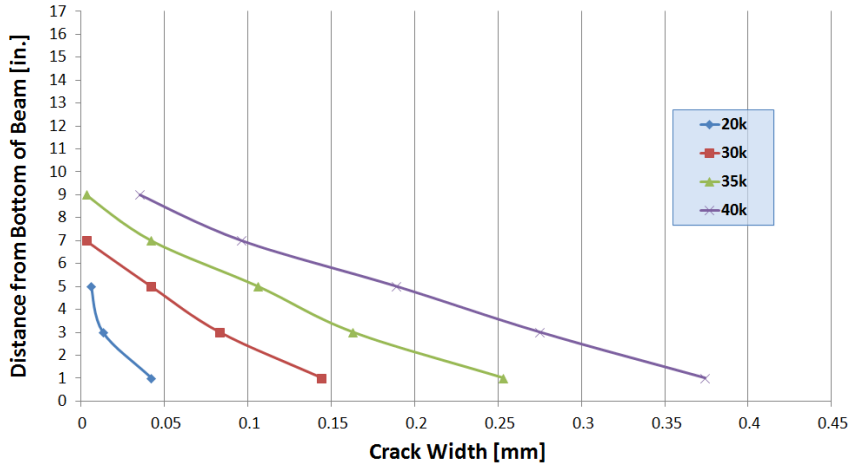

(e)

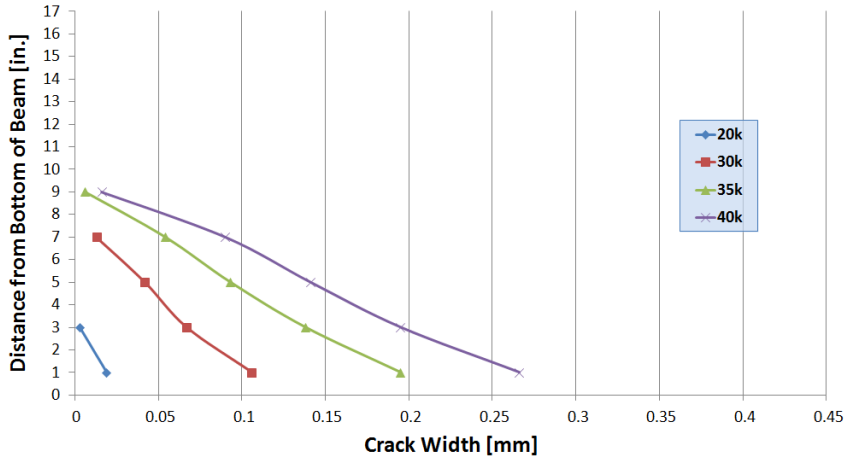

(f)

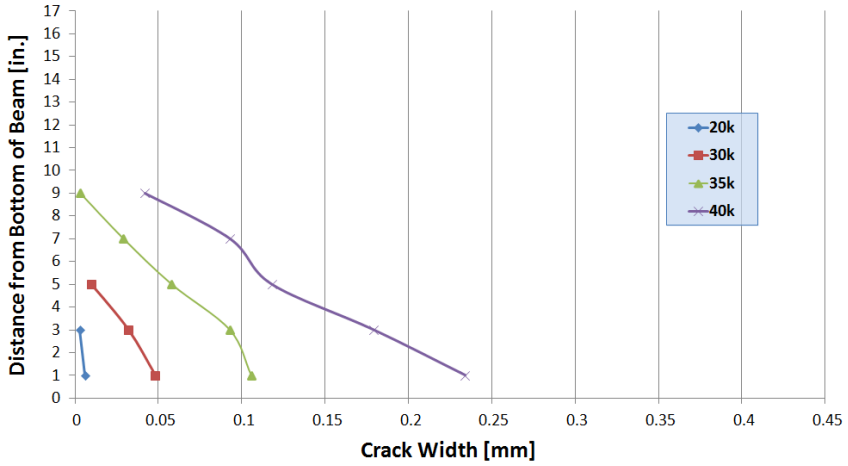

(g)

Figure 4-32 Crack profiles at select loadings for Cracks (a) #1, (b) #2, (c) #3, (d) #4, (e) #5, (f) #6, and (g) #7.

4.5.1.1.3 Decompression Study 2 – Ultrasonic and Visual

Secondary investigations to assess the decompression loading of the beam were done to explore the feasibility of utilizing different techniques for determining the load that causes decompression at the bottom of the beam. The first method used ultrasonic techniques, with the amplitude of a sinusoidal wave transmitted through the crack used as an indicator of the crack opening. The second method utilized the USB digital scope described in the previous subsection to visually observe the crack width at various loads. The clip gage and the concrete strain gage measurements discussed in the "Decompression Study 1" section were also used as a basis of comparison.

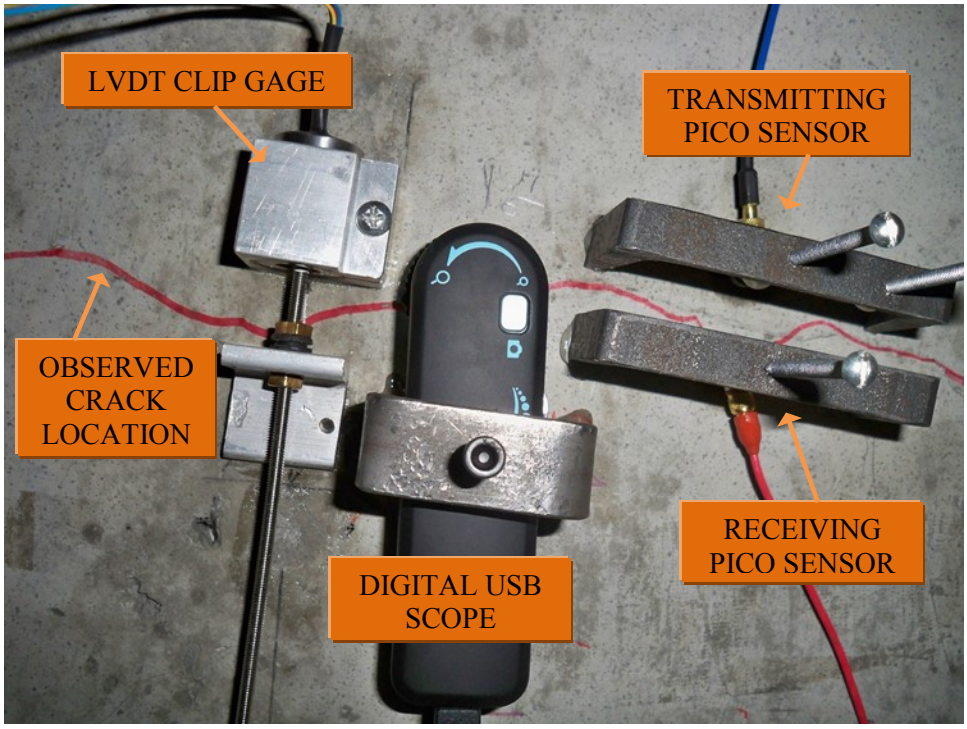

Figure 4-33 Instruments as affixed to underside of beam for decompression study.

Two pico sensors were used for the ultrasonic test; one pulser was constantly transmitting a signal that was detected by the receivers, while one receiver was on the opposite side of the crack as the pulser (~1 inch apart). The pico sensors and digital scope were attached using metal brackets that

were adhered to the bottom surface of the beam, as shown in Figure 4-33. Ultrasonic gel was used on the beam-sensor interface to ensure sufficient signal transmission throughout testing. A Stanford Research Model DS345III 30MHz Function Generator was used to control the output of the pulser. The signals of the receiving sensor were amplified using an Olympus ultrasonic preamplifier.

The transmitted wave was a continuous sine wave; typical signals received using the cross-crack sensor during the baseline measurement can be seen in Figure 4-34. A National Instruments data acquisition system connected to a laptop was used to monitor, process and record signals detected by the receiving sensor.

Loading was applied to the beam in the same fashion as had been done during previous load tests of the prestressed/precast box beam, with similar load, deflection and strain data being recorded using the System 5000 data acquisition system. At a number of points during testing, loading was halted, and signals received from the receiving pico sensor were collected along with crack information from the digital scope.

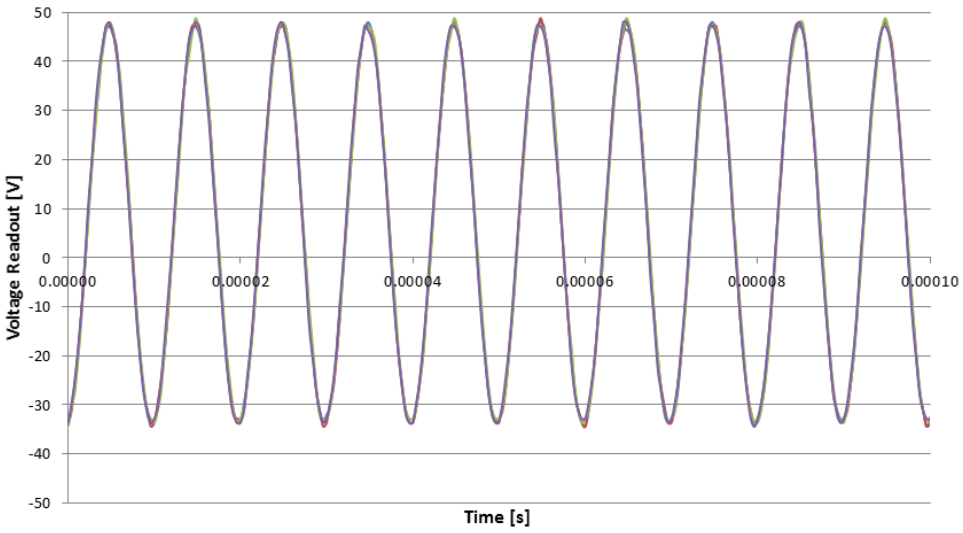

Figure 4-34 Cross-crack signals received by pico sensor during ultrasonic decompression study.

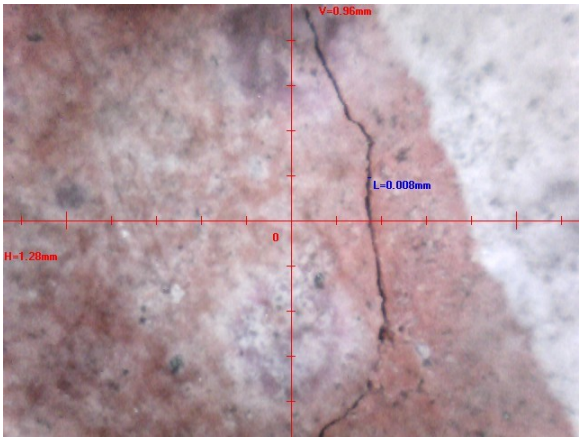

(a)

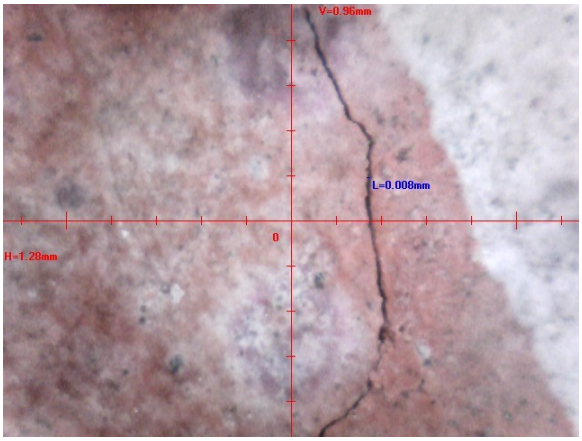

(b)

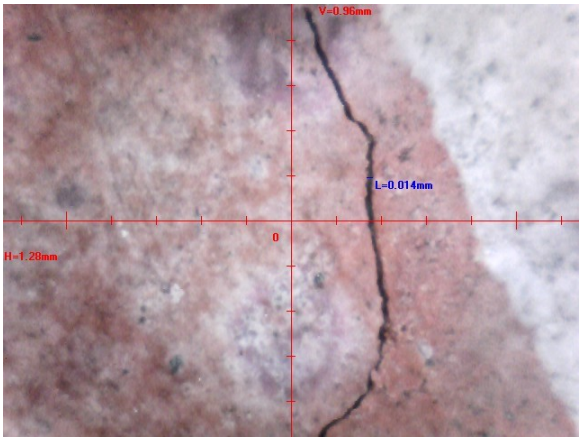

(c)

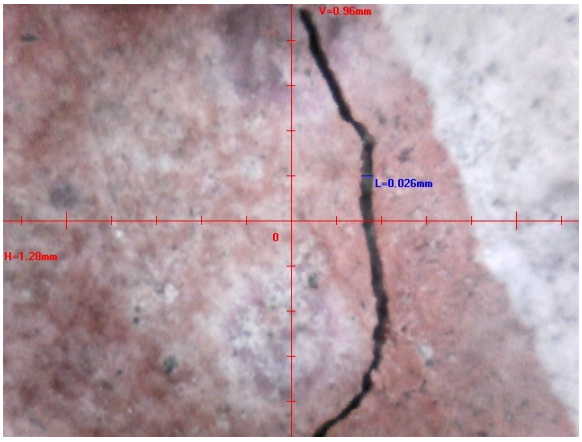

(d)

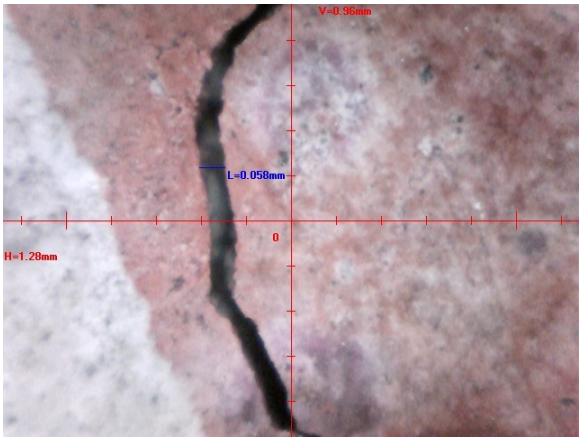

(e)

Figure 4-35 Crack width as measured using USB scope with PL of (a) 0k, (b) 5k, (c) 10k, (d) 15.2k, and (e) 20k.

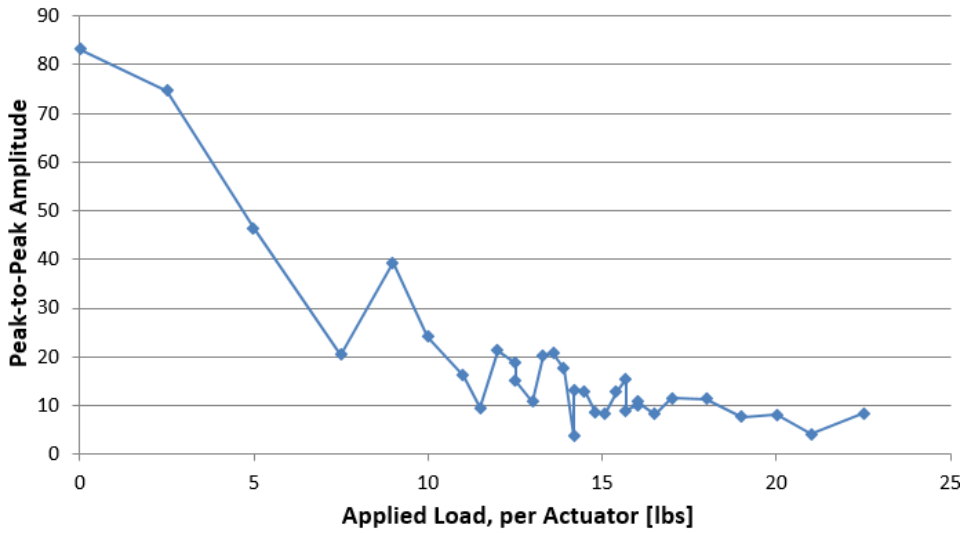

Figure 4-36 Change in amplitude with loading of cross-crack signal received during decompression testing.

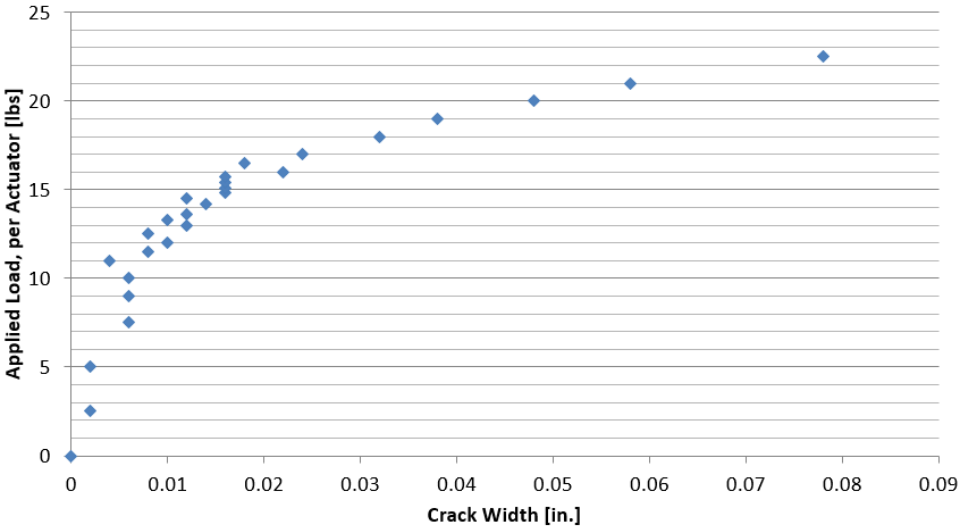

Figure 4-37 Relationship between measured crack width and loading during decompression study.

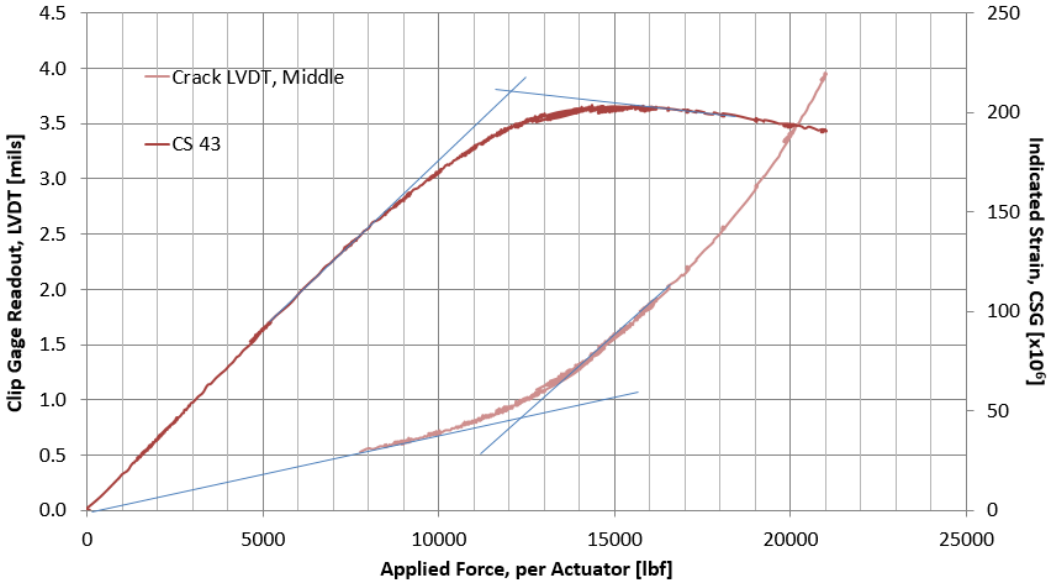

Figure 4-38 Readings from Clip Gage and concrete strain gage during final loading of decompression study.

In addition to the ultrasonic signals, visual observations of the crack width were simultaneously made using a digital scope. The changes in the measured crack width observed when the beam was subjected to various loads can be seen in Figure 4-35.

Based on the changes in peak-to-peak amplitude of the ultrasonic waves with loading (Figure 4-36) and the changes in crack widths (Figure 4-37), the decompression loading was significantly smaller for this round of testing than it was for the decompression testing described previously. From Figure 4-36, it appears that the signal strength falls to and remains below about 25% of its original strength at the 10-kip load magnitude, whereas the crack width measurements appear to change at a high rate after reaching an 11-kip load magnitude.

The differences from previous decompression testing are also seen in the readings taken from the clip gage and the concrete surface strain gage during this testing, as shown in Figure 4-38. As can be seen in these figures, significant changes in the readings from all three types of gages occurred well before the 18 kips determined to be the decompression loading from the previous discussion; the

difference is believed to be the more advanced damage state of the beam at the time of the second decompression study, which will be discussed more in Section 4.5.1.4.

4.5.1.2 Theoretical Models for Static Behavior

Prior to loading of the beam, design values for material and section properties were first used to predict the performance of the beam when loaded with the above configuration. The design values for concrete strength, tendon strength, and prestress loss were used to assess the anticipated behavior of the beam, as were the transformed cross sectional properties. The general procedure for the calculation was as follows:

1. The designer's prestress loss calculations were used to determine the effective prestress in the prestressing strands, P_e.
2. The cracking moment was calculated using Equation (**3**).
3. The live load moment necessary to cause cracking was calculated by subtracting the dead load moment from the cracking moment; the corresponding point loads (using 5-ft constant moment zone setup) that are necessary to create that moment were then calculated.
4. The deflection of the beam at cracking was estimated using the principle of superposition for two point loads applied at 2.5 feet from the center of the beam on opposite sides of the center.
5. M_n was calculated using a value of f_{ps} obtained from the following relationship from PCI:
$$f_{ps} = f_{pu}\left(1 - \frac{\lambda_p * \rho_p * f_{pu}}{\beta_1 * f_c'}\right) \quad \textbf{(13)}$$
The ultimate applied load was calculated as the value of the two point loads necessary to create M_n
6. The total deflection was calculated using the bi-linear moment-deflection relationship described in PCI. The contribution of the deflection of the cracked section, based on an estimated I_{cr}, was added to the pre-cracked deflection to obtain the total at failure.

Results from the preliminary analysis using design equations can be seen in Table 4-15. Important parameters obtained from this calculation were the applied loads and deflections at which cracking and failure of the beam would be anticipated.

Since the original design of the beam did not consider the use of SCC for fabrication, it was beneficial to compare the SCC-2 laboratory beam's actual behavior to the desired behavior. To do this, analyses were done to determine the theoretical, non-factored behavior of the non-composite

beam section as designed. Additionally, the analyses were expanded to consider the measured material properties and structural behaviors of the beam to allow for the comparison of the theoretical behavior of the actual SCC-2 beam behavior to the observed behaviors of the beam, such as stiffness and decompression loading.

Table 4-15 Results of PCI analyses for theoretical behavior of SCC-2 laboratory beam.

P_e, lbs	**786,100**
R, %	**87.5**
P_L @ Cracking, lbs (per actuator)	**30,920**
Δ @ cracking, in.	**1.63**
f_{ps}, psi	**243,760**
P_L @ Failure, lbs (per actuator)	**50,190**
Δ @ failure, in.	**8.01**

The three types of analyses to be utilized for predictive behavior of the beam include the PCI design equations, moment-curvature analysis, and a reinforced beam analysis program, Response2000. The material properties and section properties used for these analyses can be found in Table D-2.

4.5.1.2.1 PCI Design Equations

The original parameters from the PCI analysis discussed above were adjusted based on the observed material properties and structural behavior to more accurately predict the SCC-2 beam behavior. The major adjustments that were made are as follows:

1. Adjust for measured material properties (linear assumption of E_c) and measured strand strain
2. Adjust P_e based on crack opening behavior (f_2=0), as determined in Section 4.5.1.1.1.
3. Adjust f_{ps} based on iterative, non-linear behavior of strands (strand behavior from Devalapura/Tadros, 1994)

A summary of the parameters used for these adjusted calculations can be seen in Table 4-16, while results are compared to the observed beam behavior in Table 4-17.

Table 4-16 Material properties, section properties and input parameters for PCI calculations.

	Design Values	1 Materials & Measured Strain	2 Crack Observations	3 Iterative f_{ps}
Concrete Properties	**Linear, Design**	**Linear, Measured**	**Linear, Measured**	**Non-Linear, Measured**
f_{ci}' [psi]	6,000	6,366	6,366	6,366
E_{ci} [psi]	4.70 x 10^6	4.45 x 10^6	4.45 x 10^6	4.45 x 10^6
f_c' [psi]	8,000	9,513	9,513	9,513
E_c [psi]	5.42 x 10^6	4.85 x 10^6	4.85 x 10^6	4.85 x 10^6
Strand Properties	**Linear, Design Values**	**Linear, from Producer**	**Linear, from Producer**	**Non-Linear, Empirical**
E_s [psi]	28.5 x 10^6	28.7 x 10^6	28.7 x 10^6	Davalapura/Tadros Eqn.
Section Properties	**Design, Transformed**	**Transformed**	**Transformed**	**Transformed**
I_t [in^4]	19,628	19,739	19,739	19,739
e [in.]	5.14	5.15	5.15	5.15
Effective Prestress, P_e	**Calculated Using Design Values**	**From Strand Strain Gages**	**From Observed Decompression**	**From Observed Decompression**
Strand Stress @ Ultimate Stage, f_{ps}	**ACI 318-05 Eq 18-3**	**ACI 318-05 Eq 18-3**	**ACI 318-05 Eq 18-3**	**Iterative Calculation of f_{ps}**

Table 4-17 Comparison of results of ACI analyses for theoretical behavior of SCC-2 laboratory beam.

	Design Values	1 Materials & Measured Strain	2 Crack Observations	3 Iterative fps
P_e, lbs	**786,100**	**699,460**	**707,520**	**707,520**
R, %	**87.5**	**83.3**	**84.4**	**84.4**
P_L @ Cracking, lbs (per actuator)	**30,920**	**26,440**	**26,760**	**26,760**
Δ @ cracking, in.	**1.63**	**1.55**	**1.57**	**1.57**
f_{ps}, psi	**243,760**	**261,690**	**261,690**	**251,690**
P_L @ Failure, lbs (per actuator)	**50,190**	**53,560**	**53,560**	**51,440**
Δ @ failure, in.	**8.01**	**10.72**	**10.63**	**9.91**

4.5.1.2.2 Moment-Curvature Analysis

Based on the methodology outlined in Chapter 2, a moment-curvature analysis was done in addition to the ACI analysis in order to get a more complete representation of the beam's behavior under the 4-point bending scenario. A simple Excel spreadsheet was adequate for determining the sectional response prior to cracking. Since the iterative post-cracking analysis of the member is more tedious, a MATLAB program was developed that could automatically generate the points for moments

exceeding M_{cr}. The moment-curvature relationship developed for the concrete box beam is shown in Figure 4-39.

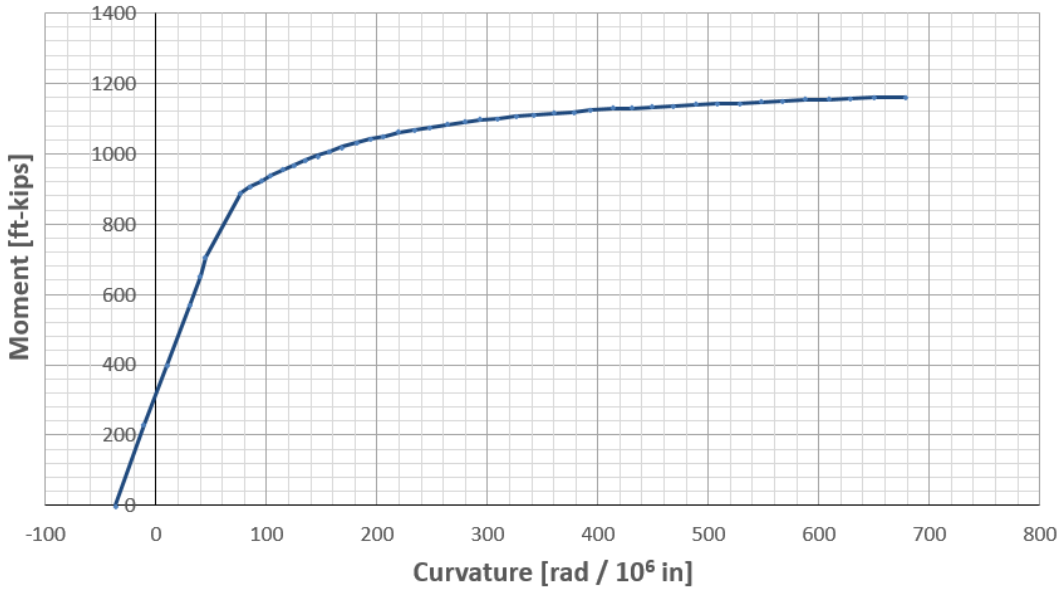

Figure 4-39 Box beam Moment-Curvature relationship from hand calculations.

The moment-curvature calculations indicate that cracking of the section would occur when subjected to a moment of 704.7 ft-kips. When assuming that the dead load moment of the beam is 174.5 ft-kips, and placed in the loading configuration depicted in Figure 4-25, this would correlate to a non-factored applied live load at cracking of P_L=27.9 kips per actuator. Similarly, this model predicts failure of the beam, based on the compressive fiber reaching a threshold of 2,650 με, to occur under a load of 1,162.2 ft-kips, corresponding to an applied load of P_L=52.0 kips per actuator.

Using the 4-point setup as was shown previously, and the relationship given in Equation (7 the load-deflection behavior of the beam can be established. The relationship between the magnitude of the point load and the maximum deflection of the beam, as obtained from this program, can be seen in Figure 4-40. The results indicate an initial camber of 1.57 inches, with an increase in deflection of 2.33 inches to reach the cracking load of P_L=27.9 kips, and an increase in deflection of 11.08 inches to reach the ultimate load of P_L=52 kips.

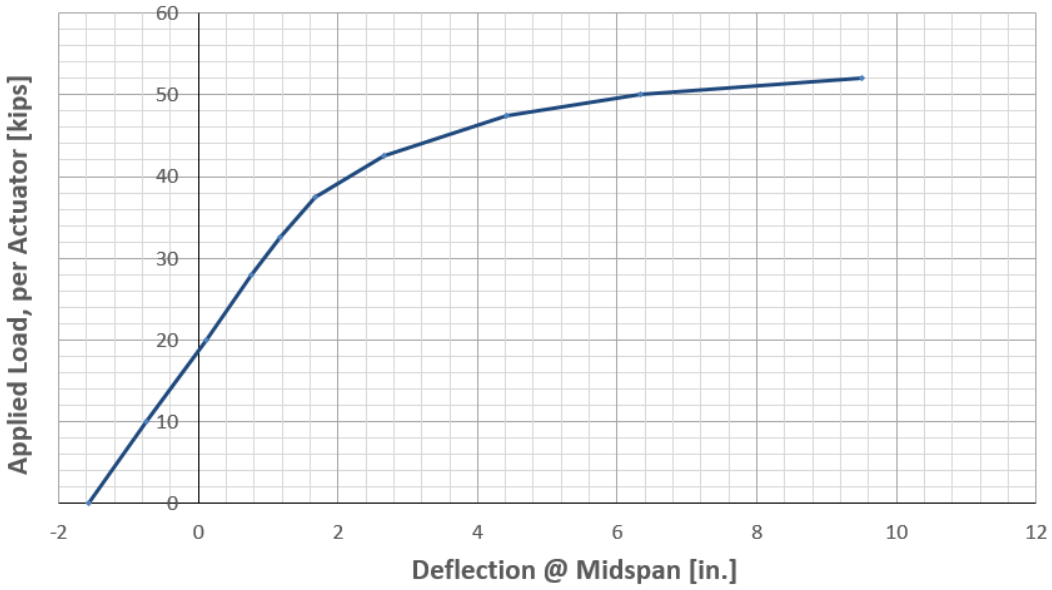

Figure 4-40 Load-deflection relationship obtained from moment-curvature member analysis.

4.5.1.2.3 Response-2000 Analysis

Further analysis was done using a reinforced concrete beam analysis program, Response-2000. Although this program does not facilitate the analysis of prestressed box sections, the cross-section of the laboratory beam was idealized as an I-section with a web thickness equal to the combined sidewall thickness of the box beam. Since it was not possible to recreate the chamfered edges of the beam's void, the web thickness was adjusted to reproduce a section with approximately the same moment of inertia as the actual box beam. The prestressing strands in this model were placed in three rows, located at the same depths as in the design for the box beam. The stress-strain behavior of the beam concrete (APPENDIX B.1) was approximated using piecewise linear segments of the stress-strain curves; the behaviors of the strands were generated by the program according to user inputs. The section parameters for the I-beam can be seen in Figure 4-41.

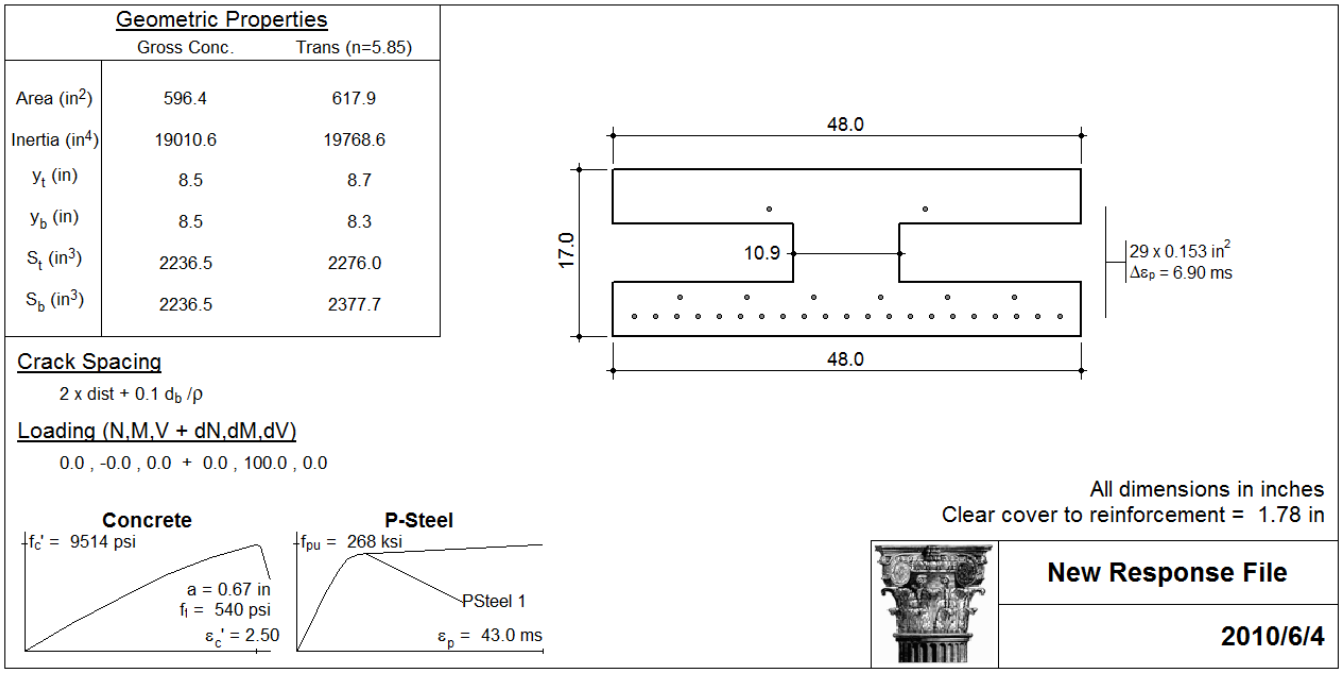

Figure 4-41 Screen capture from Response-2000 software indicating I-beam cross-section and material properties used for analysis.

Using this cross section, a sectional response can be done to obtain the moment-curvature relationship for the section. The characteristic moment-curvature response curve obtained for the section can be seen in Figure 4-42. This plot represents 34 load conditions for which a complete analysis was performed. At any of these load conditions, the user can further investigate numerous characteristics of the beam's behavior, including strain data, depth of neutral axis, strand stresses, and internal forces.

The sectional analysis first indicates the presence of cracking at the section under a loading of 786.5 ft-kips. The peak load in Figure 4-42 is 1176.5 ft-kips, corresponding to a loading of P_L=61.9 kips for the same loading configuration.

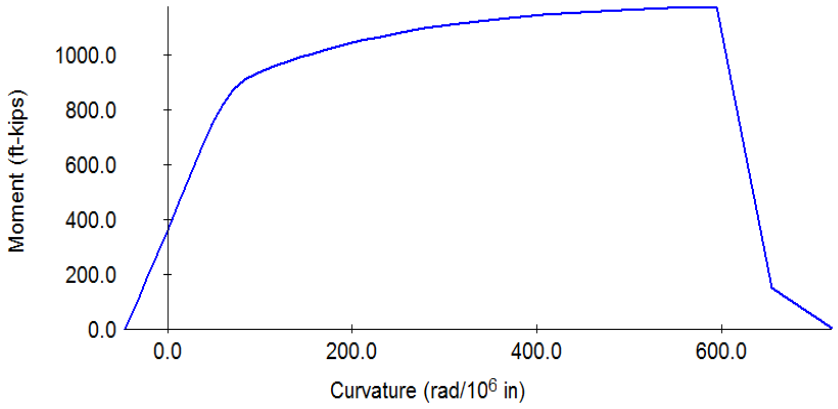

Figure 4-42 Moment-curvature relationship obtained from Response-2000 sectional analysis.

Once the sectional analysis is completed, a full-member analysis can be done. The load configuration for this analysis is again the 4-point setup as was shown previously. The relationship between the magnitude of the point load and the maximum deflection of the beam, as obtained from this program, can be seen in Figure 4-43. The results indicate an initial camber of 1.57 inches, with an increase in deflection of 2.48 inches to reach the cracking load of P_L=41.4 kips, and an increase in deflection of 4.91 inches to reach the ultimate load of P_L=55.2 kips. There is a difference between the ultimate loads obtained from the sectional and member responses because of the dead weight of the beam, and also because the member analysis accounts for an averaged curvature after cracking [the curvature in a cracked member is known to vary greatly within a cracked zone, with localized maximums at the locations of cracks and localized minimums between cracks.]

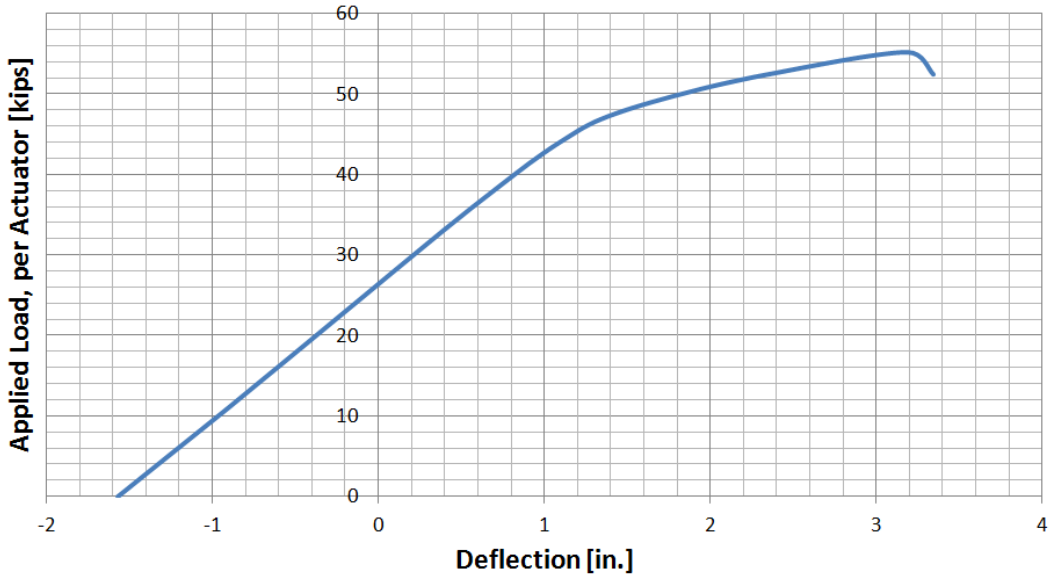

Figure 4-43 Load-deflection relationship obtained from Response-2000 member analysis.

4.5.1.3 Results and Discussion from Static Loading

4.5.1.3.1 Beam Camber at Onset of Testing

As was shown in Table 4-10, the laboratory beam had an initial camber upon detensioning of 1-1/8 in. Upon delivery, the camber had risen to above 2-1/2 in., with a measured camber of 2-5/8 in. at the initiation of static testing, approximately one year after casting. This behavior was compared to the theoretical method for determining camber (described in Chapter 2) in order to determine its efficacy in regards to describing the beam behavior.

The initial camber was calculated based on the measured material properties, using the modulus of elasticity of the concrete at the time of release, and the transformed section properties at the time of release; the long-term adjustments are calculated using the long-term modulus of elasticity of concrete and long term section properties. Adjustments for the long-term camber occur from the prestress losses. In our case, the prestress loss was calculated based on the strand strain gage readings taken immediately after detensioning and the readings from the same strands taken prior to the start of testing, resulting in a loss of 22.96 ksi.

The final component of the long-term camber is the upward camber resulting from the creep of concrete. In the case of the laboratory beam, a creep coefficient of 2.58 was used for these calculations, which was based on the material properties discussed in Section Creep of Beam Concrete.

A comparison of the calculated cambers and the observed cambers measured upon prestress release and at one year after fabrication can be seen in Table 4-18. It can be seen that there was 21.8% difference between the theoretical and observed cambers at the initial stage, with virtually no difference in long-term cambers. When using this method of camber prediction for high-strength prestressed SCC beams, Brewe and Myers also saw the most significant differences in the early ages, with fairly accurate prediction of camber behavior beyond 50 days (Brewe and Myers 2010).

Table 4-18 Comparison of theoretical and observed cambers of SCC-2 laboratory beam.

	Theoretical Camber [in.]	Observed Camber [in.]	% Difference
Immediate (1hr)	**0.90**	**1.12**	**21.8**
Long-term (1yr)	**2.65**	**2.63**	**0.8**

4.5.1.3.2 Cracking

During the first loading to 25 kips, non-linearity was detected in the data taken from some of the mid-span strain gages, as shown in Figure 4-44. It can be seen in this figure that the readings of the lower concrete surface gages [CS43 and CS44] diverge at approximately 9¼ minutes, whereas other gages remain fairly consistent. This phenomenon would coincide with a crack appearance on the bottom surface of the beam. It is believed that the crack would be sufficiently close to CS44 (if not directly beneath the gage) to produce a disproportionately large increase in strain, whereas the rate of strain increase in CS43 decreases at that time due to a stress release from the crack. It also appears that the strain rate of surface strain gage SSG6 increases more rapidly than expected shortly thereafter, a possible indication that the crack propagated to the level of the lower prestressing strands at that time.

This phenomenon is even better illustrated when plotting the strain readings versus the applied loading, P_L, as shown in Figure 4-45. It can be seen from this plot that the major divergence of the readings occurred at a loading of approximately 23,500 lbs per actuator. When comparing Figure 4-44 and Figure 4-45, one can deduce that the effects of cracking were first experienced by SSG6 at a loading of approximately 23,500 lbs per actuator, which is significantly lower than the aforementioned design value of around 30,900 lbs per actuator. It is also below the PCI predictions calculated using more realistic material behaviors.

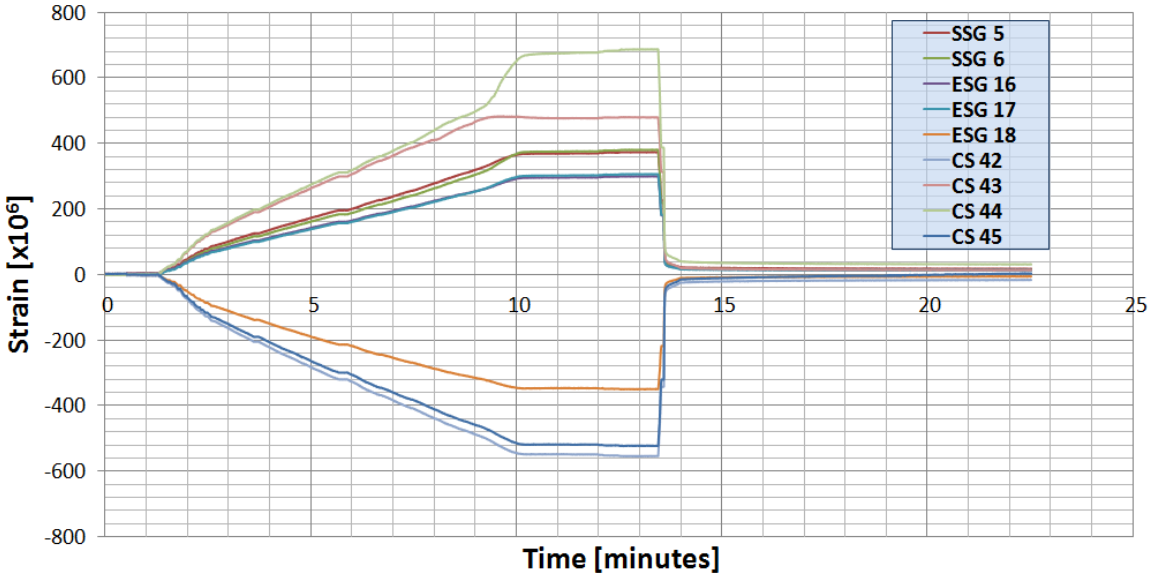

Figure 4-44 Strain data recorded with mid-span gages; first 25-kip loading of laboratory beam.

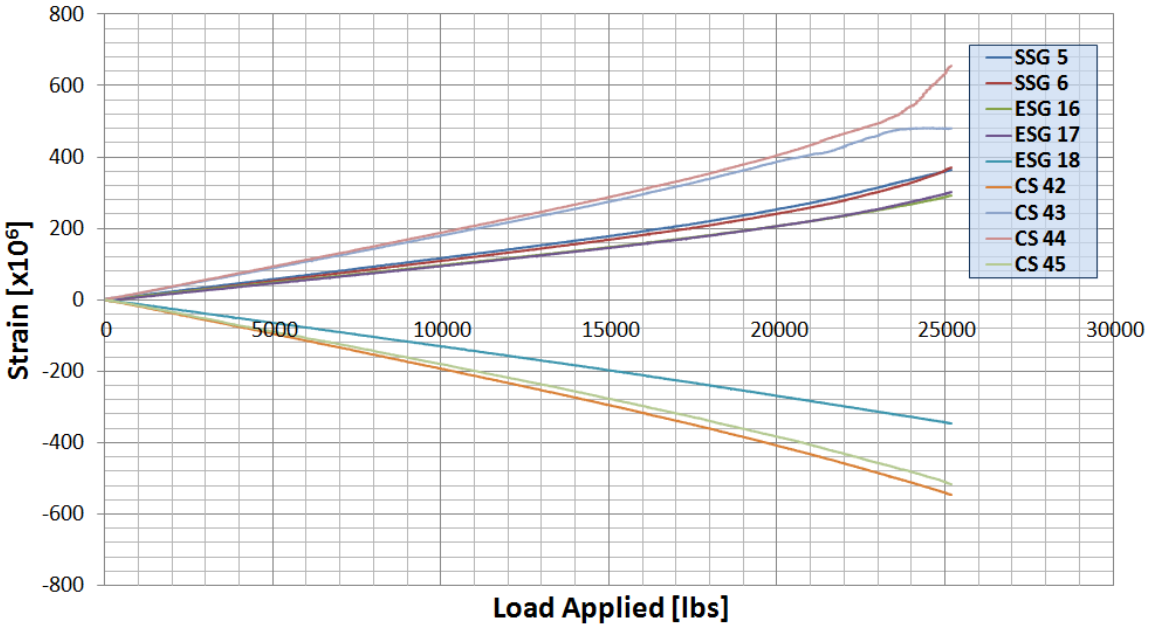

Figure 4-45 Strain data from mid-span gages versus applied load, PL; first 25-kip loading of laboratory beam.

4.5.1.3.3 Load-Deflection Behavior of Laboratory Beam

The mid-span load-deflection data from the initial loading, as well as the reloading portions of later tests, are presented in Figure 4-46 for small loads (prior to decompression). In this figure, the deflection measurements represent the average of the two mid-span LVDTs, while the load data represents the average of the two load cell readouts. This shows that at small loads, a relatively linear, repeatable load-deflection behavior is seen up through the 47.5 kip loading. Minor variations in the observed behavior do not appear to directly correlate to the damage state of the beam, so these variations likely result from small changes in alignment between tests, with the possibility of minor effects stemming from ongoing creep and creep recovery behaviors of concrete due to the previous load states.

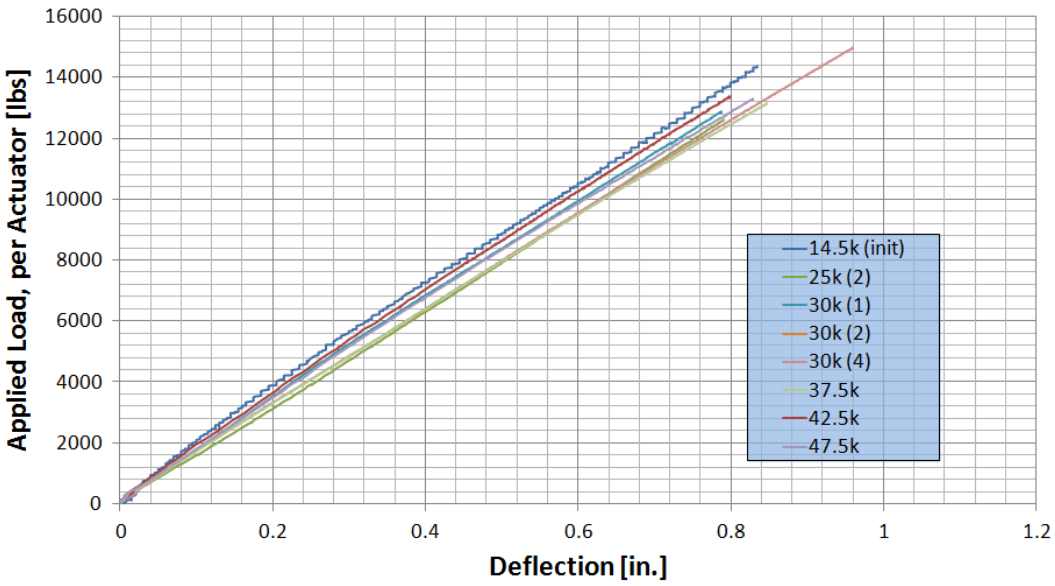

Figure 4-46 Load vs. deflection of laboratory beam subjected to small loads.

The load-deflection behavior of the beam as observed for each test can be seen in Figure 4-47. In this figure, the deflection readings are zeroed prior to each test in order to remove any permanent deflection that might have previously occurred. For the most part, the load-deflection behavior of the prestressed beam followed approximately the same path, at least until the final two loadings. Even then, while the beam stiffness was reduced at points during those two loadings, the path seemed to converge to the same envelope at loads exceeding the highest previous loading.

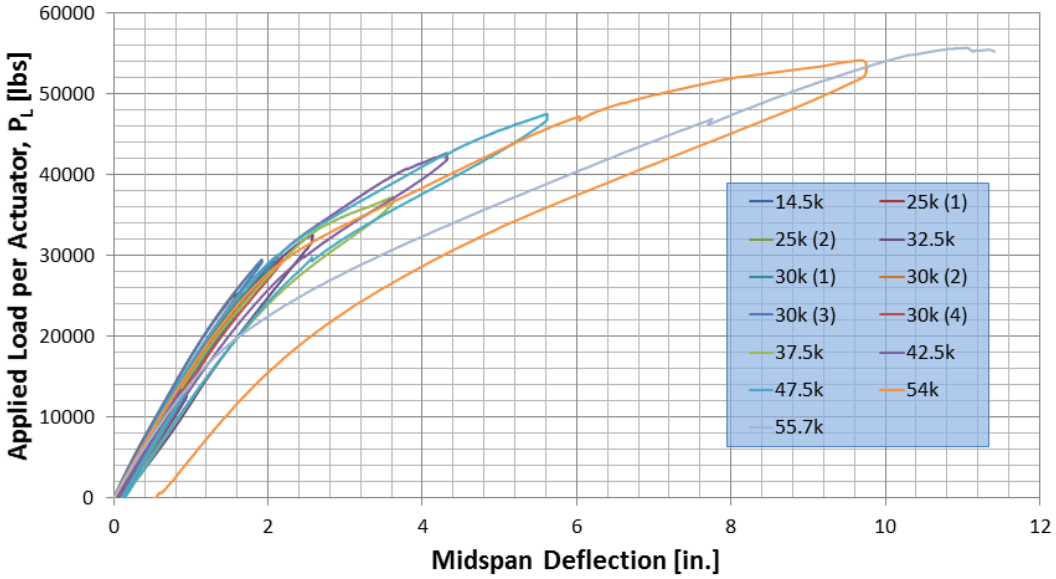

Figure 4-47 Midspan deflection (zeroed) versus applied load from static loading of laboratory beam.

For most load cycles, the beam's mid-span deflection became very small immediately upon unloading, with the exception of the 54-kip loading data. This would indicate that very little plastic deformation occurred within the beam prior to that load cycle. The camber data collected in between cycles confirms this, with only small changes detected prior to the 54-kip loading, as shown in Table 4-19.

Table 4-19 Observed changes in laboratory beam camber throughout static load testing regimen.

Maximum Previous Load Case [kips]	Measured Camber [in.]	Cumulative Change in Camber [in.]
0	**2 5/8**	**--**
32.5	**2 17/32**	**- 3/32**
42.5	**2 ½**	**- 1/8**
47.5	**2 15/32**	**- 5/32**
54.0	**2 1/32**	**- 19/32**

Based on these observations, the data from Figure 4-47 can be adjusted to reflect the plastic deformation that was present prior to each loading; this is shown in Figure 4-48. This is similar to the previous figure, but with a slightly altered envelope when accounting for plastic deformations.

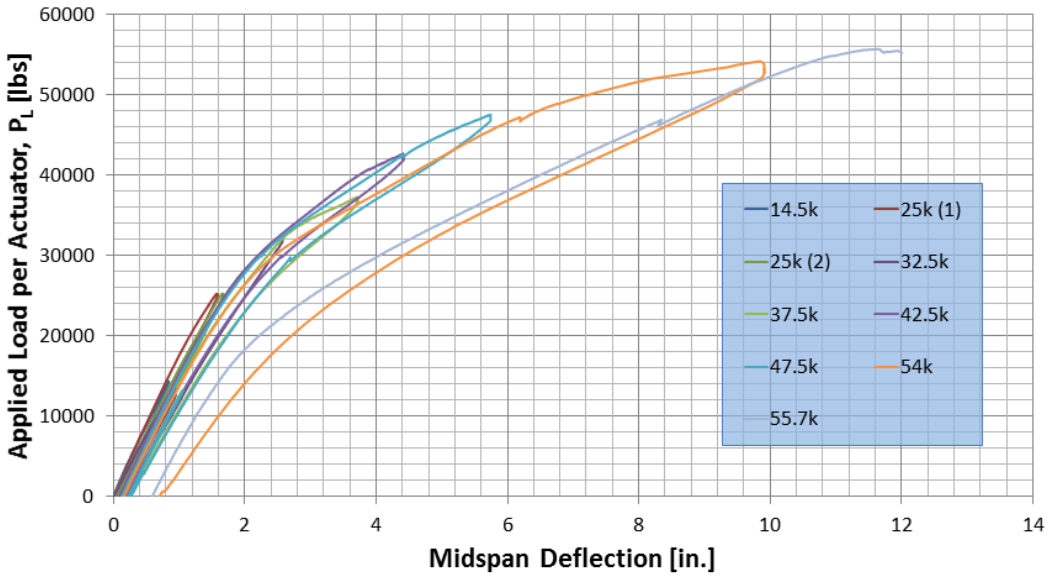

Figure 4-48 Midspan deflection (w/plastic deformations) versus applied load from static loading of laboratory beam.

The loading portion of these curves was then compared to the theoretical behavior of the beam, as shown in Figure 4-49. It can be seen from this figure that the beam cracked at a load below the design strength and all predictions, and with a smaller deflection. However, the ultimate load of the beam exceeded the design values, as well as the moment-curvature and PCI predictions, in both load magnitude and deflection.

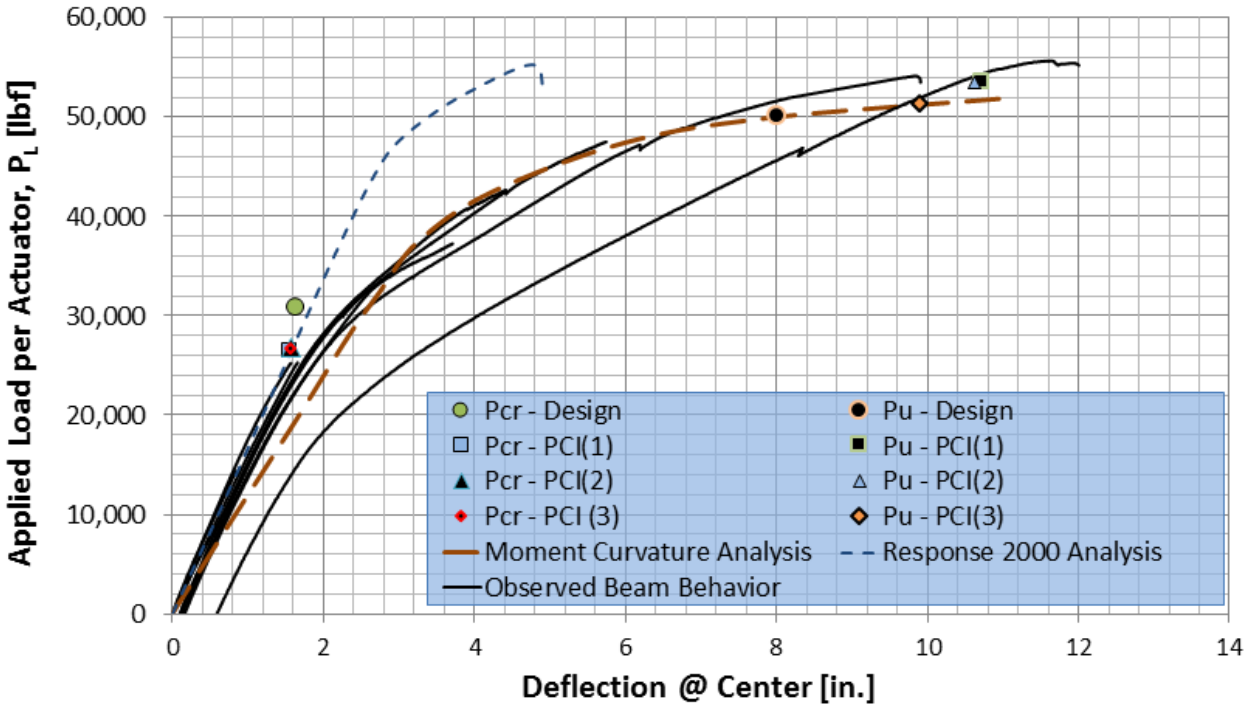

Figure 4-49 Observed load-deflection behavior of laboratory beam compared to theoretical behavior.

4.5.1.3.4 Strain Profile

Data collected for observation of the pre-cracking behavior was limited to the first loading of 14.5 kips per actuator, and the majority second loading, during which cracking was observed. As expected, the beam exhibited particularly linear behavior prior to cracking. This is evident when observing the strains recorded from sensors in the constant-moment zone versus loading for the first load magnitude, 14.5 kips, as shown in Figure 4-50. In this figure, an increase in strain is representative of an elongation at the location of the gage. It can be seen that all gages behave in a predominantly linear fashion with changes in strain almost exactly proportional to increases in loading.

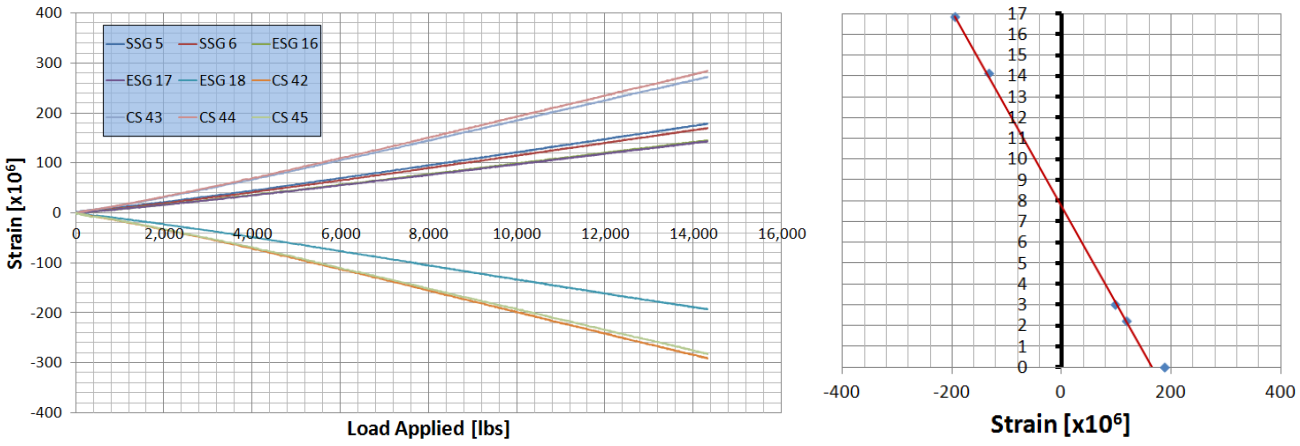

(a) (b)

Figure 4-50 Strain readings (microstrain) at mid-span during application of 14.5-kip loading to laboratory prestressed beam. (a) All gage readings vs. P_L; (b) Reading vs. gage depth (in.) when P_L = 10 kips.

As can already be seen from the mid-span strain data shown in the cracking discussion (Figure 4-44 and Figure 4-45), as well as the load-deflection data (Figure 4-47 through Figure 4-49), the overall behavior of the beam becomes much more non-linear after cracking. This can be observed for the mid-span strains at loads beyond the cracking moment; Figure 4-51 shows the strains in the constant moment zone for the 32.5 kip loading. The strains on the top portion of the beam, while slightly curved, appear to follow a reasonable stress-strain pattern for concrete in compression. Readings on the bottom of the beam appear to be more dependent on their vicinity to cracking, as illustrated by the divergence of the two lower concrete surface gages (CS43 and CS44).

Figure 4-52 illustrates that the linearity of the strain readings exhibited in Figure 4-50(b) was seen to fade at higher loads, particularly beyond a live load magnitude of P_L=20 kips. Beyond that load state, the strains from the concrete surface strain gages on the bottom side of the beam do not increase at the same rate as the strand strain gages. Also, the strain readings from the concrete embedment gages immediately above the strand strain gage (depth=3 in.) do not increase at the same rate beyond P_L=25 kips.

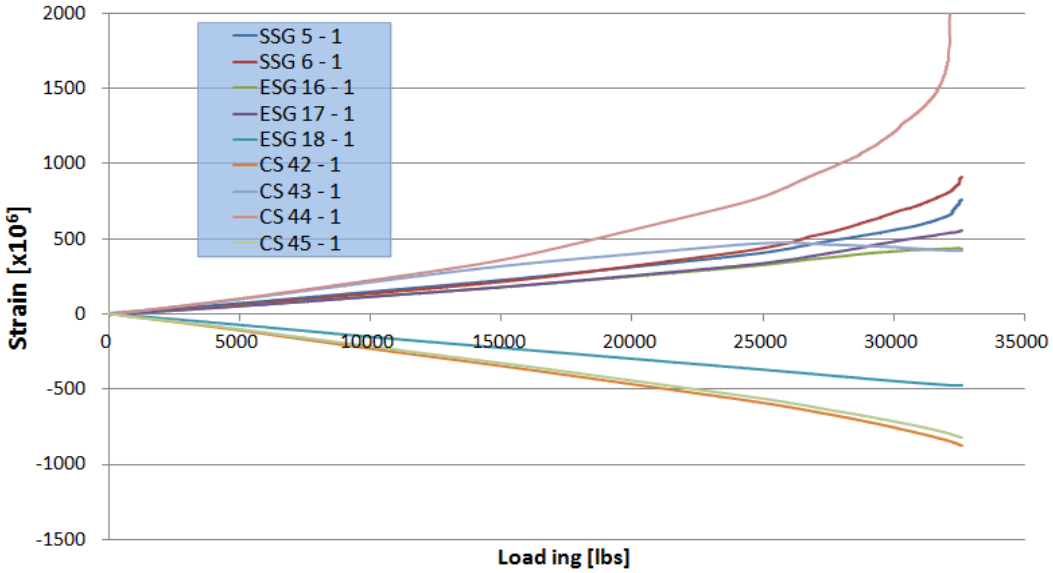

Figure 4-51 Strain data from mid-span gages versus applied load, PL; 32.5-kip loading of laboratory beam.

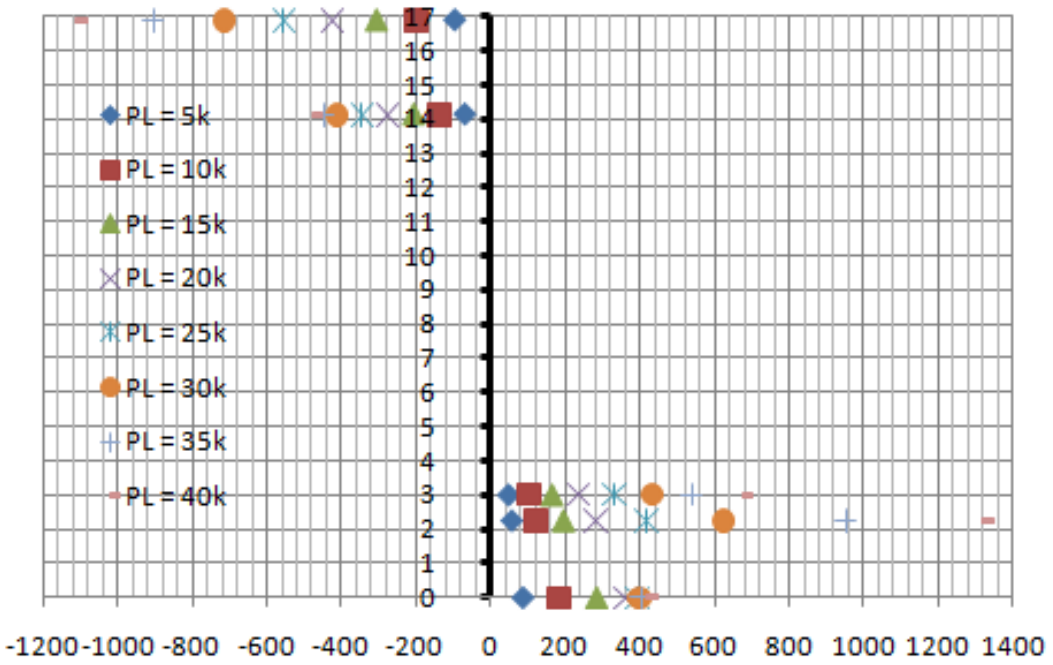

Figure 4-52 Mid-span strain readings (microstrain) at various loads, shown vs. depth (in.), during application of 42.5-kip loading to laboratory prestressed beam.

The likely cause of the reduction in the rate of the strain increase at those locations is the vicinity of the gages to cracks propagating from the bottom of the beam, which would subsequently

provide stress relief at those locations. The proximity of the gage to the crack, as well as its proximity to the bonded strand, would ultimately determine the response of the gages at that location, as illustrated by the readings of concrete surface strain gages CS 43 and CS 44 in Figure 4-51; while both gages are mounted on the bottom of the beam, and would be essentially the same distance from the bonded strands, a crack was seen to propagate directly beneath where Gage CS 44 was mounted, whereas the location of CS 43 was between two cracks.

When considering the strain readings from only the strand strain gages and the concrete gages in the compressive zone, a relatively linear relationship can still be seen at higher loads, as depicted in Figure 4-53. This figure shows theoretical linear strain profiles based on the strain readings of the strands and those of the concrete surface strain gages on the outermost compressive fibers of the beam.

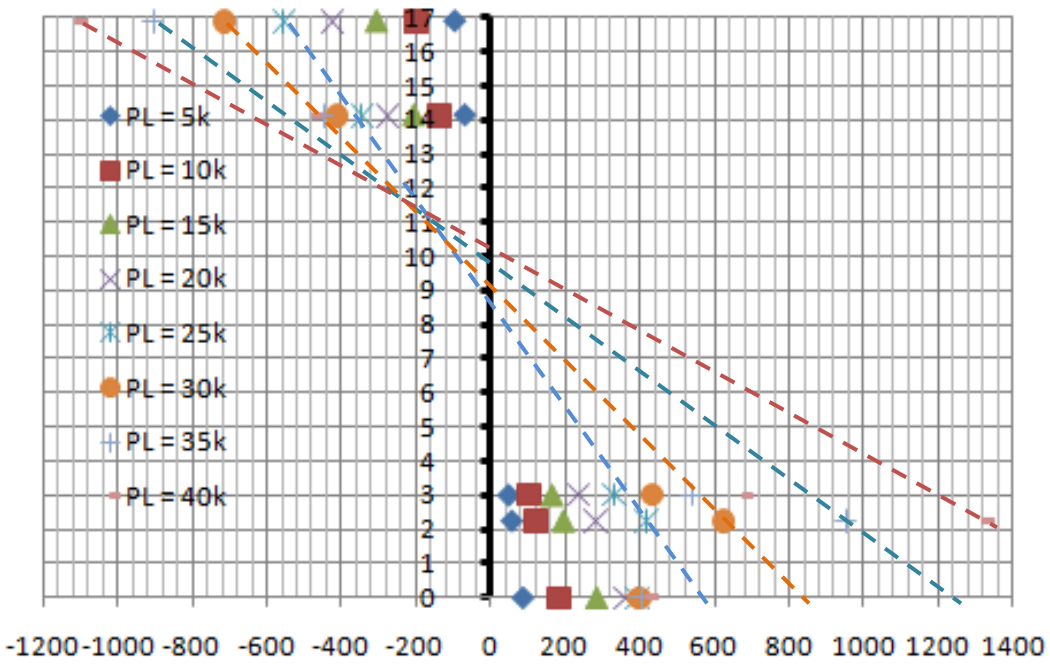

Figure 4-53 Mid-span strain readings (microstrain) at various loads, shown vs. depth (in.), during application of 42.5-kip loading to laboratory prestressed beam.

As expected, the depth of the compressive zone is seen to reduce under higher loadings based on the theoretical strain profiles. However, while this figure initially shows a relatively linear

relationship, the reading from the concrete embedment strain gage in the compressive zone (depth = 14 in.) does not show a linear response beyond the 30-kip loading.

4.5.1.3.5 Concrete Stiffness from Strain Measurements

The test specimens used to establish the concrete properties shown in Table 4-12 were moved to a curing room shortly after detensioning, so these did not experience identical ambient conditions to those experienced by the test beam. Therefore, it was of interest to determine how representative the concrete properties established using these cylinders were of the actual beam concrete. This was done by correlating the changes in strain at the top of the beam with the theoretical changes in strain due to increased loading, making it was possible to estimate the stiffness of the beam concrete. Since the post-cracking behavior becomes more complex than the assumed pre-cracking behavior, estimations were done based on data from early loadings of small load magnitude.

For a pre-determined load range, the stress was assumed to increase based on uniform sectional properties using the relationship:

$$\Delta\sigma_1 = \frac{\Delta M \cdot c_1}{I_c} \quad \textbf{(14)}$$

For these calculations, the values of c_1 and I_c that were used were 8.68 in. and 19,739 in^4, respectively; the calculations of these section properties are shown in APPENDIX D. The average strain change from the readings of the two concrete surface strain gages located on top of the beam was used to define the deformation of the concrete when subjected the corresponding stress change. The stiffness was then approximated as a chord modulus for each load range by calculating the proportion of the increase in stress to the corresponding increase in strain for that range.

The average of the two strain gage readings from the top two concrete surface strain gages, CS 42 and CS 45, was used to calculate the concrete stiffness for the 14.5k loading, and the first and

second 25k loadings (see Figure 4-45, Figure 4-50 and Appendix C). These results are shown in Table 4-20. Some variation in data could be due to minor differences in alignment of the spreader beam, which was removed and replaced between tests. It can be seen from the latter two tests that a slight decrease in calculated stiffness occurs when considering the higher load range, 0k to 20k, as opposed to 0k to 14k. The results from the first two loads would indicate a concrete stiffness that is at or slightly above the 28-day cylinder results that were shown in Table 4-12, which indicated an average stiffness of 4.93 $x10^6$ psi for cylinders taken during casting of the WVU Lab Beam. The concrete stiffnesses obtained from the second 25k loading are slightly below that obtained from the cylinder testing.

Table 4-20 SCC-2 stiffness, as calculated from beam loading data.

Load Range	ΔM_L [ft-lbs]	Change in Stress [psi]	Modulus of Elasticity		
			14.5k Loading [psi]	**1st 25k Loading [psi]**	**2nd 25k Loading [psi]**
0k to 14k	38000	1,403.6	**5,021,200**	**5,296,200**	**4,697,600**
0k to 20k	38000	2,005.7	**--**	**5,074,700**	**4,618,800**

4.5.1.3.6 Debonding of Strands

As was mentioned in Section 4.5.1.1.2, it was determined from the crack profiles that some debonding of the interface between the strands and concrete could have occurred by the time that testing was conducted (after the beam was subjected to a loading of 47.5 kips). The data collected from strain gages on the lower portion of the beam was used to further explore this phenomenon. This included strain gage measurements from the concrete as well as data from the prestressing strand gages. The objective of this portion of the study is to indirectly detect changes in the level of constraint provided by the interfacial bond by observing changes in the overall beam behavior, particularly localized changes at the locations of the strain gages.

The gage readings taken from the strand strain gage SSG 5 during key loadings are compared in Figure 4-54. In this figure, the readings taken during the progressively increasing load cycles, as well as representative samples of those during the initial debonding study and second decompression study, are plotted in chronological order (see Figure 4-24) to show the change in beam response at this location. As can be seen in this figure, there is a relatively consistent response from this gage until after the 54.0-kip loading.

Reasons for changes in the response after the 54.0-kip loading could include the occurrence of permanent damage, such as concrete microcracking or plastic deformation of the prestressing strands, or changes in constraint conditions of the strands due to debonding at the steel-concrete interface. Since it was seen in Table 4-19 that significant changes in camber had occurred after the 54-kip loading, coupled with the fact that the initial strand strain of around 5,500 με was raised to beyond 8,500 με because of the 54-kip loading, it is reasonable to believe that some yielding of the prestressing strand had occurred during the 54-kip loading.

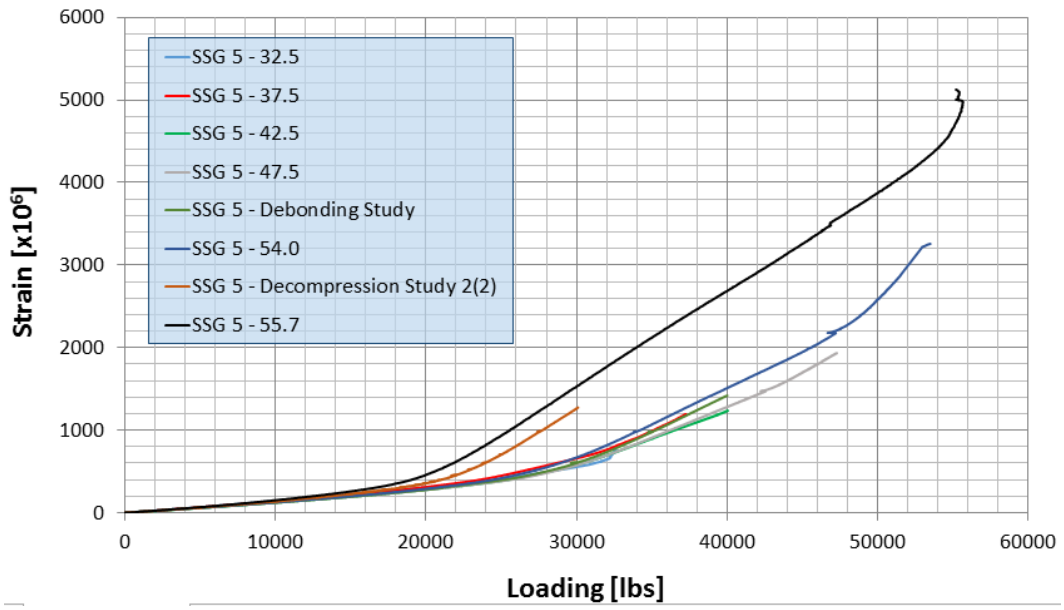

Figure 4-54 Response history of strand strain gage SSG5 throughout static load testing of beam.

While the change in response of the strands may be primarily due to yielding of the strands, the responses of the concrete gages may give more indication as to whether debonding had occurred. To further explore this topic, the readings from concrete surface strain gage CS 43 were plotted for the same loadings as those for the strand strain gage, which are shown in Figure 4-55. When comparing this to Figure 4-54, one can see that there were much larger changes in the readings from the concrete surface gage throughout testing than what had occurred with the surface strain gages.

Crack propagation near the gage location would change the boundary conditions at the location, and ultimately affect the readings. This is evident in the 32.5-kip loading, during which there was a noticeable stress release due to the initiation of cracking, apparent by the decrease in strain after a load of about 25 kips was reached. It is reasonable that there is a slight reduction in the response at the location of the gage as the cracks propagate and microcracking occurs within the concrete, since more and more concrete loses its ability to withstand tensile forces. The difference between the 37.5 kip response and the 42.5 kip response could be due in part to small variations in the alignment of the spreader beam and the load cells, which were removed and replaced between tests.

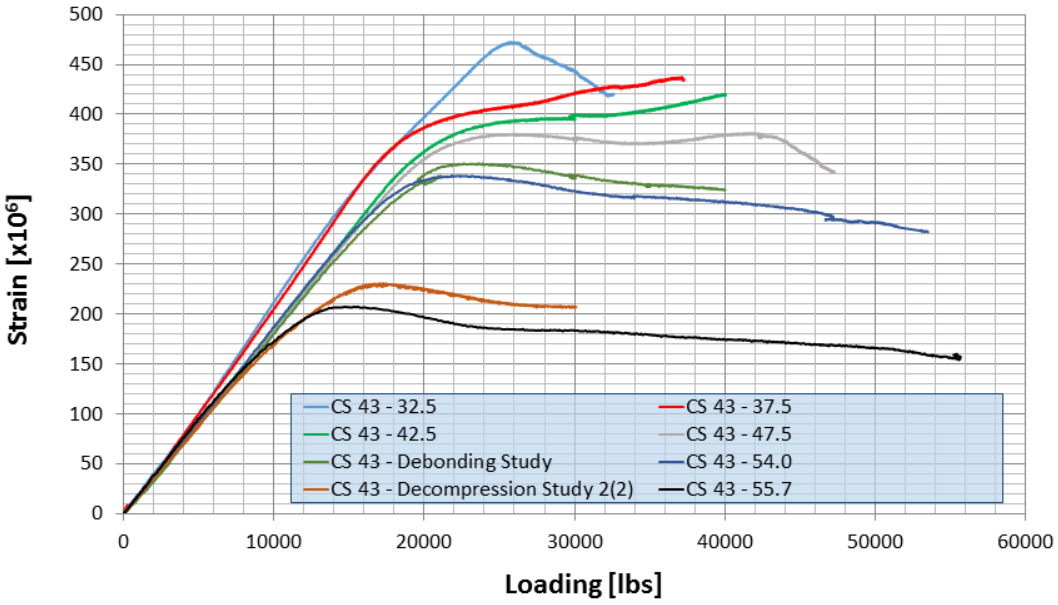

Figure 4-55 Response history of concrete surface strain gage CS43 throughout static load testing of beam.

With a consistent bond between concrete and the prestressing steel, the effect of crack propagation should become minimal, though, as the tip of the crack gets further from the location of the gage. Furthermore, with a layer of fully-bonded prestressing strands located less than two inches from the bottom surface of the beam, the significant elongation of the strands with increased loading would be accompanied by at least a slight elongation of the bottom fibers of the beam. However, during the 47.5-kip loading and after, there are times when the concrete strain readings are actually decreasing with an increase in load. This could indicate an ongoing change in restraint conditions at the location of the gage, which could be due to the appearance of more cracks in the vicinity of the gage, an ongoing loss of bond between the concrete and prestressing strands, or a combination of the two. While the sharp drop toward the end of the 47.5-kip loading might have been due to initiation of a new crack, the gradual decrease in strain with increased loading could be indicative of an insufficient bond at that location.

More evidence of debonding can be seen when observing the behavior of the concrete embedment gage that is located only ½" above the bottom row of prestressing strands. It was shown in Figure 4-52 that the strain readings from these embedment gages become disproportionately small when compared to those from the strand strain gages. While it is possible that the proximity to cracking would come into play as a release for the embedment gages, it is unlikely that they could deform so differently from the prestressing strands if a perfect bond existed between the steel and the concrete.

4.5.1.3.7 Comparison of Methods for Decompression Assessment

The previous discussion in Section 4.5.1.1 indicated that there was a significant reduction in load that would cause decompression of the concrete on the bottom of the beam by the time the second decompression study was conducted. It was already discussed in Section 4.5.1.3.6 that the strand strains exceeded 8,500 με prior to the second decompression study, so the plastic deformation of the

prestressing strands is the likely cause of this reduced decompression load, along with an increased presence of microcracking within the concrete. Since the results of the first decompression study were already given in Section 4.5.1.1.1, this section will focus on the results of the second decompression study, and in particular on comparing the results from the various methods used during that study.

The results from the ultrasonic test warrant more investigation. The peak-to-peak amplitudes of the time-domain signals received from the cross-crack sensor were determined at different load magnitudes during the loading and unloading of the beam, as shown in Figure 4-56. In multiple trials, the amplitude was seen to exhibit an overall drop in amplitude with increasing loads, with a localized peak around 9-10 kips when loading, and a localized peak around 10-11 kips while unloading.

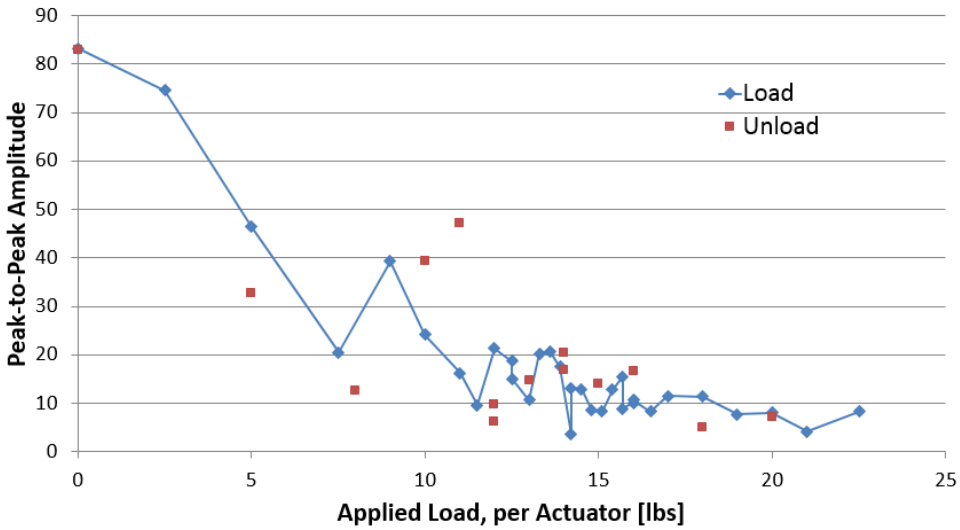

Figure 4-56 Peak-to-peak amplitudes of cross-crack signals received during ultrasonic decompression study.

A spectral analysis was done using the Signal Express software to further analyze the signals received, which is shown in Figure 4-57. For all tests, the predominant peak appeared at 100,000 Hz, and another consistent peak appeared at 200,000 Hz. The magnitudes of the 100 kHz peak and the 200 kHz peak were compared throughout the loading and unloading of the beam. The trends observed in

the time-domain are further exemplified when observing the magnitudes of the 100 kHz and 200 kHz components of the power spectral density of the signal, as shown in Figure 4-58 and Figure 4-59.

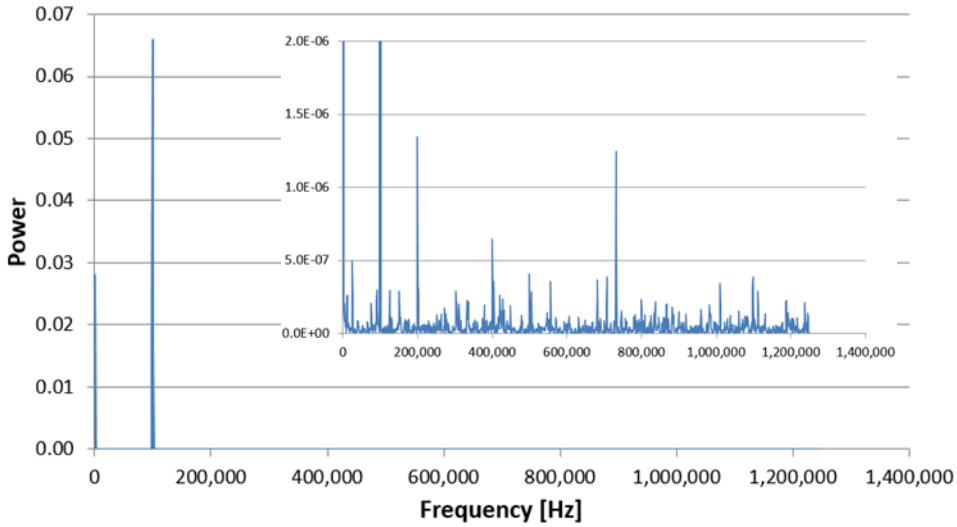

Figure 4-57 Power Spectral Density (PSD) of cross-crack signal received when beam is subjected to PL=7.5 kips.

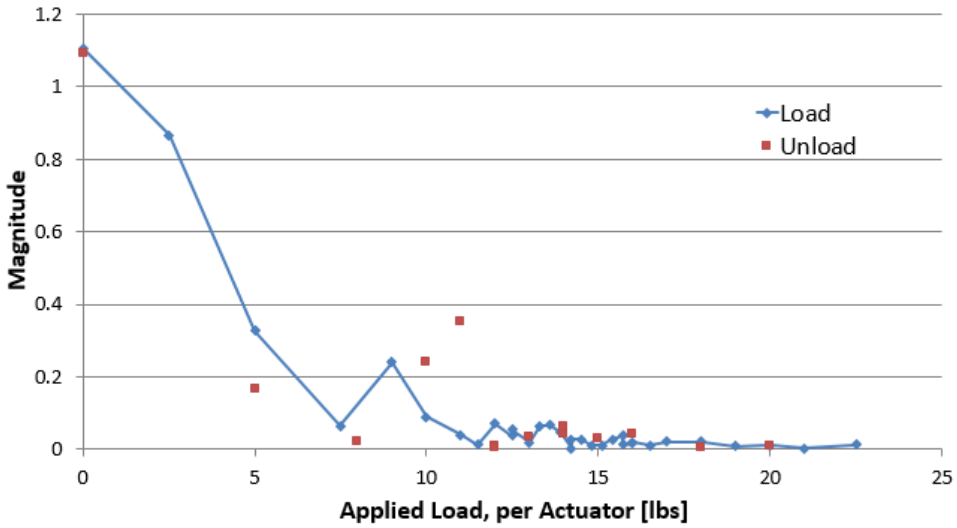

Figure 4-58 Magnitude of 100 kHz component of PSD of cross-crack signals at various load states.

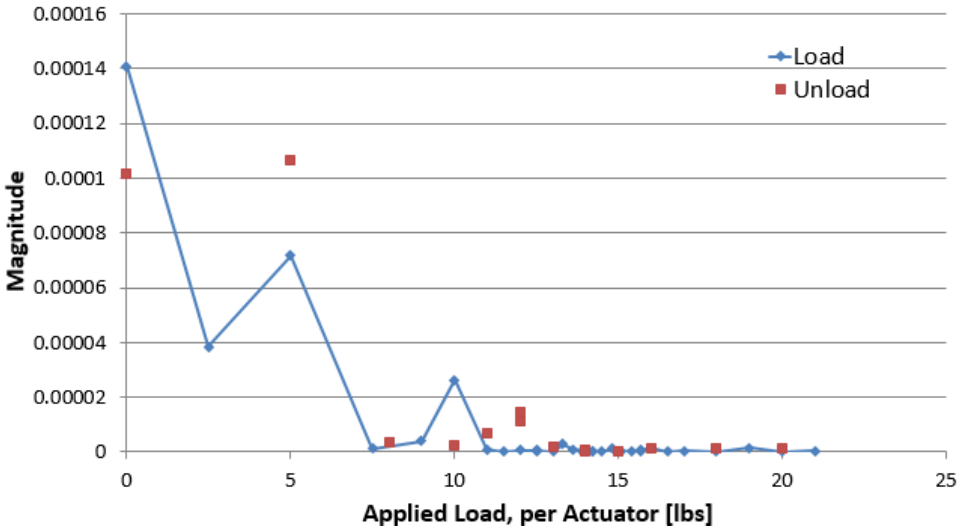

Figure 4-59 Magnitude of 200 kHz component of PSD of cross-crack signals at various load states.

The crack width data taken using the digital scope (Figure 4-35) indicated a widening of the crack after a load of 11 kips. Similarly, data from the crack clip gage and concrete surface gage CS43 (Figure 4-38) indicate decompression loads in the range of 12-12.5 kips. From the data shown in Figure 4-56, Figure 4-58 and Figure 4-59, it would seem that the 200 kHz component of the PSD for the unloading of the beam gives the best correlation to the results from the other methods, with a peak appearing at 12 kips.

4.5.1.3.8 Mechanism of Beam Failure

There was some plastic deformation of the prestressing strands prior to the ultimate failure of the beam. Small amounts of plastic deformation are believed to have taken place during the 47.5-kip loading, with much more significant amounts taking place during the 54-kip loading. The stress-strain relationship for the prestressing strands given by Devalapura and Tadros (Devalapura and Tadros 1992), shown in Figure 4-60, indicates a strain of approximately 7,500 με as the beginning of non-linear behavior for the tendons. Based on an initial strain of 5,500 με at the onset of testing, the strands would have to undergo an additional deformation of approximately 2,000 με prior to yielding. It was seen in the response history of strand strain gage SSG5 (Figure 4-54) that the strand strain gage

underwent an increase in strain of more than 3,000 με during the 54-kip loading, which would have been enough to cause plastic deformation of the strands.

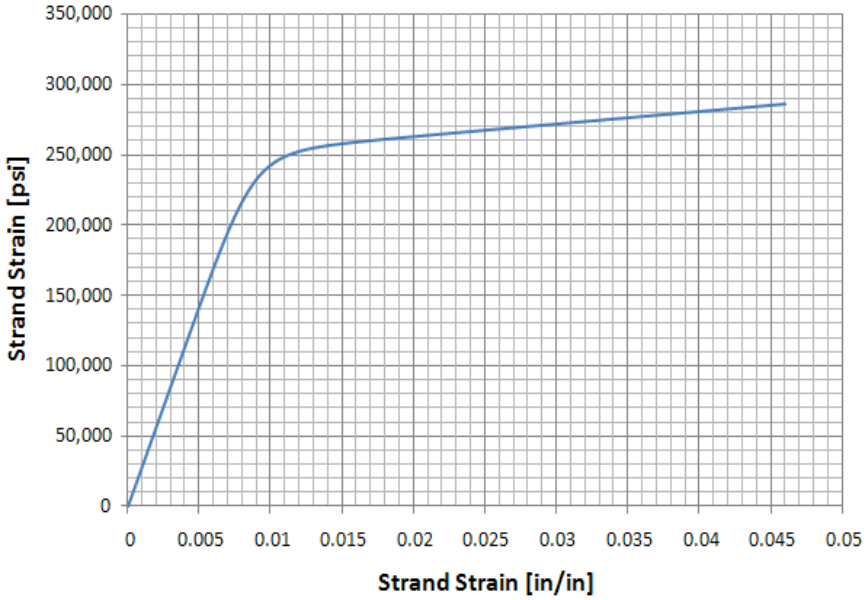

Figure 4-60 Behavior of Gr270 Low-Relaxation Strands (Devalapura and Tadros 1992).

After the yielding of the prestressing strands, the beam still underwent a significant amount of deformation before ultimate failure, which was due to compressive failure of the extreme compressive concrete. Since the failure of the beam was technically due to the yielding of the prestressing strands, the compressive failure is considered a secondary failure mechanism. Pictures of the compression failure sequence taken at mid-span are shown in Figure 4-61.

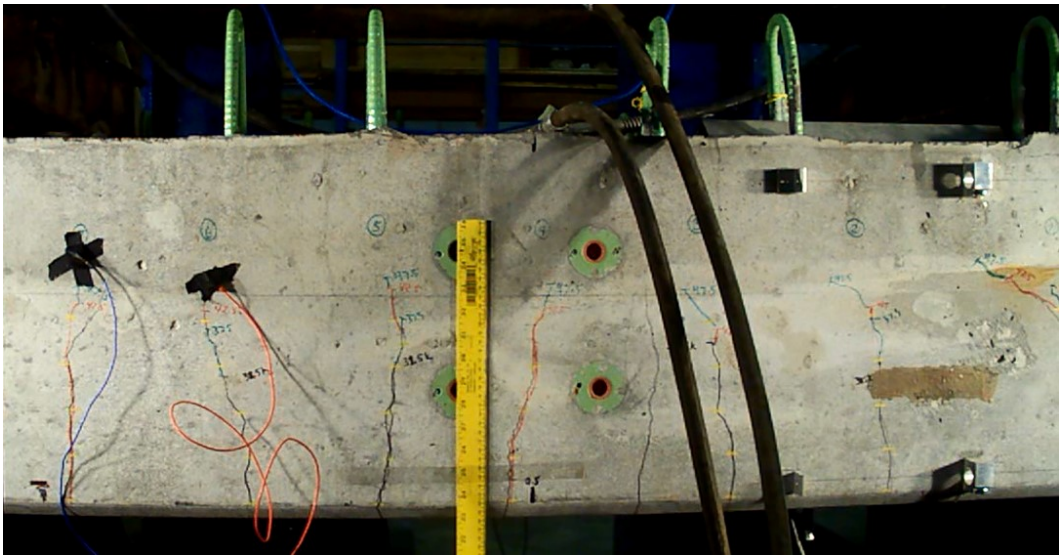

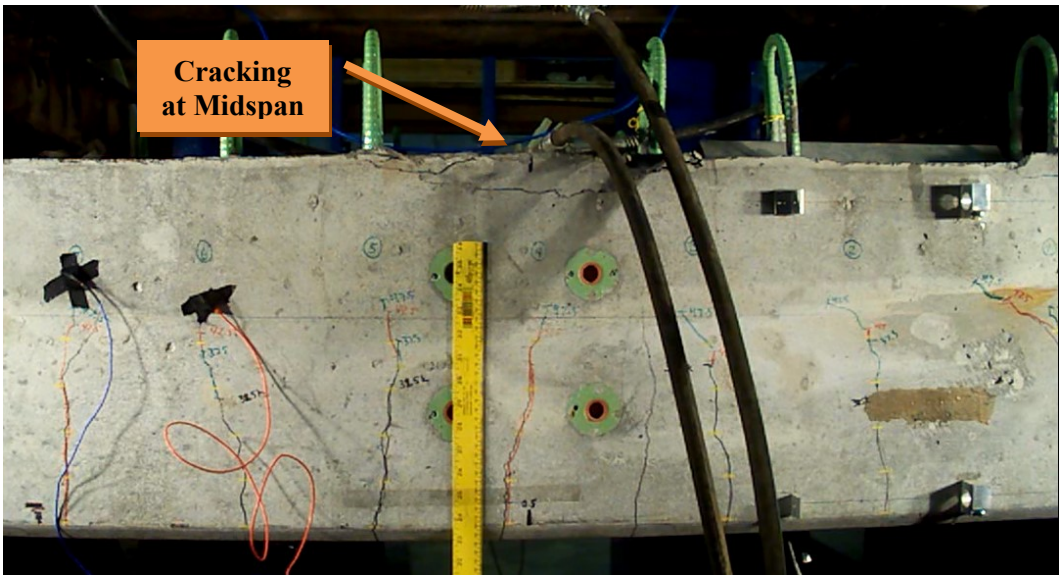
Cracking
at Midspan

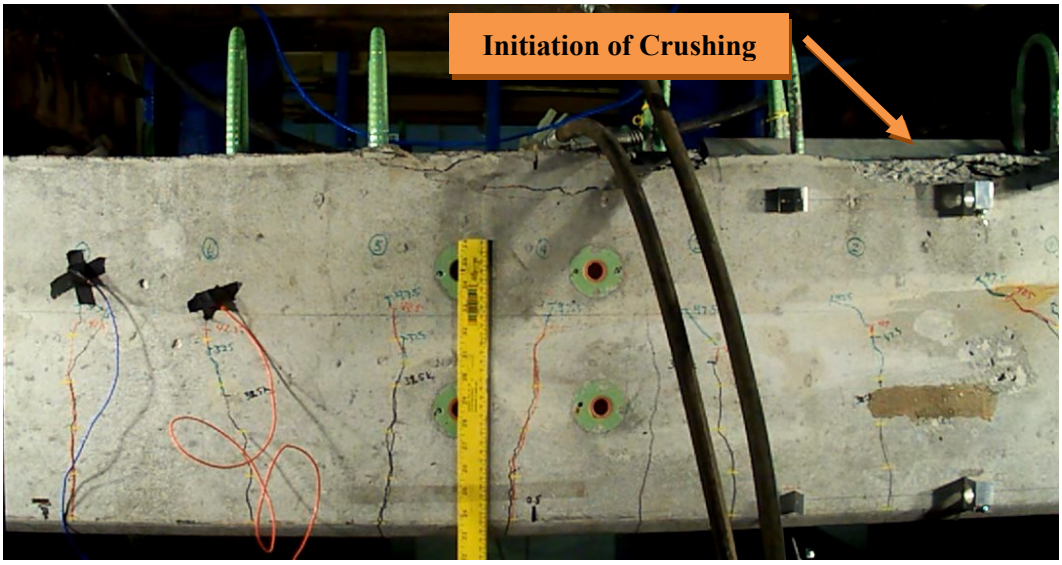
Initiation of Crushing

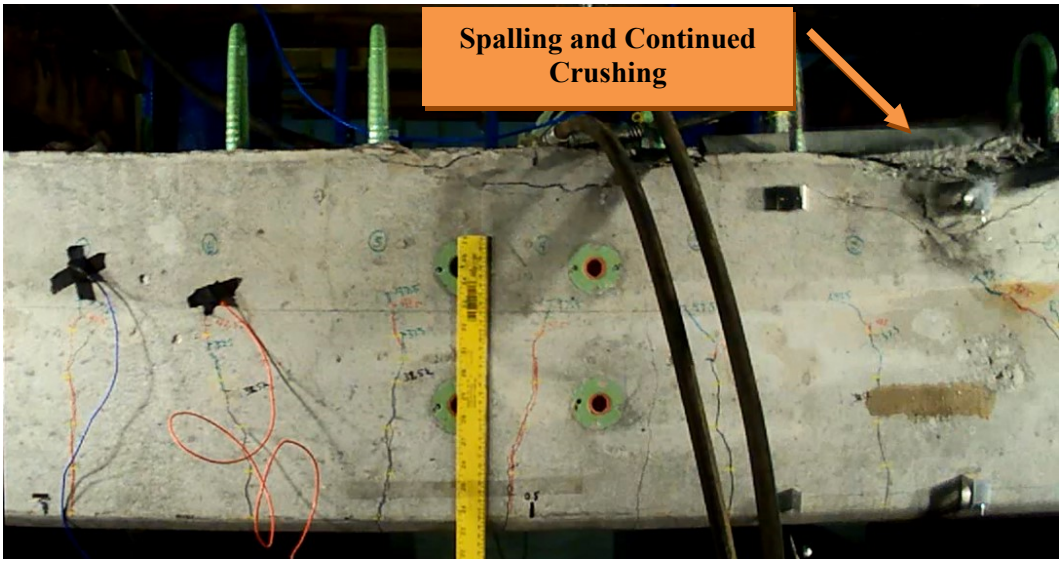
Spalling and Continued Crushing

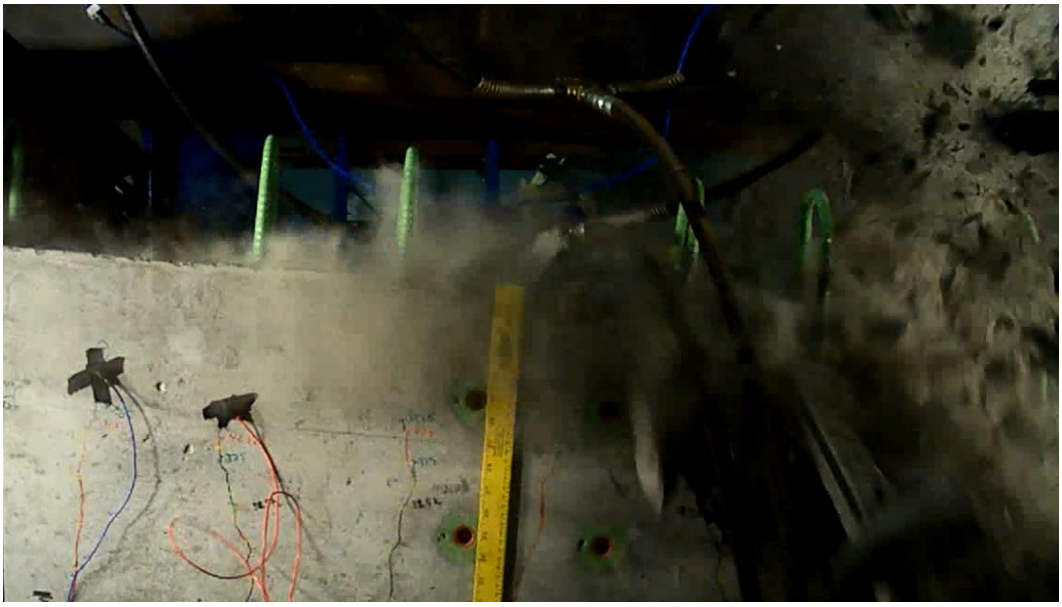

Figure 4-61 Secondary compressive failure of laboratory beam.

4.5.2 Modal Analysis of Beam

Dynamic testing was carried out on the laboratory beam to determine baseline characteristics prior to destructive testing of the beam, as well as at times in between loadings, as was shown in Figure 4-24. Modal analysis includes a simple mathematical manipulation to allow for determination of the beam's natural frequencies, as well as the shapes of vibration at those frequencies. This was done to see the effect that the damage from loading would have on the vibrational response of the beam, as well as to assess the merit of using such a technique for damage detection in prestressed beam structures. The methodology, results and findings from this testing will be discussed throughout this section.

4.5.2.1 Methodology

By observing the response of the beam when excited at multiple points, it is possible to determine the shape of its vibration using a modal analysis. This test was done to compare the vibration response of the beam when it is subjected to an increasing amount of damage.

An instrumented sledgehammer was used to excite the beam and mounted accelerometers were used to record the dynamic response of the beam. Excitation was done at points in increments of 0.05 times the beam span (L=43 ft.) in order to allow for later analysis at 19 points along the length of the beam. The hammer was swung by an operator standing on the floor next the beam Figure 4-62, as opposed to standing on top of the beam, in order to avoid any inertial effects from the swinging motion. All points of impact were at the top of the beam at mid-width to minimize torsional effects on the beam. The accelerometers were mounted on the underside of the beam at locations 0.45L and 0.55L using a mounting plate and threaded rod, as shown in Figure 4-63.

Figure 4-62 Delivery of impact during modal analysis of test beam using instrumented sledgehammer.

Figure 4-63 Accelerometer and mounting hardware for modal analysis of test beam.

The target magnitude of the impact was 4,000 lbs; typical magnitudes were within 5% of the target, and results were recorded so long as magnitudes were within 10% of the target. Samples of the recorded hammer impulse and accelerometer response can be seen in Figure 4-64 and Figure 4-65.

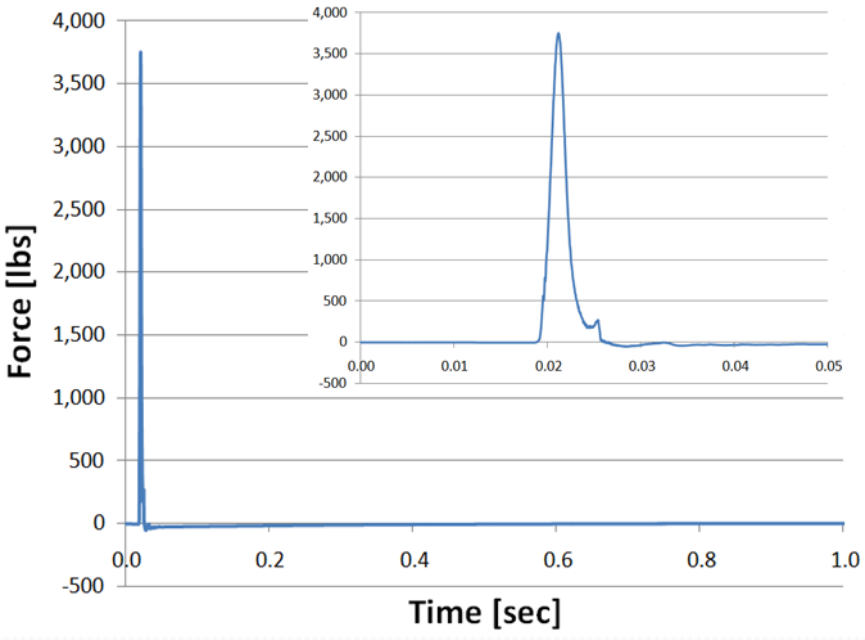

Figure 4-64 Impact waveform from instrumented sledgehammer.

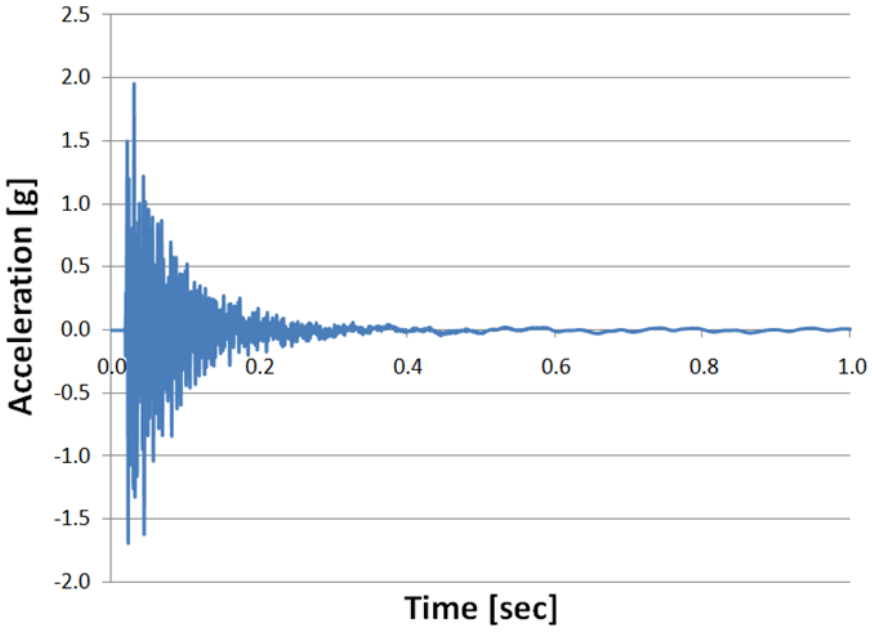

Figure 4-65 Beam response waveform as measured by accelerometer at 0.45L.

Once the force and acceleration data was recorded from the impact at each location, it was converted into the frequency domain using a Fourier transform to determine the frequency response function (FRF). The Fourier transform is determined as:

$$G(\omega) = \int_{-\infty}^{\infty} g(t)\, e^{-i2\pi\omega t}\, dt \tag{15}$$

where *g(t)* is the function in time domain and *G(ω)* is the transferred function in frequency domain. The FRF was obtained from the imaginary portion of the transfer function, *T(ω)*, or the ratio between the dynamic response, *U(ω)*, and the excitation force, *P(ω)*, both in the frequency domain.

A typical FRF is shown in Figure 4-66. In this figure, each of the peaks corresponds to a particular mode of vibration, and this method resulted in three clearly distinguishable peaks. In order to see the higher modes more clearly, more energy would need to be imparted into the beam than that of which the instrumented sledge is capable. However, by comparing the magnitudes of these peaks as obtained from an average of at least three impacts at each location along the length of the beam, the

mode shapes of vibration can be generated, as shown in Figure 4-67 through Figure 4-69. In these figures, the amplitudes are normalized for each respective mode by dividing by the absolute value of the maximum amplitude for the respective mode.

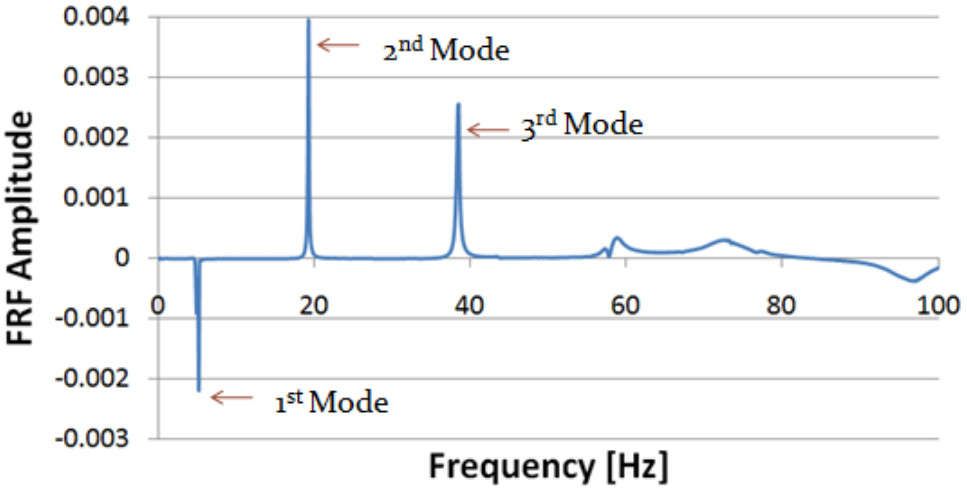

Figure 4-66 Typical frequency response function from excitation of laboratory beam.

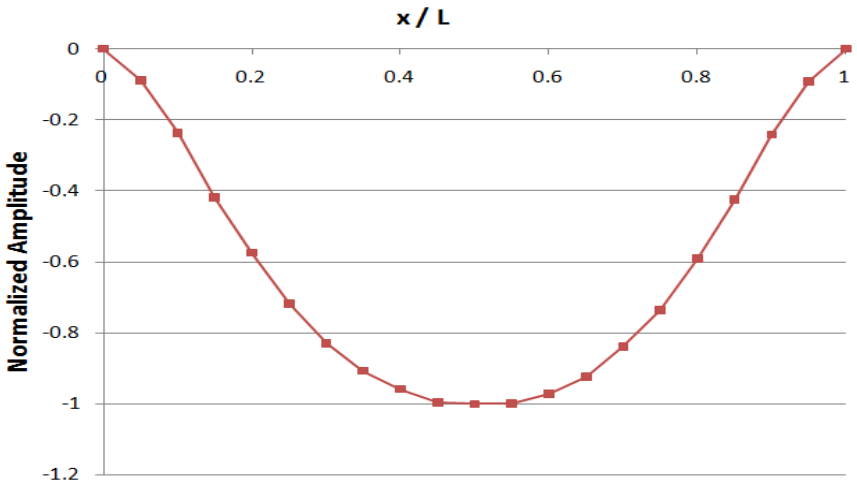

Figure 4-67 Shape of first mode of vibration for the SCC-2 prestressed bridge girder prior to static loading.

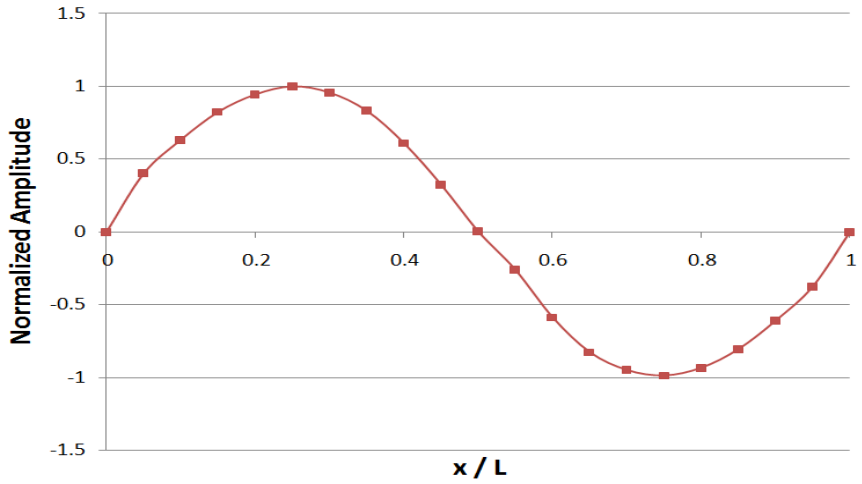

Figure 4-68 Shape of second mode of vibration for the SCC-2 prestressed bridge girder prior to static loading.

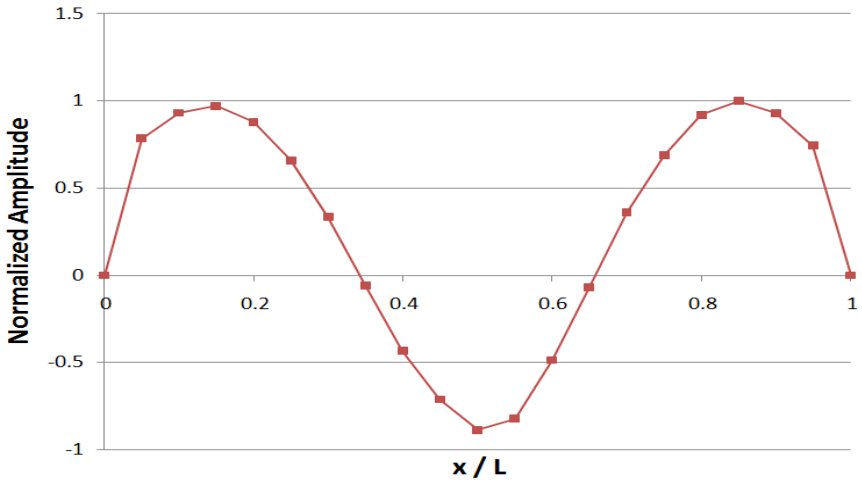

Figure 4-69 Shape of third mode of vibration for the SCC-2 prestressed bridge girder prior to static loading.

4.5.2.2 Results and Discussion of Modal Analysis

The measured natural frequencies of the prestressed laboratory beam for each test are summarized in Figure 4-70. In this figure, the Mode 1 frequency was seen to undergo a slight reduction from 4.98 Hz to 4.88 Hz (a 2.0% drop), Mode 2 reduced from 19.34 Hz to 18.75 Hz (a 3.1% drop), and Mode 3 gradually reduced from 38.98 Hz to a minimum of 36.82 Hz (a 5.5% drop). The

resolution of the FRF was only about 0.1 Hz, though, which likely was not small enough to accurately assess the changes in natural frequency, particularly for the first two modes.

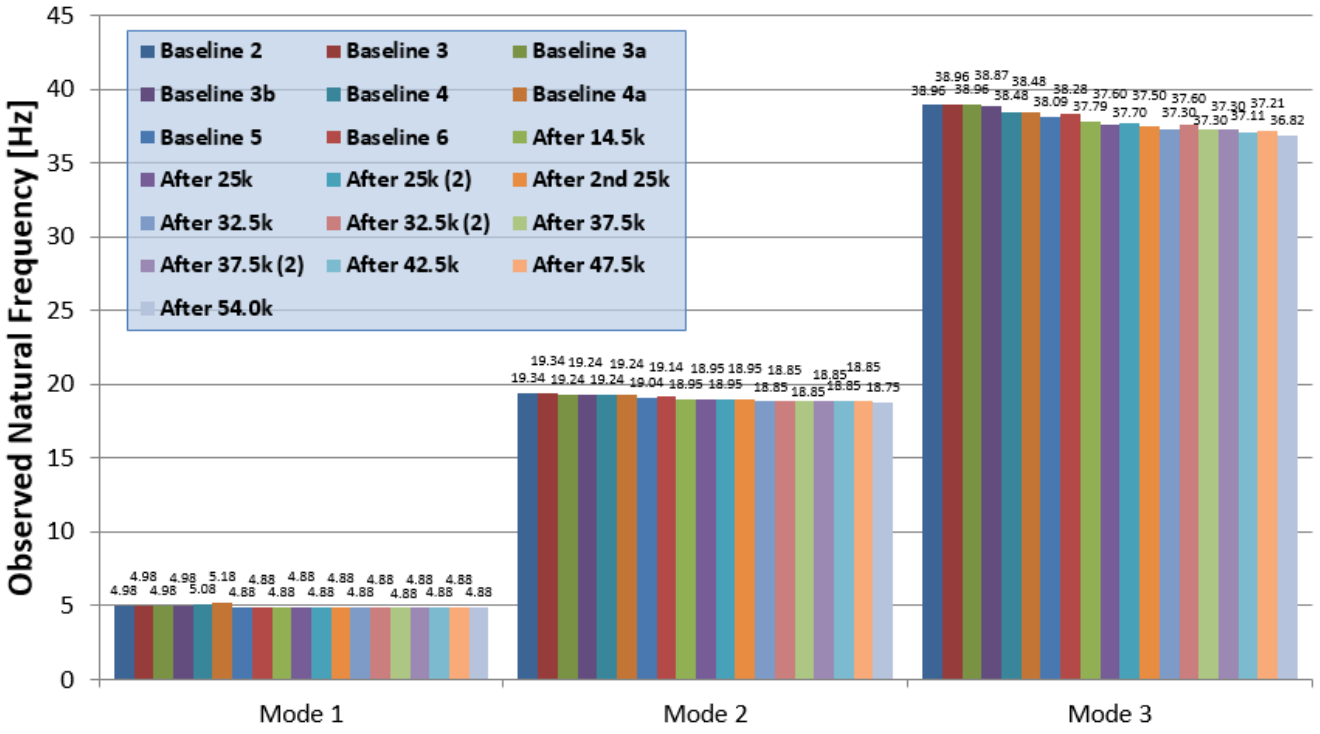

Figure 4-70 Changes in first three natural frequencies of vibration of prestressed laboratory beam.

Aside from the natural frequencies, the mode shapes were constructed for the first three modes of vibration at each time of testing. These are given for the first three modes in Figure 4-71 through Figure 4-73.

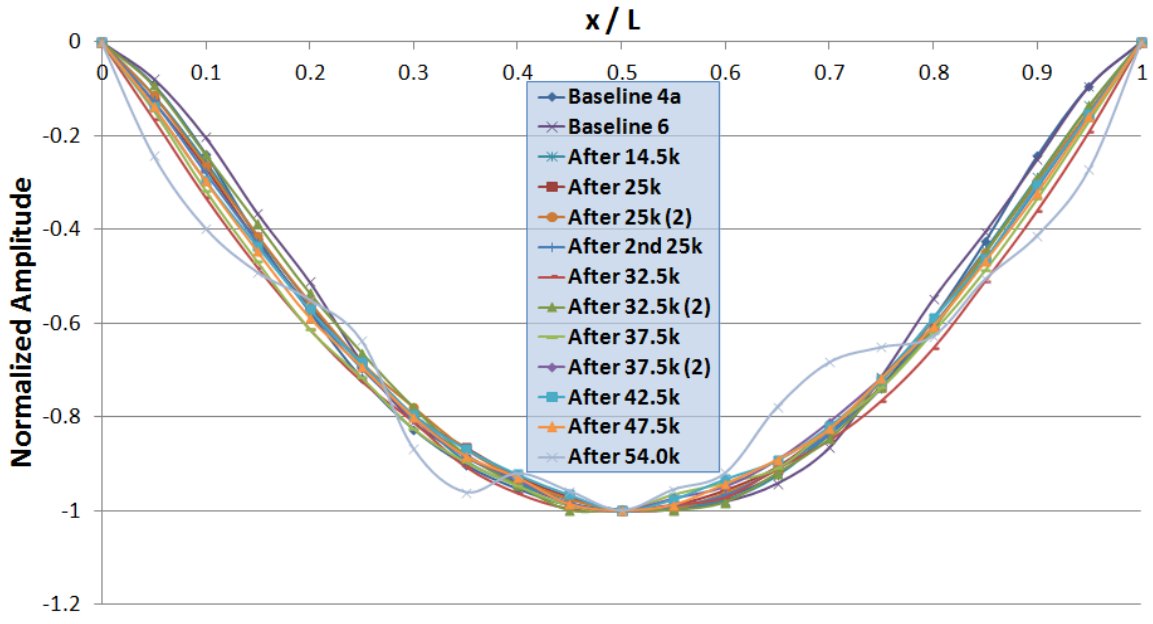

Figure 4-71 Comparison of mode shapes for first mode of vibration, prestressed laboratory beam.

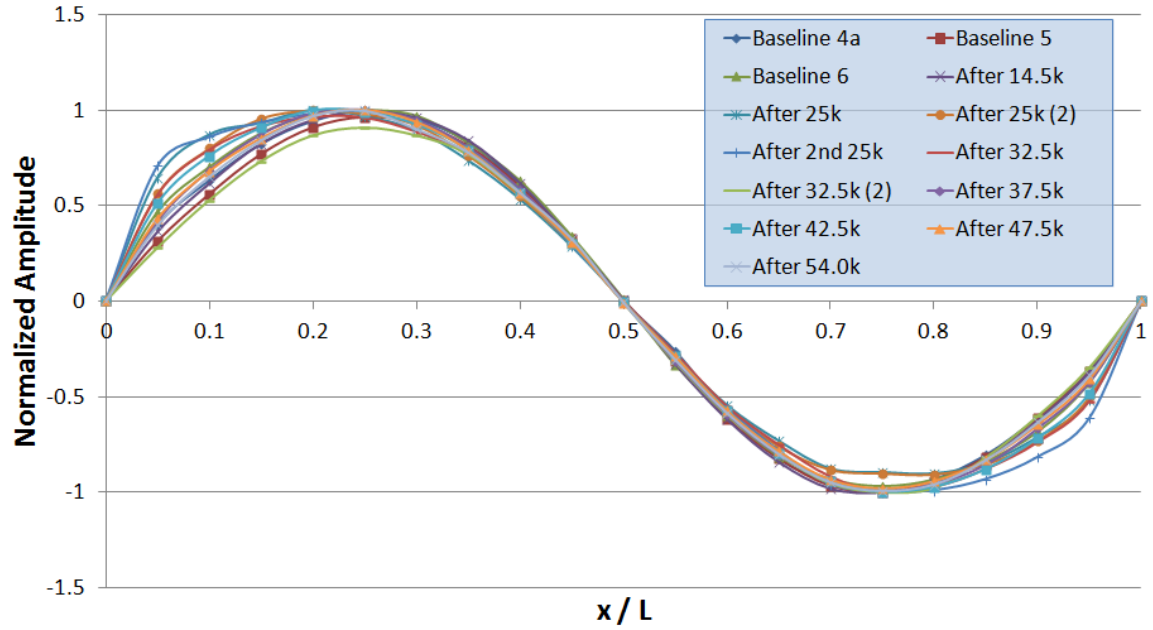

Figure 4-72 Comparison of mode shapes for second mode of vibration, prestressed laboratory beam.

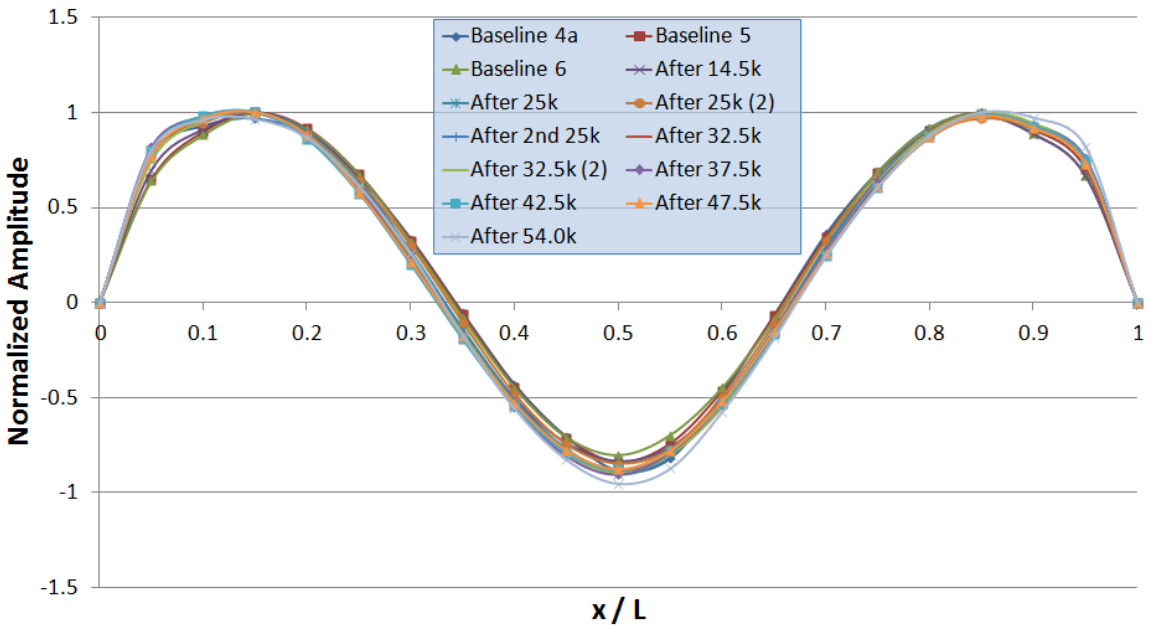

Figure 4-73 Comparison of mode shapes for third mode of vibration, prestressed laboratory beam.

One would expect the majority of damage from static loading to occur at midspan, due to the 4-point bending scheme, and consequently that the larges differences in damaged mode shapes would occur within Mode 1 and Mode 3. However, aside from the Mode 1 and Mode 3 results obtained after the 54-kip loading, it is difficult to observe a consistent, discernible relationship between damage state and vibrational mode shape.

4.6 Summary of Results from Precast/Prestressed Box Beams

Special Provisions written for SCC-2 were more stringent than those for the caisson SCC since the hardened properties of the beam concrete are so critical to the structural integrity of the bridge. In addition to strength requirements, the provisions for mix qualification included requirements for testing modulus of elasticity, splitting tensile strength, creep, shrinkage, rapid chloride permeability and freeze-thaw durability of concrete, as well as evaluating bond between concrete and prestressing strands.

Three box beams were fabricated at Eastern Vault facilities using a traditional, high-strength concrete mix for prestress applications, and another three were fabricated using SCC-2. Fabrication using the traditional vibrated concrete (TVC) mix took the majority of a work day, approximately 6½ hours for completion of casting. Use of SCC-2 simplified the work required on the day of casting, and all concrete was placed in just over three hours. It took only one night of steam curing for the TVC to reach the desired compressive strength at detensioning, 6,000 psi, while the SCC beams needed two nights of steam curing to reach the necessary compressive strength. A slight reduction of the paste volume and/or the *w/cm* of the SCC-2 mix could be sufficient to reach the detensioning strength after only one night.

Prior to fabrication, a number of gages were affixed to the casting bed for later monitoring of each beam. These included prestressing strand strain gages, concrete embedment gages, and two different types of temperature gages. During production of the beams, strains were monitored during tensioning of the prestressing strands, throughout casting and curing of the concrete, and during the release of the prestressing forces into the beams; temperatures were monitored throughout casting and curing of the concrete. Temperature data collected during curing of the beams indicated maximum temperatures of around 160°F to 170°F, which fall below the PCI prescribed 180°F threshold.

Midspan strand strain data collected during detensioning of the SCC-2 beams indicated a fairly consistent reduction in strain, with values ranging from 442 με to 479 με for the six gages. Similar data from the TVC beams had a larger range and slightly smaller magnitudes (ranging from 352 με to 446 με) than those of the SCC-2 beams. This is consistent with the TVC beams exhibiting, on average, smaller initial cambers than the SCC-2 beams.

Specimens taken from the fabrication of both types of beams give comparable average compressive strengths at detensioning and at 28 days for the SCC-2 and TVC concrete, although the SCC-2 detensioning took place after two nights of steam curing, as opposed to one for the TVC.

Results from modulus of elasticity testing indicate that, on average, the TVC has a higher modulus of elasticity than the SCC-2 concrete, both at detensioning (19% higher) and at 28 days (21.0% higher). Splitting tensile strength results for both types of concrete were somewhat sporatic, but higher initial and similar average tensile strengths were seen for the SCC-2 in comparison to the TVC.

Durability testing of SCC-2 specimens indicate that the SCC-2 concrete from production may not be freeze-thaw durable, and not all specimens exhibited the required durability factor of 80% per project specifications, with average durability factors of 65 (3"x3"x11" specimens) and 90; the TVC was freeze-thaw durable. Results of RCPT testing of both types of concrete would classify SCC-2 as having mostly "moderate" permeability, while many of the TVC results would indicate that the concrete has a "high" permeability.

A full-scale prestressed SCC-2 box beam was transported and tested in the WVU laboratories. Both destructive and non-destructive tests were utilized to gain an understanding of the beam's behavior. Non-destructive modal analysis testing was conducted in attempts of ascertaining a relationship between the damage state of the beam and the vibrational characteristics; while some minor changes were seen throughout testing, the frequency and mode shape changes were not significant until the beam had undertaken a critical amount of damage.

Destructive testing included loading of the beam in a 4-point configuration to progressively higher magnitude loads. Cracking was observed at a smaller load and higher deflection than that predicted using PCI analysis based on the beam's design parameters, as well as the PCI analysis using properties that were adjusted to better account for the behavior of the actual beam materials. Strain profiles from the load data were considerably linear prior to cracking, and began exhibiting non-linear behavior at loads exceeding the cracking load; this is particularly true for concrete gages in locations that experience stress relief from a nearby crack.

By observing the decompression behavior on the lower concrete fibers of the beam, the effective prestress in the beam (Pe = 707.5 kips or fpe = 159.7 ksi) was determined to be within 1.5% of a direct measurement of the residual strain based on strand strain readings, which was based on the strand strain gages upon delivery of the beam to WVU facilities. Strain gage and clip gage readings were initially used to determine the load at which the crack began to open; later methods for further assessment included ultrasonic pulse detection and visual observation using a digital scope.

It is believed that there were small changes in the level of constraint provided to the concrete in the tensile zone by the prestressing strands; this is based on observations of the strain data taken from concrete gages in the tensile zone. After large loads had been sustained by the beam, plastic deformation of the prestressing strands occurred. Final failure of the beam was due to secondary compressive failure of concrete after the plastic deformation of the strands.

The final failure load and failure deflection were calculated using the measured concrete properties. Both the ultimate load and the deflection at failure were observed to be slightly larger than those predicted by modified PCI analyses and moment-curvature analysis for the beam.

The ultimate carrying capacity of the beam exceeded the design behavior that was determined using PCI methods and the original design parameters. However, a beam design using the assumed material properties based on the behavior of TVC significantly overestimates the stiffness and the carrying capacity of the beam at the point of cracking. Likewise, the stiffness of the beam at the point of failure would be greatly overestimated in this manner. Therefore, while the PCI equations for analysis are suitable when using reasonable estimations of the SCC properties, assuming SCC properties based on the typical values for TVC can lead to large errors in prediction of SCC beams.

5 Long-Term Monitoring of the Stalnaker Run Bridge

As was mentioned, the drilled shafts were constructed in July of 2009; the three SCC shafts for Abutment 1 were completed on the 16th of July and the three B Modified shafts for Abutment 2 were completed on the 23rd. In addition to the specimens collected for hardened testing, all drilled shafts were monitored for three days after casting via embedded concrete strain gages, surface-mounted strain gages attached to the longitudinal rebars, and both logging and analog temperature sensors.

Approximately one and one-half weeks after fabrication of the SCC-2 box beams, on October 02, 2009, the beams were delivered to the construction site. Figure 5-1 shows the beams as placed on the two abutments; in this picture the three beams closest to the camera would be constructed of traditional concrete and the two furthest would be SCC-2 beams. The locations and orientations of the beams as placed can be seen in Figure 5-2.

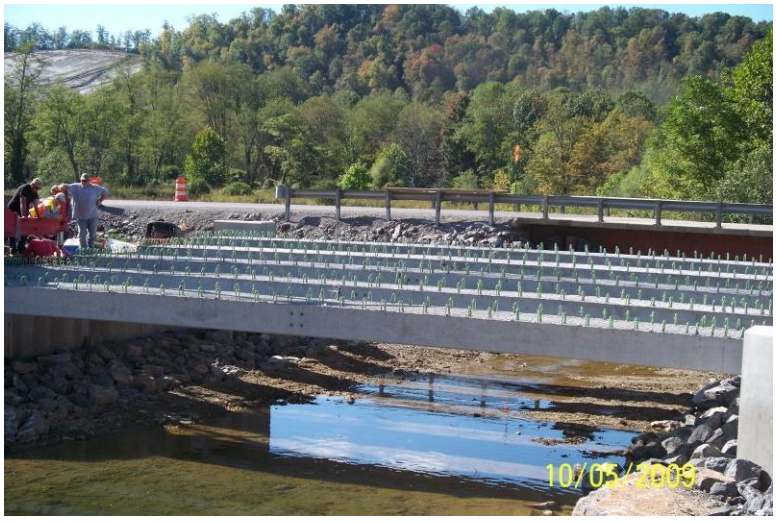

Figure 5-1 Stalnaker Run Bridge after placement of all five prestressed box beams; View from upstream location, north bank.

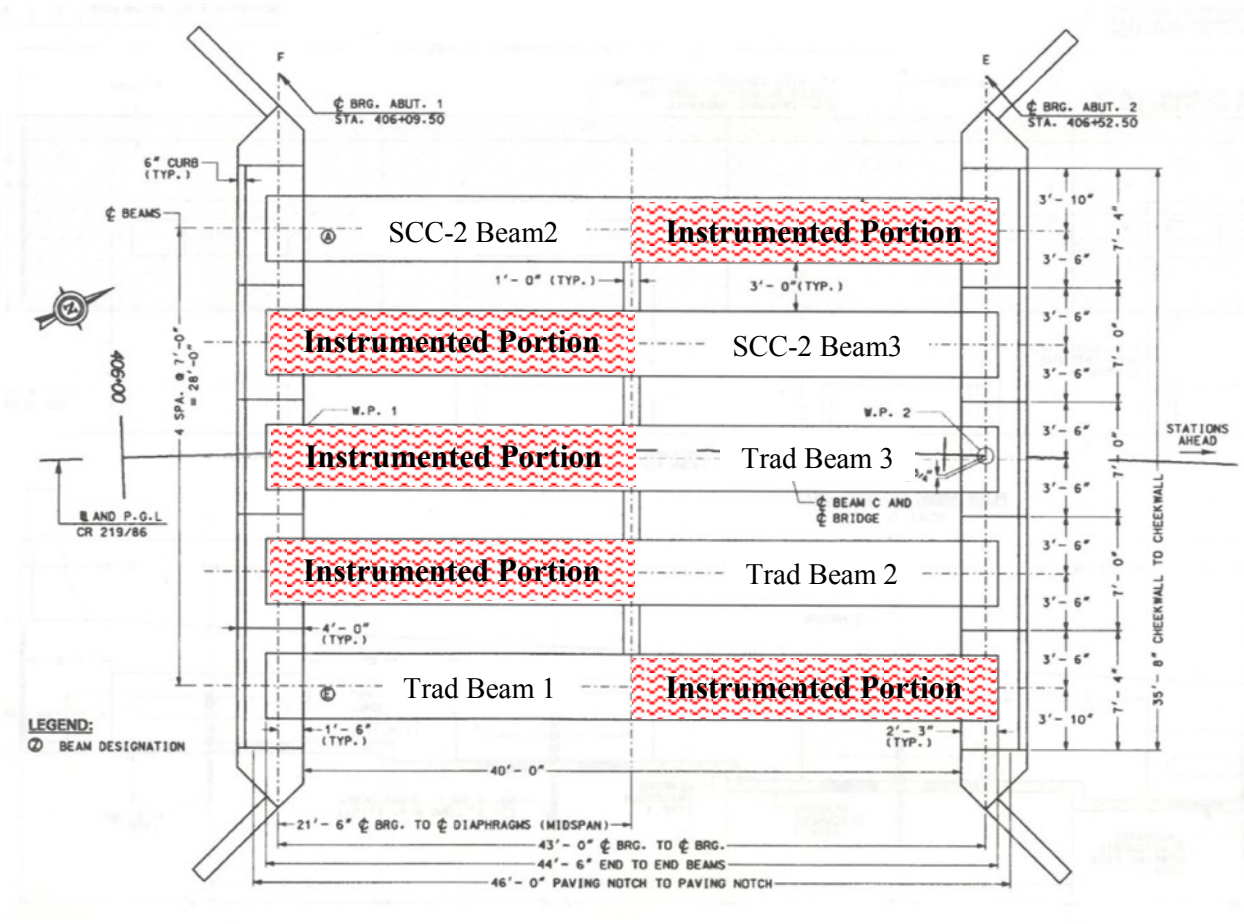

Figure 5-2 Orientation of PC beams as placed on Stalnaker Run Bridge.

Over the course of the next month, the construction of the bridge continued, and it was opened to traffic at the beginning of November. A picture of the bridge upon completion can be seen in Figure 5-3. This bridge was the first construction project for WVDOT that included the use of Self-Consolidating Concrete.

Figure 5-3 Stalnaker Run Bridge replacement after completion; View from Stalnaker Run Road (upstream, north bank).

Throughout various phases of construction, measurements were taken from the gages inside the drilled shafts and the box beams. Initially, a data acquisition system was periodically taken to the site to collect readings over a limited period of time. After completion of the bridge, however, a long-term monitoring station was set up adjacent to the bridge to house a data acquisition system capable of automatic monitoring at preset intervals. The various data collected after construction will be presented throughout this chapter.

5.1 Manual Data Collection

After completion of the bridge, individual trips were made to the bridge to collect data and to set up the long-term monitoring station. The Omega and National Instruments data acquisition systems were taken to the field at these times so that the changes in strain could be measured using wire leads; all beam strain gages were made accessible after beam placement by extending lead wires to junction boxes located near Abutment 1. Connectivity with the I-buttons was maintained using this same

process such that temperature histories could be collected. In addition to strain and temperature data, during some site visits beam cambers were measured using a taunt string line.

5.1.1 Strain Data from SCC-2 Box Beams

Figure 5-4 shows the strain readings taken from the strand strain gages in the two SCC-2 box girders, while Figure 5-5 shows the strain readings taken from the concrete embedment gages for these beams. In these figures, SCC Beam 2 refers to the outermost SCC beam, as was indicated in Figure 5-2, while SCC Beam 3 is the inner beam that is beneath the same lane. It was possible to maintain a high level of continuity among the measurements shown in these plots since the physical connections and the electrical settings of the data acquisition system remained consistent.

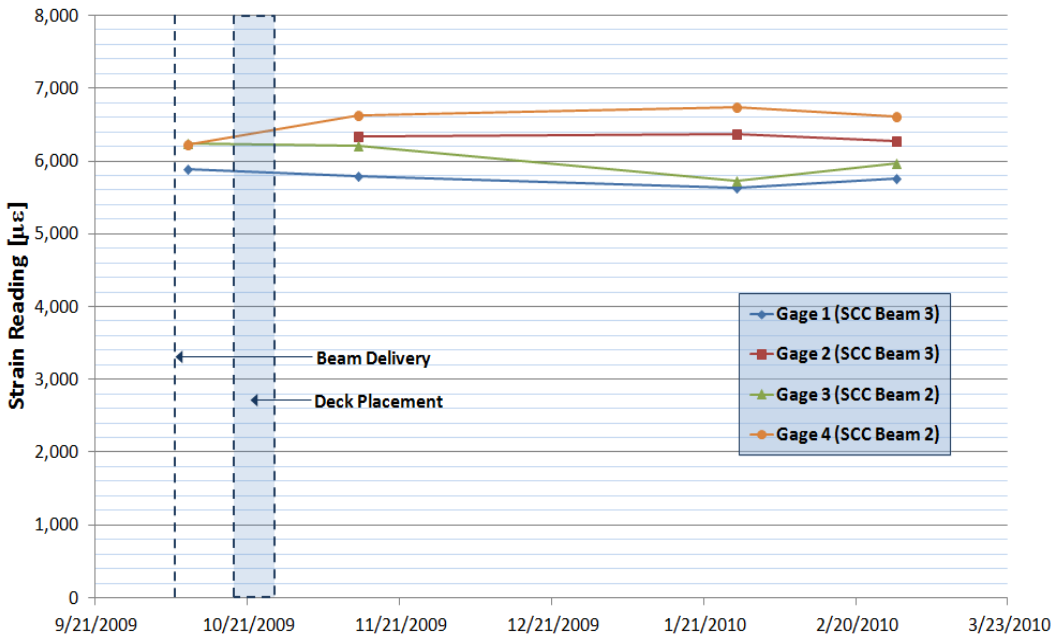

Figure 5-4 Prestressing strand strains for SCC-2 beams, measured after placement on Stalnaker Run Bridge.

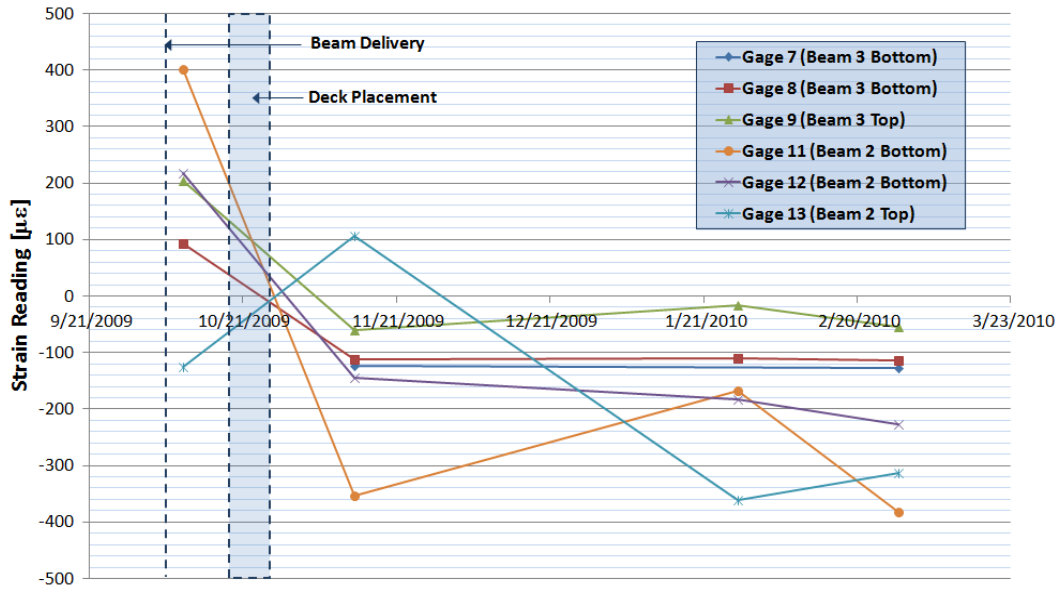

Figure 5-5 Concrete strains for SCC-2 beams, measured after placement on Stalnaker Run Bridge.

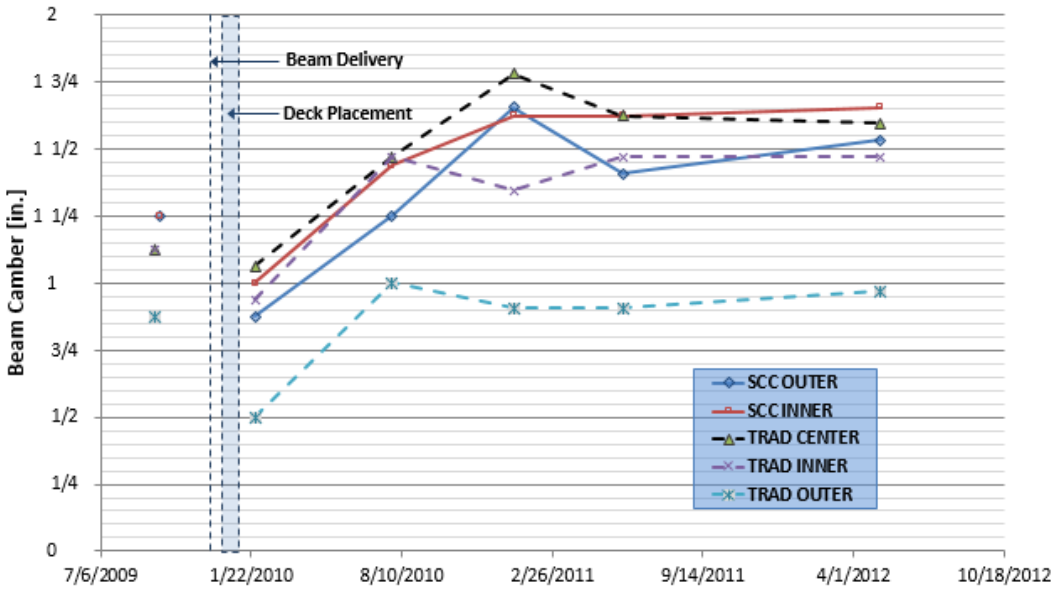

Figure 5-6 Recorded camber of Stalnaker Run Bridge beams.

5.1.2 Camber Data from Stalnaker Run Box Beams

Beam cambers were measured manually at various times after completion of the Stalnaker Run Bridge. To make these camber measurements, a string line was stretched along the length of the beam to either abutment, and a graduated rule was used to measure the distance from the string to the surface

of the beam at midspan of the bridge. A plot of these measurements with time can be seen in Figure 5-6.

5.2 Long-Term Monitoring Station

The data acquisition system is powered by a 12VDC deep-cycle battery that is recharged daily by a solar panel. The battery, the data acquisition system, and a timer that is responsible for powering on and off the system are all housed inside an electrical box, as shown in Figure 5-7. A picture of the box and the solar panel, as mounted on a pole next to the bridge, can be seen in Figure 5-8. This system, as placed in the field, has the capacity to simultaneously monitor and record measurements from up to 24 strain gages using a National Instruments cRIO data acquisition system.

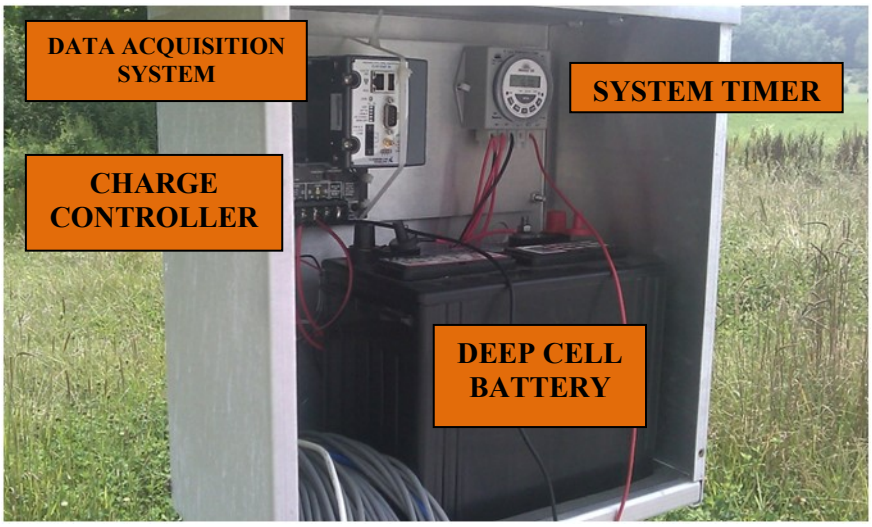

Figure 5-7 Instrumentation in long-term monitoring station for the Stalnaker Run Bridge.

Figure 5-8 Long-term monitoring station adjacent to the Stalnaker Run Bridge. Upstream location, south bank.

This setup is still in operation and continues to record data from the instrumented bridge members. The periods during which data was recorded are summarized in Figure 5-9. It can be seen that readings were taken for each date during which the data acquisition system was running, ranging from March 2010 to July 2010 and from September 2010 until the end of May 2011. In between July 2010 and September 2010, the data acquisition system was temporarily removed for use in another application. At this time, adjustments were made to the LABVIEW program which controlled the input parameters and sampling frequency of the data acquisition system when it was running. Figure 5-9 shows that the times of recording were more sporadic initially than at later dates. It is believed that an error occurred with the setup of the timer function, which was resolved during re-installation. It can still be seen that some issues still remained with the system with respect to its ability to collect data during the allotted times, though, particularly in the winter months. These issues are believed to result from insufficient recharging of the battery due to a reduction in the duration and intensity of sunlight at these times.

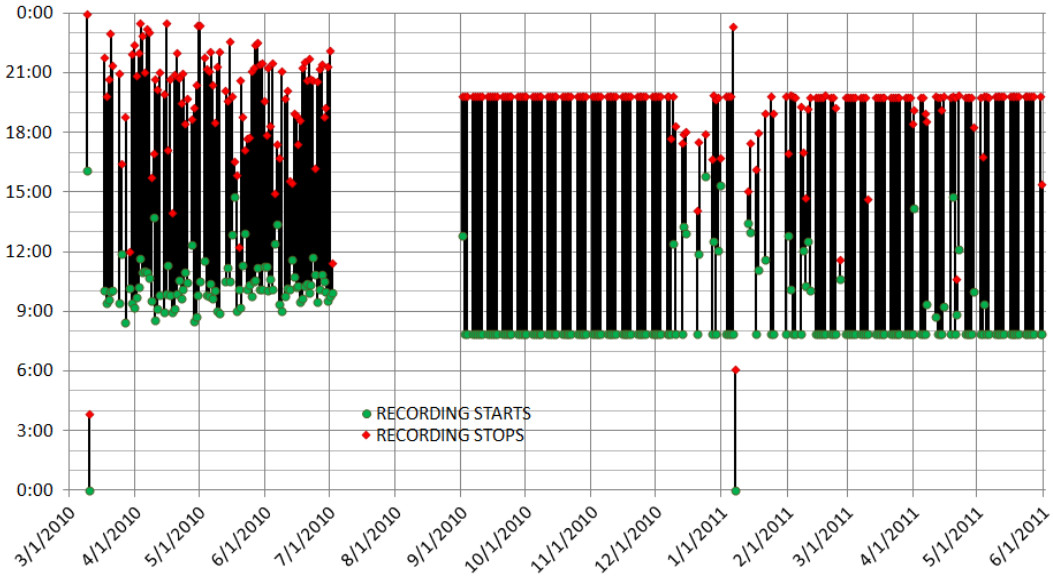

Figure 5-9 Data collection periods for long-term data collection on Stalnaker Run Bridge.

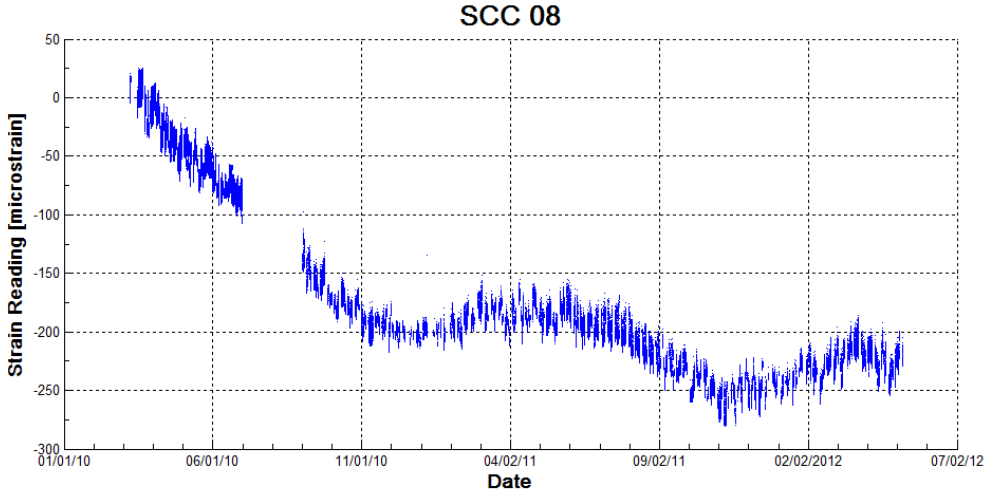

Figure 5-10 Change with time of readings from concrete embedment strain gage (SCC#8) in outer SCC beam.

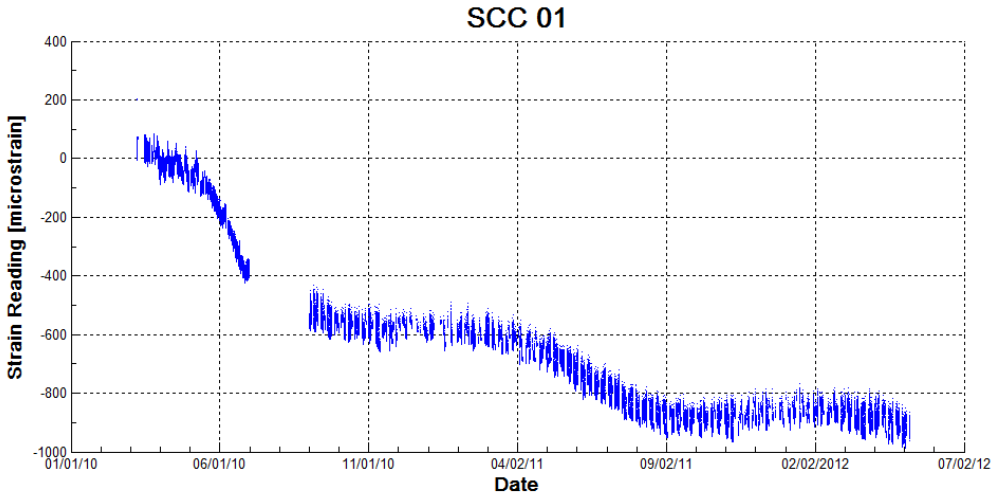

Figure 5-11 Changes in strain observed in the inner SCC box beam, as indicated by long-term observation of an affixed strand strain gage (SCC#1).

Samples of the strain data collected from one concrete embedment strain gage and one strand strain gage throughout two extended periods are respectively shown in Figure 5-10 and Figure 5-11. These plots indicate all readings taken during the prescribed data acquisition times on any given day. The readings for all strand strain gage and concrete embedment gage readings taken using the long-term monitoring system can be found in APPENDIX E.

Using this data, it is possible to observe the data collected to note any changes in the bridge's behavior with time. In particular, it would be worth watching out for any changes in the readings from the strand strain gages in order to determine the amount of prestressing forces that are being lost with time, which could be assessed using the data from Figure 5-11 in conjunction with the stress-strain relationship of the prestressing strands. For instance, using the modulus of elasticity of the prestressing strands, 28.5 x 10^6 psi, the 900 με reduction in strain depicted in Figure 5-11 would correspond to a prestress loss of 25.65 ksi in the strands.

It can be seen from these figures that the readings drop initially and then level off. Some variation in strains due to thermal expansion and contraction is expected with the changes in seasons,

so continual observation is necessary to make it clear which portion of these changes is due to seasonal variations, and what portion can be attributed to non-recoverable changes in the beam properties.

5.2.1 Comparison of SCC and Traditional Beam Strains

As was seen in Figure 5-10 and Figure 5-11, the majority of the changes observed in the beam strains occurred within the first year after beam fabrication. For the first period of regular data collection using the long-term monitoring station, from March 2010 until July 2010, the magnitudes of measured strain change in the prestressing strand gages ranged from 200 με to 400 με, and 200 με to 500 με for the SCC and TVC beams, respectively.

An apparent discontinuity of measurement does occur between the first and second installation for some data sets, such as that for SCC Strand Strain Gage 4, as shown in Figure 5-12. This could result from either changes made to the internal programming of the data acquisition system, or perhaps from changes in the physical connectivity of the gage leadwires. Nevertheless, for the sake of consistency, it is more reasonable to compare the changes in strain occurring after the second installation of the data acquisition system in order to remove any uncertainty associated with the discontinuities.

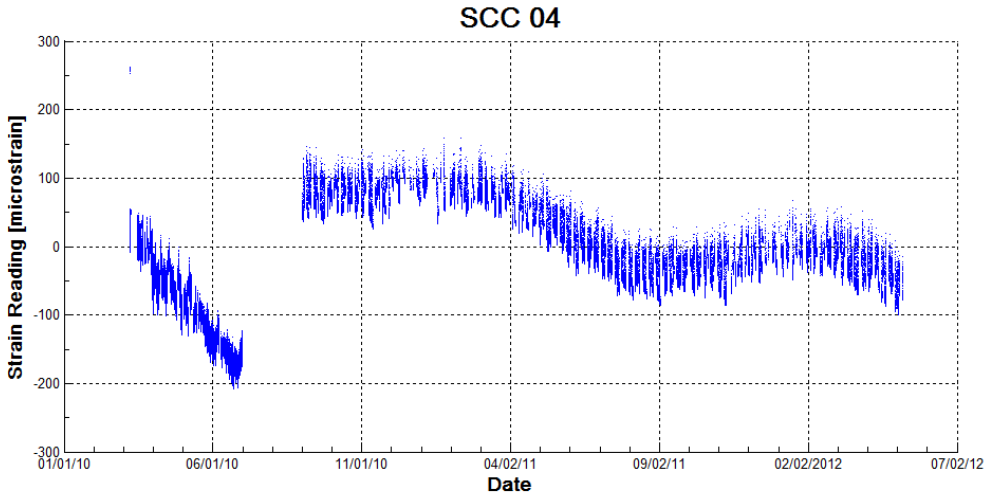

Figure 5-12 Changes in prestressing forces observed in the outer SCC box beam, as indicated by long-term observation of an affixed strand strain gage (SCC#4).

The changes in the prestressing strand strains in the SCC beams after the second installation of the data acquisition system, as observed by the strand strain gages, can be seen in Figure 5-13; similarly, those from the TVC beams are shown in Figure 5-14. It can be seen from these figures that, for the most part, the rate of strain change over this approximately 1½ year period was relatively small, with the overall strain changes measured by 6 of the 7 gages being between 200 με and 500 με. For the sake of comparison, it was mentioned above that the strain changes in some gages over the initial 3½-month period already approached 500 με. The fact that creep and shrinkage occur at higher rates initially, and then the rates reduce, allows one to deduce that the early age creep and shrinkage were the primary contributors to the large initial rate of strain reduction in the strands.

From the data presented in these figures, it appears that the seasonal variations of the strain readings are somewhat easily discernable from the long-term strain changes experienced by the beams. Most of the strand strain gages exhibited similar behavior throughout the duration of the data collection, with minimal decreases in strain (or even slight increases) during the winter months, and more noticeable decreases during the summer. By comparing readings at times where there is a relatively small rate of change in the readings, such as those taken in the months of September or

October, one can see that a slight reduction in the strain reading for all strand strain gages. Monitoring this change over time will allow for the further assessment of prestress losses incurred by the prestressed beams.

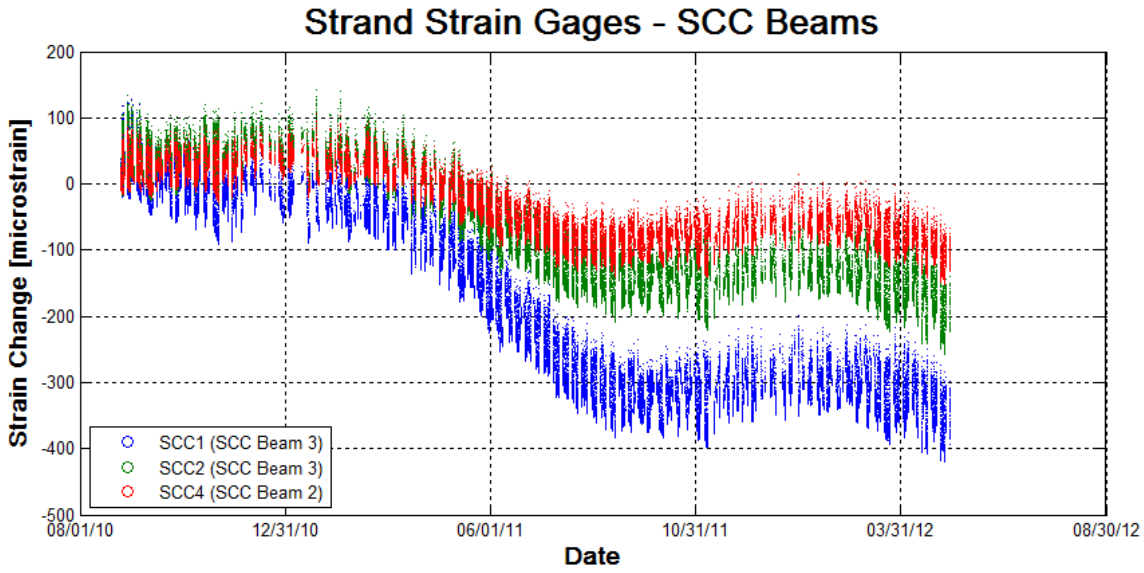

Figure 5-13 Strain changes in prestressing strands of SCC beams after second installation of long-term monitoring system.

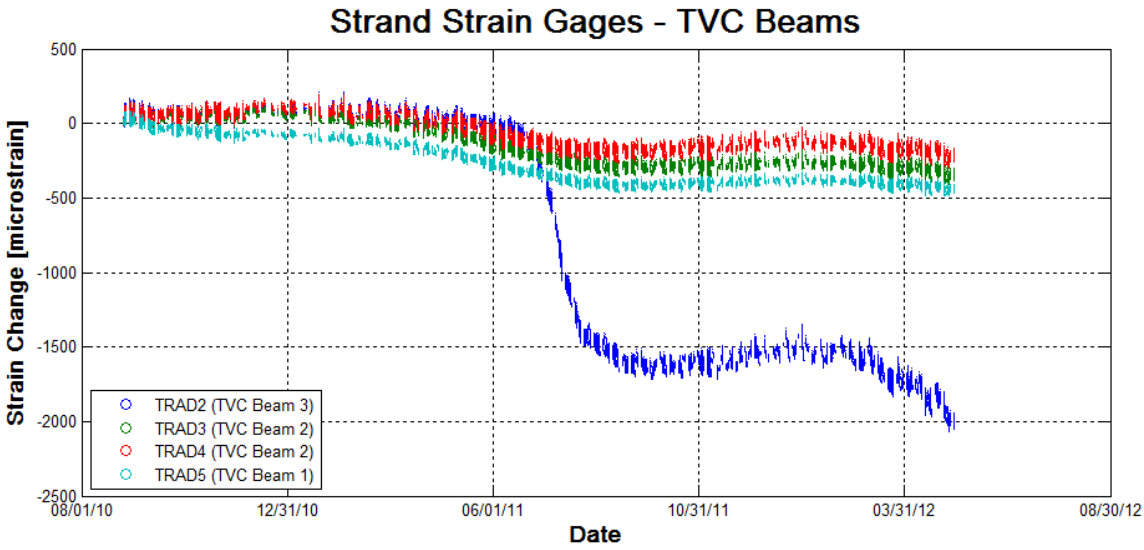

Figure 5-14 Strain changes in prestressing strands of TVC beams after second installation of long-term monitoring system.

The exception to the trends described above was the strain history from Gage TRAD2, which is located on the centermost beam of the Stalnaker Run Bridge, TVC Beam 3. Over the period of about one month, around July 2011, the strain readings from this gage dropped at a very rapid rate in comparison to those of the other six strand strain gages. While the reasons for this behavior are not completely known, it was seen from the static loading of the laboratory beam that gage readings can exhibit sharp changes in behavior when in the vicinity a crack. In addition to the possibility of a crack occurring in the beam in the vicinity of the gage, a crack or delamination could have gradually propagated in the interface between the concrete and steel strand to cause this stress relief in the strand.

The changes in readings from the concrete embedment gages located just above the lower level of reinforcement over the same time period can be seen for the SCC and TVC beams in Figure 5-15 and Figure 5-16, respectively. These figures indicate overall changes in strains at these locations that are below 150 με for each of the five beams. The steep decrease in strain reading that was seen in TVC Beam 3 based on the strand strain reading was not present in the concrete embedment gage (TRAD8) reading for the same beam.

The gage from TVC Beam 3 did exhibit the highest strain change out of the three TVC concrete embedment gage readings; the strain changes observed from this gage were similar in shape and in magnitude to those of the two embedment strain gages monitored for the SCC beams. The other two TVC gages indicated only about ½ as much strain change as the three aforementioned gages.

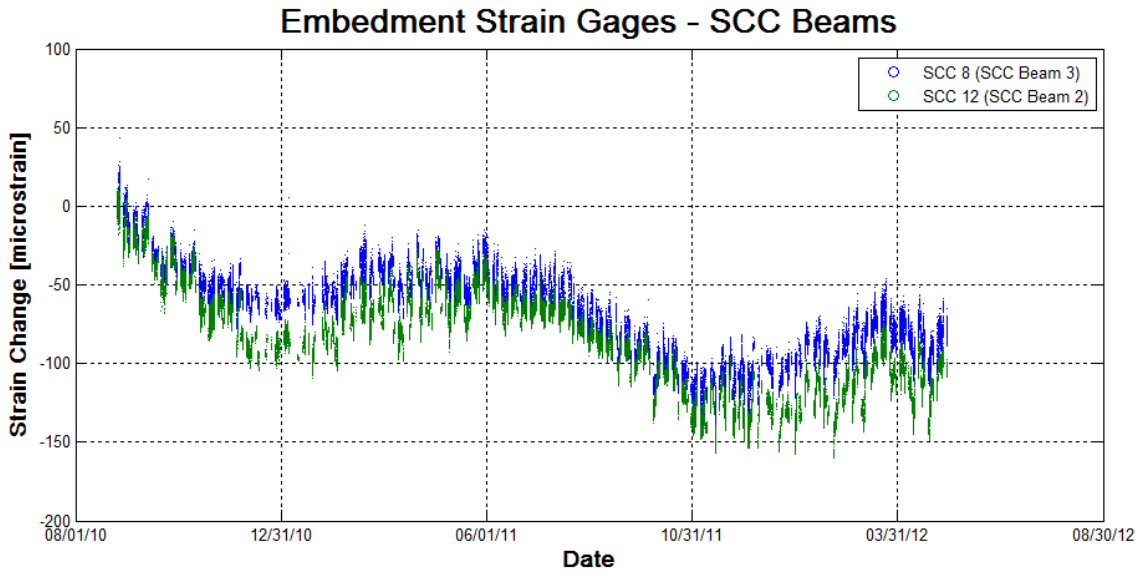

Figure 5-15 Strain changes in lower-level concrete embedment gages of SCC beams after second installation of long-term monitoring system.

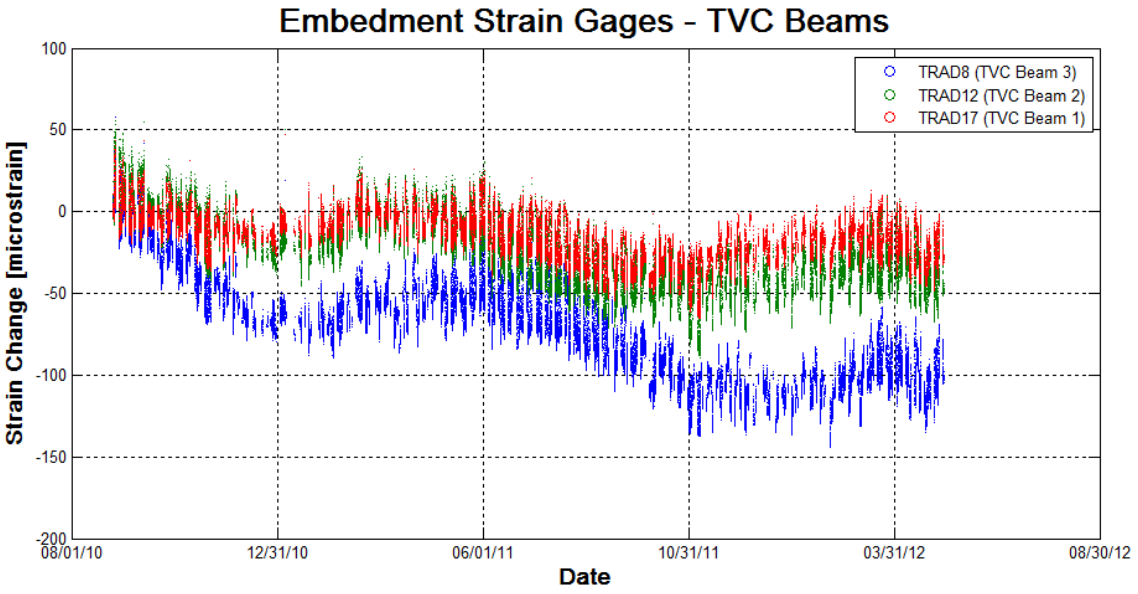

Figure 5-16 Strain changes in lower-level concrete embedment gages of TVC beams after second installation of long-term monitoring system.

5.3 Observations from Stalnaker Run Site Visits

During the site visit in May of 2011, it was observed that some longitudinal cracks had formed in the bridge deck of the Stalnaker Run Bridge. The physical locations of the cracks, shown in Figure 5-17, fall between the center beam (TVC Beam 3) and the other internal TVC beam (TVC Beam 2).

Possible reasons for this cracking include: (1) the reduction in volume of the deck concrete under restrained conditions, and/or (2) a shift in the support of the bridge deck, which would likely include differential deflection of the prestressed beams. It is noted that the SCC-2 concrete creep and shrinkage deformation, as described earlier in Chapter 3, are much higher than that from TVC, hence the difference in the long-term deformation between the SCC beams and TVC beams would be the driving force behind the latter proposed explanation. Since the second issue could potentially affect the long-term performance and structural integrity of the bridge, the condition of the bridge should continue to be monitored.

(a) **(b)** **(c)**

Figure 5-17 Observed longitudinal cracking of Stalnaker Run Bridge Deck. (a) Crack initiating at Abutment #1, (b) crack initiating at Abutment #2, and (c) crack present near midspan.

6 Future Implementation of SCC

Based on the findings and experiences of the previous sections, it is beneficial to revisit the project special provisions to reflect on their effectiveness and to consider revisions that would be helpful to those trying to implement similar construction practices in the future. This section will first address the use of SCC for cast-in-place caisson construction, and then that for precast/prestressed construction.

6.1 Special Provisions for SCC Caissons

For the most part, the project Special Provisions used for the Stalnaker Run Caissons could be utilized for other projects of similar nature. Minor modifications would be beneficial to employing them on a large scale.

One such modification would be to include ASTM C 1712, "Rapid Assessment of Static Segregation Resistance of Self-Consolidating Concrete Using Penetration Test," as one of the acceptance criteria. This test is less labor intensive and gives more immediate results than the segregation column test prescribed in the provisions. For this to happen, this test would be prescribed for mix qualification, potentially in conjunction with the static segregation column test. The replacement of the static segregation column test would help to expedite the judgment on whether or not a mix is acceptable, based on whether the penetration of the apparatus exceeds 0.5 inches.

A second would be the requirement of using an air-entraining agent in all SCC mixes. Although the SCC-1 mix tested for this project had favorable freeze-thaw performance, it has been noted by other researchers that the use of HRWRAs, particularly of the polycarboxylate type, can produce an air void structure that is unsatisfactory for freeze-thaw purposes (Khayat and Mitchell 2009). Therefore, it is recommended to check hardened air-void structure and to use an AEA to

stabilize the air voids and to improve the air void structure, even when the percentage of fresh air content appears to be satisfactory.

Another small modification would be the simplification of the determination of the "workable period" defined in the mix qualification requirements. This testing entails the periodic assessment of SCC properties to determine the point at which the concrete behavior would no longer be acceptable, with the idea that construction planning can be done based on this information. In reality, however, the ambient conditions to which the cast-in-place SCC will be subjected prior to placement could vary greatly, and this will affect the workable period. Therefore the benefit of knowing the laboratory workable period will be diminished, and the requirement for determining this parameter will only convolute the discussion of whether a particular mix should be acceptable for use. As an alternative, simply requiring that all caisson SCC mixes exhibit the desired characteristics for around 2 hours after mixing, similar to NJDOT regulations, seems to be an acceptable alternative to determining the workable period in the manner dictated by the Stalnaker Run project provisions.

Finally, the Stalnaker Run project provisions were written with the knowledge that each caisson would only take approximately one truckload of concrete to fill, so it was required to test the contents of every truck as it was to be used. However, since many projects are much larger in scale, it would be excessive to demand that every single truck undergoes a full barrage of testing. Since the performance of SCC is so dependent on the materials, it would make sense to command a higher rate of testing at first while the batch production stabilizes, and then at a normal rate after the third or fourth batch.

6.2 Special Provision for Prestressed SCC Beams

Since SCC oftentimes exhibits significantly different performance with respect to stiffness, creep and shrinkage behaviors, the use of SCC instead of TVC without properly accounting for these changes in the design could be detrimental to the performance of the structure. Therefore, the use of

SCC has to be taken into account early in the process to ensure that things such as changes in anticipated prestress loss are considered in the design. The project provisions did not use the hardened property assessment as a means of acceptance of the mix design, per se, so acceptable values or ranges of values for the material properties must be considered to ensure satisfactory structural performance.

The simplest scenario would be to have the SCC exhibit properties within the bounds of the ACI or AASHTO predictions that are typically used in the design that are currently based on the traditional prestressed concrete. This would allow the initial design to be used without making adjustments based on differing prestress losses when using SCC.

It has been shown in many cases, though, that SCC can exhibit significantly increased creep and/or shrinkage and a reduced modulus of elasticity when compared to traditional concrete of a similar strength, all of which would affect the prestress losses, deflection and long-term behavior of the prestressed beams. This means that prescribing values for these properties that are based on design using traditional concrete could be overly-restrictive when considering SCC; this could make the development and qualification of SCC mixes cost-prohibitive in some cases, and eliminate the prospect of using SCC completely in others. Therefore, it may be best to use the ACI/AASHTO values as the basis of SCC mix qualification, with the addendum that:

> "SCC exhibiting values for creep, shrinkage and modulus of elasticity that do not meet these limits can be used for production provided that the prestressed beam design calculations for prestress losses and long-term deflection are adjusted according to the measured values and approved by the WVDOT Design Engineer."

Also, due to these potential differences in the behavior between SCC and traditional prestressed concrete, it is recommended to prescribe that only one kind of concrete (either traditional or SCC) be used for all the girders of an individual beam span.

Another scenario for incorporating SCC could be that modifications to the concrete properties be used in the design for SCC beams; this could result in the presentation of two separate designs for the same beam elements.

In Special Provisions for North Carolina, and others for Virginia, as reported by Zia et al., the maximum allowable shrinkage of prestressed SCC was 0.04% (400 με) at 28 days (Zia, Nunez and Mata 2005). This actually corresponds to the lower limit of the ultimate shrinkage values considered for the AASHTO lump sum method for determining prestress loss. The shrinkage will continue to grow beyond 28 days, though, so it may be a good idea to dictate an early-age target such that the ultimate shrinkage would be within (or at least reasonably close to) the range considered for AASHTO design, 400 to 600 με.

Based on ACI 209, the following relationships are commonly used for determining the time-dependent shrinkage of steam cured and moist cured concrete:

$$(\boldsymbol{\varepsilon_{sh}})_{\boldsymbol{t}} = \left(\frac{\boldsymbol{t}}{\boldsymbol{55+t}}\right)(\boldsymbol{\varepsilon_{sh}})_{\boldsymbol{u}} \qquad \text{STEAM CURED} \qquad \textbf{(16)}$$

$$(\boldsymbol{\varepsilon_{sh}})_{\boldsymbol{t}} = \left(\frac{\boldsymbol{t}}{\boldsymbol{35+t}}\right)(\boldsymbol{\varepsilon_{sh}})_{\boldsymbol{u}} \qquad \text{MOIST CURED} \qquad \textbf{(17)}$$

where $(\varepsilon_{sh})_t$ is the shrinkage at time t, and $(\varepsilon_{sh})_u$ is the anticipated ultimate shrinkage. The time variable, t, in these relationships is measured starting with exposure to shrinkage conditions, which excludes the curing period (1-3 days of steam curing, or a standard 7-day moist curing period.) Typical values used for the ultimate shrinkage of traditional concrete in the absence of measured behavior are 730με for steam cured concrete, and 800με for moist cured concrete. As such, if using the anticipated ultimate shrinkage, the above relationships will give the possible limits for test durations of 28, 60, 90, 120 and 180 days, as listed in Table 6-1. Using this table, and a moderate test

duration of 90 days, limits can be set at 450με of shrinkage for steam cured concrete and 575με for moist cured concrete at 90 days after the initial curing period.

Table 6-1 Shrinkage (microstrain) of traditional concrete at various ages, as approximated by ACI 209 methods.

	Steam Cured	Moist Cured
28 days	**246**	**356**
60 days	**381**	**505**
90 days	**453**	**576**
120 days	**501**	**619**
180 days	**559**	**670**

Likewise, concrete will continue to creep beyond a reasonable testing period. Therefore, prescribing a creep coefficient after 180 days of 1.6, which is the low end of the range of ultimate creep coefficients used for the AASHTO lump sum method, should produce an ultimate creep coefficient within (or reasonably close to) the range considered for AASHTO design, 1.6 to 2.4. Similarly, the ACI time-dependent model for creep uses the following relationship:

$$C_t = \left(\frac{t^{0.6}}{10 + t^{0.6}}\right) C_U \tag{18}$$

where C_t is the creep coefficient of the concrete at time after loading, t, and C_U is the ultimate creep coefficient. The time variable in this relationship is based on a loading age of 7 days for moist cured concrete and 1-3 days for steam cured concrete. For normal loading conditions, the ultimate creep coefficient, as well as the anticipated values at 28, 60, 90, 120 and 180 days are as follows:

Table 6-2 Creep coefficient of traditional concrete with various strengths at different ages, as approximated by ACI 209 methods.

f_c' [psi]	C_U	C_{28}	C_{60}	C_{90}	C_{120}	C_{180}
3,000	**3.1**	**1.32**	**1.67**	**1.85**	**1.98**	**2.15**
4,000	**2.9**	**1.23**	**1.56**	**1.73**	**1.85**	**2.01**
6,000	**2.4**	**1.02**	**1.29**	**1.44**	**1.53**	**1.66**
8,000	**2.0**	**0.85**	**1.08**	**1.20**	**1.28**	**1.39**
10,000	**1.6**	**0.68**	**0.86**	**0.96**	**1.02**	**1.11**

Using this table, the acceptable creep coefficient can be set based on the desired time of testing and the design strength of the concrete.

7 Conclusions

The use of SCC for cast-in-place caisson and precast/prestressed box beam applications on the Stalnaker Run Bridge replacement was successfully demonstrated as the first bridge construction project in West Virginia, and the outcome of the project yielded a multitude of useful data and results that can be utilized for future applications with SCC. This section will summarize some of the key findings of the laboratory and field investigations discussed previously.

7.1 SCC for Cast-in-Place Caissons

- A novel testing scheme was developed to test the uniformity of cast-in-place SCC by sampling in the fresh state. The apparatus is reusable and relatively inexpensive.
- Disparities in aggregate contents throughout the trial caisson cores were not seen to necessarily correspond to detrimental hardened properties at those locations.
- SCC-1 was used for the cast-in-place construction of the caissons for Abutment 1 of the Stalnaker Run Bridge.
- Preliminary experiments showed potential in using pH measurements as an indicator of water content in fresh concrete.
- Slight modifications to the equipment used for the Thermal Integrity Testing could help this to be a viable method for anomaly detection in caissons.
- Third-party crosshole sonic logging did not discover any anomalies within the SCC-1 or TVC caissons.
- Both SCC-1 and Class B Modified concrete exceeded the 4,500 psi compressive strength requirement.
- SCC-1 exhibited a lower tensile strength, but similar modulus of elasticity as the Class B Modified concrete.

- SCC-1 had a better RCPT performance than the Class B Modified concrete, with 2 of 3 specimens being classified as "low" permeability and all others being classified as "moderate" permeability.
- SCC-1 was seen to be very freeze-thaw durable.

7.2 SCC for Precast/Prestressed Box Beams

- Special Provisions for Prestressed SCC require more hardened testing than for cast-in-place SCC.
- Use of SCC-2 for box beam application reduced time of casting by about ½.
- The SCC-2 took two nights of steam curing to reach the desired strength at detensioning (6,000 psi); a slight reduction of the *w/cm* could reduce the time needed to achieve this strength.
- Maximum temperatures measured during casting and curing of the SCC-2 and TVC Box Beams were around 160-165^{o}F, below the PCI threshold of 180^{o}F.
- Upon detensioning, the initial cambers of the SCC-2 beams were larger than the predicted values.
- Average compressive strengths for SCC-2 and TVC were comparable upon detensioning and at 28 days, although the SCC-2 took an extra day to reach the required strength for detensioning.
- Splitting tensile strengths were higher for the SCC-2 at detensioning, but similar at 28 days.
- On average, TVC had a 19% higher modulus of elasticity at detensioning and a 21% higher modulus at 28 days when compared to SCC-2.
- 4 of 6 of the SCC-2 specimens that were exposed to freeze-thaw testing did not achieve the desired durability factor of 80. The TVC was freeze-thaw durable, with DFs in the high 90s.
- Most SCC-2 Specimens would be classified as "moderately" permeable per ASTM C1202, while most TVC specimens would be classified as "high" permeability.

- The shrinkage and creep strains of the SCC-2 concrete were higher than the TVC. After 1 year, the SCC-2 shrinkage strain (609 με) was 34% higher than that of the TVC (455 με), while the creep coefficient of the SCC-2 was almost twice that of the TVC (2.58 vs. 1.31) after 1 year.
- Although calculations of the initial camber of the SCC-2 lab beam using the methodology of Brewe and Myers were lower than the observed camber, the long-term (1-year) calculation was very accurate when using the measured material and structural properties.
- A linear strain profile was seen throughout the depth of the beam for small loads, but non-linearities appeared in both the tensile and compressive zones after cracking.
- Cracking occurred in the laboratory beam at a smaller loading than predicted using PCI, moment-curvature and Response2000 analyses.
- By observing the decompression behavior on the lower concrete fibers of the beam, the effective prestress in the beam (Pe = 707.5 kips or fpe = 159.7 ksi) was determined to be within 1.5% of a direct measurement of the residual strain based on strand strain readings.
- A concrete surface gage, a clip gage, ultrasonic pico sensors, and a digital microscope were all successfully used to determine the decompression load for the beam.
- Some localized debonding likely occurred throughout testing, as evidenced by the change in reaction of the concrete surface strain gage.
- Plastic deformation of the strands, and noticeable permanent deflection of the beam, took place during the 54-kip loading.
- Modal Analysis of the beam was not sensitive enough to reflect the damage state of the beam using the first three modes of vibration until after the 54-kip loading, at which point the beam was already severely damaged.
- Failure of the beam was due to plastic deformation of the strands, with secondary compressive failure.

- PCI and moment-curvature analyses were fairly accurate in calculations for failure and deflection at failure for the beam when using the measured material properties and structural characteristics of the beam.
- PCI predictions overestimated loads and underestimated deflections of the beam at cracking when using the design values established for traditional concrete mixes; deflections were underestimated at failure using design values.
- While PCI and moment-curvature methods can accurately predict the behavior of prestressed beams made using SCC, it is important that the material properties used to do so are representative of the SCC.

7.3 Stalnaker Run Bridge

- SCC has been successfully implemented in both cast-in-place caisson and precast/prestressed box beam applications for the Stalnaker Run Bridge.
- Periodic data collection and a long-term monitoring station have made it possible to observe the long-term prestress losses of the bridge girders.
- Data collected over a period of approximately 1½ years indicates that the reductions in strain of the prestressing strands for the TVC and SCC-2 beams is now, for the most part, occurring at a similar rate.
- Strand strain gage data show a clear prestress loss in the steel strand in one of the TVC beam.
- Due to cracking of the bridge deck, it is not only of interest but important to continue to monitor the changes occurring in the bridge to ensure the safety of the bridge.

8 Works Cited

ACI Committee 237. 2007. *ACI 237-07 Self Consolidating Concrete.* Famington Hills MI: American Concrete Institute.

ACI Committee E-701. 2003. "Chemical Admixtures for Concrete." E4.1-E4.12.

ASTM. 2010. "C260/C260M-10a: Standard specification for air-entraining admixtures for concrete."

ASTM Standard C 1610. 2006. "C1610/C1610M-06 Standard Test Method for Static Segregation of Self_Consolidating Concrete Using Column Technique." *Standard Test Method for Static Segregation of Self_Consolidating Concrete Using Column Technique.*

ASTM Standard C 1611. 2005. "C1611/C1611M-05 Standard Test Method for Slump Flow of Self-Consolidating Concrete." *Standard Test Method for Slump Flow of Self-Consolidating Concrete.*

ASTM Standard C 1621. 2006. "C1621/1621M-06, Standard Test Method for Passing Ability of Self-Consolidating Concrete by J-Ring."

ASTM Standard C 1712. 2009. "C 1712-09/C 1712M-09 Standard Test Method for Rapid Assessment of Static Segregation Resistance of Self-Consolidating Concrete using Penetration Test." *Standard Test Method for Rapid Assessment of Static Segregation Resistance of Self-Consolidating Concrete using Penetration Test.*

BIMB, CEMBUREAU, ERMCO, EFCA and EFNARC. 2005. *European Guidelines for Self-Compacting Concrete.*

Bonen, D, and S P Shah. 2005. "Fresh and Hardened Properties of Self-Consolidating Concrete." *Progress in Structural Engineering Materials Journal* 7 (1): 14-26.

Brewe, Jared E, and John J Myers. 2010. "High-strength self-consolidating concrete girders subjected to elevated compressive fiber stresses, part 1: Prestress loss and camber behavior." *PCI Journal* (Fall): 60-77.

Brooks, JJ, MA Megat Johari, and M Mazloom. 2000. "Effect of admixtures on the setting times of high-strength concrete." *Cement & Concrete Composites* (22): 293-301.

Brown, D A. 2004. "Zen and the Art of Drilled Shaft Construction: The Pursuit of Quality." *Geotechnical Special Publicatioin No. 124.* Orlando: ASCE. 19-33.

Burns, Ned H. 1964. "Moment Curvature Relationships for Partially Prestressed Concrete Beams." *Journal of the Prestressed Concrete Institute* (PCI) 9 (1): 52-63.

Chatterji, S. 2003. "Freezing of air-entrained cement based materials and actions of air-entraining agents." *Cement & Concrete Composites* (25): 759-765.

Chen, HL, and K Wissawapaisal. 2002. "Application of Wigner-Ville Transform to Evaluate Tensile Forces in Seven-Wire Prestressing Strands." *Journal of Engineering Mechanics* (ASCE) 127 (6): 1206-1214.

Chen, HL, and K Wissawapaisal. 2001. "Measurement of Tensile Forces in a Seven-Wire Prestressing Strand Using Stress Waves." *Journal of Engineering Mechanics* (ASCE) 127 (6): 599-606.

Chen, HL, and L Pei. 1996. "Detection of Cracks in Concrete Using the Impact Responses." Edited by Y.K. Lin and T.C. Su. *11th Conference on Engineering Mechanics.* Ft Lauderdale, FL. 620-623.

Chen, HL, and Y He. 2001. "Analysis of an Acoustic Surface Waveguide for AE Monitoring of Concrete Beams." *Journal of Engineering Mechanics* (ASCE) 127 (1): 1-10.

Chen, R, U Halabe, Bhandarkar, and Z Sami. 1994. "Impulse Radar Reflection Waveforms of Simulated Reinforced Concrete Bridge Decks." *Material Evaluation Journal of ASNT* 52 (12): 1382-1388.

Collepardi, M. 1998. "Admixtures used to enhance placing characteristics of concrete." *Cement and Concrete Composites* (20): 103-112.

Collepardi, M. 1984. "Water Reducers/Retarders." In *Concrete Admixtures Handbook: Properties, Science and Technology*, edited by V.S. Ramachandran, 116-210. Park Ridge, NJ: Noyes Publications.

Collepardi, S, L Coppola, R Troli, and M Collepardi. 1999. "Mechanisms of actions of different superplasticizers of high-performance concrete." Edited by VM Malhotra, P Helene, LR Prudencio and DCC Dal Molin. *Performance and Quality of Concrete Structures: ACI SP-186.* 503-524.

D'Ambrosia, M D, S Altabout, C Park, and D A Lange. 2001. "Early-age tensile creep and shrinkage of concrete with shrinkage reducing admixtures." In *Creep, Shrinkage and Durability Mechanics of Concrete and Other Quasi-Brittle Materials*, 645-651. Cambridge, MA.

Damone, P L. 2007. "A Review of the Hardened Mechanical Properties of Self-Compacting Concrete." *Cement & Concrete Composites* 29: 1-12.

Devalapura, and Tadros. 1992. "Stress-Strain Modeling of 270 ksi Low-Relaxation Prestressing Strands." *PCI Journal* 100-6.

Du, Linaxiang, and Kevin J Folliard. 2005. "Mechanisms of air entrainment in concrete." *Cement and Concrete Research* (35): 1463-1471.

FDOT. 2005. *Self-Consolidating Concrete for Precast/Prestressed Concrete Products.* Vol. II, in *Materials Manual*, by Florida Department of Transportation, 8-4-1 through 8-4-12.

Ferraris, C F. 1999. "Measurement of the Rheological Properties of High Performance Concrete: State of the Art Report." *Journal of the National Institute of Standards and Technology* 104 (5): 461-478.

FHWA. 2005. "Advances in Self-Consolidating Concrete." *Focus Magazine*, November.

Florida Department of Transportation. n.d. *Wet Shafts.* Accessed February 12, 2012. http://www.dot.state.fl.us/construction/training/drill%20shaft/Wet_shafts.htm.

Folliard, Kevin J, and Neal S Berke. 1997. "Properties of high-performance concrete containing shrinkage-reducing admixture." *Cement and Concrete Research* 27 (9): 1357-1364.

Ghafoori, N, and H Diawara. 2010. "Evaluation of Fresh Properties of Self-Consolidating Concrete under Long Transportation Time and Extreme Temperature." In *Design, Production and Placement of Self-Consolidating Concrete*, by K H Khayat and Feys D, 139-150. RILEM. doi:10.1007/978-90-481-9644-7_12.

Grace Construction Products. 2005. "Self-Consolidating Concrete (SCC) Production Tips."

He, Z, ZJ Li, MZ Chen, and WQ Liang. 2006. "Properties of shrinkage-reducing admixture-modified pastes and mortar." *Materials and Structures* (39): 445-453.

Heirman, G, L Vandewalle, D Van Germert, V Boel, K Andenaert, G De Shutter, and et al. 2008. "Time-dependent deformations of limestone powder type self-compacting concrete." *Engineering and Structures* 30: 2945-2956.

Hill, Russel L, Shondeep L Sarker, Robert F Rathbone, and James C Hower. 1997. "An examination of fly ash carbon and its interactions with air entraining agent." *Cement and Concrete Research* 27 (2): 193-204.

Hodgson, D, A Schindler, D Brown, and M Stroup-Gardiner. 2005. "Self-Consolidating Concrete for Use in Drilled Shaft Applications." *ASCE Journal of Materials in Civil Engineering* 17 (3): 363-369.

Illinois Department of Transportation. 2007. "Special Provision for Self-Consolidating Concrete for Cast-In-Place Construction." Bureau of Materials and Phyisical Research.

Jakobsen, U.H., C. Pade, N. Thaulow, D. Brown, S. Sahu, O. Magnusson, S. De Buck, and G. De Schutter. 2006. "Automated air void analysis of hardened concrete - a Round Robin study." *Cement and Concrete Research* 36: 1444-1452.

n.d. *JMicroVision.* Accessed January 2009. http://www.jmicrovision.com.

Jolicoeur, Carmel, and Marc-Andre Simard. 1998. "Chemical admixture-cement interactions: Phenomology and physico-chemical concepts." *Cement and Concrete Composites* (20): 87-101.

Kasemsamrarn, N, and S Tangtermsirikul. 2005. "A Design Approach for Self-Compacting Concrete Based on Deformability, Segregation Resistance and Passing Ability Models." *First International Symposium on Design, Performance and Use of Self-Consolidating Concrete.* Changsha, China: RILEM.

Khaleel, O R, S A Al-Mishhadani, and H Abdul Razak. 2011. "Effect of Coarse Aggregate on Fresh and Hardened Properties of Self-Compacting Concrete (SCC)." *Procedia Engineering* 14: 805-813.

Khayat, K H, and D Mitchell. 2009. *Self-Consolidating Concrete for Precast, Prestressed Concrete Bridge Elements.* Report 628, National Cooperative Research Program (NCHRP): Transportation Research Board.

Khayat, K, J Assaad, and J Daczko. 2004. "Comparison of Field-Oriented Test Methods to Assess Dynamic Stability of Self-Consolidating Concrete." *ACI Materials Journal* 168-176.

Koehler, Eric P, and David W Fowler. 2007. "Aggregates in Self-Consolidating Concrete." ICAR Project 108.

Kronlof, Anna, Markku Leivo, and Pekka Sipari. 1995. "Experimental study on the basic phenomena of shrinkage and cracking of fresh mortar." *Cement and Concrete Research* 25 (8): 1747-1754.

Lazniewska-Piekarczyk, Beata. 2012. "The influence of selected new generation admixtures on the workability, air voids parameters and frost-resistance of self compacting concrete." *Construction and Building Materials* (31): 310-319.

Lin, Yiching, Shih-Fang Kuo, Chaimen Hsiao, and Chao-Peng Lai. 2007. "Investigation of Pulse Velocity-Strength Relationship of Hardened Concrete." *ACI Materials Journal* 344-350.

Logan, D. 1997. "Acceptance Criteria for Bond Quality of Strand for Pretensioned Prestressed Concrete Applications." *PCI Journal* 52-90.

Lomboy, Gilson, and Kejin Wang. 2009. "Effects of Strength, Permeability, and Air Void Parameters on Freezing-Thawing Resistance of Concrete with and without Air Entrainment." *Journal of ASTM International* 6 (10).

Nanthagopalan, P, and M Santhanam. 2009. "Experiemental Investigations on the Influence of Paste Composition and Content on the Properties of Self-Compacting Concrete." *Construction and Building Materials* 3443-3449.

Narchus, Robert, interview by Joseph Sweet. 2006. *SCC in Sidley Precast Company, PA* (May).

Neville, A M. 2004. *Properties of Concrete.* 4th. Essex: Pearson Education Limited.

NJDOT. 2007. "Section 903.06." In *Standard Specifications for Road and Bridge Construction*, by New Jersey Department of Transportation.

Ouchi, M, S Nakamura, T Osterberg, S Hallberg, and M Lwin. 2003. "Application of Self-Consolidating Concrete in Japan, Europe and the United States." *49th PCI Annual Convention and Exhibition.* Orlando, Florida.

Ouyang, Xinping, Yongxia Gou, and Xueqing Qui. 2008. "The feasibility of synthetic surfactant as an air entraining agent for the cement matrix." *Construction and Building Materials* (22): 1774-1779.

Parra, C, M Valcuende, and F Gomez. 2011. "Splitting Tensile Strength and Modulus of Elasticity of Self-Compacting Concrete." *Construction and Building Materials* 25: 201-207.

Persson, Bertil. 2001. "A Comparison between Mechanical Properties of Self-Compacting Concrete and the Corresponding Properties of Normal Concrete." *Cement and Concrete Research* 193-198.

Precast/Prestressed Concrete Institute. 2003. "Interim Guidelines for the Use of Self-Consolidating Concrete in Precast/Prestressed Concrete Institute Memeber Plants." *TR-6-03.* Chicago.

—. 1999. *MNL-116-19 Manual for quality control for plants and production of structural precast concrete products.* Fourth Edition. Chicago: PCI.

—. 1999. *PCI Design Handbook.* Fifth. Edited by Raths and Johnson, Inc. Raths. Chicago.

Rajabipour, Farshad, Gaurav Sant, and Jason Weiss. 2008. "Interactions between shrinkage reducing admixtures (SRA) and cement paste's pore solution." *Cement and Concrete Research* (38): 606-615.

Rhode Island Department of Transportation. 2006. "Revisions, Supplemental Specifications and Special Provisions." In *Standard Specifications for Road and Bridge Construction*.

Saak, A W, H M Jennings, and S P Shah. 2001. "New Methodology for Designing Self-Compacting Concrete." *ACI Materials Journal* 98 (6): 429-439.

Scheff, J, and HL Chen. 2000. "Bridge Deck Inspection Using Chain Drag and Ground Penetrating Radar." Edited by Farhad Ansari. *Condition Monitoring of Materials and Structures* (ASCE) 164-178.

Shindoh, Takefumi, and Yasunori Matsouka. 2003. "Development of Combination-Type Self-Compacting Concrete and Evaluation Test Methods." *Journal of Advanced Concrete Technology* 1 (1): 26-36.

Slag Cement Association. 2002. "Slag Cement and Fly Ash." *Slag Cement and Concrete.*

Staton, BW, NH Do, ED Ruiz, and WM Hale. 2009. "Transfer Lengths of Prestressed Beams Cast with Self-Consolidating Concrete." *PCI Journal* Spring 2009: 64-83.

Sutter, Lawrence L. 2007. *Evaluation of Methods for Characterizing Air Void Systems in Wisconsin Paving Concrete.* Final Report, School of Technology, Michigan Technological University, Madison, WI: Wisconsin Department of Transportation.

U.S. Department of Transportation - Federal Highway Administration. 2011. "Air Entrainment." April 7. Accessed July 18, 2012. http://www.fhwa.dot.gov/infrastructure/materialsgrp/airentr.htm.

Utah Department of Transportation. 2008. "2008 Standard Specifications for Road and Bridge Construction."

W.R. Grace & Co. 2006. "Technical Bulletin TB-0203: Effect of high dosage of AEA on compressive strength."

Wang, K, SP Shah, DJ White, J Gray, T Voigt, G Lu, J Hu, C Halverson, and BY Pekmezci. 2005. "Self-Consolidating Concrete - Applications to Slip Form Paving: Phase I (Feasibility Study)." Final Report to FHWA, Study TPF-5(98), 10.

Weiss, Jason, Pietro Lura, Farshad Rajabipour, and Gaurav Sant. 2008. "Performance of shrinkage-reducing admixtures at different humidities and at early ages." *ACI Materials Journal* 105 (5): 478-486.

Weiss, W J, and N S Berke. 2003. "Admixtures for reduction of shrinkage and cracking." In *Early age cracking in cementitious systems -Report of RILEM Technical Committee 181-EAS*, edited by A Bentur, 323-335. RILEM.

West Virginia Department of Transportation. 2000. *Standard Specifications for Roads and Bridges.* Charleston, West Virginia.

Wong, G S, Alexander A M, Haskins R, Poole T S, Malone P G, and Wakeley L. 2000. *Portland-Cement Concrete Rheology and Workability: Final Report.* FHWA-RD-00-025, McLean: FHWA.

Yang, Quanbing, Peirong Zhu, Xueli Wu, and Shiyuan Huang. 2000. "Properties of concrete with a new type of saponin air-entraining agent." *Cement and Concrete Research* (30): 1313-1317.

Yurtdas, I., N. Burlion, J.-F. Shao, and A. Li. 2011. "Evolution of the mechanical behaviour of a high performance self-compacting concrete under drying." *Cement & Concrete Composites* 33: 380-388.

Zhang, DS. 1996. "Air entrainment in fresh concrete with PFA." *Cement and Concrete Composites* (18): 409-416.

Zia, Paul, Roberto A Nunez, and Luis A Mata. 2005. *Implementatin of Self-Consolidating Concrete for Prestressed Concrete Girders*. Final Report, North Carolina State University, Raleigh: FHWA/NC.

APPENDIX A – Special Provisions for the Use of SCC

A.1 General Notes on Use of SCC for Stalnaker Run Project

WEST VIRGINIA DEPARTMENT OF TRANSPORTATION

DIVISION OF HIGHWAYS

SPECIAL PROVISION

FOR
STALNAKER RUN PROJECT

STATE PROJECT: _____

FEDERAL PROJECT: _____

GENERAL NOTES FOR SCC IN CONSTRUCTION PLANS
(Additions and Changes to Current Notes)

USE OF SELF-CONSOLIDATING CONCRETE

SELF-CONSOLIDATING CONCRETE (SCC) WILL BE USED IN TWO DIFFERENT EXPERIMENTAL APPLICATIONS FOR THIS CONSTRUCTION. THREE DRILLED CAISSONS, PLUS ONE TEST HOLE, WILL BE CONSTRUCTED USING READY-MIX SCC, DESIGNATED SCC-1. TWO PRESTRESSED CONCRETE BOX BEAMS, AND ONE MORE FOR FULL SCALE TESTING, WILL BE CONSTRUCTED USING PRECAST SCC, DESIGNATED SCC-2. SPECIAL PROVISIONS TO THE WVDOT STANDARD SPECIFICATIONS (SECTIONS 601 AND 603) AND MATERIALS PROCEDURES (MP 711.03.23) ARE PROVIDED WHICH INCLUDE FRESH MATERIAL REQUIREMENTS, ACCEPTANCE CRITERIA, MIXING AND HANDLING OF SCC, AND HARDENED PROPERTY REQUIREMENTS FOR BOTH CLASSES OF SCC THAT WILL BE USED IN THIS PROJECT.

FRESH PROPERTY TESTING IS IMPORTANT WHEN CONSIDERING THE OVERALL PERFORMANCE OF SCC TO ENSURE HOMOGENEITY OF CONCRETE DURING AND AFTER CASTING. TESTS THAT ARE SPECIFIC TO SCC AND WILL BE CONDUCTED ON SITE FOR ACCEPTANCE OF SCC INCLUDE, BUT ARE NOT LIMITED TO, THE SLUMP-FLOW TEST (ASTM C1611) AND J-RING TEST (ASTM C1621). ANOTHER PROPERTY REQUIREMENT OF SCC INCLUDES THE SEGREGATION RESISTANCE BY COLUMN METHOD (ASTM C1610). REQUIRED FRESH PROPERTIES FOR FIELD ACCEPTANCE OF THE CLASS SCC-1 AND CLASS SCC-2 CONCRETES ARE:

SCC-1	SPREAD = 21” ± 2”, J-RING VALUE $\leq$ 1.5”,
	VSI $\leq$ 1.5, 2SEC $\leq$ T_{50} $\leq$ 7SEC, AIR CONTENT 6% ± 1.5%
SCC-2	SPREAD: TARGET ± 2” (MAX=25’), J-RING

VALUE $\leq$1.5", VSI $\leq$ 1, 2SEC $\leq T_{50} \leq$ 7SEC, AIR CONTENT 5% ± 1%

RESEARCHERS FROM WEST VIRGINIA UNIVERSITY (WVU) WILL BE PRESENT TO CONDUCT TESTING ON ALL SCC MEMBERS CONSTRUCTED IN THIS PROJECT. THEY WILL CONDUCT TESTING AND COLLECT DATA DURING ALL PHASES OF CONSTRUCTION, INCLUDING SCC MIX QUALIFICATION, MIX ACCEPTANCE, CONSTRUCTION, AND POST-CONSTRUCTION. THE CONTRACTOR IS EXPECTED TO WORK WITH THE DIVISION IN COORDINATING THEIR CONSTRUCTION SCHEDULE TO PERMIT WVU RESEARCHERS TO CONDUCT THE RESEARCH FOR THIS PROJECT. AMPLE NOTICE (AT LEAST ONE WEEK) SHOULD BE GIVEN TO THE RESEARCHERS WHEN IMPORTANT CONSTRUCTION BENCHMARKS WILL BE REACHED. THE CONTRACTOR SHALL PROVIDE ADEQUATE ACCESS AND NECESSARY ASSISTANCE TO THE RESEARCHERS FOR CONDUCTING ALL TESTING, INSTRUMENTATION AND DATA COLLECTION ACTIVITIES.

MATERIAL SPECIFICATIONS AND DESIGN UNIT STRESSES

MATERIALS FURNISHED SHALL BE IN ACCORDANCE WITH GOVERNING SPECIFICATIONS AND SHALL MEET THE FOLLOWING REQUIREMENTS:

CONCRETE:

CLASS B	f 'c = 3,000 psi, n = 9
CLASS B MODIFIED	f 'c = 4,500 psi, n = 7
CLASS H	f 'c = 4,000 psi, n = 8
CLASS K	f 'c = 4,000 psi, n=8
PRESTRESSED	f 'ci = 6,000 psi, f 'c = 8,000 psi, n = 6
SCC-1	f 'c = 4,500 psi, n = 7
SCC-2	f 'ci = 6,000 psi, f 'c = 8,000 psi, n = 6

REINFORCING STEEL:
(NO CHANGE)

PRESTRESSING STEEL:
(NO CHANGE)

REINFORCED ELASTOMERIC BEARING PADS:
(NO CHANGE)

CONCRETE

CONCRETE FOR THE BRIDGE DECK, SEMI-INTEGRAL BACKWALLS AND DIAPHRAGMS SHALL BE CLASS H CONCRETE. THE PARAPETS SHALL BE CLASS K CONCRETE. THE ABUTMENTS, WINGWALLS AND APPROACH SLABS SHALL BE CLASS B CONCRETE. THE THREE DRILLED SHAFTS ON ABUTMENT TWO SHALL BE MODIFIED CLASS B CONCRETE. THE THREE DRILLED SHAFTS ON ABUTMENT ONE SHALL BE CLASS SCC-1 CONCRETE. TWO OF THE FIVE PRESTRESSED BOX BEAMS SHALL BE CLASS SCC-2 CONCRETE, AS SPECIFIED IN THE PLANS, AND THE OTHER THREE WILL BE CONVENTIONAL PRESTRESSED CONCRETE.

THE CLASS SCC-1 CONCRETE FOR THE DRILLED SHAFTS AND ONE TEST HOLE, AND THE CLASS SCC-2 CONCRETE FOR THREE PRESTRESSED CONCRETE BOX BEAMS, TWO FOR CONSTRUCTION AND ONE FOR FULL-SCALE TESTING BY WVU RESEARCHERS, SHALL BE AS SPECIFIED IN THE SPECIAL PROVISIONS. THE MAXIMUM AGGREGATE SIZE FOR CLASSES SCC-1 AND SCC-2 CONCRETE IS 3/4 INCH. THE MIX DESIGN REQUIREMENTS FOR ADMIXTURES, POZZOLANS, AND PERFORMANCE OF THE SCC MIXES ARE GIVEN IN THE SPECIAL PROVISIONS.

CLASS H CONCRETE FOR… (NO CHANGES TO REST OF SECTION)

PRESTRESSED CONCRETE BOX BEAMS

PRESTRESSED CONCRETE BOX BEAMS INCLUDE ALL PRESTRESSED MEMBERS COMPLETE IN PLACE, PLUS ONE MANUFACTURED FOR WVU RESEARCHERS FOR THE PURPOSE OF FULL-SCALE TESTING. THIS SHALL INCLUDE BUT NOT BE LIMITED TO ALL MEMBER COMPONENTS AND PLACEMENT, WHICH INCLUDES THE CONCRETE, MILD REINFORCING STEEL, PRESTRESSING STRANDS, LIFT DEVICES, STAY-IN-PLACE FORM INSERTS, TEMPORARY BRACING INSERTS (IF REQ'D), AND PROTECTIVE COATINGS. ALSO INCLUDED SHALL BE THE COMPLETE MECHANICAL SPLICING SYSTEM TO BE UTILIZED AS DIAPHRAGM THROUGH BEAM REINFORCEMENT. ALL MATERIAL AND PLACEMENT COSTS OF THE BARS AND COUPLERS, INCLUDING COMPONENTS TO BE PLACED DURING DIAPHRAGM CONSTRUCTION, SHALL BE CONSIDERED INCIDENTAL FOR PAYMENT AND SHALL BE INCLUDED IN THE PRICE BID FOR ITEM 603016-207, PRESTRESSED CONCRETE BOX BEAMS.

ALL MILD REINFORCING STEEL SHALL BE EPOXY COATED, AASHTO M248, GRADE 60. THE MECHANICAL SPLICING SYSTEM SHALL BE EITHER EPOXY COATED OR GALVANIZED AS APPROVED BY THE MANUFACTURER. FOR ADDITIONAL INFORMATION AND REQUIREMENTS SEE SEMI-INTEGRAL BACKWALL DETAILS, MIDSPAN DIAPHRAGM DETAILS AND BEAM DETAILS AND NOTES.

THE PRODUCTION OF THE PRESTRESSED CONCRETE BOX BEAMS WILL BE IN ACCORDANCE WITH THE REQUIREMENTS OF SECTION 603 OF THE SPECIFICATIONS AND THE SPECIAL PROVISION. A TOTAL OF SIX BOX BEAMS WILL BE PRODUCED. ONE BOX BEAM WILL BE PRODUCED FOR FULL-SCALE TESTING AT WVU USING THE CLASS SCC-2 MIX DESIGN. TWO BOX BEAMS FOR CONSTRUCTION OF THE BRIDGE WILL BE PRODUCED USING CLASS SCC-2 CONCRETE, WHILE THE OTHER THREE WILL BE PRODUCED USING THE "PRESTRESSED" CONCRETE DESIGN. THE BEAM PRODUCERS SHALL ALLOW WVU RESEARCHERS TO INSTALL EMBEDDED INSTRUMENTATION IN THE FORMWORK FOR ALL BOX BEAMS PRIOR TO CASTING OF CONCRETE FOR THE BEAMS.

THE PRESTRESSED BOX BEAM FOR FULL-SCALE TESTING SHALL BE CAST NO LESS THAN 90 DAYS PRIOR TO PRODUCTION OF THE PRESTRESSED CONCRETE BOX BEAMS THAT WILL BE USED IN CONSTRUCTION. THIS WILL BE CONSTRUCTED, CURED AND SHIPPED IN THE SAME MANNER AS THOSE PROPOSED IN THE PLANS. THE

TEST BEAM SHALL BE SHIPPED TO WVU FACILITIES FOR FURTHER INSTRUMENTATION AND LOAD TESTING.

IN ORDER FOR PRESTRESSED SCC BEAMS TO BE USED FOR CONSTRUCTION, THE PRESTRESSED CONCRETE BOX BEAM FABRICATED USING CLASS SCC-2 CONCRETE MUST DEMONSTRATE THAT THE SCC IS CAPABLE OF PRODUCING A BEAM WITH STRENGTH AND SHORT-TERM AND LONG-DEFLECTION BEHAVIORS THAT ARE COMPARABLE TO THOSE CALCULATED FOR THE DESIGN. IF THE SCC BEAMS ARE DEEMED UNSUITABLE FOR CONSTRUCTION, AND THE CONSTRUCTION SCHEDULE DOES NOT ALLOW FOR ADJUSTMENT TO THE CLASS SCC-2 MIX DESIGN, CONSTRUCTION WILL PROCEED WITHOUT DELAYS USING CONVENTIONAL PRESTRESSED CONCRETE BEAMS.

BEAM CAMBERS WERE ESTIMATED IN ACCORDANCE WITH STANDARD PROCEDURES SPECIFIED IN THE PCI DESIGN HANDBOOK. PCI RECOMMENDED MULTIPLIERS FOR CAMBER AND DEFLECTION ESTIMATION ASSUMING ELASTIC BEHAVIOR FOUND IN TABLE 4.6.2 WERE UTILIZED. DEFLECTIONS WERE COMPUTED TO COMPENSATE FOR ALL DEAD LOAD DEFLECTIONS EXCLUDING FUTURE WEARING SURFACE AND THE HORIZONTAL CURVATURE OF THE FINISHED ROADWAY. ACTUAL PRESTRESSED BEAM CAMBERS SHOULD BE DETERMINED AND HAUNCH THICKNESSES ADJUSTED ACCORDINGLY. THE MINIMUM HAUNCH THICKNESS AT BEAM CENTERLINES, 2 INCH, MUST BE MAINTAINED. THE CONTRACTOR SHALL BE REQUIRED TO COMPLETE THE INITIAL TOP OF BEAM ELEVATION TABLE PROVIDED ON SHEET B26.

THE CLASS SCC-2 CONCRETE AND THE CONVENTIONAL PRESTRESSED CONCRETE THAT ARE USED FOR THE PRESTRESSED CONCRETE BOX BEAMS SHALL GENERATE MATERIAL PROPERTIES (I.E. CREEP, SHRINKAGE, AND MODULUS OF ELASTICITY) THAT PRODUCE COMPATIBLE SHORT- AND LONG-TERM DEFLECTION, CAMBER AND PRESTRESS LOSSES. EQUATIONS OF AASHTO SECTION 5.9.5 SHALL BE USED ALONG WITH THE MEASURED CONCRETE PROPERTIES TO ENSURE COMPARABLE PRESTRESS LOSS BETWEEN THE PRESTRESSED BOX BEAMS WILL OCCUR.

IF THE ACTUAL CAMBERS ARE DETERMINED TO BE SIGNIFICANTLY DIFFERENT THAN ESTIMATED, THE DEFLECTIONS SHOULD BE RECALCULATED, THE BEAM DESIGN RE-EVALUATED AND/OR THE ROADWAY PROFILE ADJUSTED AS NECESSARY.

DRILLED CAISSONS

THE INSTALLATION OF THE DRILLED CAISSON FOUNDATIONS SHALL BE IN ACCORDANCE WITH THE REQUIREMENTS OF SECTION 625 OF THE SPECIFICATIONS AND THE SPECIAL PROVISION. THE THREE DRILLED CAISSONS FOR ABUTMENT 1 WILL USE CLASS SCC-1 CONCRETE, WHILE THE THREE DRILLED CAISSONS FOR ABUTMENT 2 WILL USE MODIFIED CLASS B CONCRETE.

THE LENGTH OF THE DRILLED CAISSON IS BASED ON THE COMBINATION OF THE END BEARING AND FRICTIONAL RESISTANCE OF THE ROCK SOCKET DURING SCOUR CONDITIONS, AND IS THE MINIMUM LENGTH REQUIRED.

TWO 42-INCH-DIAMETER TEST HOLES WILL BE CONSTRUCTED PRIOR TO CONSTRUCTION OF THE DRILLED CAISSONS. THE FIRST WILL USE MODIFIED CLASS B CONCRETE, AND SHALL BE LOCATED AT STATION 406+09.50 OFFSET 42 FEET RT. THE SECOND SHALL USE CLASS SCC-1 CONCRETE AND BE LOCATED AT STATION _____ OFFSET __ FT ___. BOTH TEST HOLES SHALL BE CONSTRUCTED IN THE SAME MANNER AND DEPTH AS THE PROPOSED FOUNDATION CAISSONS, INCLUDING PLACING REINFORCEMENT. PAYMENT FOR THE FIRST TEST HOLE, USING MODIFIED CLASS B CONCRETE, SHALL BE UNDER ITEM 625004-014. PAYMENT FOR THE SECOND TEST HOLE, USING CLASS SCC-1 CONCRETE, SHALL BE UNDER ITEM _____.

CROSSHOLE SONIC LOGGING (CSL) WILL BE REQUIRED FOR ALL CAISSONS AND ROCK SOCKETS, INCLUDING THE TEST HOLES. THE CONTRACTOR IS RESPONSIBLE FOR PERFORMING THE CSL TESTING. CSL SHALL BE IN ACCORDANCE WITH SECTION 625.2.6 OF THE SPECIFICATIONS AND THE SPECIAL PROVISION.

A.2 Special Provisions for Use of SCC-1 for Stalnaker Run Caissons

A.2.1 Modifications to Standard Specifications

WEST VIRGINIA DEPARTMENT OF TRANSPORTATION

DIVISION OF HIGHWAYS

SPECIAL PROVISION
FOR
STALNAKER RUN PROJECT

STATE PROJECT: _____

FEDERAL PROJECT: _____

SECTION 601, 625 AND 707
DRILLED CAISSON FOUNDATIONS
CLASS SCC-1 CONCRETE FOR DRILLED CAISSONS

625.4.1 – Concrete:
DELETE THE SECTION AND REPLACE WITH THE FOLLOWING:

Concrete for the selected drilled caissons noted in the plans shall be Class SCC-1 and shall conform to the requirements of Section 601 of the Standard Specifications and as modified below in this special provision.

The design 28-day compressive strength shall be not less than 4500 psi (31 MPa) unless shown otherwise in the plans. The Contractor will prepare a mix design to attain this strength in accordance with MP 711.03.23 as modified by special provision for this project. Unless otherwise specified in the plans, the cement shall be Type I.

601.1 – DESCRIPTION:
ADD THE FOLLOWING PARAGRAPHS TO THIS SUBSECTION:

Class SCC-1 concrete shall be self-consolidating concrete, and will be used for drilled shaft caissons and other elements when designated in the plans. For this project, the Class SCC-1 concrete will be placed in accordance to this section, as well as Section 625 of these Standard Specifications.

601.2 – MATERIALS:
ADD THE FOLLOWING PARAGRAPH AT THE BEGINNING OF THIS SECTION:

Class SCC-1 concrete shall consist of a homogeneous, flowable mixture of cement, fine aggregate, coarse aggregate, fly ash or ground granulated blast furnace slag, chemical admixtures and water. The mixture proportions shall be such that the Class SCC-1 concrete will resist segregation, bleeding, and the generation of foam during placement, and will need no external compaction or vibration. Establishment of the mixture proportions shall be coordinated with the manufacturers of the admixtures that will be used in the Class SCC-1 concrete.

ADD THE FOLLOWING TO THE BOTTOM OF THE TABLE:

MATERIAL	SECTION OR SUBSECTION
Viscosity-Modifying Admixture	707.16

601.3 – PROPORTIONING:

ADD THE FOLLOWING PARAGRAPH:

SCC-1 REQUIREMENTS: Self-consolidating concrete (SCC) exhibits self-leveling capabilities and therefore requires no external compaction or vibration efforts. Creating a successful SCC mix requires combining ingredients to achieve a highly-flowable product that also has the capability to resist dynamic segregation and foaming during placement, and also resist static segregation and bleeding once in place. SCC mix designs are often achieved using high-range water reducing (HRWR) admixtures, and by carefully selecting an aggregate gradation, incorporating high volumes of powder in the mix, through the use of viscosity-modifying admixtures (VMAs), or a combination of any or all of those.

For Class SCC-1 concrete, a combination of admixtures may be used that includes high-range water reducing admixtures, VMAs, air-entraining agents, and retarding admixtures. The admixtures used should all come from the same manufacturer, or measures should be taken to ensure that no adverse reactions would occur from using different sources. Also for SCC-1, it is permitted to use a combination of up to two AASHTO gradations of coarse aggregate to obtain the optimal combination of strength, self-compacting ability, and passing ability.

601.3.1 – Mix Design Requirements:

ADD THE FOLLOWING PARAGRAPHS TO THIS SUBSECTION:

The Class SCC-1 concrete mix design shall be submitted for approval at least 45 days prior to construction. Design mixture testing shall be done in accordance with MP 711.03.23, using the criteria for all classes of concrete (except Class H and concrete for specialized overlays). Modifications to MP 711.03.23 for Class SCC-1 concrete include a modification of the test for consistency, and additional tests for passing ability and segregation resistance, and are given as a separate Special Provision. Since the fresh and hardened behaviors of Class SCC-1 concrete are highly dependent upon the materials from which it is made, at the discretion of the Engineer, the mix design may be subject to re-acceptance testing as per MP 711.03.23 following a change in the source of any of the materials.

REPLACE TABLE 601.3.1A AND THE FIRST FOOTNOTES WITH:

{ENGLISH}

Class of Concrete	Design 28 Day Compressive Strength	Target Cement Factor	Maximum Water Content	Standard Size(s) of Coarse Aggregate***	Entrained Air
	Pounds per Square inch	Bags / c.y. *	Gal/bag of cement **	Number	Percent
A	3500	7¼	5¾	7, 78 or 8	7½
K	4000	7	5	57, 67	7
B	3000	6	5½	57, 67	7
C	2500	5¼	6½	57, 67	6
D	2000	4¼	7	57, 67	5½
SCC-1	4500	6.5≤C.F.≤8	4 ¾	67****, 7, 78, 8, 9	6

{METRIC}

Class of Concrete	Design 28 Day Compressive Strength	Target Cement Factor	Maximum Water Content	Standard Size(s) of Coarse Aggregate***	Entrained Air
	MPa	kg /m^3 *	L / kg of cement **	Number	Percent
A	24	404	.51	7, 78 or 8	7½
K	28	390	.44	57, 67	7
B	21	335	.48	57, 67	7
C	17	295	.58	57, 67	6
D	14	235	.62	57, 67	5½
SCC-1	31	335≤C.F.≤446	0.42	67****, 7, 78, 8, 9	6

*An equal volume of pozzolanic additive may be substituted for Portland cement up to the maximum amount in Table 601.3.1B.

** When using pozzolanic additives, volumes of these materials shall be considered as cement for purposes of establishing maximum water content.

***For SCC-1, blending up to two coarse aggregate types is permitted, but the aggregate blend must contain (at least) one aggregate type that has a maximum aggregate size of ¾ inches.

****Coarse aggregate gradation using #67 aggregates is allowed only if it is graded such that 100% of all aggregates pass through a sieve with ¾-inch nominal opening size. Such a gradation of #67 aggregate will be considered in this provision to have a maximum aggregate size of ¾ inches.

REPLACE TABLE 601.3.1B:

MATERIAL	CLASS OF CONCRETE	QUANTITY
Fly Ash	B, C, D, SCC-1	1 Bag (15%)
	A, K	1 ¼ Bags (19%)
Ground Granulated Furnace Slag	A, B, K, SCC-1	3 Bags (45%)
	C, D	2 Bags (30%)
Microsilica	All Classes	1/2 Bag (8%)

601.3.2.1 – Consistency:

REPLACE THE FIRST PARAGRAPH OF THIS SECTION WITH THE FOLLOWING:

Concrete shall have the consistency which will allow proper placement and consolidation in the required position. Every attempt shall be made to obtain a uniform consistency. For Class SCC-1 concrete, slump-flow tests will be conducted in lieu of traditional slump tests as the indication of consistency. The optimum consistency for a Class SCC-1 concrete mix varies based on things such as member geometry and rebar congestion, and therefore should be indicated on the plans of the specific project. The optimum consistency for various types of highway structures for normal concrete shall be as indicated in Table 601.3.2.

ADD THE FOLLOWING TO TABLE 601.3.2:

TYPE	***OPTIMUM CONSISTENCY Inches of slump*** (millimeters of slump***)**
vi. SCC-1	****

***The slump-flow test (ASTM C1611) is used to measure the consistency of self-consolidating concrete.

****The target slump-flow value (spread) for Class SCC-1 concrete as indicated on the construction plans (21", or 533 mm). If the Class SCC-1 concrete spread varies beyond a tolerance of 1.5 inches (38 mm) above or below the target value, the Contractor shall take immediate steps to adjust the spread for subsequent batches. If the spread of the Class SCC-1 concrete exceeds two inches (51 mm) above or below the target value, the concrete will be rejected.

601.3.2.2 – Air Content:

REPLACE WITH THE FOLLOWING:

The target value of the entrained air at the point of placement shall be as shown in Table 601.3.1A. If the air content exceeds the target value plus 1.5 percentage points (4.5% < Air Content < 7.5%) the concrete-shall be rejected. When the concrete is delivered in a truck mixer and the air content is less than the target value minus 1.5 percentage points the concrete shall be rejected, or the Contractor may use additional air entraining agent in an amount that is intended to achieve the target value specified. The addition is permitted under the following conditions:

i. The air entraining agent is the same as used in the approved mix design and is thoroughly mixed with a maximum of 0.2 gallons (757 mL) of water per cubic yard of concrete contained in the truck. The solution will be directed to the front of the mixer.
ii. The mixer is turned a minimum of 30 revolutions, at mixing speed, or the number of revolutions established in tests to comply with uniformity requirements, whichever is more.
iii. Immediately after mixing, the air content and other acceptance criteria shall be measured by a certified inspector or technician.

An air adjustment may be attempted twice per truck. If after the second addition the specified air content is not achieved, the concrete shall be rejected. These procedures do not alter the limits placed on time to discharge, the total revolutions of the mixing drum, or the specified slump.

601.3.2.4 – Total Solids Ā

REPLACE THE FIRST PARAGRAPH WITH THE FOLLOWING:

The combined grading of the coarse aggregate, fine aggregate, and cement used in the structural concrete shall conform to the design mix Ā plus or minus the tolerance specified in Table 601.3.2.4 for the coarse aggregate size used. All coarse aggregate blends for Class SCC-1 concrete shall use a tolerance of ± 0.15.

601.4 – TESTING:

601.4.1 – Sampling and Testing Methods:

ADD THE FOLLOWING TESTING METHODS:

Slump-Flow of Self-Consolidating Concrete	ASTM C 1611
Passing Ability of Self-Consolidating Concrete using J-Ring	ASTM C 1621
Static Segregation of Self-Consolidating Concrete using Column Technique	ASTM C 1610

ADD THE FOLLOWING:

NOTE 2 - In the performance of quality control or acceptance testing of Class SCC-1 concrete, fill cylinder molds, slump flow cones, and air buckets in one lift. Do not vibrate, rod, or tap to consolidate the SCC.

601.4.2 –Contractor's Quality Control:

REPLACE WITH THE FOLLOWING:

Quality control of the structural concrete is the responsibility of the Contractor as designated in MP 601.03.50. The Contractor shall maintain equipment and qualified personnel, including at least one certified Portland cement concrete technician who shall direct all field inspection, sampling and testing necessary to determine the magnitude of the various properties of concrete governed by the Specifications and shall maintain these properties within the limits of this Specification. The quality control plan designated in MP 601.03.50 shall be submitted to the Engineer at the preconstruction conference. The quality control plan for Class SCC-1 concrete shall include on-site testing of each truckload of Class SCC-1 concrete for spread (19"(483 mm) $\leq$ Spread $\leq$ 23" (584 mm)), Visual Stability Index (VSI $\leq$ 1.5), T_{50} (2 to 7 sec.) , J-Ring Value ($\leq$ 1.5"), Air Content (4.5 % $\leq$ air content $\leq$ 7.5 %), T_{50} (2 to 7 sec.) and casting of three specimens for 28-day compressive strength testing and two for hardened VSI determination. Work shall not begin until the plan is reviewed for conformance with the contract documents.

WVU Researchers, with the permission of the Division, may implement additional quality control methods for field acceptance. The Contractor is responsible for providing material for testing purposes. The additional testing method can also be implemented into MP 711.03.23 Section 3.4.1 for acceptance of the mix design.

601.4.4

As noted in Section 601.4.1, when using Class SCC-1 concrete, fill cylinder molds in one lift. Do not vibrate, rod, or tap to consolidate the SCC.

601.5.3 – Mixers and Agitators:

ADD THE FOLLOWING TO THE END OF THE FIRST PARAGRAPH:

For Class SCC-1 concrete, all wash water must be completely discharged from the mixing drum prior to addition of any materials for the subsequent batch.

601.7 – MIXING:

ADD THE FOLLOWING PARAGRAPH AFTER THE THIRD PARAGRAPH:

During truck delivery of Class SCC-1 concrete, the drum shall mix the concrete at a rate of 1-2 revolutions per minute during transport. Upon arrival at the construction site, the SCC shall be agitated at mixing speed for a period of at least 3 minutes before testing and discharge. The total number of revolutions of the truck's mixing drum from the time the cement is added to the aggregates until expulsion shall not exceed 300 revolutions.

ADD THE FOLLOWING SENTENCES TO THE FOURTH PARAGRAPH:

When using Class SCC-1 concrete, under no circumstances shall water be used to adjust the consistency of the mix. If it is necessary to adjust the Class SCC-1 concrete's consistency when delivered in truck mixers, this shall be done, at the Engineer's discretion. This shall be accomplished through the addition of chemical admixtures using the procedures i.–iii. described for air entraining agents in subsection 601.3.2.2 before any Class SCC-1 concrete is discharged. If in accordance with the admixture manufacturers' recommendations, multiple admixtures may be added to the same batch of dilution water. A maximum of two adjustments to reach the appropriate acceptance tolerances, including those for air content, is allowed before rejection of the batch.

601.10 – PLACING CONCRETE:

ADD THE FOLLOWING SUBSECTIONS:

601.10.1.1 – Test Hole Requirements

Two test holes will be constructed in accordance with 625.2.5 in order to verify the techniques of the Contractor, as well as the integrity of both the Type B Modified concrete and the Class SCC-1 concrete mix designs. The first test hole will be constructed using traditional Type B Modified Concrete, and the second will use Class SCC-1 concrete. Both test holes will require steel reinforcement cage as per plan, in addition both test holes will also require the insertion of tubes for Cross-hole Sonic Logging (CSL) non-destructive testing, as per 625.2.6. Both test holes will assume construction under "wet" conditions, requiring either tremie placement or pumping, as outlined in 625.5.1(g) and 625.5.4. The construction and placement of concrete of these test holes must take place at least 35 days prior to the construction of the actual bridge caissons to allow adequate time for evaluation of the integrity of each. WVU Researchers will be present for the casting of both test holes. The Contractor will be responsible for conducting CSL testing after completion of the test holes, and will provide the Division and the WVU Researchers with all data collected from these tests. The Contractor will provide means of retrieving 4-inch-diameter core samples from the two test holes for the entire depth.

601.10.1.2 – Instrumentation of Drilled Caissons

Instrumentation of the drilled caissons shall be done by WVU Researchers in cooperation with the Contractor. The Contractor shall provide suitable working space and access to the drilled caissons and their components, and allow adequate time for such actions as the placement of instrumentation and gages, and the collection of data. Fabrication of the reinforcing steel cage shall be performed prior to concrete placement to allow for installation of gages and instrumentation by the Researchers. The Contractor shall provide any required assistance for implementation of the instrumentation, and uphold the coordination and scheduling of these activities as determined by the Division.

601.10.3 – Vibrating:

ADD THE FOLLOWING PARAGRAPH:

When Class SCC-1 concrete is used, the plans for delivery and placement of the SCC to the jobsite should ensure that construction of the caisson is completed during the workable period of the concrete established in MP 711.03.23, such that no vibration of the concrete is necessary at any point during construction. Batching, transportation and delivery of the Class SCC-1 shall be planned by the Contractor such that there is a continuous feed into the tremie and, therefore, at no time shall there be a pause or delay in the pouring of the caissons. If a delay shall occur due to an uncontrollable event, the Division Engineer may allow minimal vibration to occur if the mixture was qualified during production of a mockup at or near the maximum slump flow for the type and duration of vibration applied during production.

601.10.5 – Depositing Concrete Underwater:

ADD THE FOLLOWING SENTENCES TO THE END OF THE LAST PARAGRAPH:

All Class SCC-1 concrete used for drilled caissons is assumed to be considered underwater construction and must be placed by either tremie or pumping, in accordance with 625.5.1(i) and 625.5.4. If the Contractor wants to pump Class SCC-1 concrete using a pumping mechanism (such as a concrete pump truck), a demonstration of the pumpability of the SCC-1 mix design must be given to the Division and the WVU Researchers at least 30 days prior to the date of intended use of the pumping mechanism; in this demonstration, the Contractor must show that no additional segregation, bleeding, or air migration would result from the effects of pumping. Upon satisfactory demonstration, the Division will then approve the conditional use of the pumping mechanism.

625.5.4 – Placing of Concrete

ADD THE FOLLOWING PARAGRAPHS AFTER THE FOURTH OF THE SECTION:

At the time of placement of drilled caisson concrete, the concrete temperature shall not exceed the highest concrete temperature recorded during the testing described in Sections 3.4.1 and 3.4.2 of MP 711.03.23 by more than 9°F. If such a temperature difference is anticipated, the slump-flow tests described in those sections shall be re-run at the higher temperature.

At the time of placement of drilled caisson concrete, the workable period established in MP 711.03.23 must exceed the actual concrete placement time by at least 30 minutes. If a longer placement time is anticipated, the amount of retarding admixtures in the mix shall be increased, and the tests described in Sections 3.4.1 and 3.4.2 of MP 711.03.23 shall be re-run to ensure an acceptable workable period.

ADD THE FOLLOWING SENTENCE TO THE LAST PARAGRAPH:

No external or internal vibration shall take place when using Class SCC-1 concrete for drilled caissons.

ADD THE FOLLOWING SECTIONS:

707.16 – VISCOSITY MODIFYING ADMIXTURES FOR CONCRETE:

707.16.1-Acceptance Requirements for Approval of Viscosity Modifying Admixtures: Viscosity Modifying Admixtures (VMAs) for concrete shall be tested in accordance with AASHTO M 194, and exhibit the properties described in the next section.

707.16.2-Performance Requirements for VMAs:

707.16.2.1-The effects of using VMAs may vary widely with different types of cement, cement from different mills, aggregate proportions, aggregates from different sources and of different gradation, and changes in water-cement ratio. Therefore, no hydration control admixture shall be used until the concrete of the specified class, designed in accordance with these Specifications and made with the ingredients proposed for use by the Contractor, including hydration control admixtures as specified or permitted under this Specification, is shown to meet the requirements of AASHTO M 194 for water reduction and compressive strength increases at ages 3, 7, and 28 days.

Upon completion of mixing of this trial batch, air content and slump tests (or air content and slump-flow tests in the cases of Classes SCC-1 and SCC-2 concrete) in accordance with Section 601.4.1 shall be performed on the plastic concrete containing the VMA. A test to establish the initial and final times of setting of the concrete mix shall also be performed in accordance with ASTM C403.

Viscosity Modifying Admixtures (VMAs) for concrete, when evaluated according to the test methods and mix design proportions in AASHTO M 194, shall conform to the following physical requirements:

1. For initial and final set times, the allowable deviation of the test concrete from the reference concrete is not more than 1.0 hour earlier or 1.5 hours later.
2. For compressive and flexural strengths, the minimum allowable strength of the test concrete is 90 percent of the reference concrete strength at 3, 7, and 28 days.
3. The maximum allowable length change of the test concrete is 135 percent of the reference concrete. However, if the length change of the reference concrete is less than 0.030 percent, the maximum allowable length change of the test concrete is 0.010 percentage units more than the reference concrete.
4. The minimum allowable relative durability factor of the test concrete is 80 percent.

707.16.2.2 – The quantity of admixture used shall adhere to the recommended range provided by the manufacturer at the prevailing temperature.

707.16.3-Certification of Viscosity Modifying Admixtures: When a Contractor proposes to use an approved VMA, the procedure set forth in 707.2.4 shall apply.

707.16.4-Additional Test Requirements for Viscosity Modifying Admixtures (Optional): Either prior to or at any time during construction, the Engineer may require the selected admixture to be tested further to determine its effect on the strength of the concrete. When so tested, the VMA shall meet the requirements specified in 707.16.2.

A.2.2 Modifications to Mix Qualification for Class SCC-1 Concrete

WEST VIRGINIA DEPARTMENT OF TRANSPORTATION

DIVISION OF HIGHWAYS

SPECIAL PROVISION
FOR
STALNAKER RUN PROJECT

STATE PROJECT: _____

FEDERAL PROJECT: _____

MP 711.03.23
MIX DESIGN FOR PORTLAND CEMENT CONCRETE
SELF-CONSOLIDATING CONCRETE (SCC-1) FOR DRILLED CAISSONS

3.2
ADD THE FOLLOWING SENTENCE AT THE END OF THE PARAGRAPH:
For Class SCC-1 concrete, use Attachment 1a.

3.2.1
ADD THE FOLLOWING SENTENCE AT THE END OF THE PARAGRAPH:
For Class SCC-1 concrete, use Attachment 2a.

ADD THE FOLLOWING SUBSECTION
3.2.2
Viscosity-modifying admixtures (VMA) may be used for Class SCC-1 concrete with approval from the Division. To do this, a written request must be filed that contains the following information:

1. Name and contact information for the manufacturer of the admixture.
2. Name and designation of the product that is to be evaluated.
3. Documentation that includes results of testing that shows adherence to Section 707.17 of the Special Provisions for of the WVDOT Standard Specifications.
4. Documentation showing that the tests mentioned above were completed in a Division approved laboratory.
5. A materials safety data sheet for the product.

For Class SCC-1 concrete, approval of the VMA is limited the particular mix design for which it will be used, and acceptance is on a project-to-project basis. Re-approval of the product shall be necessary if there are changes in the SCC materials used or in the mix designs.

3.3.2
ADD THE FOLLOWING AT THE END OF THE FIRST PARAGRAPH:
This batch will not be necessary for Class SCC-1 concrete.

3.4

REPLACE WITH THE FOLLOWING PARAGRAPHS:

Each batch of concrete shall be tested in its plastic state for air, consistency and yield. Each batch shall be adjusted as necessary to produce a concrete having plastic properties within a reasonable laboratory working tolerance. The following tolerances shall be used as a guide for all classes of concrete except SCC-1: Air content, ± ½ %; Consistency, ± ½" (± 12 mm) of slump or ball penetration; Yield, ± 2%. See Subsection 3.4.1 for testing criteria of Class SCC-1 concrete.

ADD THE FOLLOWING SUBSECTIONS

3.4.1

Prior to testing ready-mix Class SCC-1 concrete, the approximate time after batching at the ready-mix plant for transport to the job site shall be estimated for the particular project for which it will be used, and this shall represent the time of initial testing at the project site, T_{IT}. The use of the same delivery trucks, similar mixing drum speeds, and similar timing for the addition of admixtures shall done to simulate those conditions that are expected in the field. Initial testing of the fresh properties of Class SCC-1 concrete shall take place at the anticipated time after batching, T_{IT}. For the test batches, the slump-flow shall be in the upper one-half of the acceptable working range given in the construction plans. The following values shall be used as a guide for air, consistency and yield of SCC-1 at T_{IT}: Air content (ASTM C173), 6 % ± 0.5 %; Consistency (ASTM C1611), spread 21" to 23" (533 mm to 584 mm), a T_{50} time of 2 to 7 seconds, and a Visual Stability Index (VSI) of not greater than 1.0; Yield, ± 2%. SCC-1 should also meet the following tolerances: Passing Ability (ASTM C1621), J-Ring Value not greater than 1.0" (51 mm); Segregation Resistance (ASTM C1610), less than 12% segregation by column technique.

For Class SCC-1 concrete, consistency and passing ability tests of all batches will be conducted for each batch immediately after batching (T_0), then at T_{IT}, then 30, 60 and 90 minutes after T_{IT}, and then every 30 minutes thereafter until the spread falls below 12". Segregation resistance tests of all batches will be conducted at 60 minutes after initial testing. Time elapsed after batching for all tests except the segregation resistance test will be recorded upon completion of each test as T_0, T_{IT}, T_{30}, T_{60}, T_{90}, etc., until T_F. Time elapsed after batching for the segregation resistance tests will be recorded upon placement of the concrete into the column apparatus as T_{IT} and T_{60}.

WVU Researchers, with the permission of the Division, may implement additional quality control methods for mix design acceptance. The Contractor is responsible for providing material for testing purposes. The additional testing method can also be implemented into 601.3.4 section for acceptance of the concrete in the field.

3.4.2

For each time of testing of the consistency and the passing ability described in Section 3.4.1, the slump-flow and j-ring values will be plotted versus the time after batching. From this, the "workable period," defined as the amount of time after batching during which the SCC has acceptable fresh properties, will be found through linear interpolation of the data by determining the time at which either the spread falls below the lower acceptance limit (19" or 486 mm) or the J-ring value exceeds the acceptance limit (1.5" or 38mm). The workable period obtained can aide Contractors in project planning, however it should be noted that significant differences in environmental conditions during construction, such as temperature and humidity effects, may cause large changes to this value.

3.5

REPLACE WITH THE FOLLOWING:

When the properties of a concrete batch have been established within acceptable limits, seven standard concrete cylinders shall be made from each batch produced in Section 3.3 (or 3.3.1) and 3.3.2 and tested in compression at the following ages: one cylinder at age 24 hours ± 4 hours (the exact age to the nearest hour at time of test shall be noted on the report); one cylinder at age 3 days; one cylinder at age 7 days; one cylinder at age 14 days; and three cylinders at age 28 days. For Class SCC-1 Concrete, three additional cylinders shall be cast for later assessment of the hardened Visual Stability Index. All cylinders using Class SCC-1 concrete for purposes of compression testing and hardened VSI determination shall be cast in a single layer with no rodding or vibration. The values of the physical properties of each mix shall be the average of the physical properties established in each of the two batches produced in section 3.3 (or 3.3.1). These values shall be listed in Attachment 3 for all concrete classes except SCC-1, and in Attachment 3a for Class SCC-1.

3.5.1

REPLACE WITH THE FOLLOWING:

The following properties of each batch of concrete produced in Sections 3.3 (or 3.3.1) and 3.3.2 for all concrete types, excluding SCC-1, shall be listed in Attachment 2: A-Bar of Total Solids, Consistency, Air Content, Unit Weight & Yield, Water / Cement Ratio, and Temperature. For SCC-1, the following properties, and appropriate times for each batch produced shall be listed in Attachment 2a: A-Bar of Total Solids, Consistency, Passing Ability, Segregation Resistance, Air Content, Unit Weight & Yield, Water / Cement Ratio, and Temperature.

ADD THE FOLLOWING SUB-SECTION:

5.2.3

Although a Class SCC-1 concrete may meet the necessary strength requirements and exhibit acceptable fresh properties at the time of initial testing, the Division could require a re-design of the mix based on other criteria, such as: insufficient retention of the slump flow for the mix, poor hardened VSI results, excessive foam buildup, etc.

5.3

The submittal for a proposed mix design shall include completed copies of Attachments 1 and 3 (or 1a and 3a for SCC-1). It shall also include a completed copy of Attachment 2 (or 2a) for the reference batch, a completed copy of Attachment 2 (or 2a) for each of the batches at the minimum cement factor, and a completed copy of Attachment 2 (or 2a) for each of the batches at the minimum cement factor plus one bag (when applicable). All pertinent information supporting these attachments and pertaining to the information in them should be submitted also.

A.2.2.1 Attachment 1(a) – Class SCC-1 Concrete Materials

MP 711.03.23
ORIGINAL ISSUANCE: APRIL 1971
REVISED: DRAFT COPY
ATTACHMENT 1a (SCC-1)

Source: _____

Source Location: _____

Design Laboratory: _____

Class of Concrete: _____

Date: _____

Cementitious Material Data		
Data	Cement	Pozzolan
Name		
Type		
Source		
Source Location		
Specific Gravity		

Admixture Data				
Data	Air Entrainment	Additional Admixture 1	Additional Admixture 2	Additional Admixture 3
Name				
Type				
Source				
Source Location				

Aggregate Data			
Data	Coarse Aggregate #1	Coarse Aggregate #2	Fine Aggregate
Class/Size			
Type			
Source			
Source Location			
Specific Gravity			
A-Bar			
Absorption			
Fineness Modulus			
Unit Weight			

A.2.2.2 Attachment 2(a) – Class SCC-1 Concrete Trial Batch Report

MP 711.03.23
ORIGINAL ISSUANCE: APRIL 1971

REVISED: DRAFT COPY
ATTACHMENT 2a (SCC-1)

Souce: _____ Class of Concrete: _____

Souce Location: _____ Date: _____

Design Laboratory: _____

Check The Appropriate Box For Designated Batch:	Reference Batch	Minimum Cement Factor		Minimum Cement Factor + 1 Bag		Additional Batch
		Batch 1	Batch 2	Batch 1	Batch 2	

Material	Mass	Units	Volume		Units
Cement		lb (kg)			ft^3 (m^3)
Pozzolan 1		lb (kg)			ft^3 (m^3)
Latex Admixture		lb (kg)	gal (L)		ft^3 (m^3)
Water		lb (kg)	gal (L)		ft^3 (m^3)
Air Content, by volume		lb (kg)			ft^3 (m^3)
Coarse Aggregate 1		lb (kg)			ft^3 (m^3)
Coarse Aggregate 2		lb (kg)			ft^3 (m^3)
Fine Aggregate		lb (kg)			ft^3 (m^3)
Total		lb (kg)			ft^3 (m^3)
Air Entraining Admixture		oz/Cwt (mL/100kg)			fl. Oz. (mL)
Chemical Admixture 1		oz/Cwt (mL/100kg)			fl. Oz. (mL)
Chemical Admixture 2		oz/Cwt (mL/100kg)			fl. Oz. (mL)
Chemical Admixture 3		oz/Cwt (mL/100kg)			fl. Oz. (mL)

Mixture Test Data							
Time of Test	Slump Flow	T50	VSI	J-Ring	Seg. Resist.	Concrete Temperature	
T_0							
T_{IT}							
T_{30}							
T_{60}							
T_{90}							
T_F							

Additional Mixture Test Data							
	Yield	W/C Ratio	Cement Factor	Unit Weight	Air Content	A-bar Tot. Sol.	
T_{IT}							

Compressive Strength, psi (Mpa)							
Specified Test Age:	24 Hours +/- 4 Hours	3 days	7 days	14 days	28 days	28 days	28 days
Actual Test Age (hours)							
Compressive Strength							

Shrikage Testing						
Test Age:	4 Days	7 Days	14 Days	28 Days	56 Days	90 Days
% Length Change:						

Rapid Chloride Permeability Testing	
Age of Specimen at Time of Test (days):	Total Adjusted Charge Passed (coulombs):

A.2.2.3 Attachment 3(a) – Summary of Class SCC-1 Concrete

MP 711.03.23
ORIGINAL ISSUANCE: APRIL 1971
REVISED: DRAFT COPY
ATTACHMENT 3a (SCC-1)

SUMMARY

Source: _____
Source Location: _____
Design Laboratory: _____
Class of Concrete: _____
Date: _____

	Reference		Minimum Cement Factor		Minimum Cement Factor + 1 Bag	
Material	Mass	Units	Mass	Units	Mass	Units
Cement		lb (kg)		lb (kg)		lb (kg)
Pozzolan 1		lb (kg)		lb (kg)		lb (kg)
Water		lb (kg)		lb (kg)		lb (kg)
Coarse Aggregate #1		lb (kg)		lb (kg)		lb (kg)
Coarse Aggregate #2		lb (kg)		lb (kg)		lb (kg)
Fine Aggregate		lb (kg)		lb (kg)		lb (kg)
Total		lb (kg)		lb (kg)		lb (kg)
Air Entrain. Admixture		oz/Cwt (mL/100kg)		oz/Cwt (mL/100kg)		oz/Cwt (mL/100kg)
Chemical Admixture 1		oz/Cwt (mL/100kg)		oz/Cwt (mL/100kg)		oz/Cwt (mL/100kg)
Chemical Admixture 2		oz/Cwt (mL/100kg)		oz/Cwt (mL/100kg)		oz/Cwt (mL/100kg)
Chemical Admixture 3		oz/Cwt (mL/100kg)		oz/Cwt (mL/100kg)		oz/Cwt (mL/100kg)
Total A Bar Solids						
Water Cement Ratio						
Cement Factor						
Temperature		°F (°C)		°F (°C)		°F (°C)
Spread @ T_{IT}		inches (mm)		inches (mm)		inches (mm)
T_{50} @ T_{IT}		seconds		seconds		seconds
VSI @ T_{IT}		---		---		---
J-Ring Value @ T_{IT}		inches (mm)		inches (mm)		inches (mm)
Seg. Resistance @ T_{IT}		%		%		%
Workable Period		h min		h min		h min
Air Content		%		%		%
Unit Weight		lb/ft³ (kg/m³)		lb/ft³ (kg/m³)		lb/ft³ (kg/m³)
Yield		ft³ (m³)		ft³ (m³)		ft³ (m³)

Compressive Strength	Reference	Minimum Cement Factor	Minimum Cement Factor + 1 Bag
1 Day			
3 Days			
7 Days			
14 Days			
28 Days			
28 Days			
28 Days			
Avg. 28 Day Strength			

A.3 Special Provisions for Use of SCC-2 for Stalnaker Run Prestressed Box Beams

A.3.1 Modifications to Standard Specifications

WEST VIRGINIA DEPARTMENT OF TRANSPORTATION

DIVISION OF HIGHWAYS

SPECIAL PROVISION
FOR
STALNAKER RUN PROJECT

STATE PROJECT: _____

FEDERAL PROJECT: _____

SECTION 603 AND 707
PRESTRESSED CONCRETE MEMBERS
SELF-CONSOLIDATING CONCRETE (SCC) FOR BOX BEAMS

603.1 – DESCRIPTION:
ADD THE FOLLOWING PARAGRAPHS TO THIS SUBSECTION:

Class SCC-2 shall be self-consolidating concrete for precast/prestressed applications that will be used for prestressed concrete box beams as designated in the plans. For this project, the Class SCC-2 concrete will be placed in accordance to this section.

603.2.1 – MATERIALS:
ADD THE FOLLOWING PARAGRAPH:

Class SCC-2 concrete shall consist of a homogeneous, flowable mixture of cement, fine aggregate, coarse aggregate, fly ash or ground granulated blast furnace slag, chemical admixtures and water. The mixture proportions shall be such that the Class SCC-2 concrete will resist segregation, bleeding, and the generation of foam during placement, and will need no external compaction or vibration. Establishment of the mixture proportions shall be coordinated with the manufacturers of the admixtures that will be used in the Class SCC-2 concrete.

ADD THE FOLLOWING TO THE ADMIXTURES PORTION OF THE TABLE:

PRECAST / PRESTRESSED CONCRETE MATERIALS	SECTIONS / SUBSECTIONS
Viscosity-Modifying Admixture	707.16

ADD SENTENCE TO END OF FOOTNOTE *:

* For SCC-2, the maximum size of coarse aggregate shall not exceed the dimension described in the previous sentence, or ¾", whichever is smaller. It is permissible to use #67 aggregates as long as 100% passes through a sieve with a ¾" nominal opening size.

603.6 – CONCRETE:

603.6.1 General:

ADD THE FOLLOWING PARAGRAPHS AT THE END OF SUBSECTION:

SCC-2 REQUIREMENTS: Self-consolidating concrete (SCC) exhibits self-leveling capabilities. Creating a successful SCC mix requires combining ingredients to achieve a highly-flowable product that also has the capability to resist dynamic segregation and foaming during placement, and also resist static segregation and bleeding once in place. SCC mix designs are often achieved using high-range water reducing (HRWR) admixtures, and by carefully selecting an aggregate gradation, incorporating high volumes of powder in the mix, through the use of viscosity-modifying admixtures (VMAs), or a combination of any or all of those.

For Class SCC-2 concrete, a combination of admixtures may be used that includes high-range water reducing admixtures, VMAs, air-entraining agents, and retarding admixtures. The admixtures used should all come from the same manufacturer, or measures should be taken to ensure that no adverse reactions would occur from using different sources. Also for SCC-2, it is permitted to use a combination of up to two AASHTO gradations of coarse aggregate to obtain the optimal combination of strength, self-compacting ability, and passing ability.

603.6.2 – Mix Design:

ADD THE FOLLOWING PARAGRAPHS TO THIS SUBSECTION:

The Class SCC-2 concrete mix design shall be submitted for approval at least 45 days prior to use in casting the prestressed box beams for full-scale laboratory testing. Design mixture testing shall be done in accordance with MP 711.03.23, using the criteria for Class H and concrete for specialized overlays. Modifications to MP 711.03.23 for Class SCC-2 concrete include a modification of the test for consistency, and additional tests for passing ability and segregation resistance, and are given as a separate Special Provision. Also, for Class SCC-2 concrete, additional hardened tests are required to ensure adequate performance in prestressed applications; these include creep, shrinkage and modulus of elasticity, freeze thaw resistance, rapid chloride permeability, hardened visual stability index (VSI) and bond tests. Since the fresh and hardened behaviors of Class SCC-2 concrete are highly dependent upon the materials from which it is made, at the discretion of the Engineer, the mix design may be subject to re-acceptance testing as per MP 711.03.23 following a change in the source of any of the materials.

603.6.3 Proportioning of Concrete:

ADD THE FOLLOWING PARAGRAPH:

For prestressed members using Class SCC-2 content, the concrete shall contain a minimum amount of water per sack of cement to obtain satisfactory workability and the specified minimum strength. Allowable mixture proportions for Class SCC-2 concrete are given in Table 603.6.3A. Concrete for all Class SCC-2 concrete members shall be air entrained with a target air content of five percent, and a working tolerance of plus or minus one percentage point will be allowed. When the ambient temperature is 90 ºF (32º C) or higher, a retarding admixture shall be added to the concrete mixture. The Engineer may permit the use of retarding or water-reducing admixture when necessary.

For Class SCC-2 concrete, mix design shall be the responsibility of the beam manufacturer. The target slump-flow value shall be determined by the manufacturer such that complete filling of the formwork occurs without the occurrence of excessive bleeding, segregation or appearance of foam as a result. If necessary, Division-approved VMAs (see Section 707.16) shall be used to control these effects from the increased fluidity of the SCC.

Table 603.6.3A

Class of Concrete	Design 28 Day Compressive Strength	Maximum Water Content	FA / TA	Entrained Air
	Pounds per Square inch	Gal/bag (L/kg) of cement *	%	%
SCC-2	8000	4 ¾ (0.42)	≤ 50%	5

*An equal volume of one type of pozzolanic additive may be substituted for Portland cement up to the maximum amount in Table 603.6.3B. When using pozzolanic additives, volumes of these materials shall be considered as cement for purposes of establishing maximum water content.

TABLE 603.6.3B:

MATERIAL	CLASS OF CONCRETE	QUANTITY
Fly Ash	SCC-2	1 Bag (15%)
Ground Granulated Furnace Slag	SCC-2	2 Bags (30%)
Microsilica	SCC-2	1/2 Bag (8%)

603.6.4 – Sampling and Test Methods:

REPLACE SUBSECTION WITH THE FOLLOWING TABLE:

Sampling Freshly Mixed Concrete	AASHTO T 141
Slump of Hydraulic Cement Concrete	AASHTO T 119
Unit Weight / Yield of Concrete	AASHTO T 121
Air Content of Freshly Mixed Concrete	AASHTO T 152 or ASTM C 173
Compressive Strength of Cylindrical Concrete Specimens	AASHTO T 22
Static Modulus of Elasticity and Poisson's Ratio of Concrete in Compression	ASTM C469
*Making and Curing Concrete Test Specimens in the Field	AASHTO T 23
Slump-Flow of Self-Consolidating Concrete	ASTM C 1611
Passing Ability of Self-Consolidating Concrete using J-Ring	ASTM C 1621
Static Segregation of Self-Consolidating Concrete using Column Technique	ASTM C 1610
Standard Method of Test for Rapid Determination of the Chloride Permeability of Concrete	AASHTO T 277 Or ASTM C 1202
Standard Test Method for Resistance of Concrete to Rapid Freezing and Thawing	AASHTO T 161 Or ASTM C 666
Standard Test Method for Creep of Concrete in Compression	ASTM C 512
Length Change (Drying Shrinkage) of Hardened Concrete	ASTM C 157

* Cylinders shall be manipulated and cured by methods identical to those used in curing the concrete members.

** As modified by special provision for MP 711.02.23.

ADD THE FOLLOWING:

NOTE - In the performance of quality control or acceptance testing of Class SCC-2 concrete, fill cylinder molds, slump flow cones, and air buckets in one lift. Do not vibrate, rod, or tap to consolidate the SCC.

ADD THE FOLLOWING SUBSECTION

603.6.4.1 – Acceptance Testing:

The acceptance testing for Class SCC-2 concrete shall include on-site testing of each batch of Class SCC-2 concrete, or for every 10 yd^3 delivered using central mixed concrete. The acceptance criteria include slump-flow, target spread ± 2" (51 mm) up to a maximum spread of 25" (635 mm), Visual Stability Index (VSI $\leq$ 1.0) , T_{50} (2 to 7 sec.), J-Ring Value $\leq$1.5" (38mm), air content (4% $\leq$ air content $\leqq$ 6%), and casting of three specimens for 28-day compressive strength testing and two for hardened VSI determination. WVU researchers must be present on the day of casting for the purpose of data collection.

603.6.6 – Batching and Mixing:

ADD THE FOLLOWING TO THE END OF THE SECTION:

For Class SCC-2 concrete, all wash water must be completely discharged from the mixing drum prior to addition of any materials for the subsequent batch. When using Class SCC-2 concrete, under no circumstances shall water be used to adjust the consistency of the mix. If it is necessary to adjust the Class SCC-2 concrete's consistency, this shall be done through the addition of chemical admixtures only, and adequate mixing after the adjustment must occur before any Class SCC-2 concrete is discharged into the formwork.

603.6.7 – Placing Concrete:

ADD THE FOLLOWING PARAGRAPH AT THE END OF THE SECTION:

When Class SCC-2 concrete is used, the batching and placement operations should be planned to ensure that casting of the prestressed box beams is completed during the workable period of the concrete established in MP 711.03.23,such that no vibration of the concrete is necessary at any point during construction. Batching, transportation and delivery of the Class SCC-2 shall be planned by the Beam manufacturer such that there is a continuous feed of SCC into the formwork, and therefore, no delay between subsequent layers.

603.7.7 Detensioning:

ADD THE FOLLOWING SENTENCES TO THE END OF PARAGRAPH:

Bond confirmation tests shall be performed by measuring strand pull-in or draw-in after strand release. The average strand draw-in shall not exceed 0.15 inches.

ADD THE FOLLOWING SUBSECTIONS:

603.12.1 – Laboratory Testing of Prestressed Concrete Box Beams

At least 90 days prior to casting of the prestressed concrete box beams to be used for the bridge construction, one prestressed concrete box beams will be produced by the manufacturer and transported to WVU facilities for full-scale testing by the WVU Researchers. This beams will have the same dimensions, material properties and prestressing characteristics as specified in the construction plans for all prestressed concrete box beams. The box beam will use Class SCC-2 concrete that is produced in accordance with the Special Provisions provided. As described in Section 603.12.2 of these provisions, access shall be granted to the beam so that WVU researchers can install instrumentation before casting shall be provided by the beam manufacturer. WVU researchers must be present for the casting of the test beams.

603.12.2 – Instrumentation of Prestressed Concrete Box Beams

Instrumentation of the precast concrete box beams shall be done by WVU Researchers in cooperation with the beam manufacturer. If feasible, instrumentation of the beams will be done while still at the precast plant before transportation to the job site, but instrumentation and data collection will also take place at the location of construction. The beam manufacturer shall provide suitable working space and access to the precast concrete box beams and their components while still at the precast plant, and allow adequate time for such actions as the placement of instrumentation and gages, and the collection of data. Likewise, the Contractor shall provide access to the box beams after delivery to the construction site. The beam manufacturer shall provide any required assistance for implementation of the instrumentation, and uphold the coordination and scheduling of these activities as determined by the Division.

ADD THE FOLLOWING SECTIONS:

707.16 – VISCOSITY MODIFYING ADMIXTURES FOR CONCRETE:

707.16.1-Acceptance Requirements for Approval of Viscosity Modifying Admixtures: Viscosity Modifying Admixtures (VMAs) for concrete shall be tested in accordance with AASHTO M 194, and exhibit the properties described in the next section.

707.16.2-Performance Requirements for VMAs:

707.16.2.1-The effects of using VMAs may vary widely with different types of cement, cement from different mills, aggregate proportions, aggregates from different sources and of different gradation, and changes in water-cement ratio. Therefore, no hydration control admixture shall be used until the concrete of the specified class, designed in accordance with these Specifications and made with the ingredients proposed for use by the Contractor, including hydration control admixtures as specified or permitted under this Specification, is shown to meet the requirements of AASHTO M 194 for water reduction and compressive strength increases at ages 3, 7, and 28 days.

Upon completion of mixing of this trial batch, air content and slump tests (or air content and slump-flow tests in the cases of Classes SCC-1 and SCC-2 concrete) in accordance with Section 601.4.1 shall be performed on the plastic concrete containing the VMA. A test to establish the initial and final times of setting of the concrete mix shall also be performed in accordance with ASTM C403.

Viscosity Modifying Admixtures (VMAs) for concrete, when evaluated according to the test methods and mix design proportions in AASHTO M 194, shall conform to the following physical requirements:

1. For initial and final set times, the allowable deviation of the test concrete from the reference concrete is not more than 1.0 hour earlier or 1.5 hours later.
2. For compressive and flexural strengths, the minimum allowable strength of the test concrete is 90 percent of the reference concrete strength at 3, 7, and 28 days.
3. The maximum allowable length change of the test concrete is 135 percent of the reference concrete. However, if the length change of the reference concrete is less than 0.030 percent, the maximum allowable length change of the test concrete is 0.010 percentage units more than the reference concrete.
4. The minimum allowable relative durability factor of the test concrete is 80 percent.

707.16.2.2-The quantity of admixture used shall adhere to the recommended range provided by the manufacturer at the prevailing temperature.

707.16.3-Certification of Viscosity Modifying Admixtures: When a Contractor proposes to use an approved VMA, the procedure set forth in 707.2.4 shall apply.

707.16.4-Additional Test Requirements for Viscosity Modifying Admixtures (Optional): Either prior to or at any time during construction, the Engineer may require the selected admixture to be tested further to determine its effect on the strength of the concrete. When so tested, the VMA shall meet the requirements specified in 707.16.2.

A.3.2 Modifications to Mix Qualification for Class SCC-2 Concrete

WEST VIRGINIA DEPARTMENT OF TRANSPORTATION

DIVISION OF HIGHWAYS

SPECIAL PROVISION
FOR
STALNAKER RUN PROJECT

STATE PROJECT: _____

FEDERAL PROJECT: _____

MP 711.03.23
MIX DESIGN FOR PORTLAND CEMENT CONCRETE
SELF-CONSOLIDATING CONCRETE FOR PRESTRESSED CONCRETE BOX BEAMS
(SCC-2)

2.1
ADD THE FOLLOWING SENTENCE TO THE END OF THE SECTION:
However, these acceptance criteria shall apply for Class SCC-2 concrete when used for those elements described in Section 603.

3.2
ADD THE FOLLOWING SENTENCE AT THE END OF THE PARAGRAPH:
For Class SCC-2 concrete, use Attachment 1b.

3.2.1
ADD THE FOLLOWING SENTENCE AT THE END OF THE PARAGRAPH:
For Class SCC-2 concrete, use Attachment 2b.

ADD THE FOLLOWING SUBSECTION
3.2.2
Viscosity-modifying admixtures (VMA) may be used for Class SCC-2 concrete with approval from the Division. To do this, a written request must be filed that contains the following information:

6. Name and contact information for the manufacturer of the admixture.
7. Name and designation of the product that is to be evaluated.
8. Documentation that includes results of testing that shows adherence to Section 707.16 of the Special Provisions for the WVDOT Standard Specifications.
9. Documentation showing that the tests mentioned above were completed in a Division approved laboratory.
10. A materials safety data sheet for the product.

For Class SCC-2 concrete, approval of the VMA is limited the particular mix design for which it will be used, and acceptance is on a project-to-project basis. Re-approval of the product shall be necessary if there are changes in the SCC materials or mix designs.

3.3
REPLACE THE FIRST SENTENCE WITH THE FOLLOWING:
All classes of the concrete (except Class H, Class SCC-2, and concrete for specialized overlays) for the proposed design shall be batched in at least four separate batches.

3.3.1
REPLACE AS FOLLOWS:
Class H concrete, Class SCC-2 concrete, and concrete for specialized overlays (as set forth in Section 679 of the Specifications) for the proposed design shall be batched in at least two separate batches.

The batches for Class SCC-2 concrete shall be made to comply with the construction plans. The rapid chloride permeability test (in accordance with AASHTO T 277) and dry shrinkage test (in accordance with ASTM C 157) specified in Section 603.6.2 shall be performed on each of these batches. Also, for Class SCC-2 concrete for precast/prestressed applications, testing for creep, shrinkage, modulus of elasticity, freeze thaw resistance, hardened visual stability index (VSI) and bond with steel strand will be required.

3.3.2
ADD THE FOLLOWING AT THE END OF THE FIRST PARAGRAPH:
This batch will not be necessary for Class SCC-2 concrete.

3.4
REPLACE WITH THE FOLLOWING PARAGRAPHS:
Each batch of concrete shall be tested in the plastic state for air, consistency and yield. Each batch shall be adjusted as necessary to produce a concrete having plastic properties within a reasonable laboratory working tolerance. The following tolerances shall be used as a guide for all classes of concrete, except SCC-2: Air content, ± ½ %; Consistency, ± ½" (± 12 mm) of slump or ball penetration; Yield, ± 2%. See Subsection 3.4.1 for testing criteria of Class SCC-2 concrete.

ADD THE FOLLOWING SUBSECTION
3.4.1
For Class SCC-2 concrete, testing will begin at the time immediately after the mixing sequence is completed, T_0. For the test batches, the spread shall be in the upper one-half of the acceptable working range given in the construction plans. The following tolerances shall be used as a guide for air, consistency and yield of SCC-2 at T_0: Air content, 4.5 % to 5.5 %; Consistency (ASTM C1611), slump-flow target spread as proposed by manufacturer up to maximum allowable spread (target plus 1" (51mm), or 25" (635 mm), whichever is smaller), a T_{50} time of 2 to 7 seconds, and a Visual Stability Index (VSI) of not greater than 1; Yield, ± 2%. SCC-2 should also meet the following tolerances: Passing Ability (ASTM C1621), J-Ring Value not greater than 1.0" (51 mm); Segregation Resistance (ASTM C1610), less than 12% segregation by column technique.

For Class SCC-2 concrete, consistency and passing ability tests of all batches will be conducted for each batch at 0, 30, 60 and 90 minutes after batching, and then every 30 minutes thereafter until the spread falls below 15". Segregation resistance tests of all batches will also be conducted at 60 minutes

after batching. Time elapsed after batching for all tests except the segregation resistance test will be recorded upon completion of each test as T_0, T_{30}, T_{60}, T_{90}, etc., until T_F. Time elapsed after batching for the segregation resistance tests will be recorded upon placement of the concrete into the column apparatus as T_0 and T_{60}.

3.4.2

For each time of testing of the consistency and the passing ability described in Section 3.4.1, the slump-flow and j-ring values will be plotted versus the time after batching. From this, the "workable period," defined as the amount of time after batching during which the SCC has acceptable fresh properties, will be found through linear interpolation of the data by determining the time at which either the spread falls below the lower acceptance limit (target slump-flow minus two inches (51 mm)), or the J-ring value exceeds the acceptance limit (1.5" or 38mm).

3.5

REPLACE WITH THE FOLLOWING:

When the properties of a concrete batch have been established within acceptable limits, seven standard concrete cylinders shall be made from each batch produced in Section 3.3 (or 3.3.1) and 3.3.2 and tested in compression at the following ages: one cylinder at age 24 hours ± 4 hours (the exact age to the nearest hour at time of test shall be noted on the report); one cylinder at age 3 days; one cylinder at age 7 days; one cylinder at age 14 days; and three cylinders at age 28 days. For Class SCC-2 concrete batches, seven more cylinders will be cast to undergo modulus of elasticity testing according to the same schedule as the compression tests. Three additional cylinders shall be cast for later assessment of the hardened Visual Stability Index of the Class SCC-2 concrete to ensure that no excessive segregation or air migration occurs.

For determination of bond with prestressing strands, strand bond tests shall be run for the SCC-2 mix and the conventional prestressed concrete mix used in this project. This comparison is to verify that the bond with SCC is comparable to, or better than, the conventional mix design with equal strand. Bond characteristics of the concrete to the strands shall be determined by the Moustafa test [1].

Table 3.5 lists the number, size, and testing schedule for the creep, shrinkage, freeze-thaw, and rapid chloride permeability tests. All specimens using Class SCC-2 concrete for purpose of testing compressive strength, creep, shrinkage, modulus of elasticity, freeze thaw resistance, rapid chloride permeability, hardened visual stability index (VSI) and bond with prestressing steel tendons shall be cast in a single layer with no rodding or vibration. The values of the physical properties of each mix shall be the average of the physical properties established in each of the two batches produced in Section 3.3 (or 3.3.1). These values shall be listed in Attachment 3 for all concrete classes except SCC-2, and in Attachment 3b for Class SCC-2.

TEST	TESTING STANDARD	# OF SPECIMENS	SPECIMEN SIZE	LOAD MAGNITUDE	AGE AT INITIATION OF LOADING
Creep	ASTM C 512	6	6" (152 mm) x 12" (305 mm) cylinders	40% of Compressive Strength	2 days
Drying Shrinkage	ASTM C 490	3	3" x 3" x 10"	Air Exposure	7 days
Rapid Chloride Permeability	AASHTO T277	3	4" (102mm) x 2" (51 mm) cylinders	60 ± 0.1 V	90 days

Freeze-Thaw	AASHTO T161	6	3" x 4" x 16"	(freeze-thaw cycles)	14 days

3.5.1

REPLACE WITH THE FOLLOWING:

The following properties of each batch of concrete produced in Sections 3.3 (or 3.3.1) and 3.3.2 for all concrete types, excluding SCC-2, shall be listed in Attachment 2: A-Bar of Total Solids, Consistency, Air Content, Unit Weight & Yield, Water / Cement Ratio, and Temperature. For SCC-2, the following properties, and appropriate times for each batch produced shall be listed in Attachment 2b: A-Bar of Total Solids, Consistency, Passing Ability, Segregation Resistance, Air Content, Unit Weight & Yield, Water / Cement Ratio, and Temperature.

ADD THE FOLLOWING SUBSECTION:

4.4

In addition to the compressive strength requirements for Class SCC-2 concrete, the following criteria also must be met for approval of the mix design:

	90-day Permeability Test Results	Freeze-Thaw Durability Factor	Drying Shrinkage	Compressive Creep	28-day Modulus of Elasticity
	(coulombs)	After 300 cycles	%	%	ksi (GPa)
SCC-2	1500	80	Per Design Requirements (See Notes)	Per Design Requirements (See Notes)	Per Design Requirements (See Notes)

ADD THE FOLLOWING SUB-SECTION:

5.2.3

Although a Class SCC-2 concrete may meet the necessary strength requirements and exhibit acceptable fresh properties at the time of initial testing, the Division could require a re-design of the mix based on other criteria, such as insufficient retention of the slump flow for the mix, poor hardened VSI results, excessive foam buildup, etc.

5.3

The submittal for a proposed mix design shall include completed copies of Attachments 1 and 3 (or 1b and 3b for SCC-2). It shall also include a completed copy of Attachment 2 (or 2b) for the reference batch, a completed copy of Attachment 2 (or 2b) for each of the batches at the minimum cement factor, and a completed copy of Attachment 2 (or 2b) for each of the batches at the minimum cement factor plus one bag (when applicable). All pertinent information supporting these attachments and pertaining to the information in them should be submitted also.

REFERENCE:

[1] Logan, D. "Acceptance Criteria for Bond Quality of Strand for Pretensioned Prestressed Concrete Applications," *PCI Journal*, March-April 1997, pp. 52-90.

A.3.2.1 Attachment 1(b) – Class SCC-2 Concrete Materials

MP 711.03.23
ORIGINAL ISSUANCE: APRIL 1971
REVISED: DRAFT COPY
ATTACHMENT 1b (SCC-2)

Source: _____

Source Location: _____

Design Laboratory: _____

Class of Concrete: _____

Date: _____

Cementitious Material Data		
Data	Cement	Pozzolan
Name		
Type		
Source		
Source Location		
Specific Gravity		

Admixture Data				
Data	Air Entrainment	Additional Admixture 1	Additional Admixture 2	Additional Admixture 3
Name				
Type				
Source				
Source Location				

Aggregate Data			
Data	Coarse Aggregate #1	Coarse Aggregate #2	Fine Aggregate
Class/Size			
Type			
Source			
Source Location			
Specific Gravity			
A-Bar			
Absorption			
Fineness Modulus			
Unit Weight			

A.3.2.2 Attachment 2(b) – Class SCC-2 Concrete Trial Batch Report

MP 711.03.23
ORIGINAL ISSUANCE: APRIL 1971

REVISED: DRAFT COPY
ATTACHMENT 2b (SCC-2)

Souce: _____ Class of Concrete: _____

Souce Location: _____ Date: _____

Design Laboratory: _____

Check The Appropriate Box For Designated Batch:	Reference Batch	Minimum Cement Factor		Minimum Cement Factor + 1 Bag		Additional Batch
		Batch 1	Batch 2	Batch 1	Batch 2	

Material	Mass	Units	Volume		Units
Cement		lb (kg)			ft^3 (m^3)
Pozzolan 1		lb (kg)			ft^3 (m^3)
Latex Admixture		lb (kg)	gal (L)		ft^3 (m^3)
Water		lb (kg)	gal (L)		ft^3 (m^3)
Air Content, by volume		lb (kg)			ft^3 (m^3)
Coarse Aggregate 1		lb (kg)			ft^3 (m^3)
Coarse Aggregate 2		lb (kg)			ft^3 (m^3)
Fine Aggregate		lb (kg)			ft^3 (m^3)
Total		lb (kg)			ft^3 (m^3)
Air Entraining Admixture		oz/Cwt (mL/100kg)			fl. Oz. (mL)
Chemical Admixture 1		oz/Cwt (mL/100kg)			fl. Oz. (mL)
Chemical Admixture 2		oz/Cwt (mL/100kg)			fl. Oz. (mL)
Chemical Admixture 3		oz/Cwt (mL/100kg)			fl. Oz. (mL)

Mixture Test Data							
Time	Slump Flow	T50	VSI	J-Ring	Seg. Resist.	Concrete Temperature	
T_0							
T_{30}							
T_{60}							
T_{90}							
T_F							

Additional Mixture Test Data							
	Yield	W/C Ratio	Cement Factor	Unit Weight	Air Content	A-bar Tot. Sol.	
T_0							

Compressive Strength, psi (Mpa)							
Specified Test Age:	24 Hours +/- 4 Hours	3 days	7 days	14 days	28 days	28 days	28 days
Actual Test Age (hours)							
Compressive Strength							

Shrikage Testing						
Test Age:	4 Days	7 Days	14 Days	28 Days	56 Days	90 Days
% Length Change:						

Rapid Chloride Permeability Testing	
Age of Specimen at Time of Test (days):	Total Adjusted Charge Passed (coulombs):

A.3.2.3 Attachment 3(b) – Summary of Class SCC-2 Concrete

MP 711.03.21
ORIGINAL ISSUANCE: APRIL 1969
REVISED: DRAFT COPY
ATTACHMENT 3b (SCC-2)

SUMMARY

Source:	
Source Location:	
Design Laboratory:	
Class of Concrete:	
Date:	

	Reference		Minimum Cement Factor	
Material	Mass	Units	Mass	Units
Cement		lb (kg)		lb (kg)
Pozzolan 1		lb (kg)		lb (kg)
Water		lb (kg)		lb (kg)
Coarse Aggregate #1		lb (kg)		lb (kg)
Coarse Aggregate #2		lb (kg)		lb (kg)
Fine Aggregate		lb (kg)		lb (kg)
Total		lb (kg)		lb (kg)
Air Entrain. Admixture		oz/Cwt (mL/100kg)		oz/Cwt (mL/100kg)
Chemical Admixture 1		oz/Cwt (mL/100kg)		oz/Cwt (mL/100kg)
Chemical Admixture 2		oz/Cwt (mL/100kg)		oz/Cwt (mL/100kg)
Chemical Admixture 3		oz/Cwt (mL/100kg)		oz/Cwt (mL/100kg)
Total A Bar Solids				
Water Cement Ratio				
Cement Factor				
Temperature		°F (°C)		°F (°C)
Spread @ T_{fT}		inches (mm)		inches (mm)
T_{50} @ T_{fT}		seconds		seconds
VSI @ T_{fT}				
J-Ring Value @ T_{fT}		inches (mm)		inches (mm)
Seg. Resistance @ T_{fT}		%		%
Workable Period		h min		h min
Air Content		%		%
Unit Weight		lb/ft³ (kg/m³)		lb/ft³ (kg/m³)
Yield		ft³ (m³)		ft³ (m³)

	Compressive Strength			Mod. of Elasticity	
	Reference	Min. Cement Factor		Reference	Min. Cement Factor
1 Day			1 Day		
3 Days			3 Days		
7 Days			7 Days		
14 Days			14 Days		
28 Days			28 Days		
28 Days			28 Days		
28 Days			28 Days		
Avg. 28 Day Strength			Avg. 28 Day Strength		

APPENDIX B – Test Methods Used for Hardened Property Assessment

B.1 RCPT Testing

Rapid Chloride Permeability Testing (RCPT) is done in accordance with ASTM C1202 to determine the extent to which non-uniformity of constituents within the member could potentially affect the durability of the concrete at different locations. The specimen preparation, test methodology and results of such testing will be discussed in this section.

The chloride permeability of concrete is determined in accordance with ASTM C1202 using a 2 inch (50 mm) thick, 4 inch (100 mm) diameter disc cut from the 4 x 8 inch (100 x 200 mm) cylinder prepared in the laboratory and vacuum saturated under a pressure less than 1 mm-Hg. The disc specimens are fixed between two cells containing ionic solutions. One of the cells is filled with 0.3N sodium hydroxide (NaOH) solution and the other with 3.0% sodium chloride (NaCl) solution. A 60 Volt DC was applied between the two cells. The resistance of concrete to chloride ion penetration is represented by the total charge passed in coulombs during a test period of 6 hours.

A schematic of the RCPT experimental set-up, as well as a picture of the actual equipment used, is shown in Figure B-1. The RCPT specimen is placed between two acrylic cells, one of the acrylic cells is filled with 250 ml of 0.3 mole/L of NaOH solution and another cell was with 250 ml of 0.52 mole/L (3%) NaCl solution. Two mesh electrodes (10 cm diameter, #20 mesh brass screens) are placed on two sides of the specimen in such a way that the electrical field is applied primarily across the test specimen. The cells are connected to the 60 V DC power source. The cathode is connected to the negative pole and the anode is connected to the positive pole of the power supply. The electrical current is measured and recorded at 5 minutes intervals for 6 hours using a data logger.

The electrical current passed through the specimen in 6 hours is measured and the total charge passed, Q_T is determined using the following equation:

$$Q_T = \int_0^{360} I(t)dt \tag{19}$$

where $I(t)$ is the time-dependent total electrical current and t is the elapsed time in minutes. The total charge passed in 6 hours is used to specify the ability of concrete to resist chloride ions penetration.

After 6 hours of testing, the specimen is removed from the cells and then split into two pieces for the silver nitrate ($AgNO_3$) spray test. The silver nitrate ($AgNO_3$) spray test method is known as a colorimetric method, based upon the reaction of free chlorides with a silver nitrate solution sprayed onto the cross section of a freshly split concrete sample. The silver nitrate reacts with unbound chlorides and produces silver chloride on the surface of the split-open cross-section.

After splitting into two pieces, the newly-exposed surface of the specimen is sprayed immediately with a 0.1 M silver nitrate solution to determine the depth of penetration of chloride ions. The average chloride penetration depth, x_d, is defined as the distance between the chloride-exposed surface and the borderline between the chloride-contaminated and chloride-free zones. This value is used to calculate the non-steady-state chloride migration coefficient (D_{nssm}) as shown [NT BUILD 492]:

$$D_{nssm} = \frac{RT}{zFE} \cdot \frac{x_d - \alpha\sqrt{x_d}}{t} \quad \textbf{(20)}$$

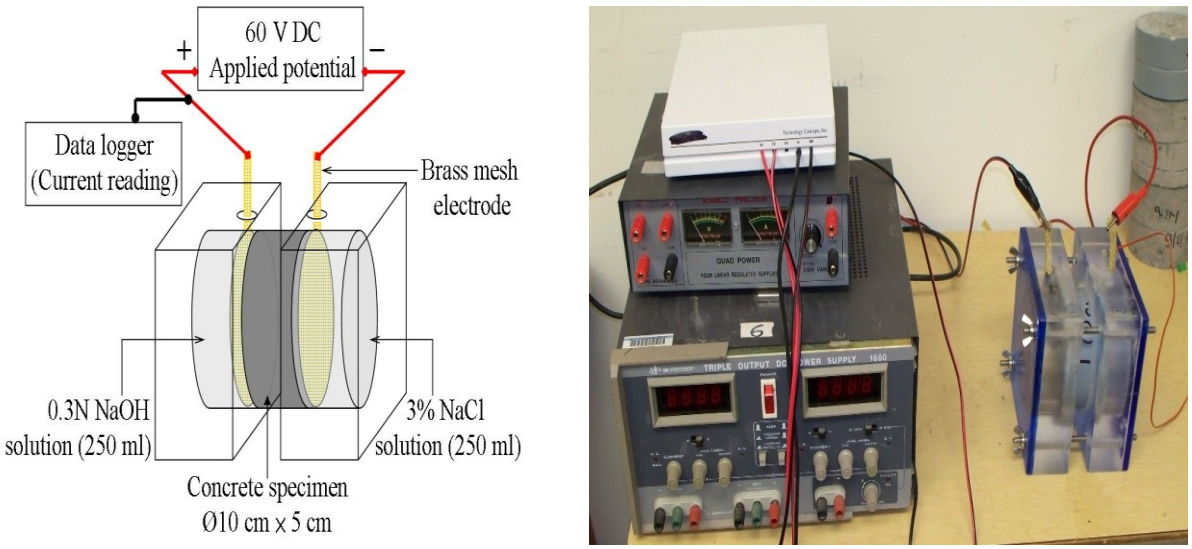

Figure B-1 Schematic and actual RCPT setup.

B.2 Freeze-Thaw Durability Testing

3”x4”x16” prisms are used for the purpose of freeze-thaw testing in accordance with ASTM C666. These specimens are water cured until the start of testing. Testing follows Procedure A of ASTM C666 (samples remained surrounded by water throughout freezing and thawing), and each specimen is placed in its own container such that it can be surrounded by the prescribed amount of water.

The chamber used for testing is a Z-16 Test Chamber from Cincinnati Sub-Zero. The specimens are placed into their containers and covered with the appropriate amount of water prior to initiating the freeze-thaw cycles. Additionally, one 3”x4”x16” specimen instrumented with an internal thermocouple, housed in its own water-filled container, is added to each group to ensure the appropriate temperature ranges are achieved. A sample of the 4-hour ambient temperature cycles used to achieve the desired internal temperatures can be seen in Figure B-2.

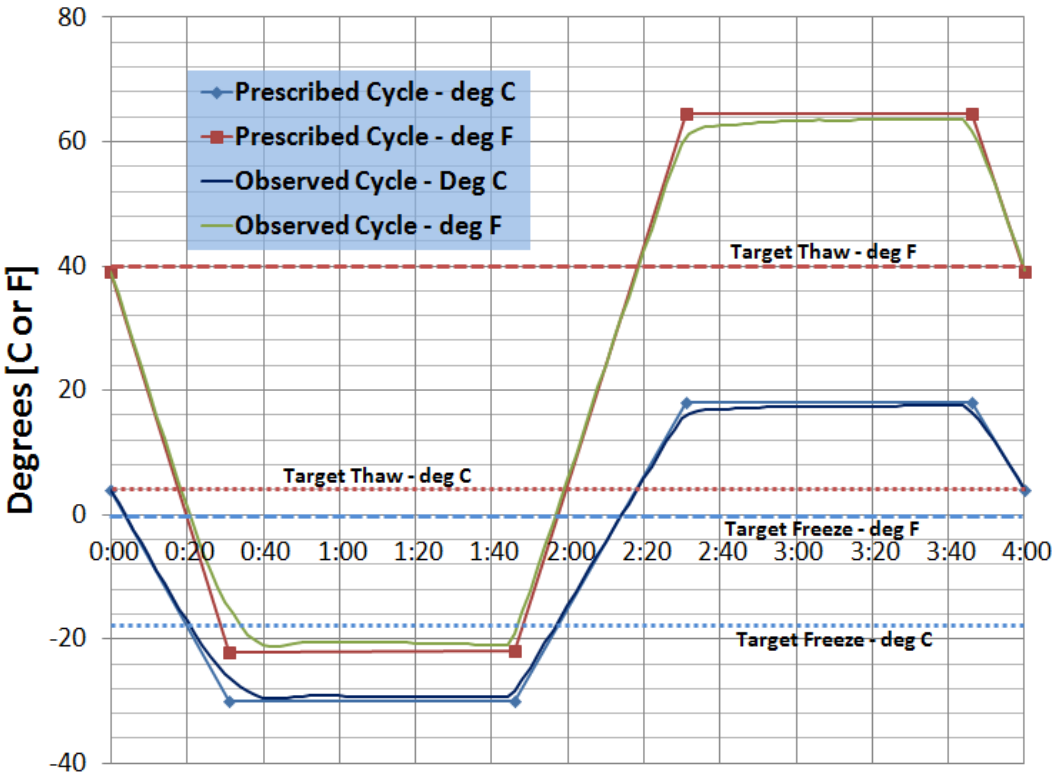

Figure B-2 Ambient temperature cycle used to achieve target core temperatures for freeze-thaw testing.

Periodic testing is done on specimens, starting after 30 cycles, and every 30 cycles thereafter until 300 cycles is reached. For the time between completion of the freeze-thaw cycles and the conclusion of testing, the Z-16 Chamber is set to maintain a constant temperature of 3^0C so the specimens are tested under consistent conditions. The specimens are removed one-by-one for their individual testing and promptly replaced to avoid drying or a significant increase in temperature. Measurements taken for each specimen at each time of testing included:

- Mass
- All Outer Dimensions
- Fundamental Longitudinal Frequency, per ASTM C215 (driver / pickup method)
- Fundamental Transverse Frequency, per ASTM C215 (impact /accelerometer method)

The test apparatuses and procedures used for determining the Fundamental Longitudinal and Transverse Frequencies are shown in Figure B-3 and Figure B-4, respectively.

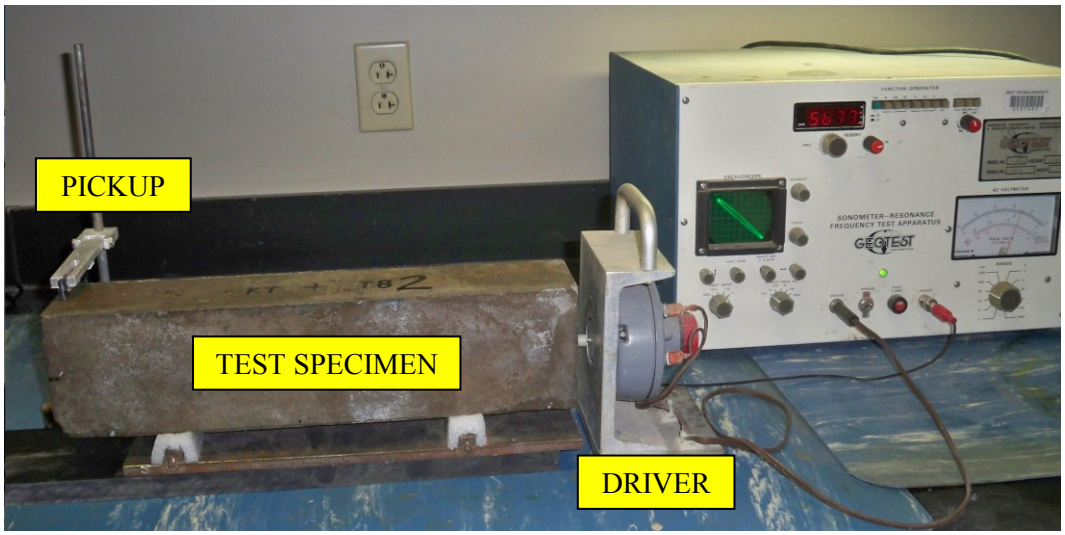

Figure B-3 Test setup for measurement of fundamental longitudinal frequencies of freeze-thaw specimens.

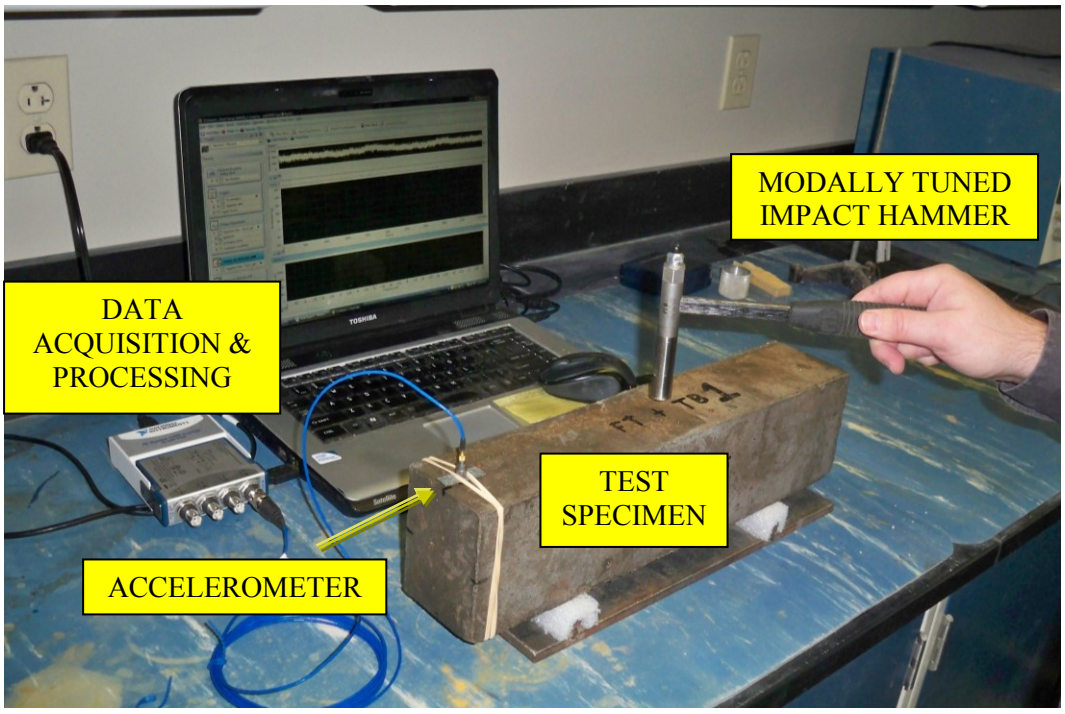

Figure B-4 Test setup for measurement of fundamental transverse frequencies of freeze-thaw specimens.

The relative dynamic modulus of elasticity is calculated based on ASTM C666 using the following relationship:

$$P_c = \left({n_1}^2 / {n^2}\right) \times 100 \quad \textbf{(21)}$$

where P_c is the relative dynamic modulus after c cycles, n is the fundamental frequency at 0 freeze-thaw cycles, and n_1 is the fundamental frequency after c freeze-thaw cycles. The fundamental frequencies used for these calculations were those measured using the respective longitudinal or transverse technique.

Alternate Specimens for Optional Length Change Measurements

Per ASTM, 3”x3”x11” specimens can also be used for freeze-thaw testing. In this case, the specimens are outfitted with gage studs at either end to allow for precise measurement of the specimen’s length. Curing conditions and storage of these specimens should be identical to the larger 3”x4”x16” specimens. Since the containers used during the freeze-thaw cycles were designed for 3”x4”x16” specimens, small concrete blocks are placed at the end of the smaller specimens in order to reduce the amount of water surrounding the specimen, as can be seen in Figure B-5.

Figure B-5 Configuration of 3"x3"x11" specimens with blocks during freeze-thaw testing.

These specimens are tested at the same frequency as the larger 3”x4”x16” freeze-thaw specimens, with minor modifications. Aside from having a slightly smaller base for transverse testing, the length change of the 3”x3”x11” specimens was measured using a length comparator (Figure B-6)**Error! Reference source not found.Error! Reference source not found.**. The percent elongation of each of the Shrinkage specimens was calculated as:

$$\%\, Elongation = \frac{L - L_0}{L_0} \times 100 \qquad \textbf{(22)}$$

Figure B-6 Length comparator with reference bar, as used for shrinkage and elongation monitoring.

B.3 Ultrasonic Pulse Velocity Testing

The ultrasonic equipment that is used for the pulse velocity testing includes an Ultran BP-9400A ultrasonic burst pulser, an Ultran BR-640A broadband receiver, and two Ultran WD100-0.125 transducers. Signals are monitored using a Tektronix 2024B oscilloscope, which can be controlled externally via a laptop computer running the Tektronix Edition of National Instruments' LABVIEW SignalExpress software. In addition to controlling the oscilloscope functions, this software is also used to record signals directly to the computer's hard drive. A schematic of the setup can be seen in Figure B-7.

The sensors used are dry-coupling, direct contact transducers that produce shear waves and have a frequency of 125 kHz. The pulser is limited to producing single, repetitive bursts in the shape of square waves.

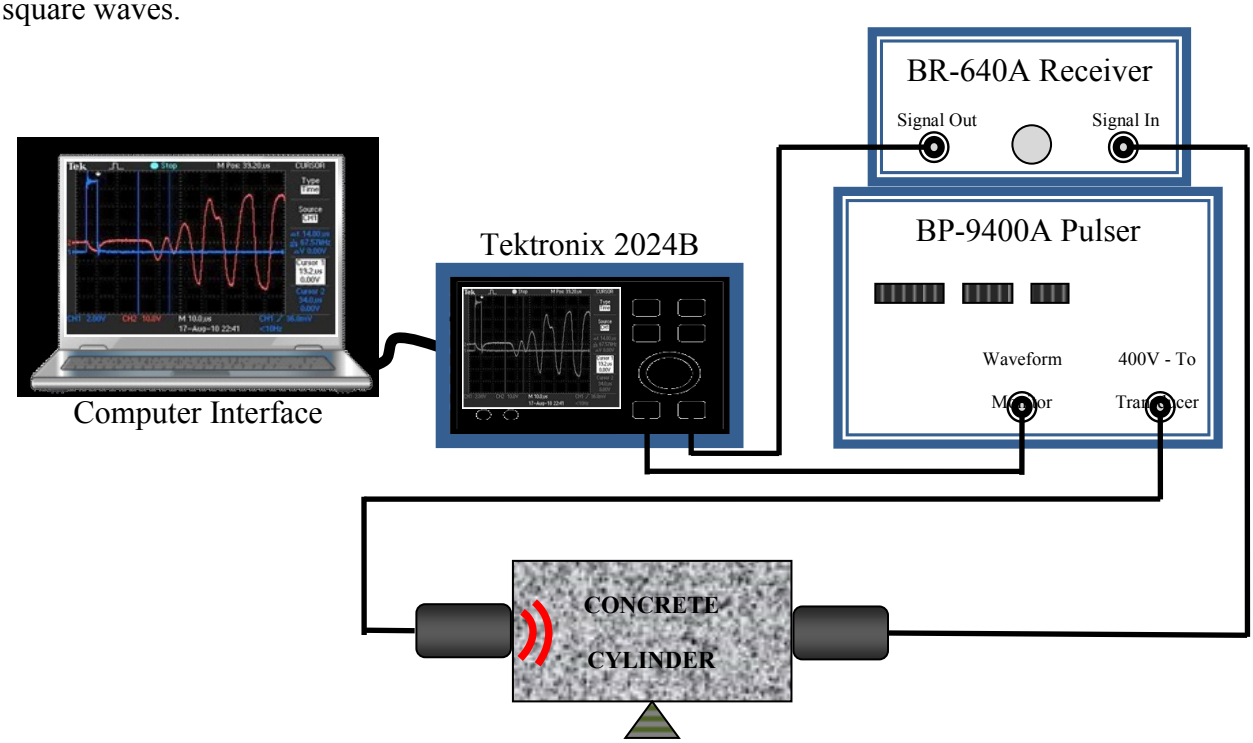

Figure B-7 Setup used for ultrasonic pulse velocity testing.

The pulse velocity of compressive waves, V_P, can simply be calculated as the proportion of the time of flight of compressive waves as they travel through a medium to the distance that the waves travel within that medium. To correctly determine V_P, it is not only necessary to be able to precisely determine the arrival time of the wave, but it is also critical to be able to accurately quantify the delay time of the system used for testing. Accounting for delay time of the system, V_P can be represented as:

$$V_P = \frac{t_t - t_d}{d} \tag{23}$$

where t_t is the total time observed from the initiation of the pulse to the first arrival, t_d is the adjustment to the time of flight of the signal due to the system delay, and d is the distance between transducer faces, as measured for each specimen using a sliding digital caliper. The delay time is determined by holding the sensors face to face and transmitting multiple 500ns pulses; it was determined that the average delay time for this particular system was 6.09 μs.

Since it is necessary to precisely determine the distance between transducers for each sample in order to obtain an accurate determination of the pulse velocity, a sliding digital caliper is used to take multiple measurements for each specimen. The caliper, seen in its entirety in Figure B-8, can measure with a precision of 0.01 mm. However, since the depth of the slide is not adjustable on this apparatus, it is not possible to measure directly at the center of the specimens. Therefore, each specimen is measured at four different points, each approximately ¾" outside of the center of the specimen, with the average of these readings taken as the distance between transducers.

Figure B-8 Sliding digital caliper used to measure length of core specimens.

Once the delay time and length of each specimen is established, the total time to arrival is determined at least three times for each specimen. To do this, the transducers are manually held in place against the cylinder ends during testing, with both points of contact being reset between each data collection. Since these are dry-coupling transducers, no ultrasonic gel is used for the contact. The pulse width used for this portion of the investigation is 1 μs. The initial arrival of a typical signal from this testing, along with the timing of the burst, can be seen in Figure B-9.

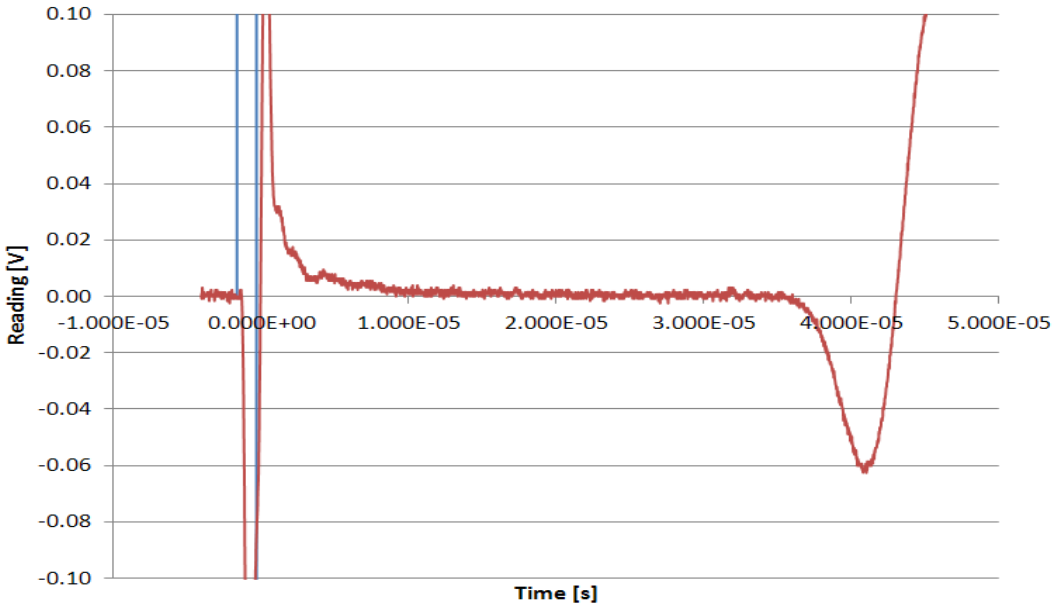

Figure B-9 Signal obtained after transmission of 1μs pulse through core specimen.

ASTM defines the relationship between pulse velocity, V, and Dynamic modulus of elasticity of concrete, E, as:

$$E = \frac{V^2 \cdot \rho \cdot (1+\mu)(1-2\mu)}{(1-\mu)} \quad \textbf{(24)}$$

where ρ is the density and μ is the dynamic Poisson's Ratio [ASTM C597—09]. To compare the elastic behavior of the concrete at different locations, the densities are calculated for each specimen using measured weights and average top and bottom diameters, and the dynamic Poisson's Ratio, μ, is assumed to be constant for all specimens.

B.4 Compressive Creep of Concrete

Creep behavior for an individual time of loading is assessed using a total of 6 – 6”x12” cylinders. In the case of steam cured concrete, these specimens would be steam cured for the appropriate number of days prior to removal from their molds. After removal of each specimen from the molds, two sets of DEMEC points (stainless steel contact points) are attached with a gage length of 8 inches on opposite sides of each specimen, and the specimens are capped with a sulphur-graphite compound on both ends. Two-part, 5 minute epoxy is used to glue the DEMEC points onto the concrete surface.

Three specimens are loaded for creep measurements about one day after application of the DEMEC points, and three specimens are kept in a non-loaded state beside the creep frame for shrinkage measurements. All cylinders that are loaded are placed into a creep frame capable of sustaining the applied load, and stored in the WVU Laboratory (indoor) with an ambient temperature of 21±1°C and relative humidity of 15±4 %; the non-loaded specimens were kept adjacent to the frames in the same ambient conditions.

The creep load frame consists of two 14”x14”x1.5” plates and two 16”x16”x1.5” steel plates (upper and lower jack plates and upper and lower base plates, respectively), four 7/8-inch diameter by 6-foot long fine threaded (7/8-9 Grade B7) high strength tension bars, 5 pairs of compression springs with each pair stacked in parallel. The creep apparatus is shown in Figure B-10. The five pairs of disk springs placed between the lower and upper base plates of the creep frame helped to maintain the load as the cylinders shortened due to creep and shrinkage. A single-acting spring return low height hydraulic cylinder with capacity of 100 kips was used together with a 200-kip capacity load cell and a hydraulic hand pump to load the specimens.

Figure B-10 Creep frame used for compressive creep testing of 6”x12” beam concrete specimens.

The initial gage lengths are measured on both sides of each cylinder before loading. The gage lengths of the specimens were measured using a Whittmore Gage, which has a dial indicator with 0.0001 inch graduations and a maximum travel distance of 0.3 in. A reference bar is used to eliminate temperature affects on the readings in order to ensure consistency of measurements. The specimens are carefully stacked in series before applying an axial compression force. The frames are loaded to the desired stress (f_{cci}) using a manual hydraulic jack. The four nuts above the lower jack plate are then secured such that the load would be maintained by the creep frame, and the hydraulic pressure can then be removed.

After the loading, each gage line is measured to determine initial elastic deformation of the three loaded creep cylinders. Then, at periodic time intervals, the gage lengths of the creep and shrinkage specimens are recorded. When possible, all of the measurements are made by the same operator to minimize the minor variability in the readings that may result from applying a different amount of pressure on the gage.

The initial elastic strains and the shrinkage strains obtained from the corresponding non-compressed cylinders are subtracted from the total strains to obtain shrinkage-compensated creep strain measurements, correlating to the compression-induced deformation of the specimens after loading.

The creep coefficients, defined as the ratio of creep strains to the initial elastic strains (when the cylinder is loaded for the first time), are also computed for each cylinder separately and then averaged for each concrete type.

The specific creep is sometimes used to correlate the creep behaviors of concrete that are tested at different stress levels. This is calculated by dividing the creep strain by the amount of compressive stress that was applied to the specimens.

APPENDIX C – Strain Data from Static Loading of Laboratory Beam

C.1 Strains from Constant Moment Zone Gages

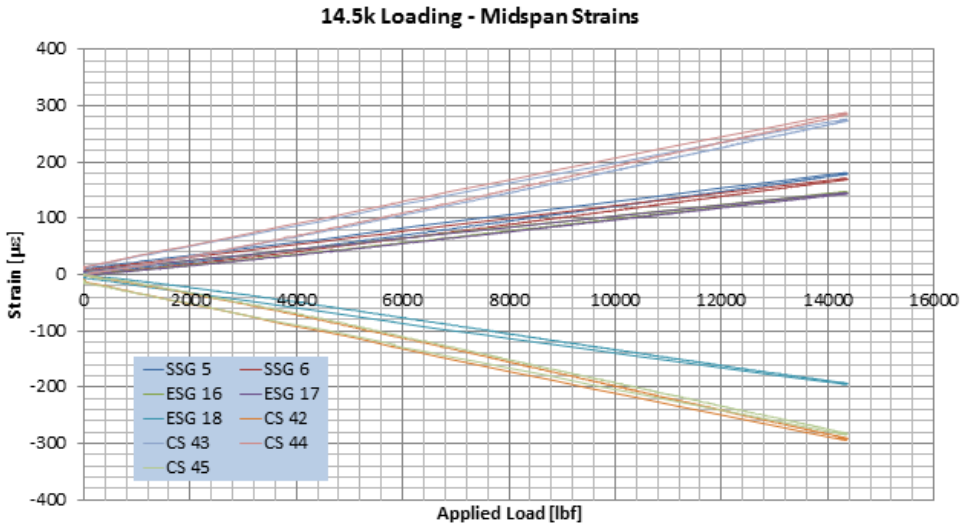

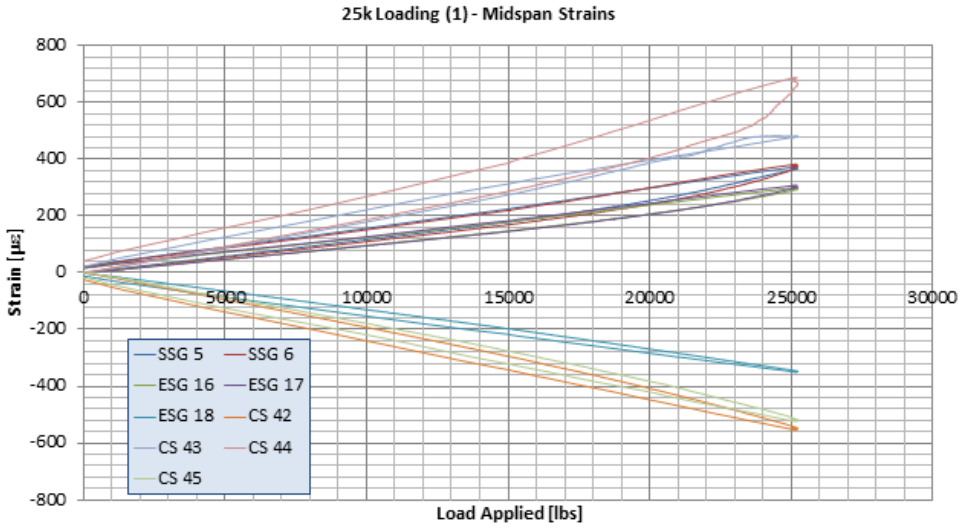

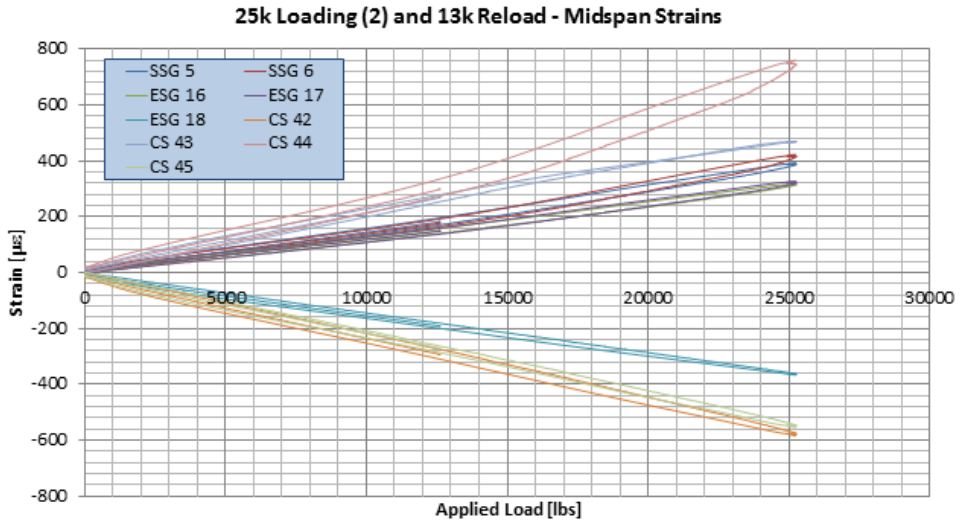
25k Loading (2) and 13k Reload - Midspan Strains
SSG 5
SSG 6
ESG 16
ESG 17
ESG 18
CS 42
CS 43
CS 44
CS 45
Strain [με]
Applied Load [lbs]

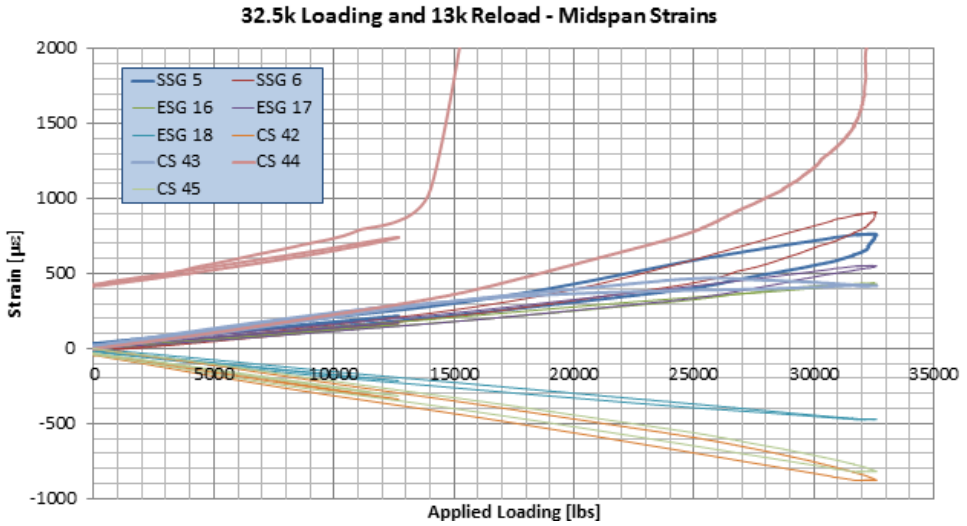
32.5k Loading and 13k Reload - Midspan Strains
SSG 5
SSG 6
ESG 16
ESG 17
ESG 18
CS 42
CS 43
CS 44
CS 45
Strain [με]
Applied Loading [lbs]

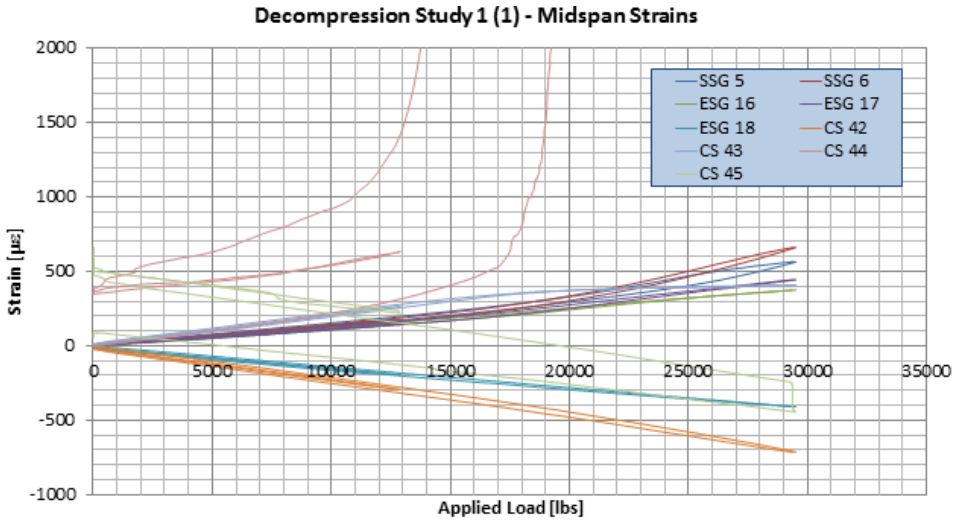
Decompression Study 1 (1) - Midspan Strains
SSG 5
SSG 6
ESG 16
ESG 17
ESG 18
CS 42
CS 43
CS 44
CS 45
Strain [με]
Applied Load [lbs]

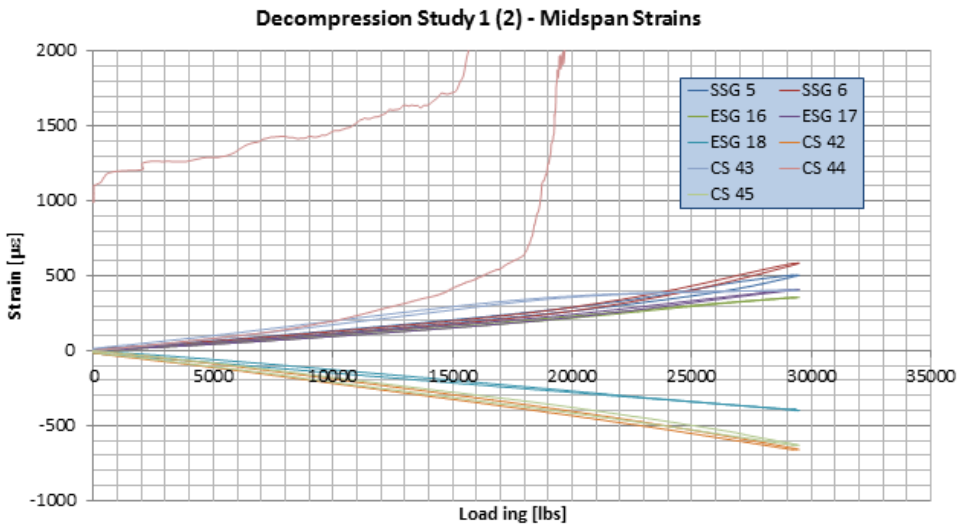
Decompression Study 1 (2) - Midspan Strains
SSG 5
SSG 6
ESG 16
ESG 17
ESG 18
CS 42
CS 43
CS 44
CS 45
Strain [με]
2000
1500
1000
500
0
-500
-1000
0
5000
10000
15000
20000
25000
30000
35000
Load ing [lbs]

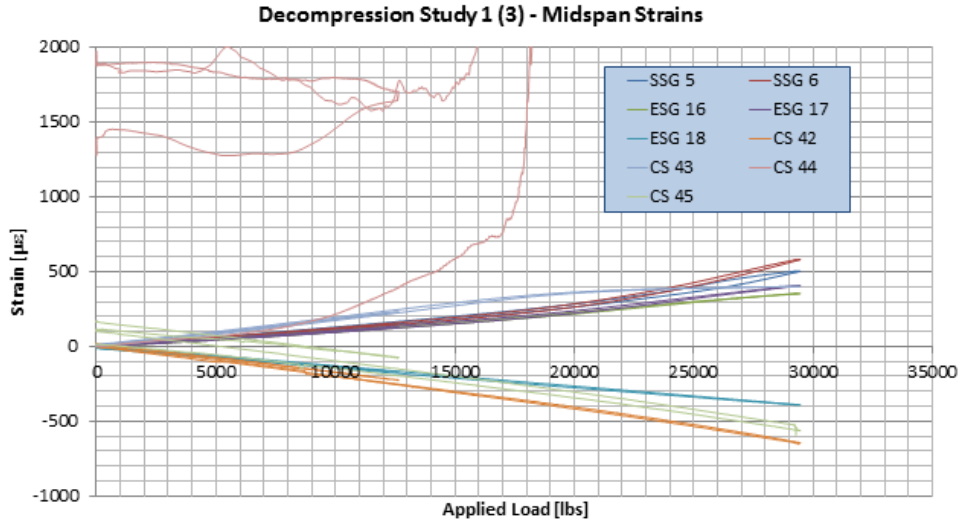
Decompression Study 1 (3) - Midspan Strains
SSG 5
SSG 6
ESG 16
ESG 17
ESG 18
CS 42
CS 43
CS 44
CS 45
Strain [με]
2000
1500
1000
500
0
-500
-1000
0
5000
10000
15000
20000
25000
30000
35000
Applied Load [lbs]

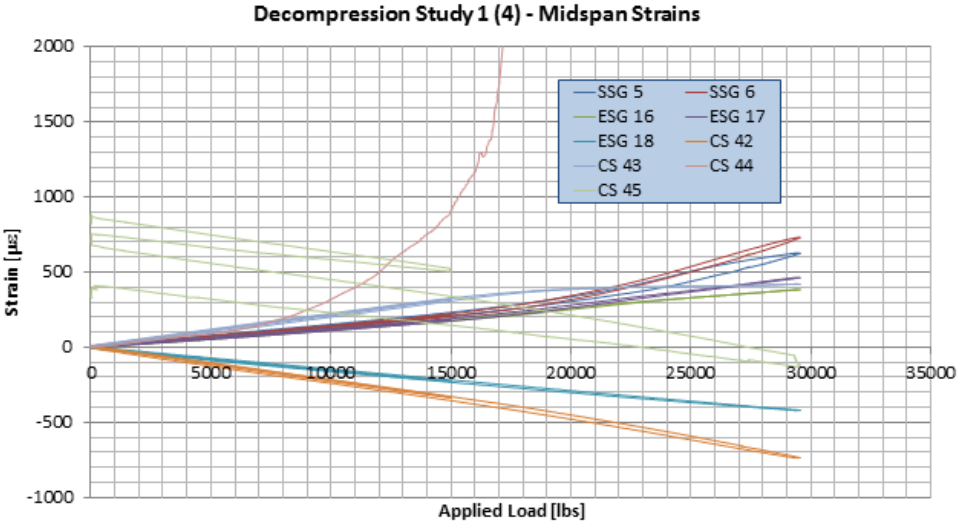
Decompression Study 1 (4) - Midspan Strains
SSG 5
SSG 6
ESG 16
ESG 17
ESG 18
CS 42
CS 43
CS 44
CS 45
Strain [με]
2000
1500
1000
500
0
-500
-1000
0
5000
10000
15000
20000
25000
30000
35000
Applied Load [lbs]

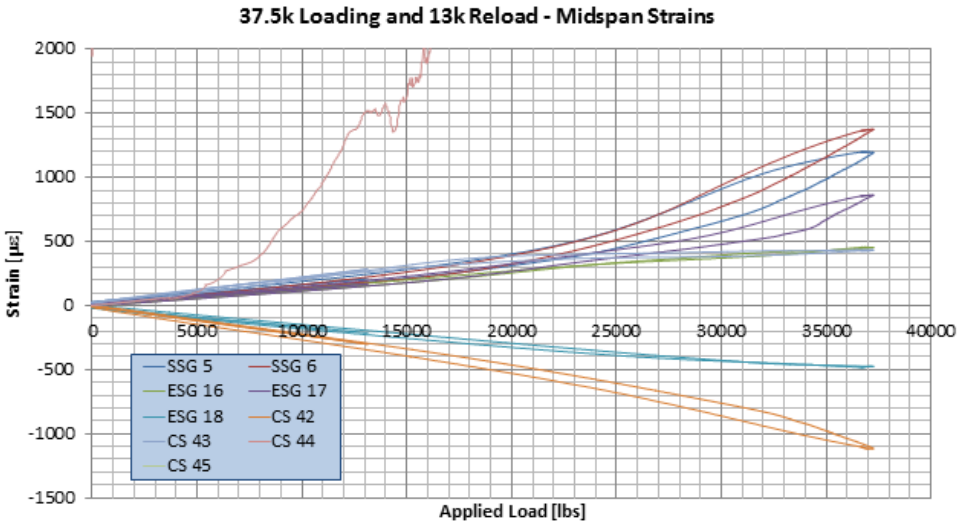
37.5k Loading and 13k Reload - Midspan Strains
Strain [με]
Applied Load [lbs]
SSG 5
SSG 6
ESG 16
ESG 17
ESG 18
CS 42
CS 43
CS 44
CS 45

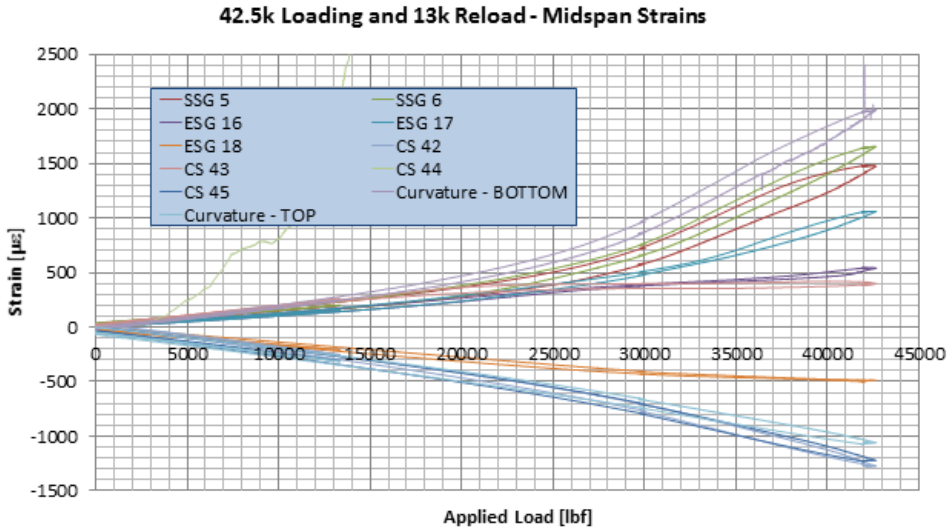
42.5k Loading and 13k Reload - Midspan Strains
Strain [με]
Applied Load [lbf]
SSG 5
SSG 6
ESG 16
ESG 17
ESG 18
CS 42
CS 43
CS 44
CS 45
Curvature - BOTTOM
Curvature - TOP

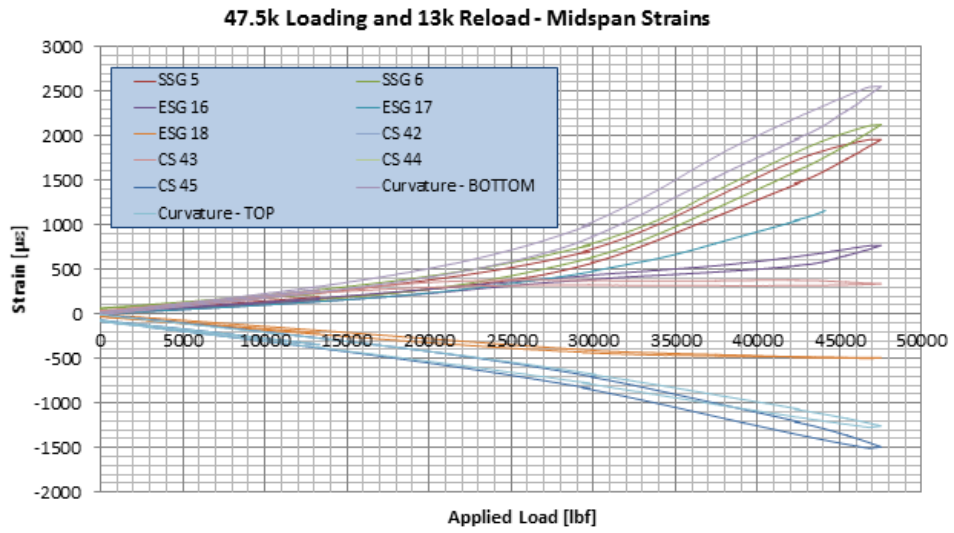
47.5k Loading and 13k Reload - Midspan Strains
SSG 5
SSG 6
ESG 16
ESG 17
ESG 18
CS 42
CS 43
CS 44
CS 45
Curvature - BOTTOM
Curvature - TOP
Strain [με]
Applied Load [lbf]

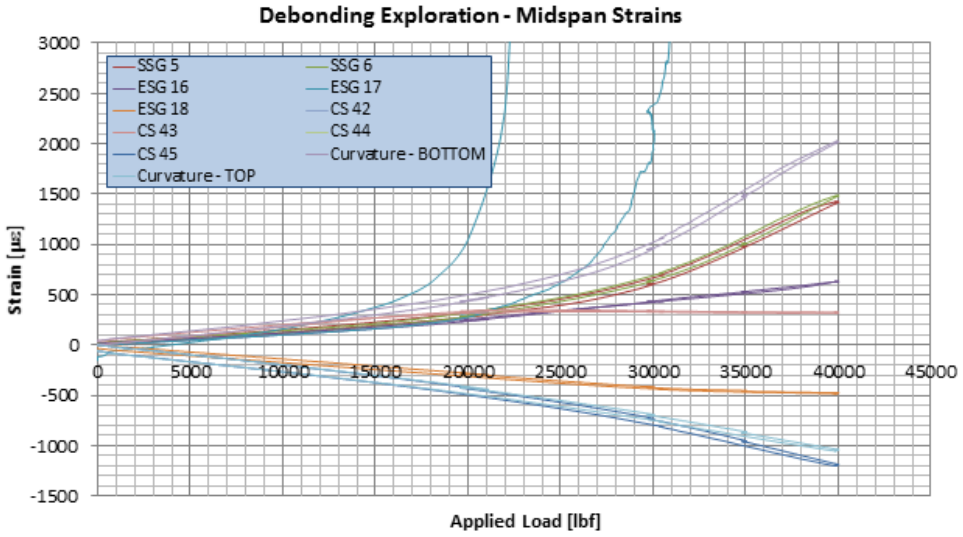
Debonding Exploration - Midspan Strains
SSG 5
SSG 6
ESG 16
ESG 17
ESG 18
CS 42
CS 43
CS 44
CS 45
Curvature - BOTTOM
Curvature - TOP
Strain [με]
Applied Load [lbf]

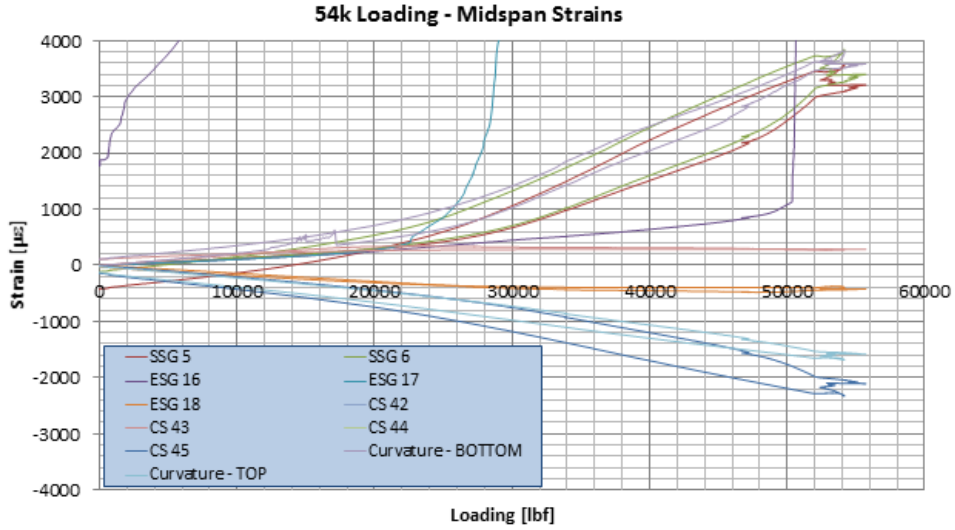
54k Loading - Midspan Strains
SSG 5
SSG 6
ESG 16
ESG 17
ESG 18
CS 42
CS 43
CS 44
CS 45
Curvature - BOTTOM
Curvature - TOP
Strain [με]
Loading [lbf]

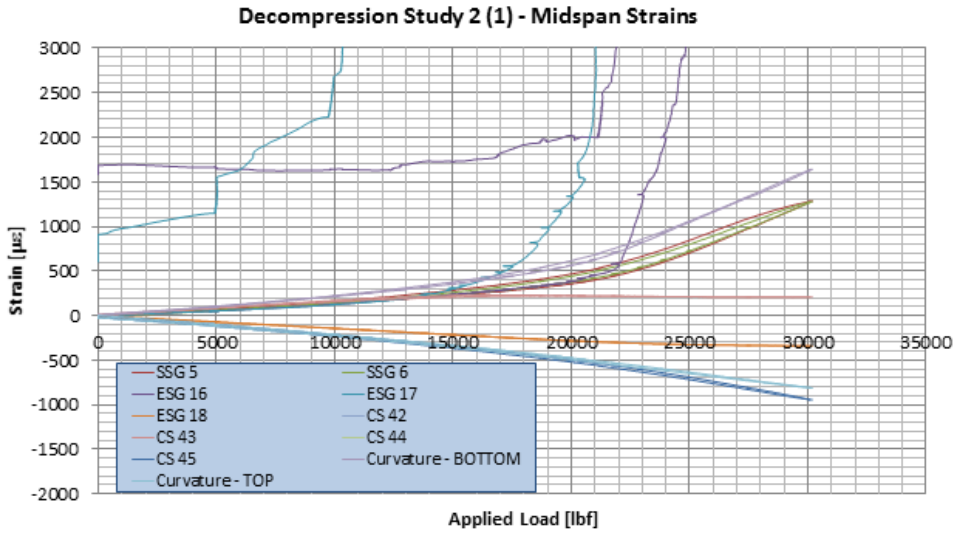
Decompression Study 2 (1) - Midspan Strains
Strain [με]
Applied Load [lbf]
SSG 5
SSG 6
ESG 16
ESG 17
ESG 18
CS 42
CS 43
CS 44
CS 45
Curvature - BOTTOM
Curvature - TOP

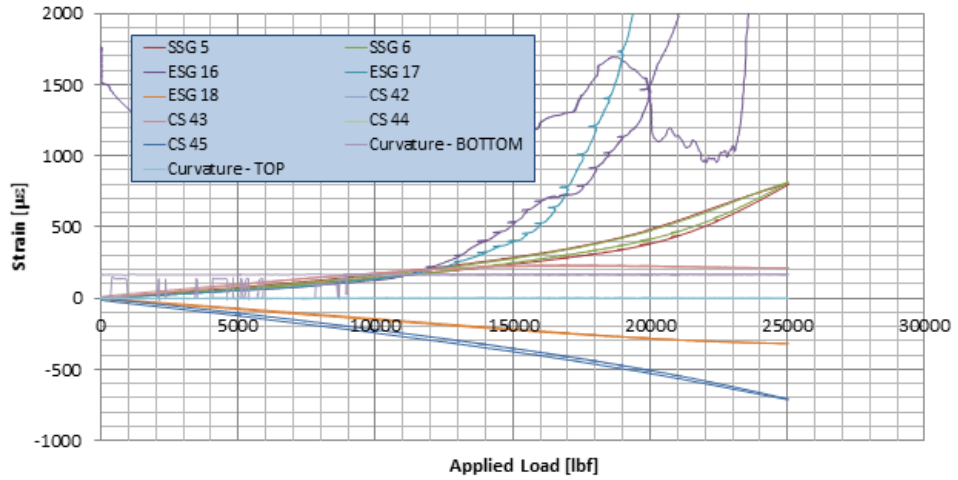
Debonding Study 2 (2) - Midspan Strains
Strain [με]
Applied Load [lbf]
SSG 5
SSG 6
ESG 16
ESG 17
ESG 18
CS 42
CS 43
CS 44
CS 45
Curvature - BOTTOM
Curvature - TOP

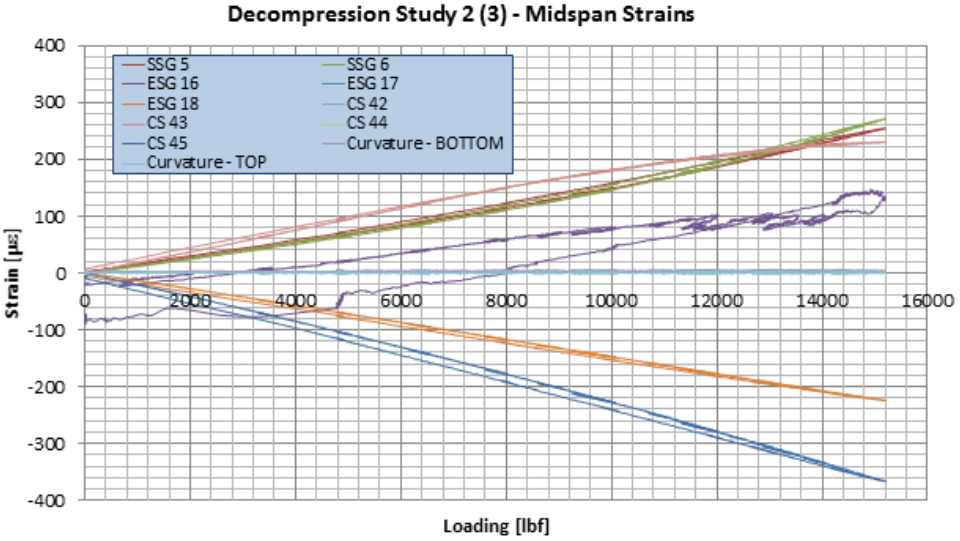
Decompression Study 2 (3) - Midspan Strains
Strain [με]
Loading [lbf]
SSG 5
SSG 6
ESG 16
ESG 17
ESG 18
CS 42
CS 43
CS 44
CS 45
Curvature - BOTTOM
Curvature - TOP

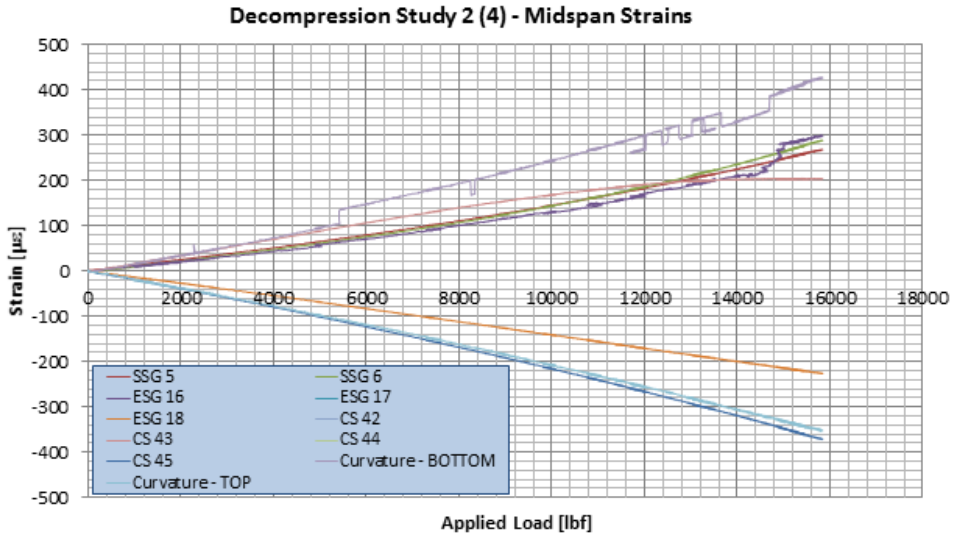
Decompression Study 2 (4) - Midspan Strains
Strain [με]
Applied Load [lbf]
SSG 5
SSG 6
ESG 16
ESG 17
ESG 18
CS 42
CS 43
CS 44
CS 45
Curvature - BOTTOM
Curvature - TOP

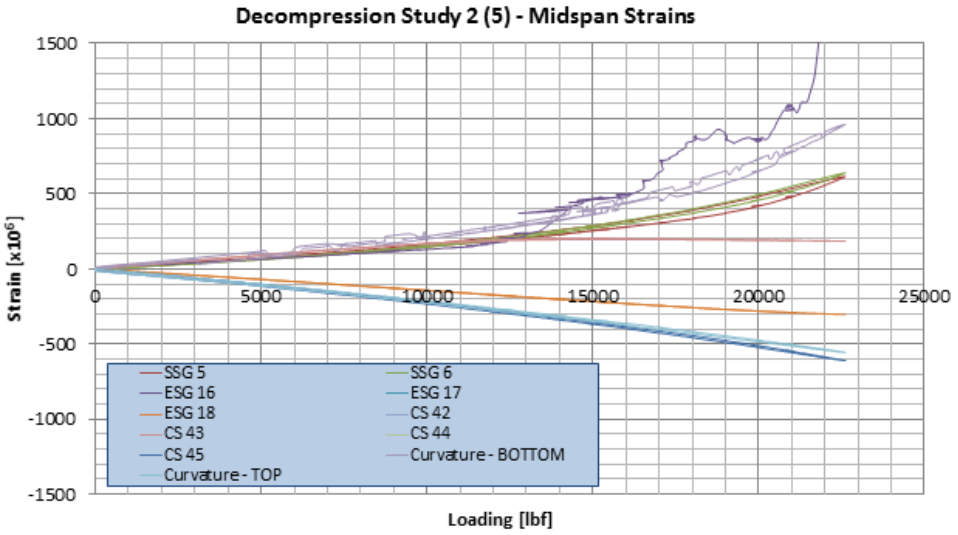
Decompression Study 2 (5) - Midspan Strains
Strain [x10⁶]
Loading [lbf]
SSG 5
SSG 6
ESG 16
ESG 17
ESG 18
CS 42
CS 43
CS 44
CS 45
Curvature - BOTTOM
Curvature - TOP

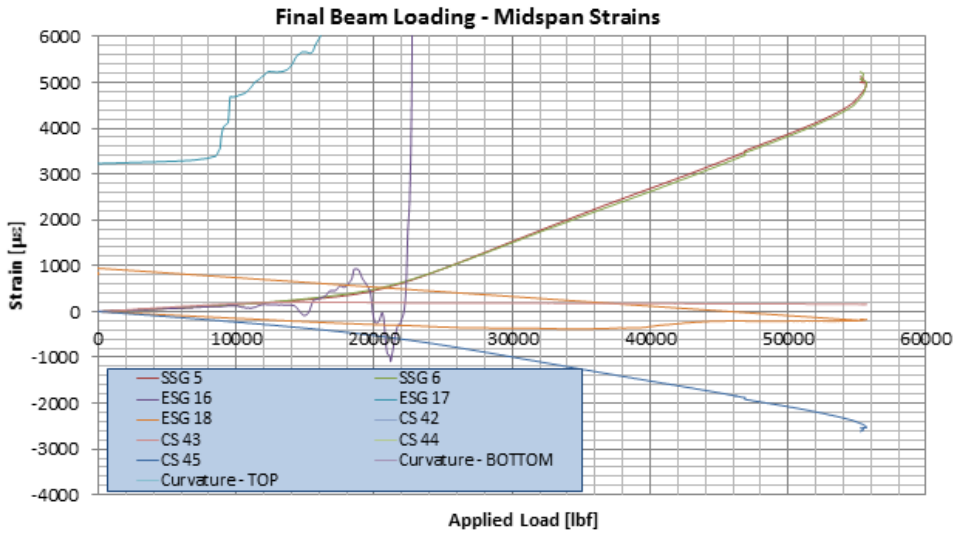

C.2 Strains from Section C-C Gages

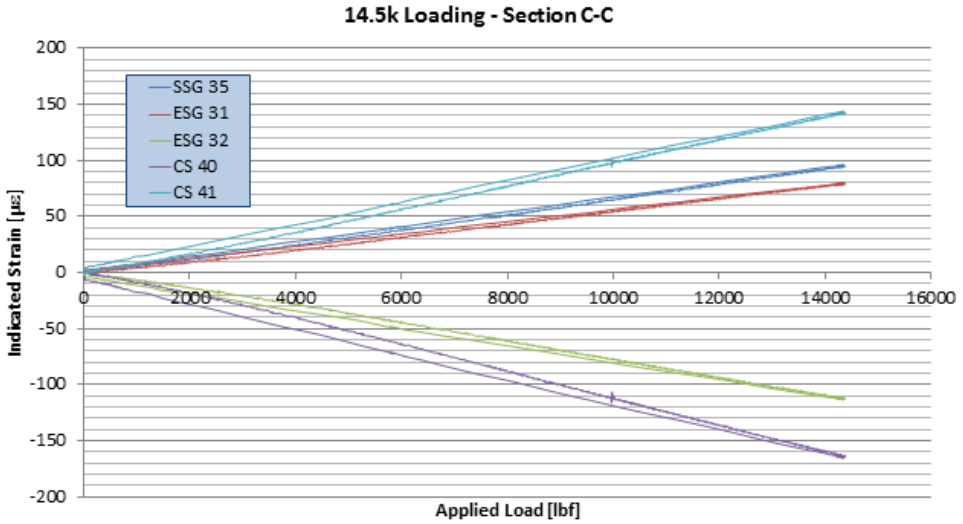

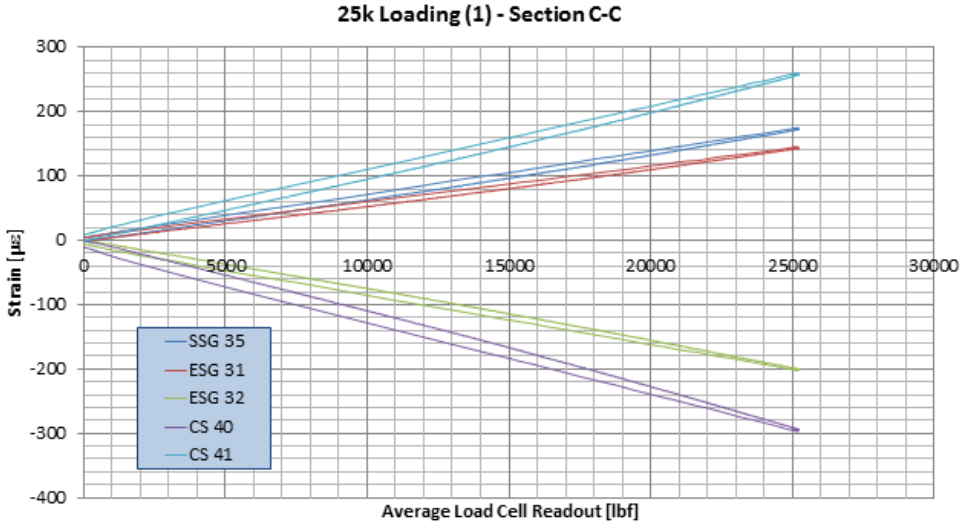

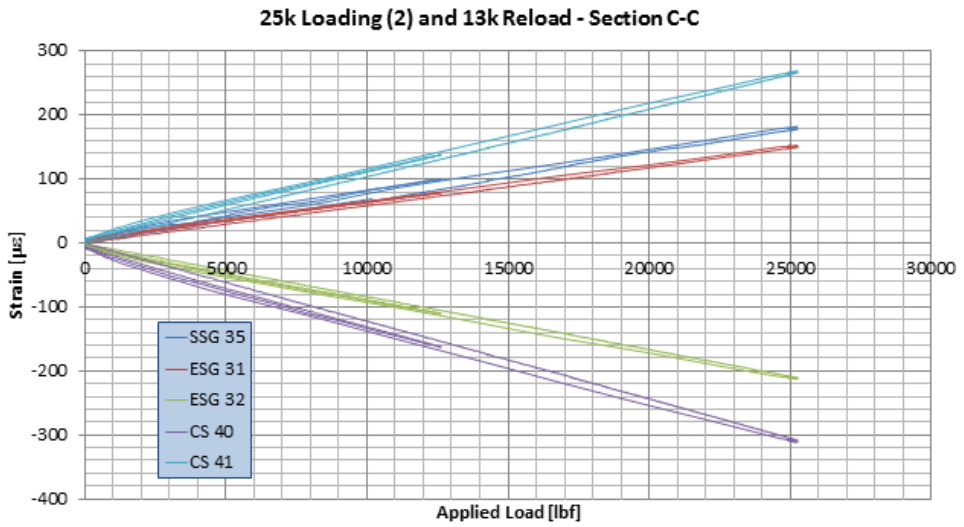
25k Loading (2) and 13k Reload - Section C-C
Strain [με]
Applied Load [lbf]
SSG 35
ESG 31
ESG 32
CS 40
CS 41

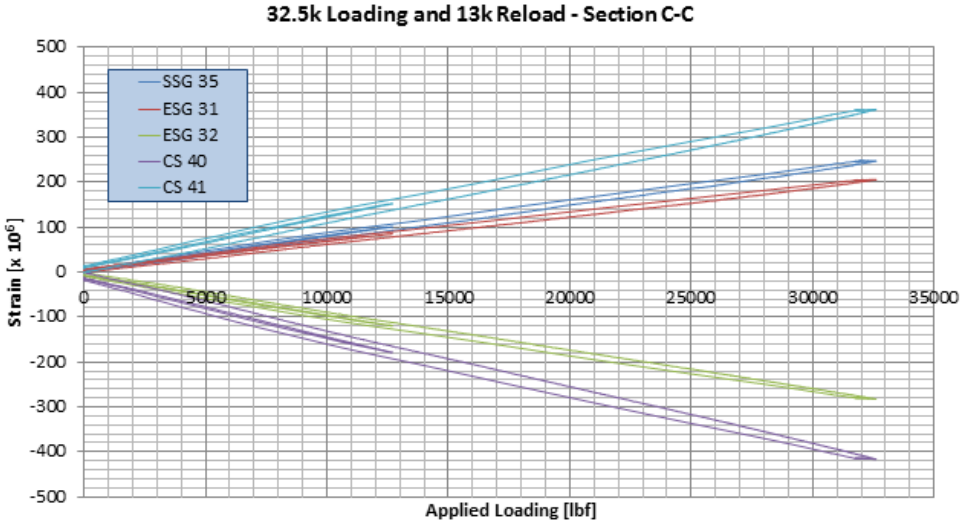
32.5k Loading and 13k Reload - Section C-C
Strain [x 10⁶]
Applied Loading [lbf]
SSG 35
ESG 31
ESG 32
CS 40
CS 41

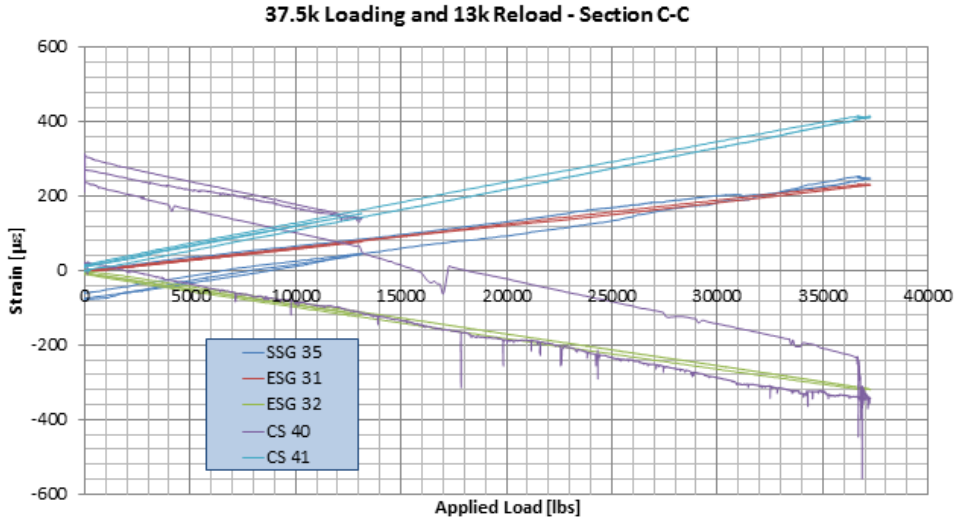
37.5k Loading and 13k Reload - Section C-C
Strain [με]
Applied Load [lbs]
SSG 35
ESG 31
ESG 32
CS 40
CS 41

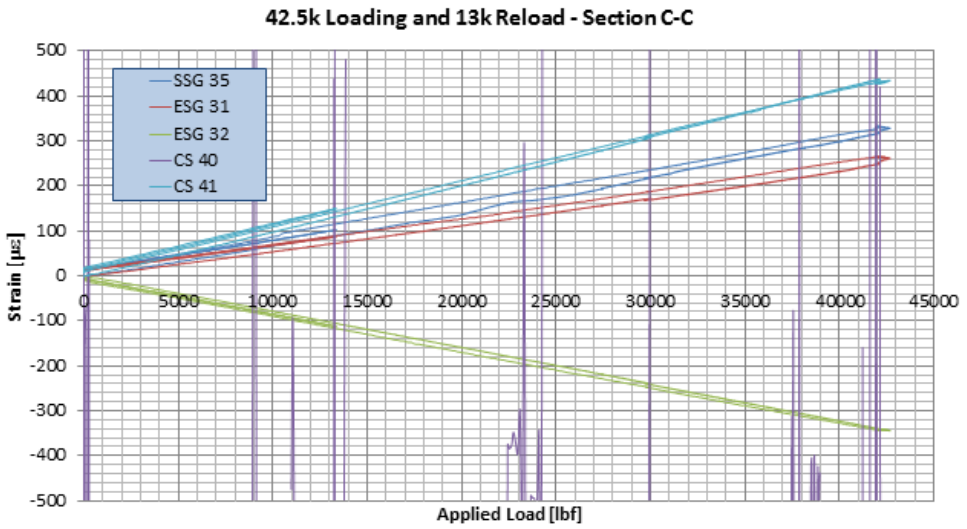
42.5k Loading and 13k Reload - Section C-C
SSG 35
ESG 31
ESG 32
CS 40
CS 41
Strain [με]
Applied Load [lbf]
500
400
300
200
100
0
-100
-200
-300
-400
-500
0
5000
10000
15000
20000
25000
30000
35000
40000
45000

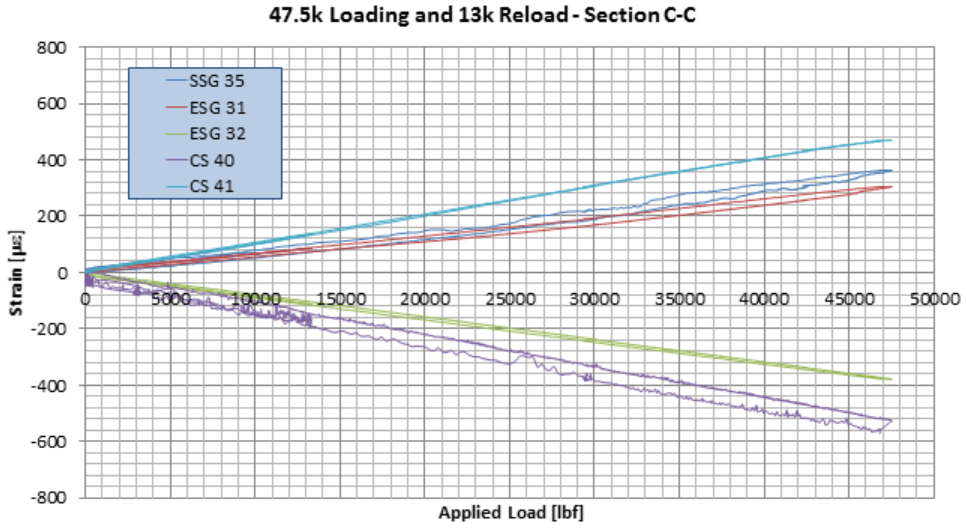
47.5k Loading and 13k Reload - Section C-C
SSG 35
ESG 31
ESG 32
CS 40
CS 41
Strain [με]
Applied Load [lbf]
800
600
400
200
0
-200
-400
-600
-800
0
5000
10000
15000
20000
25000
30000
35000
40000
45000
50000

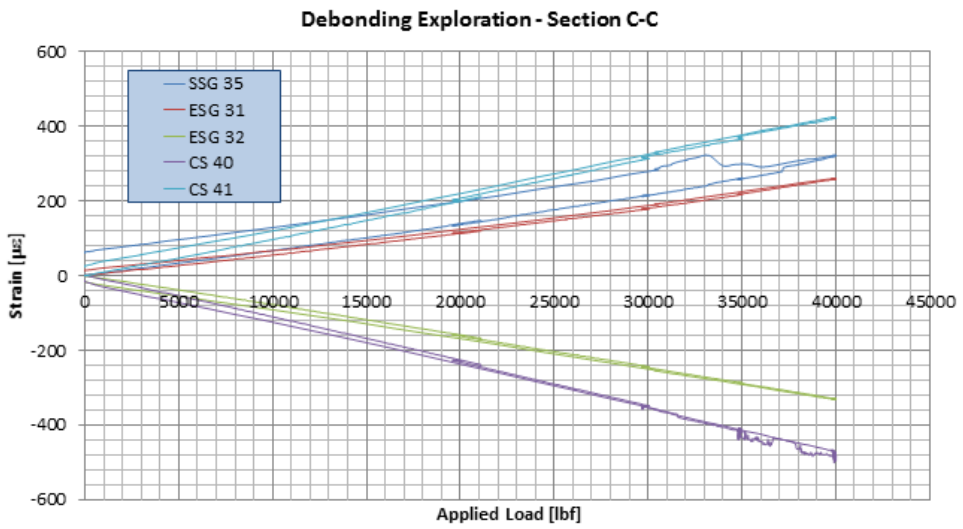
Debonding Exploration - Section C-C
SSG 35
ESG 31
ESG 32
CS 40
CS 41
Strain [με]
600
400
200
0
-200
-400
-600
0
5000
10000
15000
20000
25000
30000
35000
40000
45000
Applied Load [lbf]

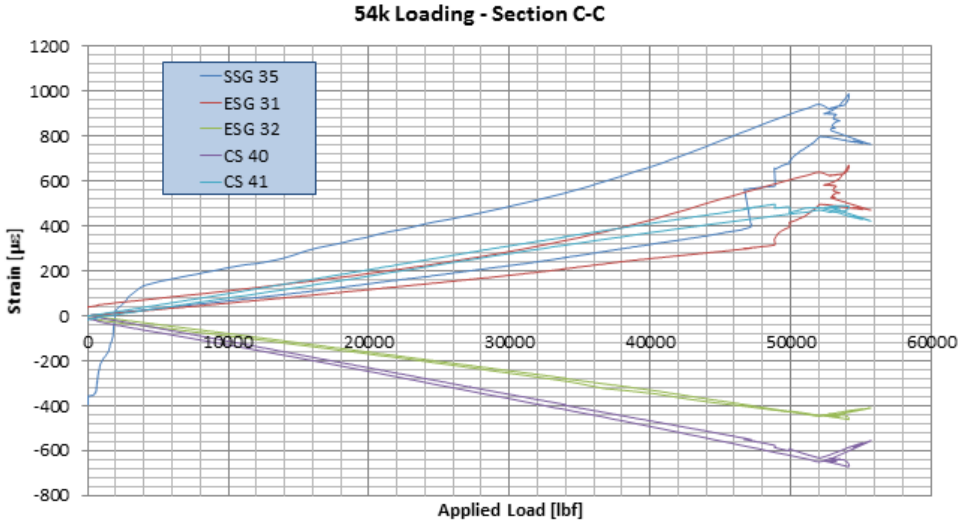
54k Loading - Section C-C
SSG 35
ESG 31
ESG 32
CS 40
CS 41
Strain [με]
1200
1000
800
600
400
200
0
-200
-400
-600
-800
0
10000
20000
30000
40000
50000
60000
Applied Load [lbf]

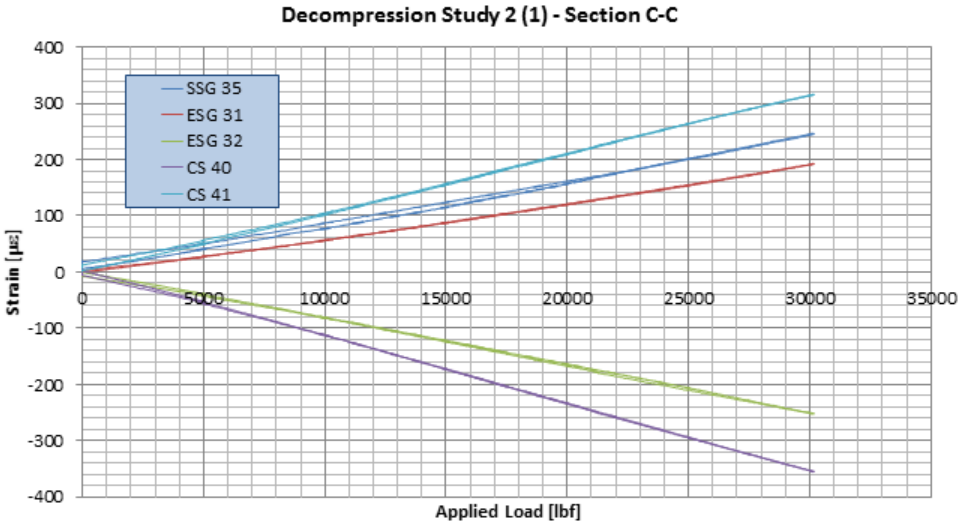
Decompression Study 2 (1) - Section C-C
SSG 35
ESG 31
ESG 32
CS 40
CS 41
Strain [με]
400
300
200
100
0
-100
-200
-300
-400
0
5000
10000
15000
20000
25000
30000
35000
Applied Load [lbf]

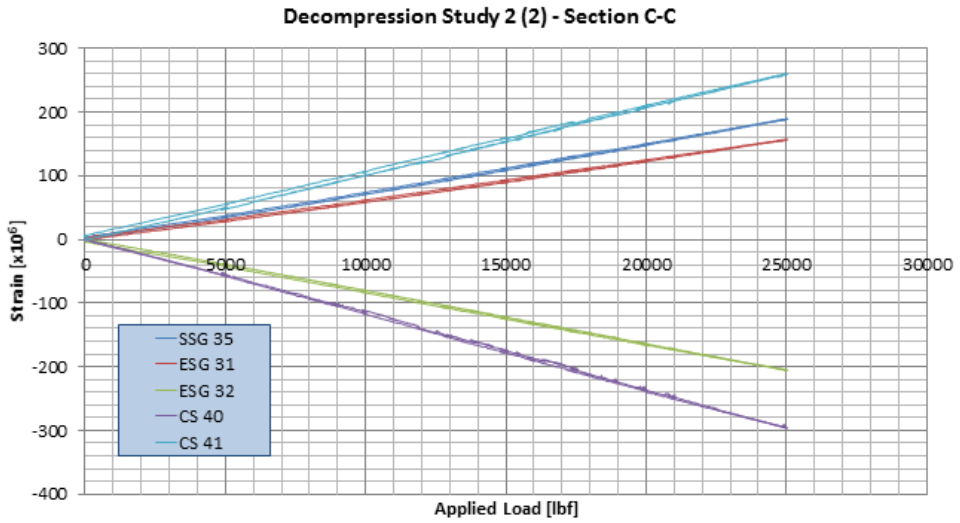
Decompression Study 2 (2) - Section C-C
Strain [x10⁶]
Applied Load [lbf]
SSG 35
ESG 31
ESG 32
CS 40
CS 41

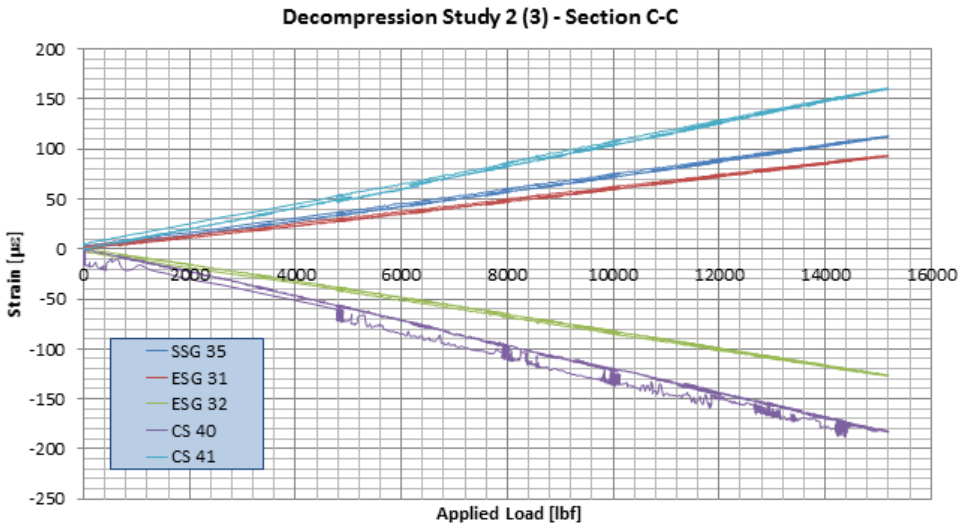
Decompression Study 2 (3) - Section C-C
Strain [με]
Applied Load [lbf]
SSG 35
ESG 31
ESG 32
CS 40
CS 41

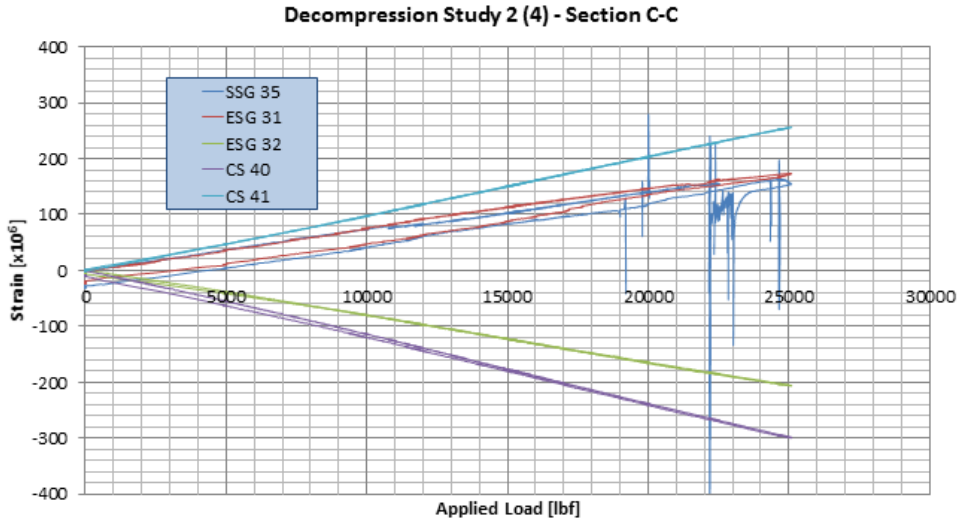
Decompression Study 2 (4) - Section C-C
Strain [x10⁶]
Applied Load [lbf]
SSG 35
ESG 31
ESG 32
CS 40
CS 41

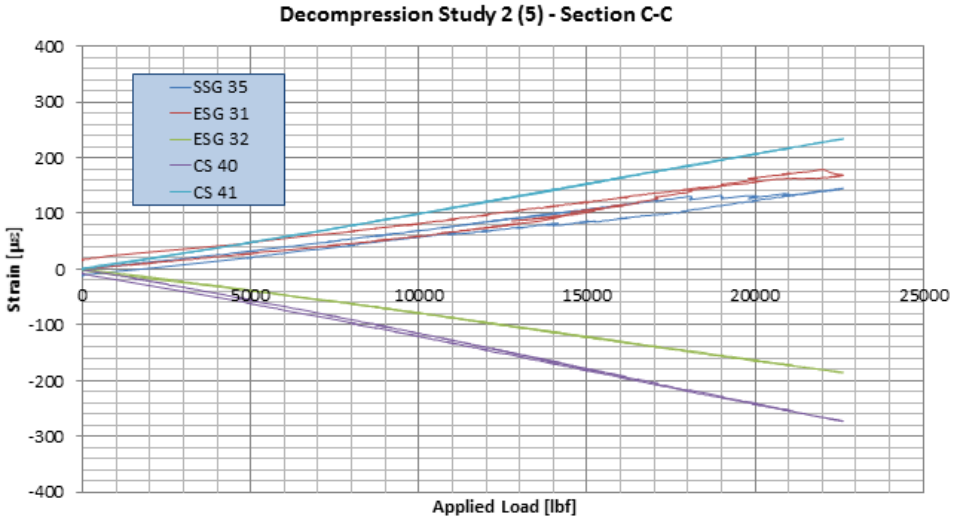
Decompression Study 2 (5) - Section C-C
SSG 35
ESG 31
ESG 32
CS 40
CS 41
Strain [με]
Applied Load [lbf]
400
300
200
100
0
-100
-200
-300
-400
0
5000
10000
15000
20000
25000

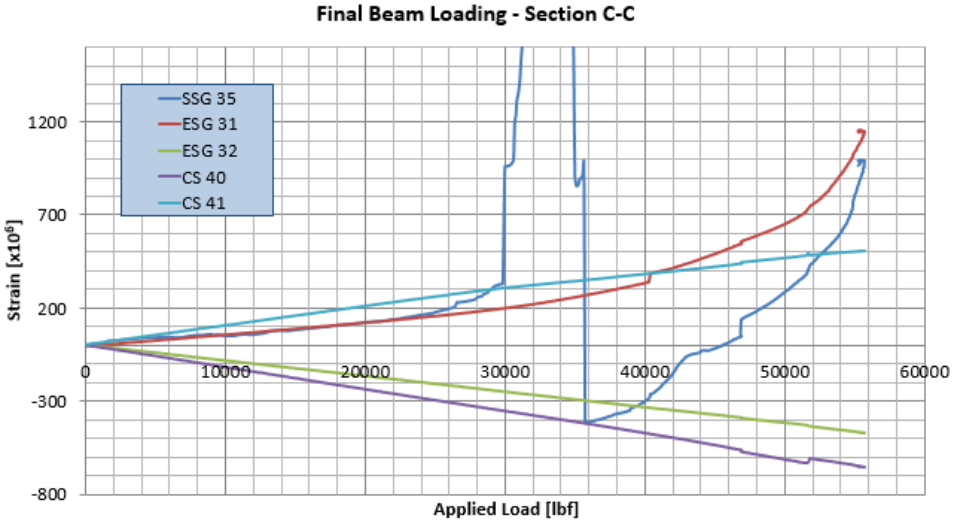
Final Beam Loading - Section C-C
SSG 35
ESG 31
ESG 32
CS 40
CS 41
Strain [x10⁶]
Applied Load [lbf]
1200
700
200
-300
-800
0
10000
20000
30000
40000
50000
60000

APPENDIX D – Properties Used for Non-Linear Analyses of Beam

D.1 Non-Linear SCC-2 Behavior

Samples were taken on the day of casting from the SCC-2 batches used to fabricate the laboratory beam. Testing was done at various ages to determine the following hardened properties: compressive strength, splitting tensile strength and modulus of elasticity. A summary of the compressive strength, tensile strength and modulus of elasticity properties obtained for the laboratory beam specimens are summarized in Table D-1, along with the values used for the original bridge design.

Table D-1 Summary of hardened properties for SCC-2 laboratory beam specimens.

	2 days	16 days	28 days	20 months	24 months
Compressive Strength, 4"x8" [psi]	**6,370**	**8,130**	**8,320**	**8,790**	
Compressive Strength, 6"x12" [psi]	**5,890**	**6,920**	**7,370**		**9,514**
Design Compressive Strength [psi]	***6,000***		***8,000***		
Modulus of Elasticity [psi]	**4,448,000**	**4,335,000**	**4,928,000**		**4,851,000**
Design Modulus of Elasticity [psi]	***4,696,000***		***5,422,450***		
Splitting Tensile Strength [psi]	**492**	**439**	**585**		

For the sake of moment-curvature analysis, it is desirable to investigate the non-linear behavior of the concrete in addition to the linear behaviors shown in Table D-1. Therefore, a compressometer instrumented with three LVDTs (see Figure D-1) along with a manual triggering mechanism were used for the 24-month tests, in lieu of the dial-type compressometer and load readout used previously.

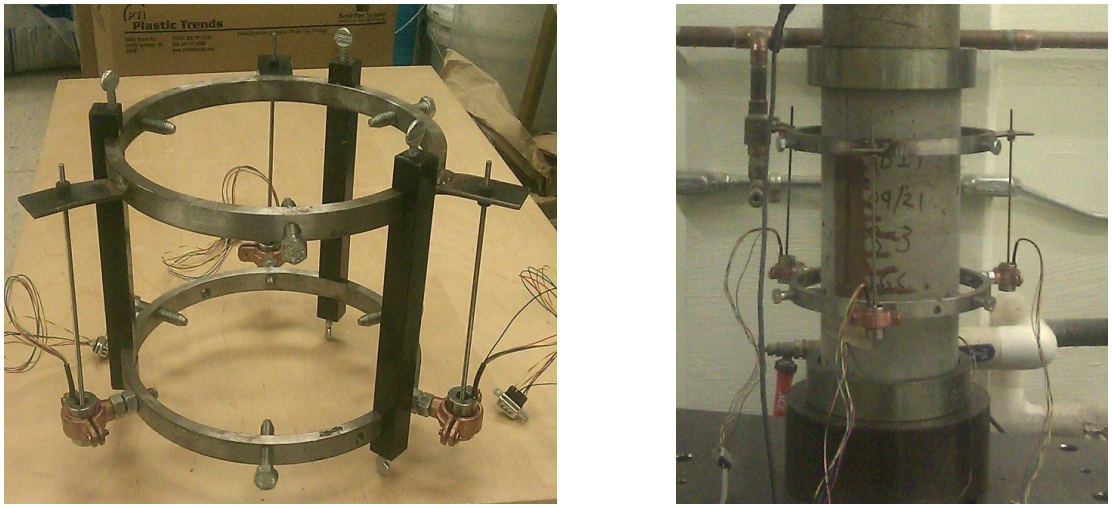

(a) **(b)**

Figure D-1 Compressometer (a) before mounting, and (b) as used for testing concrete specimen.

The stress-strain curves obtained for the two specimens tested at 24 months can be seen in Figure D-2. In addition, the 24-month values were incorporated into the following formulae to represent the ascending and descending branches of the stress-strain relationship:

Ascending Branch:

$$f = f_c' \left(1 - \left(1 - {}^{\varepsilon}/_{\varepsilon_0}\right)^{A}\right) \quad \textbf{(25)}$$

where: $f_c' = 9{,}514\ psi$ **(observed from data)**

$\varepsilon_0 = 0.0025\ in/in$ **(observed from data)**

$$A = E_c * {}^{\varepsilon_0}/_{f_0}$$

$E_c = 5{,}081{,}580\ psi$ **(adjusted to fit data)**

Descending Branch:

$$f = f_0 \cdot e^{\left(-k(\varepsilon - \varepsilon_0)^{2.5}\right)} \quad \textbf{(26)}$$

where: $k = 175{,}000 * f_c'$

In our case, without confinement, the term f_r equals 0. This representation, as calculated using the measured properties, can be seen in Figure D-2, and is indicated by the curve labeled "Equation for Analysis." In cases where non-linear analysis was done, this representation of SCC-2 was used for analysis; in cases where a linear representation of the SCC-2 was all that was needed, the appropriate value from Table D-1 was used.

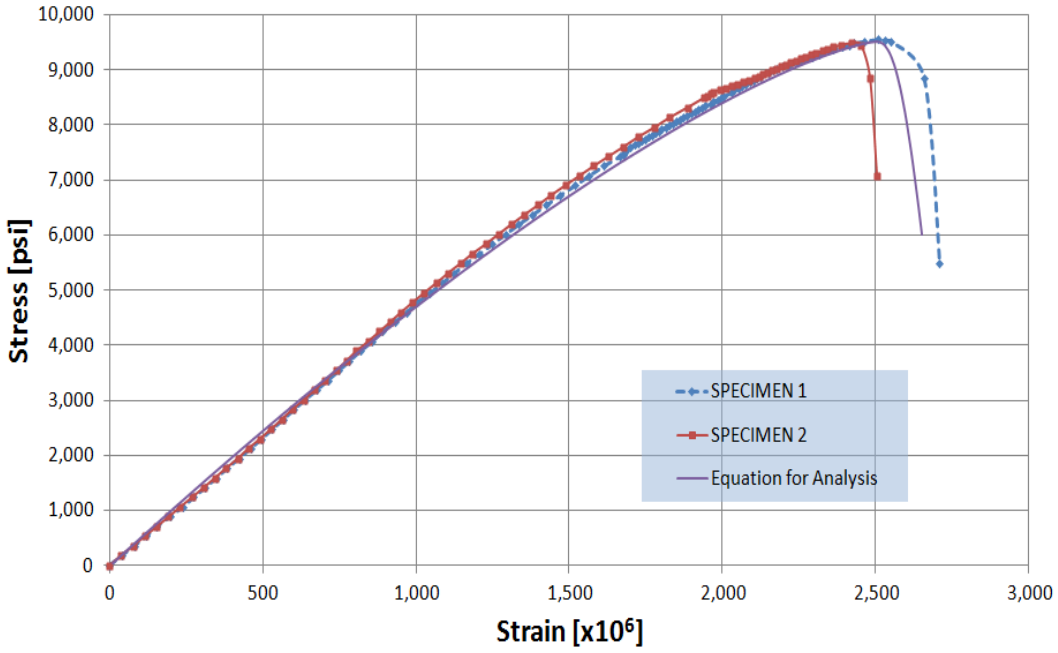

Figure D-2 Stress-Strain relationships from SCC-2 cylinders tested at 24 months.

D.2 Non-Linear Steel Strand Behavior

For analyses that only required a linear approximation of the stress-strain relationship of the Grade 270, low-relaxation steel prestressing strands, the manufacturer-specified values of 286.5 ksi for tensile strength and 28,700 ksi for elastic modulus were used. For more advanced analyses that needed the entire stress-strain curve, a better model for the strand behavior was needed. To do this, the behaviors of the strands were modeled from a study on this particular relationship by Devalapura and Tadros, appearing in the PCI Journal (Devalapura and Tadros 1992). In their study of Gr270 low-relaxation strands, they gave the following correlation for the stress-strain relationship:

$$f_{ps} = \varepsilon_{ps} * \left[A + \frac{B}{\left\{1 + \left(C\varepsilon_{ps}\right)^{D}\right\}^{1/D}} \right] \leq f_{pu} \qquad (27)$$

where: f_{ps} and ε_{ps} are the stress and strain in the strand, respectively, f_{pu} is the specified ultimate stress, and A, B, C and D are constants. For ½-inch 270 ksi strands with $f_{py}/f_{pu} = 0.9$, they experimentally found the constants to be A=887, B=27613, C=112.4 and D=7.360. Using this relationship and the manufacturer-specified tensile strength (286.5 ksi) and elastic modulus (28,700 ksi) of the prestressing strands used for the Stalnaker Run Bridge beams, the stress-strain curve used for analysis can be calculated, and is shown in Figure D-3**.**

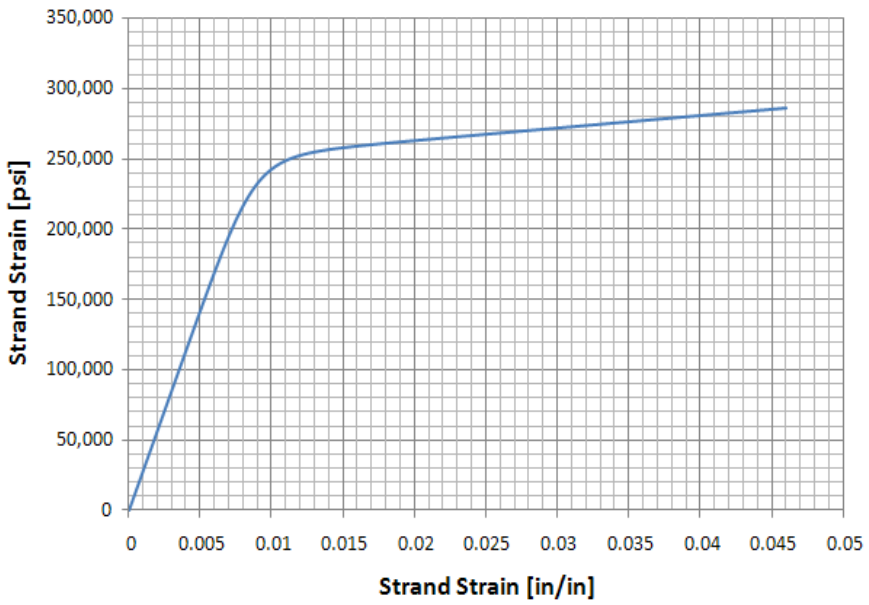

Figure D-3 Assumed behavior of Gr270 Low-Relaxation Strands, based on Devalapura and Tadros (2004).

D.3 Transformed Section Properties

As was shown previously, the outer dimensions of the box beam are 17" tall by 48" wide, and the section includes a 6" tall by 38" wide void (2" chamfered corners) in the center that extends throughout the majority of the length of the beam. A total of 29 half-inch, oversized Grade 270, low-relaxation prestressing strands were used to apply the prestressing force: 21 were in a row 2" from the bottom surface; 6 were in a row 4" from the bottom, and 2 were in a row 13" from the bottom. Figure D-4 shows a typical cross section in locations other than midspan and the very end of the beam where no void is present. It should be noted that some non-prestressed reinforcement has been removed from the depiction in Figure D-4 for clarity, although all reinforcement is in fact symmetric about the center of beam as constructed.

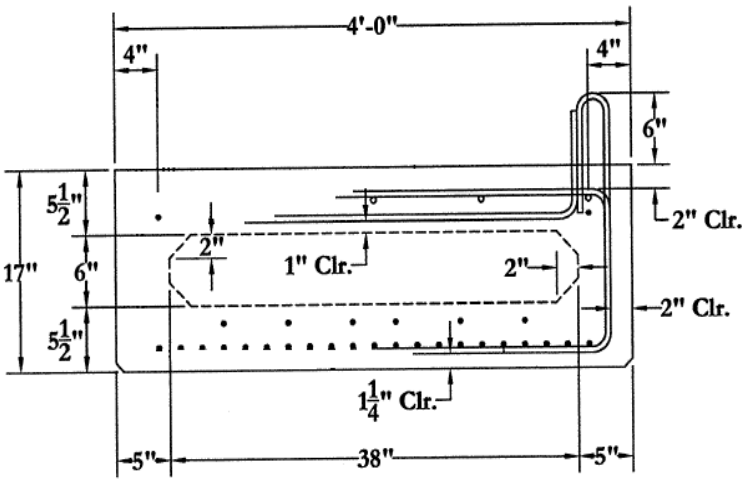

Figure D-4 Typical box beam cross-section, with void (some non-prestressed reinforcement removed for clarity).

Section properties were then established for the transformed section considering the contribution of the prestressing strands as well as that of the concrete; effects from non-prestressing rebars were not considered. It was noted in the design file that for the design values, the non-composite box beam section (prior to contribution from bridge deck) was transformed using the design stiffness of the strands (28,500 ksi) and the design stiffness of the concrete at release (2,696 ksi).

The revised calculations utilized the manufacturer-provided elastic modulus for the steel strands (28,700 ksi) and the 24-month elastic modulus of the concrete (5,082 ksi). The adjustment was made using the ratio of prestressing strand stiffness to concrete stiffness, denoted as n, to represent the prestressing strands as equivalent areas of concrete. The centroid of the section, $\bar{y}$, was obtained by summing the moments about the bottom surface of the beam. The general equation used for calculating the transformed moment of inertia is as follows, with the subscript k being used for concrete sections and the subscript j being used for the prestressing steel:

$$I_t = \sum_{k=0}^{n}\left[\frac{b_k {h_k}^3}{12} + bh(z_k - \bar{y})\right] + \sum_{j=0}^{n}\left[(n-1)A_{p,j}(z_j - \bar{y})\right] \quad \textbf{(28)}$$

The transformed section properties seen in the design documents and those calculated using observed SCC-2 material properties can be seen in Table D-2.

.

Table D-2 Prestressed box beam section properties used for analysis.

	Design Values	Adjusted per Materials
A_t [in^2]	618.5	616.6
I_t [in^4]	19,628	19,739
h [in]	17	17
c_1 [in]	8.69	8.68
c_2 [in]	8.31	8.32
r [in]	5.766	5.658
S_1 [in^3]	2,259	2,275
S_2 [in^3]	2,362	2,372
y_{cg} [in]	3.17	3.17
e [in]	5.14	5.15

APPENDIX E - Strain Readings from Stalnaker Run Bridge

E.1 Strand Strain Gages from SCC-2 Box Beams

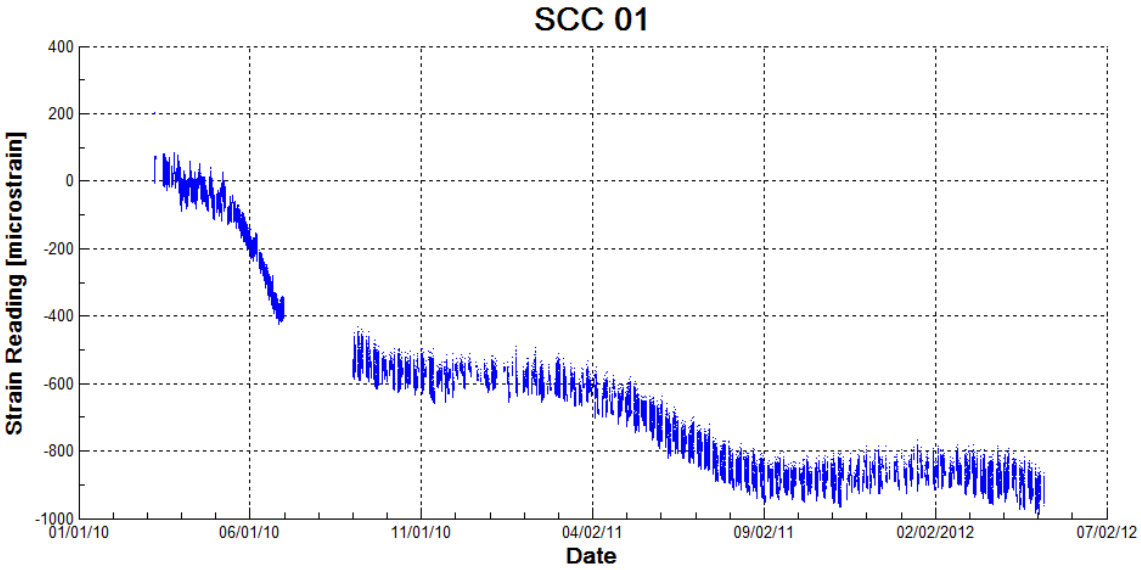

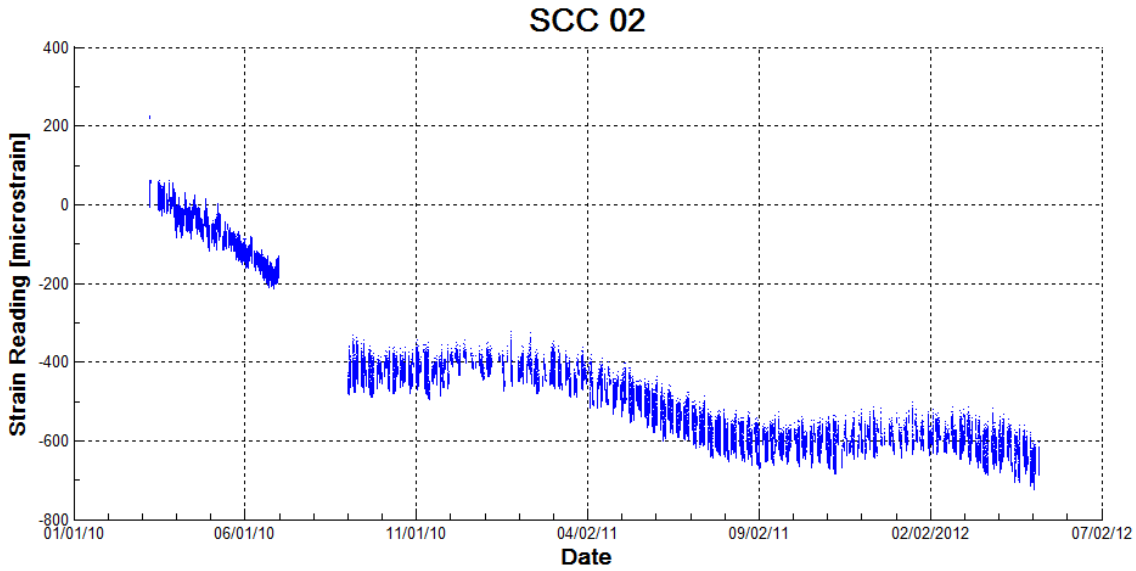

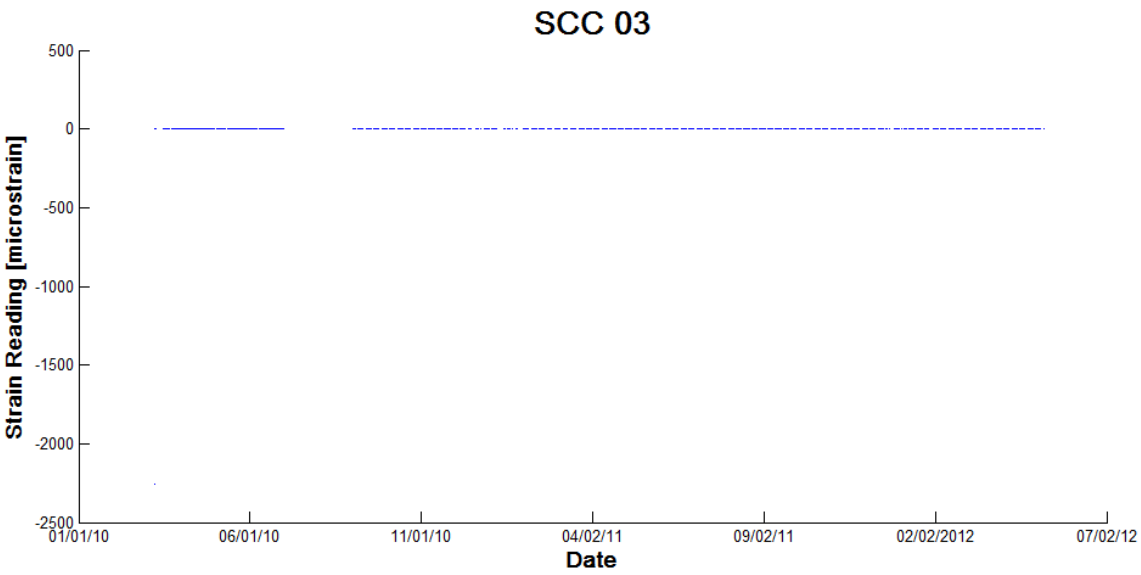
SCC 03
Strain Reading [microstrain]
500
0
-500
-1000
-1500
-2000
-2500
01/01/10
06/01/10
11/01/10
04/02/11
09/02/11
02/02/2012
07/02/12
Date

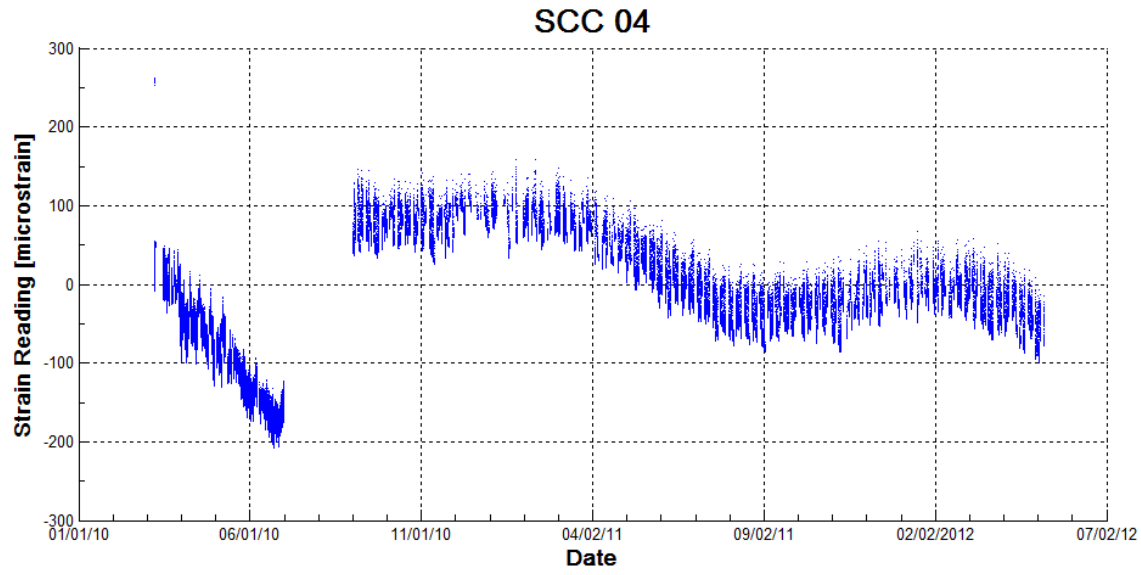
SCC 04
Strain Reading [microstrain]
300
200
100
0
-100
-200
-300
01/01/10
06/01/10
11/01/10
04/02/11
09/02/11
02/02/2012
07/02/12
Date

E.2 Strand Strain Gages from Traditional Box Beams

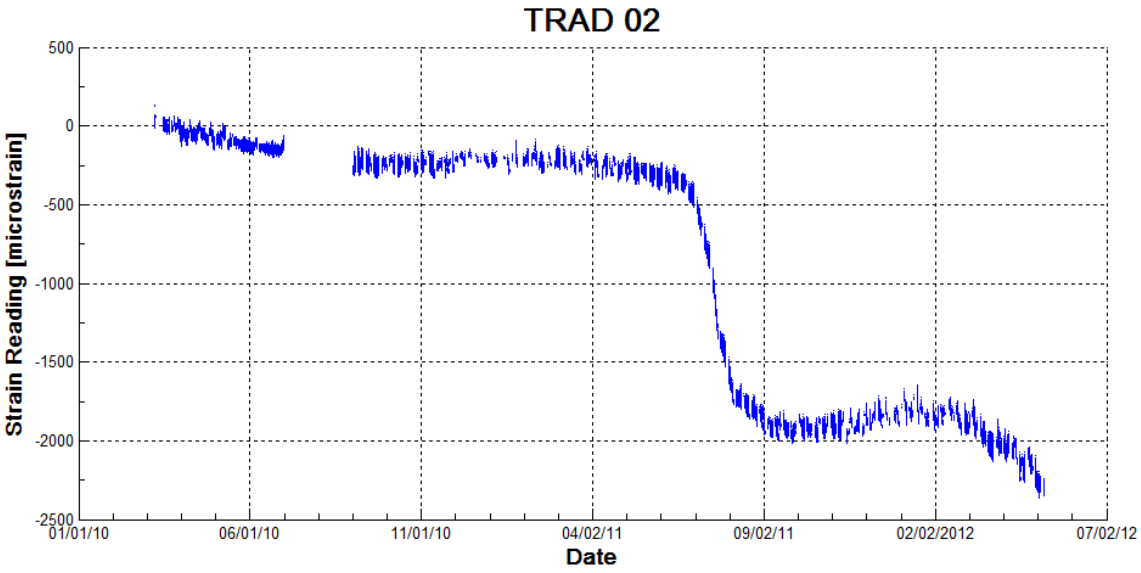

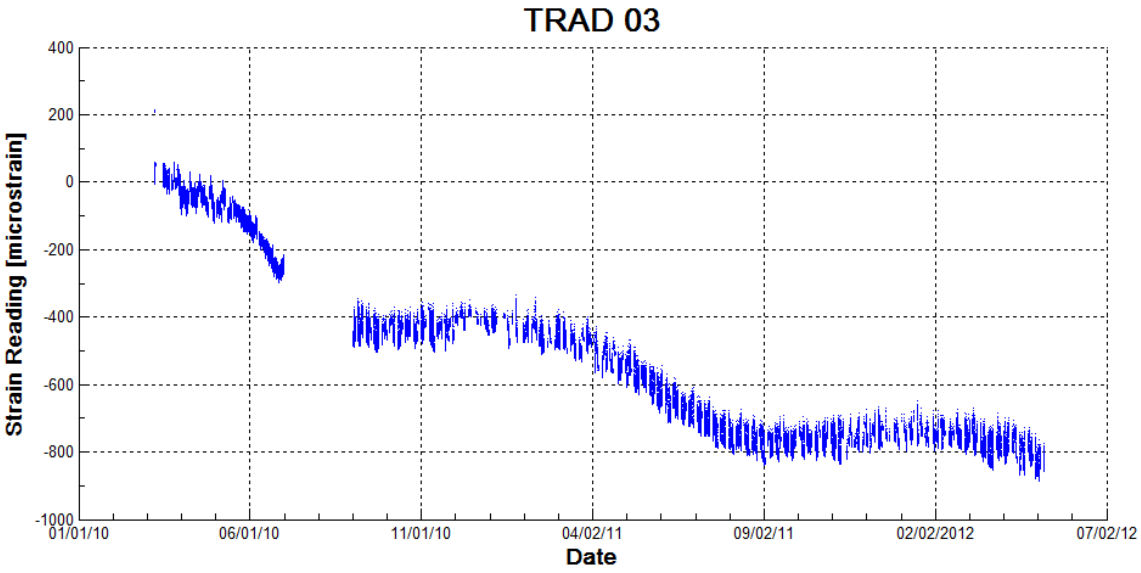

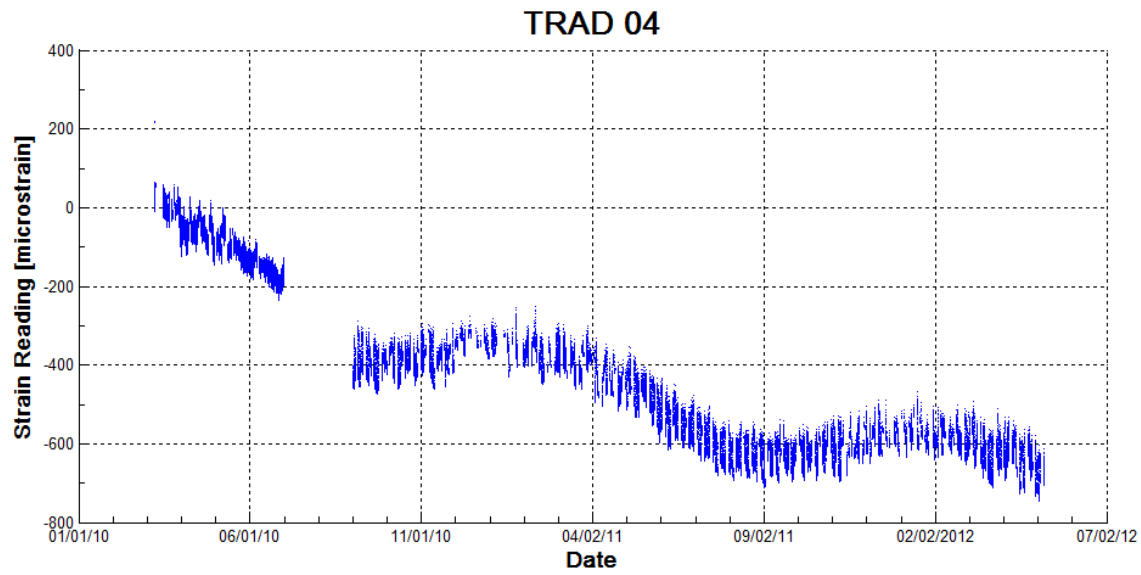
TRAD 04
Strain Reading [microstrain]
400
200
0
-200
-400
-600
-800
01/01/10
06/01/10
11/01/10
04/02/11
09/02/11
02/02/2012
07/02/12
Date

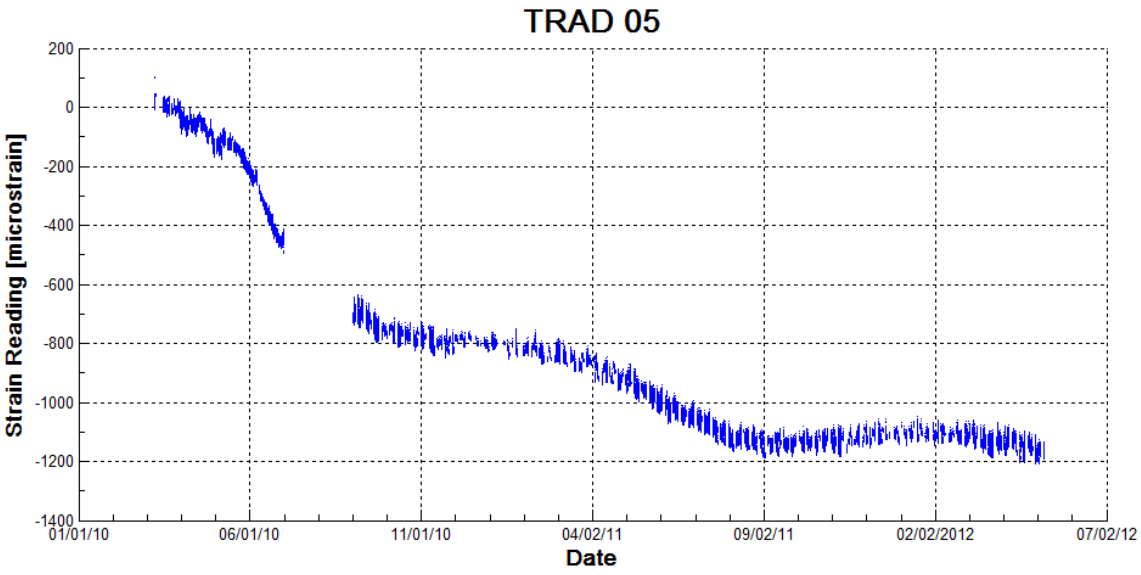
TRAD 05
Strain Reading [microstrain]
200
0
-200
-400
-600
-800
-1000
-1200
-1400
01/01/10
06/01/10
11/01/10
04/02/11
09/02/11
02/02/2012
07/02/12
Date

E.3 Concrete Embedment Gages from SCC-2 Box Beams

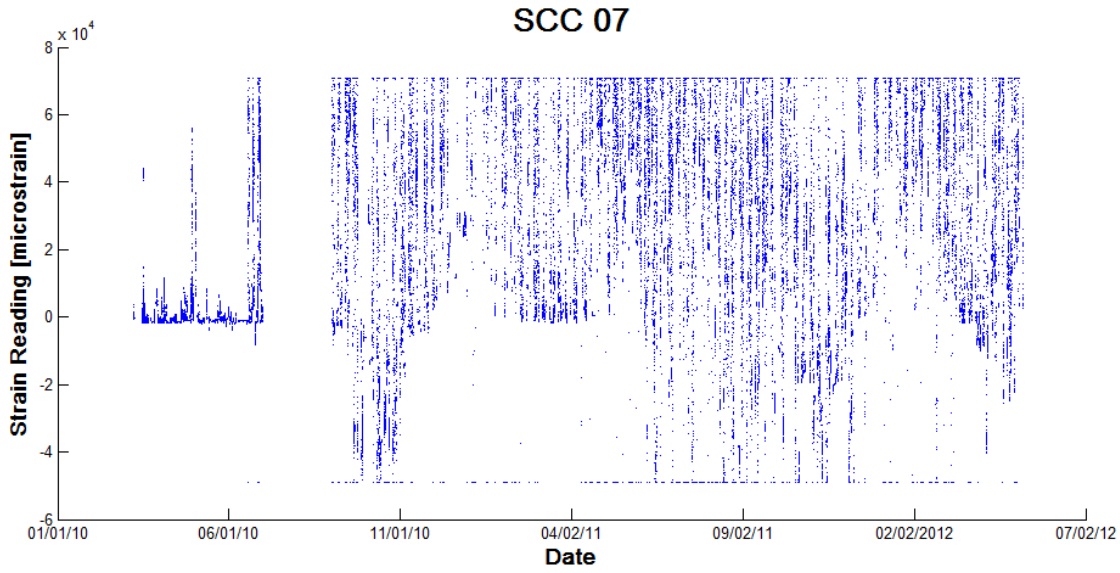

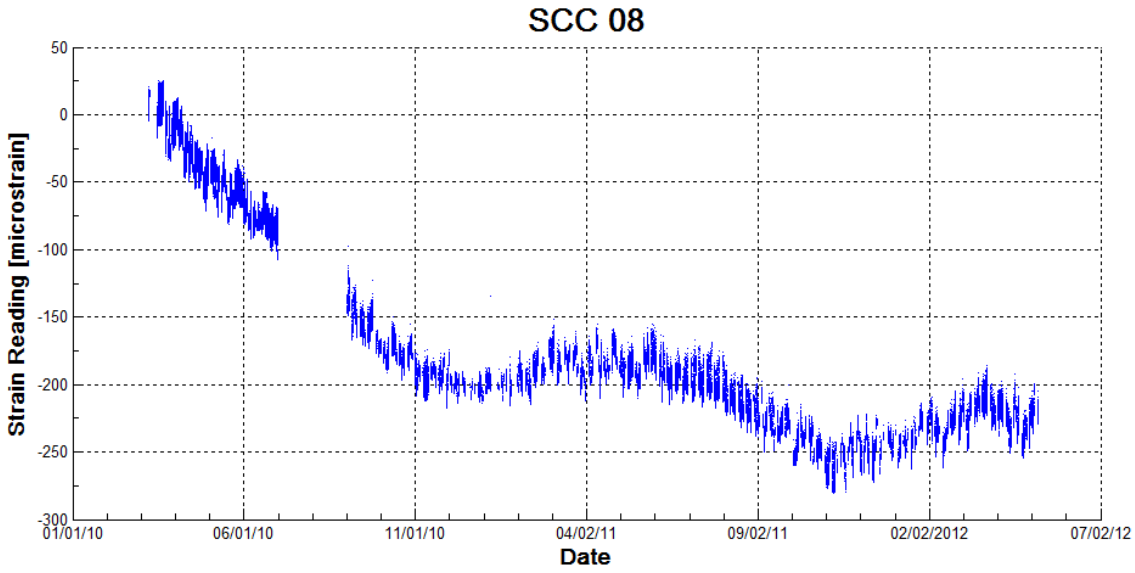

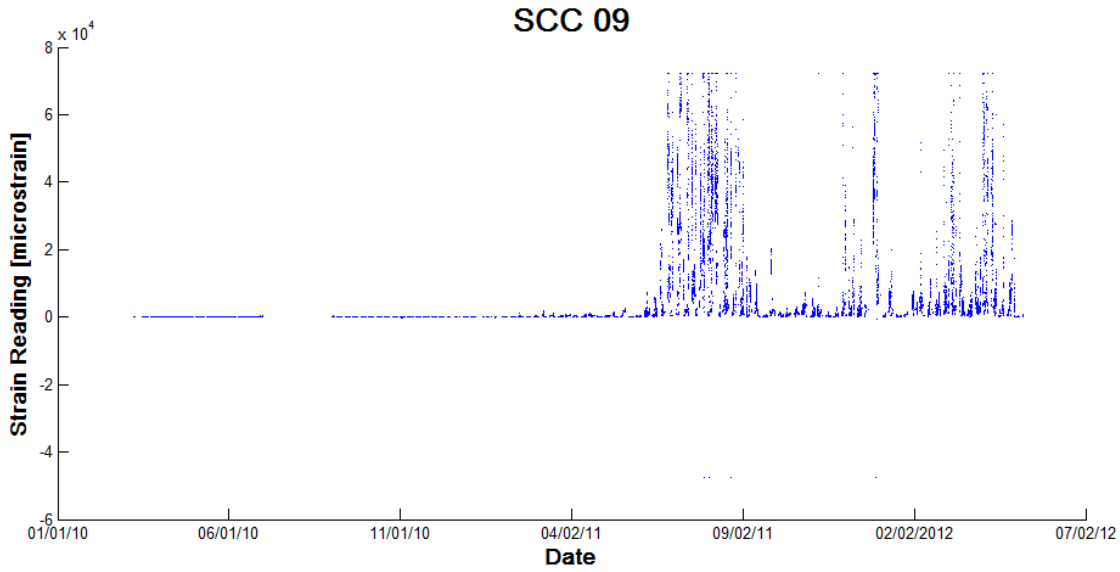
SCC 09
x 10^4
8
6
4
2
0
-2
-4
-6
Strain Reading [microstrain]
01/01/10
06/01/10
11/01/10
04/02/11
09/02/11
02/02/2012
07/02/12
Date

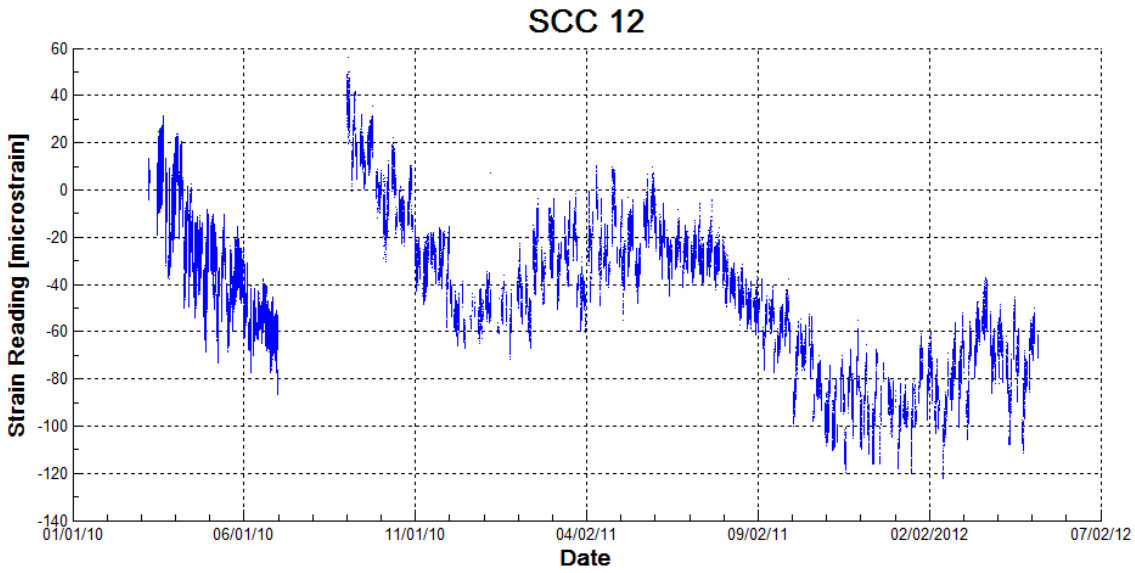
SCC 12
60
40
20
0
-20
-40
-60
-80
-100
-120
-140
Strain Reading [microstrain]
01/01/10
06/01/10
11/01/10
04/02/11
09/02/11
02/02/2012
07/02/12
Date

E.4 Concrete Embedment Gages from Traditional Box Beams

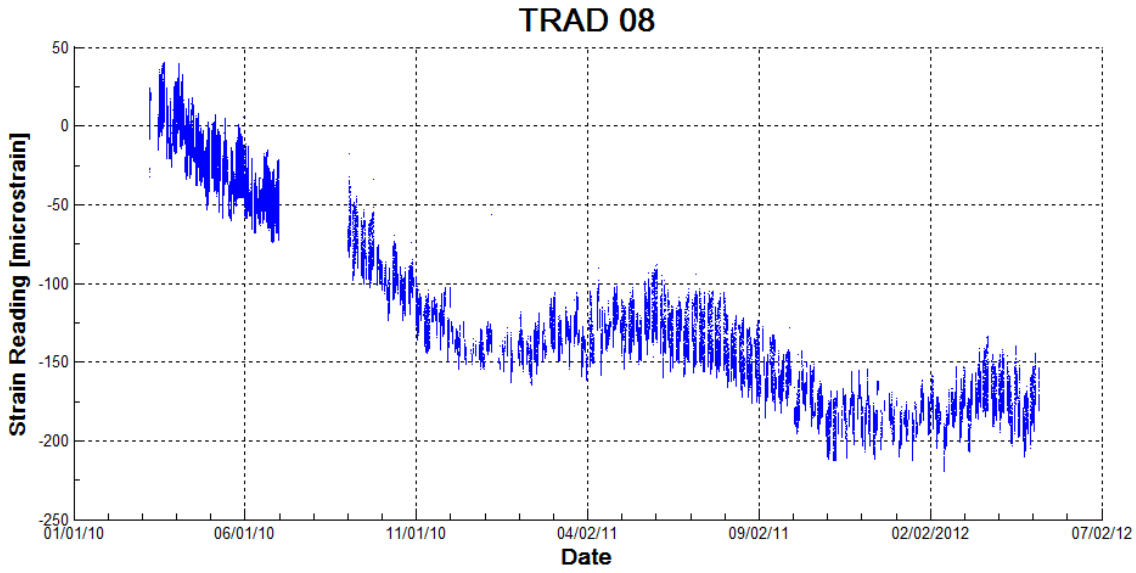

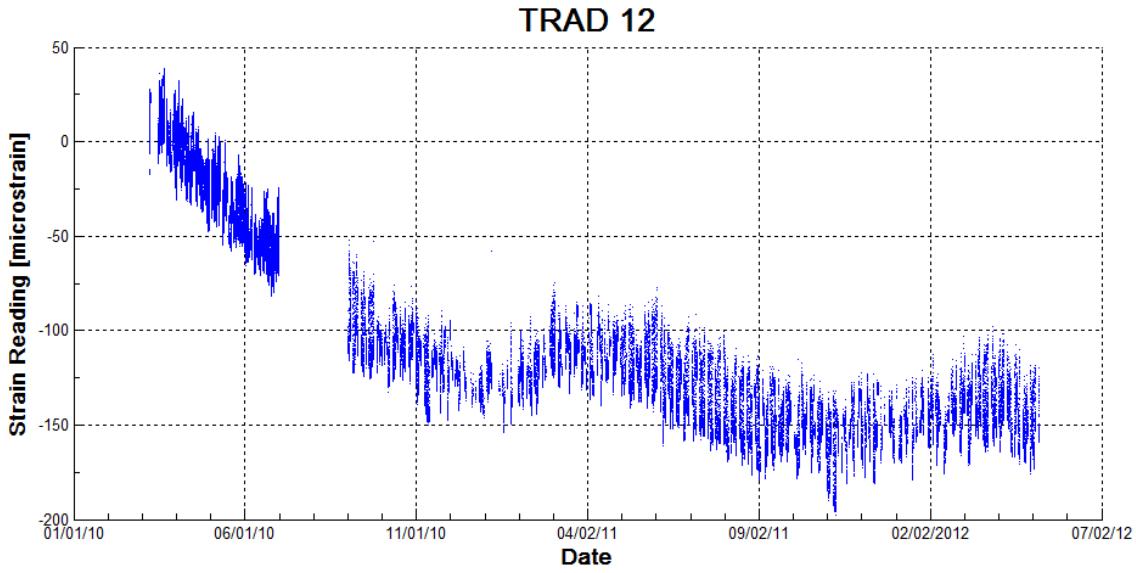

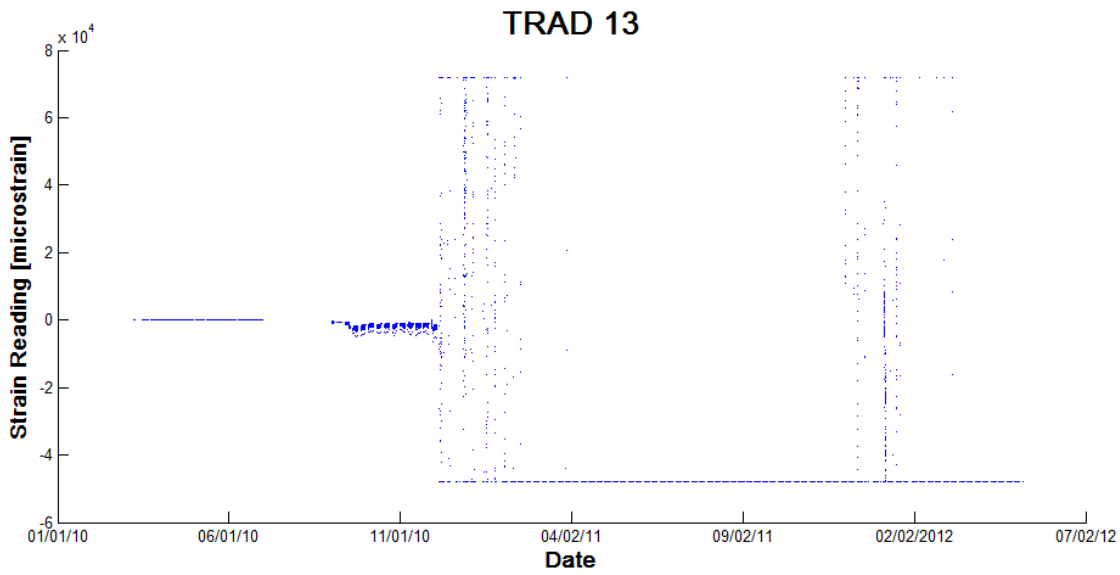
TRAD 13
x 10^4
8
6
4
2
0
-2
-4
-6
Strain Reading [microstrain]
01/01/10
06/01/10
11/01/10
04/02/11
09/02/11
02/02/2012
07/02/12
Date

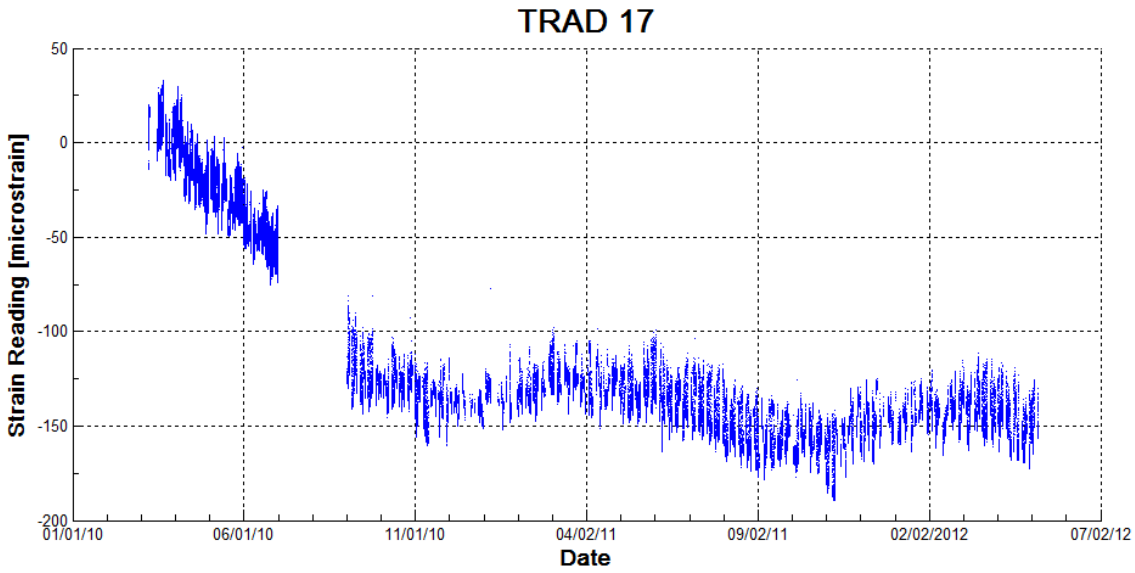
TRAD 17
50
0
-50
-100
-150
-200
Strain Reading [microstrain]
01/01/10
06/01/10
11/01/10
04/02/11
09/02/11
02/02/2012
07/02/12
Date

E.5 Strain Gages from SCC-1 Caissons

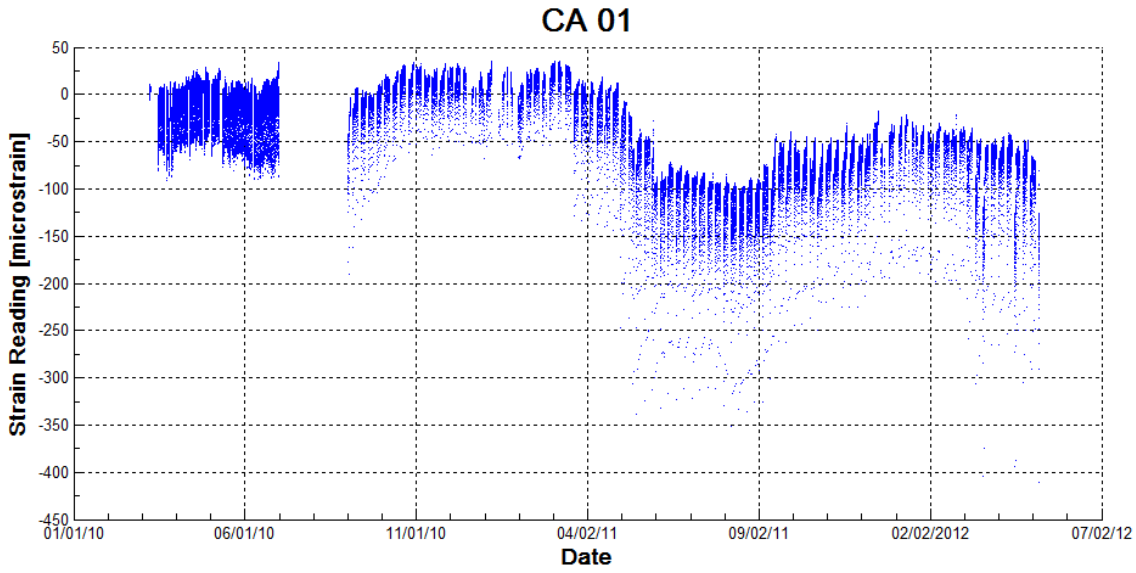

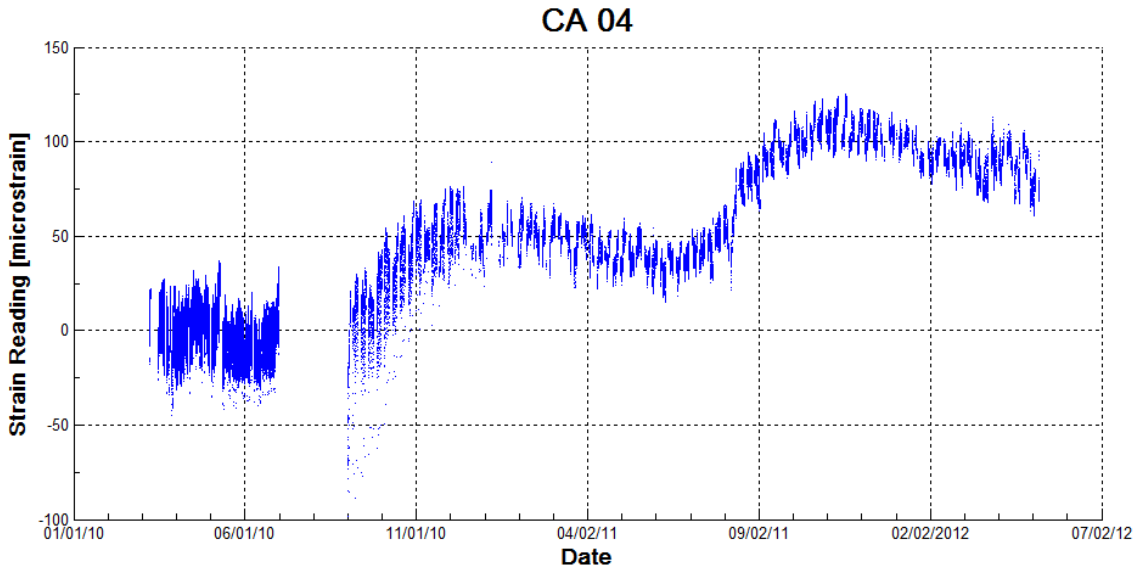

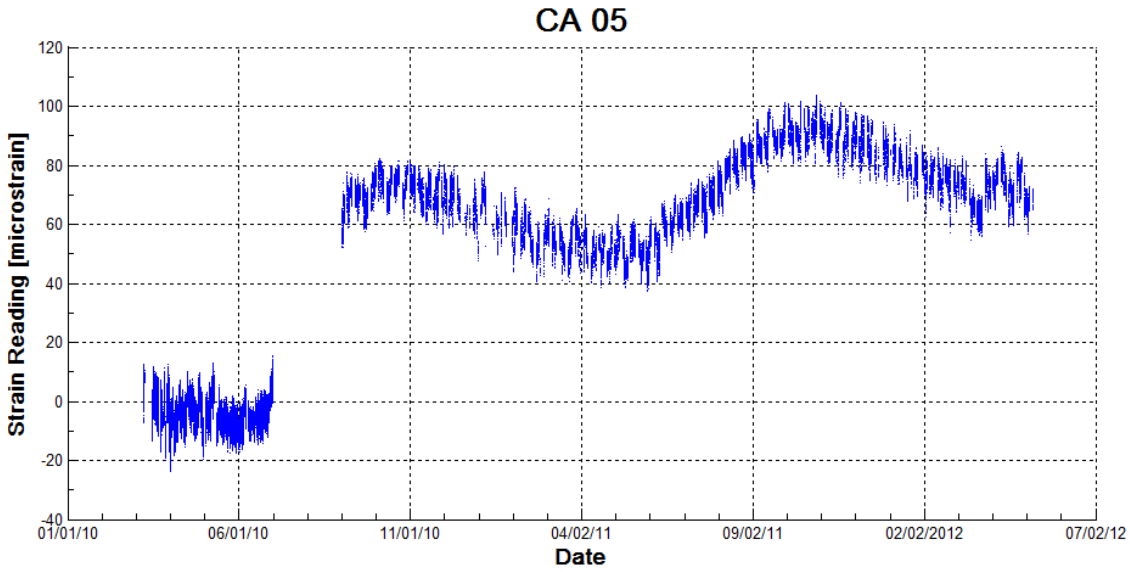
CA 05
Strain Reading [microstrain]
120
100
80
60
40
20
0
-20
-40
01/01/10
06/01/10
11/01/10
04/02/11
09/02/11
02/02/2012
07/02/12
Date

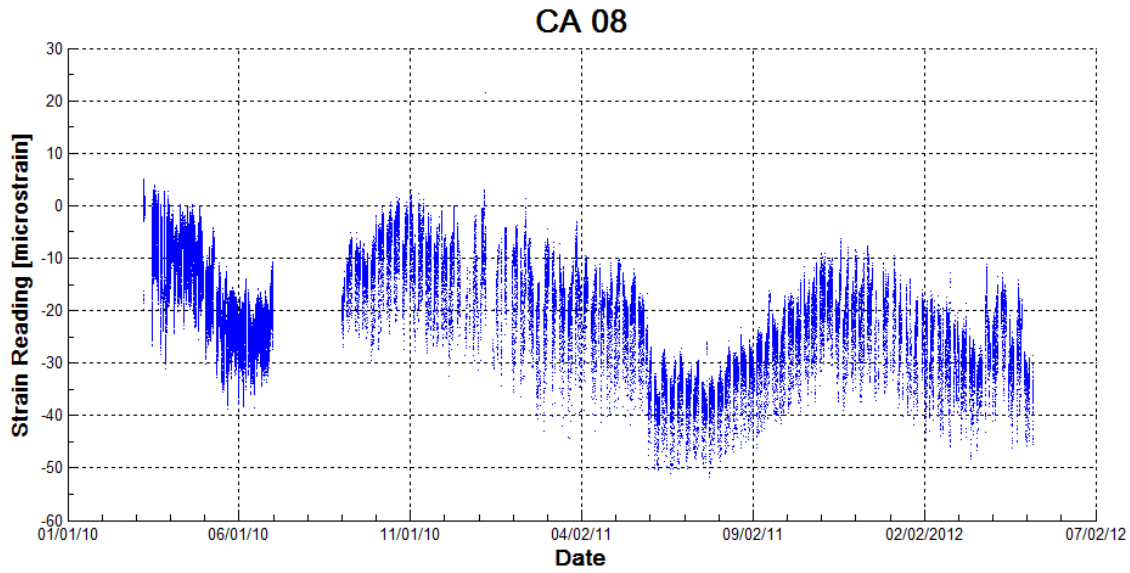
CA 08
Strain Reading [microstrain]
30
20
10
0
-10
-20
-30
-40
-50
-60
01/01/10
06/01/10
11/01/10
04/02/11
09/02/11
02/02/2012
07/02/12
Date

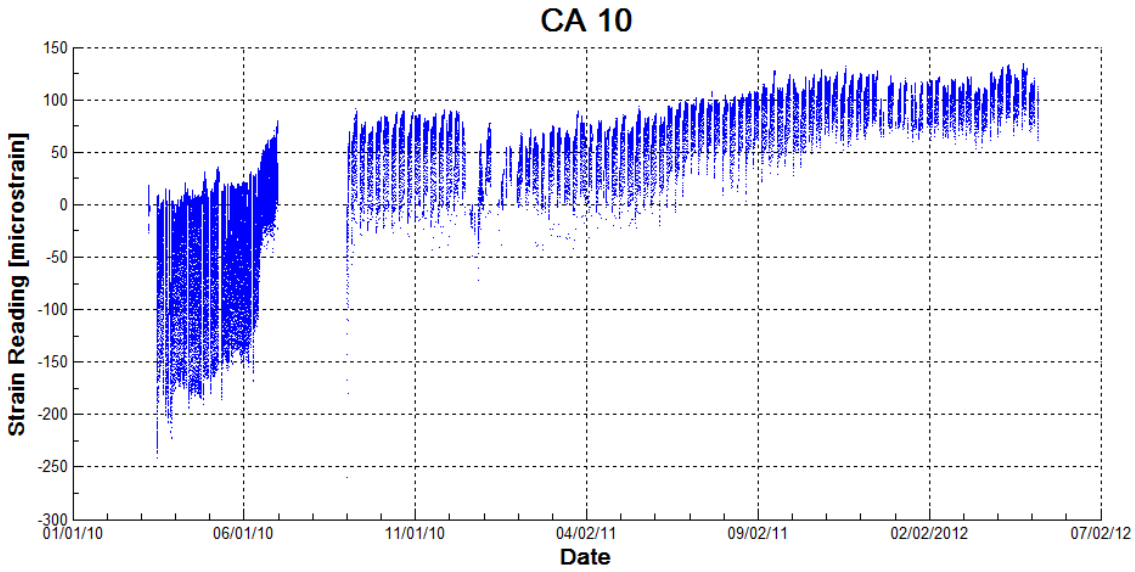
CA 10
Strain Reading [microstrain]
150
100
50
0
-50
-100
-150
-200
-250
-300
01/01/10
06/01/10
11/01/10
04/02/11
09/02/11
02/02/2012
07/02/12
Date

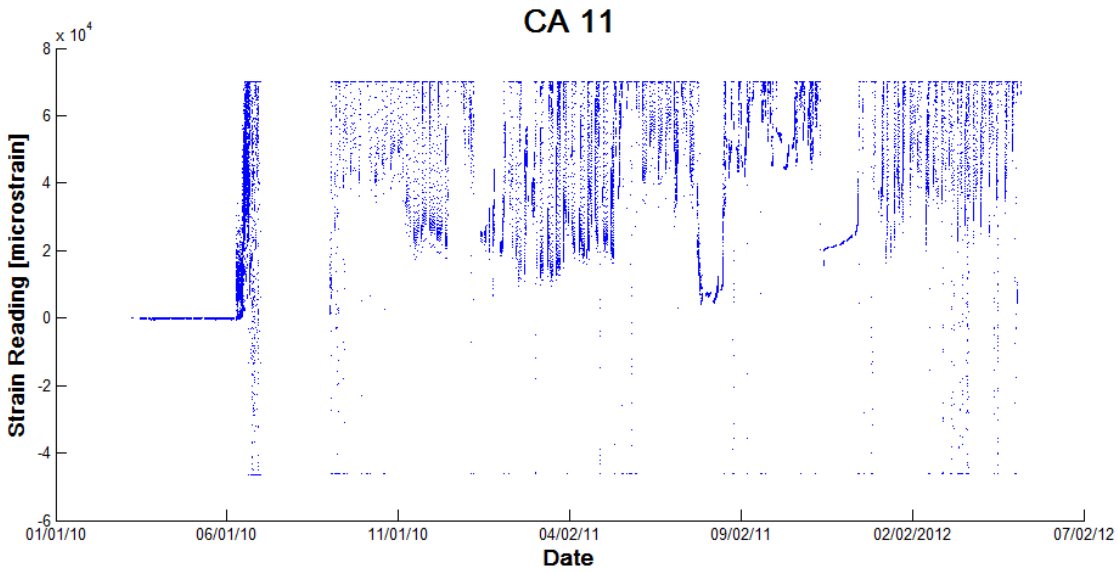
CA 11
x 10^4
Strain Reading [microstrain]
8
6
4
2
0
-2
-4
-6
01/01/10
06/01/10
11/01/10
04/02/11
09/02/11
02/02/2012
07/02/12
Date

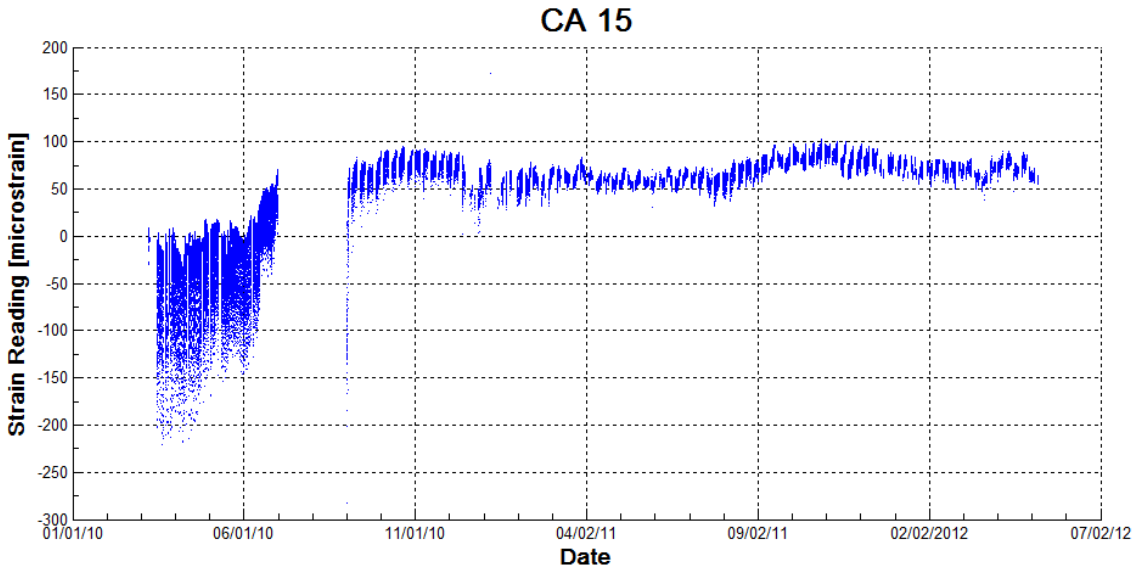
CA 15
Strain Reading [microstrain]
200
150
100
50
0
-50
-100
-150
-200
-250
-300
01/01/10
06/01/10
11/01/10
04/02/11
09/02/11
02/02/2012
07/02/12
Date

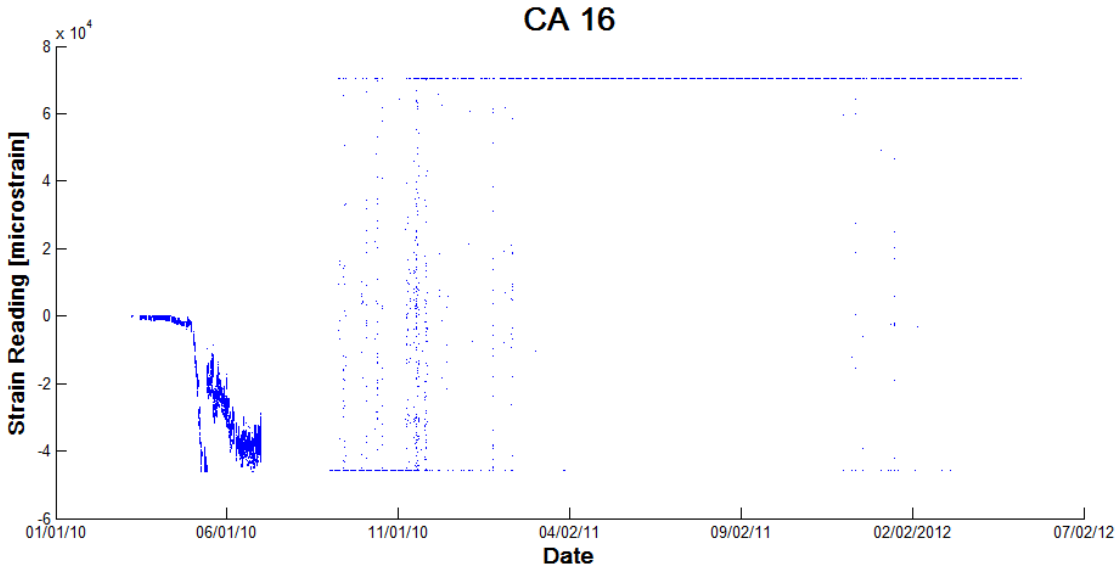
CA 16
x 10^4
Strain Reading [microstrain]
8
6
4
2
0
-2
-4
-6
01/01/10
06/01/10
11/01/10
04/02/11
09/02/11
02/02/2012
07/02/12
Date